# Experimental Investigations for the Enrichment of Biogas Employing Biomass-Based Scrubbing Agents and Bio-Electrochemical Approaches

*A Thesis*
*Submitted in Partial Fulfillment of the Requirements for the Award of the Degree of*

**DOCTOR OF PHILOSOPHY**

By

**DEEP BORA**

**School of Energy Science and Engineering**
**Indian Institute of Technology Guwahati**
**Guwahati – 781 039, Assam, India**
**November 2022**

*This thesis is dedicated to my*

*Family*

*&*

*Mentors*

*Whose endless faith, support and blessings always inspired me to move forward*

INDIAN INSTITUTE OF TECHNOLOGY GUWAHATI

**SCHOOL OF ENERGY SCIENCE AND ENGINEERING**

# DECLARATION

I do hereby declare that the content embodied in this thesis entitled **"Experimental Investigations for the Enrichment of Biogas Employing Biomass-Based Scrubbing Agents and Bio-Electrochemical Approaches"** is the result of investigation carried out by me at School of Energy Science and Engineering, Indian Institute of Technology Guwahati, Guwahati, India under the guidance of Prof. Pinakeswar Mahanta and Dr. Lepakshi Barbora.

In keeping with the general practice of reporting scientific observations, due acknowledgements have been made wherever the work described is based on the findings of others investigators.

*November 2022*

Deep Bora
(Roll No. 156151008)
School of Energy Science and Engineering
Indian Institute of Technology Guwahati
Guwahati, Assam, India

INDIAN INSTITUTE OF TECHNOLOGY GUWAHATI

**SCHOOL OF ENERGY SCIENCE AND ENGINEERING**

# CERTIFICATE

This is to certify that the work described in this thesis entitled **"Experimental Investigations for the Enrichment of Biogas Employing Biomass-Based Scrubbing Agents and Bio-Electrochemical Approaches" by Mr. Deep Bora (Roll No. 156151008)** for the award of degree of **Doctor of Philosophy** is an authentic record of the results obtained from the research work carried out under our supervision in the School of Energy Science and Engineering, Indian Institute of Technology Guwahati, India and this work has not been submitted elsewhere for a degree.


**Prof. Pinakeswar Mahanta**
Professor
Department of Mechanical Engineering
Indian Institute of Technology Guwahati
Guwahati -781039, Assam, India

**Dr. Lepakshi Barbora**
Technical Officer Grade I
School of Energy Science and Engineering
Indian Institute of Technology Guwahati
Guwahati – 781039, Assam, India

# *Acknowledgements*

*I would like to take this opportunity to express my gratitude to them, whose contribution has made this thesis possible.*

*The tenure in IIT Guwahati as a PhD student has been an amazing and challenging experience for me which I will cherished in my journey to life. It is full of my patience, support and encouragement from numerous individuals. I take my utmost pleasure to express my deepest gratitude to each and every one who supported me in several ways to complete my PhD Dissertation.*

*The first and foremost gratitude to my supervisors Prof. Pinakeswar Mahanta and Dr. Lepakshi Barbora for their patience, valuable suggestions, and constant support throughout my research work, which enabled me to work towards a successful completion. I earnestly thank them for their humbleness, spending their valuable time and effort for imbibing scientific temperament and appreciable work ethics in me.*

*I would like to express my sincere gratitude to all my doctoral committee members Prof. Kaustubha Mohanty, Prof. Vaibhav V. Goud and Dr. Priyadarshi Satpati for their encouragement and insightful advice during my seminars and progress reviews that has led to the successful completion of my thesis.*

*I wish to acknowledge the support received from various departments, schools and centres; School of Energy Science and Engineering, Centre for Environment, Chemical Engineering, Mechanical Engineering, Department of Physics and Central Instrument Facility (CIF) for permitting me to use the analytical facilities of the department. I would like to thank Prof. Vinayak Narayan Kulkarni, Dr. Pankaj Kalita, Dr. Deepmoni Deka, Mr. Debarshi Baruah, Mr. Dhiren Huzuri, and Mr. Parag Jyoti Sharma, for their all possible support and facilities to carry out my research work.*

*I would like to acknowledge my sincere thanks to Dr. Anita Mahanta, Dr. Saptarshi Mahanta and Navarshi Mahanta for their support, motivation and*

*encouragement in tough times and help in completing my journey. I would also like to express my sincere thanks to Mr. Jon Mani Kalita, Kuldeep, Arup, Rishiraj, Dipti di, Aparupa ba, Dhananjay, and Moon da for their all possible support to carry out my research work.*

*I will be always grateful to my friends at IIT Guwahati, Saurav da, Arup da, Nilkamal, Sashankar, Sanjay Da and Rubul for making my stay comfortable and cheerful in campus.*

*At last but not the least, I am highly indebted to my parents; Mr. Nakul Bora (Deuta), Mrs. Dipamoni Bora (Maa) and my brother, Pranjit Bora for all the sacrifices they have made for my better future, to have faith in me and giving me freedom to take my own decision. My Ph.D endeavor could not be completed without them.*

*I would like to gratefully acknowledge the financial support of the Ministry of New and Renewable Energy, Government of India (256/3/2017-BIOGAS, 56/4/2020-BIOGAS) for this work.*

*My sincere apology goes to them whom I forget to mention but helped me at any part of the research work.*

***Place: IIT Guwahati***

***Date : 15.11.2022*** ***Deep Bora***

# ABSTRACT

Continuously rising environmental pollution and global demand for energy due to an increase in the population and the depletion of fossil fuels have generated the necessity for alternate sustainable technologies based on renewable economic resources. Biogas produced from anaerobic digestion of organic waste is one of the potential alternative biofuels and is economically feasible, which might benefit the future energy supply demands as well as contribute to a reduction of greenhouse gas emissions. Biogas is primarily composed of methane ($CH_4$) and carbon dioxide ($CO_2$) as the major constituents, with trace amounts of other components like water vapour, hydrogen sulphide ($H_2S$), hydrogen ($H_2$), and nitrogen ($N_2$). The presence of $H_2S$ in biogas needs special attention for cooking, power generation, as well as upgrading to bio-methane due to its foul-smelling odor, corrosion, health issues, regeneration, and environmental problems. Scrubbing of $CO_2$ is also essential for the upgradation of biogas, which increases the calorific value of the treated gas and enhances its efficiency for being used as vehicular fuel and power generation. Various purification technologies are employed to attain selective separation of $CO_2$ and $H_2S$ from biogas, such as physical or chemical absorption, adsorption on solid surfaces, membrane separation, cryogenic separation, pressure swing adsorption, and so on. However, among all the methods, the absorption and adsorption methods are found to be simple, cost-effective, and easy to operate for the decentralized biogas plants. The use of different alkaline chemicals in the chemical absorption and adsorption processes is a common technique for the removal of $CO_2$ and $H_2S$ from biogas. But, the problem arises in the disposal of the used chemicals due to their toxic and environmentally unfriendly nature. Subsequently, a lot of research has been directed to the scrubbing of biogas for $CH_4$ enrichment, and simultaneously, there has also been a search for alternative scrubbing agents with all the desirable properties.

Using a natural base ash solution prepared by ashing different parts of banana plant is a traditional practice amongst the rural communities of Assam, India. As a contribution to the research on the purification of biogas, this thesis aimed to synthesize, characterize, and apply natural base ash solutions and locally available biomass-derived adsorbents for $CO_2$ and $H_2S$ removal from biogas and to alleviate the adverse effects of using chemical bases. Six different scrubbing agents and adsorbents, namely, banana pseudostem (BPS) ash solution, *Musa balbisiana* peel (MBP) ash solution, *Musa acuminata* peel (MAP) ash solution, bamboo biochar (BB), banana peel biochar (BPB), and biochar-clay composite (BCC) were chosen out of ten based on their physico-chemical properties for $CO_2$ and $H_2S$ removal from raw biogas using absorption and adsorption techniques.

The maximum average pH measured for these three natural base ash solutions, BPS, MBP, and MAP, was 11.48, 12.77, and 11.63, respectively. Flame photometry analysis showed that the potassium quantity in MBP was slightly higher (228.40 mg $g^{-1}$) than in MAP (209.72 mg $g^{-1}$) and BPS (189.64 mg $g^{-1}$), which was also supported by EDX. The surface average pH values recorded for BB, BPB, and BCC were 10.67, 10.95, and 9.96, respectively. Results of high pH, rich mineral compositions, and porosity indicated that the scrubbing agents and adsorbents are naturally alkaline and can be utilized for the removal of $CO_2$ and $H_2S$ from raw biogas.

The selected biomass-derived adsorbents, *viz.*, BB, BPB, and BCC, were used for the removal of $H_2S$ from raw biogas. The biogas was scrubbed directly from a 3 $m^3$ Deenbandhu model biogas plant where cattle dung was the only feed material. The characteristics and mechanisms of $H_2S$ adsorption from raw biogas on BB, BPB, and BCC were also investigated with the help of analytical techniques. It was found that BPB could effectively remove 89.2% $H_2S$ from raw biogas, followed by BB (87.7%) and BCC (78.4%) in a fixed bed adsorption scrubber. However, the saturation period was different for all the respective

adsorbents. For a comparative study, the compositional, morphological, and structural properties of all the three adsorbents before and after treatment were analyzed using pH, EDX, FESEM, XRD, and FT-IR. The adsorption of $H_2S$ strongly depends on pH, oxygen, BET surface area, mineral compositions, and textural properties of the adsorbents. Also, the calculated equilibrium adsorption value ($q_e$) obtained from the pseudo-second-order kinetic model (BB, $q_{e\ cal}$ = 3.53 mg $H_2S$ $g^{-1}$ biochar; BPB, $q_{e\ cal}$ = 3.57 mg $H_2S$ $g^{-1}$ biochar; and BCC, $q_{e\ cal}$ = 1.41 mg $H_2S$ $g^{-1}$ biochar) was best fitted for all the adsorbents, with the experimental data having a correlation coefficient, $R^2$ = 0.99. The observed results indicate that BB, BPB, and BCC can be used for $H_2S$ adsorption at a much lower cost compared to commonly used chemicals.

The effects of natural base ash solutions (BPS, MBP, and MAP) with different molar concentrations of KOH (0.1, 0.3, 0.5, 0.7, and 1.0 M) on $CO_2$ scrubbing from biogas were investigated and compared. The scrubber with natural base ash solution from MBP could enrich the $CH_4$ content in biogas from 56.9% to 86.3%, followed by MAP (78.4%) and BPS (76.8%), which is nearly equivalent to 0.3 M KOH (88.6%). The highest $CO_2$ absorption of ~68% was achieved with MBP with a saturation time of 19 minutes, approximately at a flow rate of 200 ml/min. Also, the kinetic study shows that the rate constant *k* for MBP was nearly equivalent to that of 0.5 M and 0.7 M KOH, with an $R^2$ value of 0.99. The experimental results also indicated that $CO_2$ absorption by various chemicals as well as NBA solutions is transient and has to be replaced once it reaches its saturation level. The experiments revealed that banana peel ash solutions had the nearly equivalent potential to KOH for $CO_2$ absorption from biogas. The biomass availability, easy preparation method, and environment-friendly nature of the scrubbing agents and adsorbents render them potential candidates for $CO_2$ and $H_2S$ removal from decentralized biogas plants installed in rural areas.

Additionally, a single chamber, above-ground, portable anaerobic digester (AD) was developed, which was hybridized with a membrane electrode assembly (MEA) to facilitate the generation of enriched biogas and electricity as a byproduct. The analysis showed enrichment of $CH_4$ in biogas, while the AD was hybridized with the MEA. The highest concentration of $CH_4$ and $CO_2$ in control was 56.3±1.5% and 43.7±0.9% whereas in AD-MEA the concentration of $CH_4$ increased to 73.7±3.9% and $CO_2$ reduced to 26.3±0.5 respectively. Enrichment of $CH_4$ concentration in the hybridized AD-MEA system proved that the presence of a conductive surface in the anaerobic chamber of the AD-MEA system could promote the enrichment of methane by stimulating a synergistic mechanism between exoelectrogens and hydrogenotrophic methanogens for the conversion of $CO_2$ directly to $CH_4$. The hybridized AD-MEA setup could produce as much as 496±7 mV of OCV with a maximum average power density of 2.87 $mW/m^2$ and a 70 $mA/m^2$ current density, respectively. Also, the average experimental data of biogas production obtained from the control and AD-MEA systems were fitted using three different non-linear mathematical models. The kinetic parameters evaluated from the three models confirm that the modified Gompertz model ($R^2$ = 0.99) was best fitted to the experimental biogas production data, followed by the Logistic and Transference function models.

***Keywords:*** *Anaerobic digestion; Biogas; Natural base ash solution; Biomass-derived adsorbents; $CO_2$ and $H_2S$ removal; Absorption; Adsorption; Kinetics study, Hybridized AD-MEA , Methane Enrichment; Electricity*

# CONTENTS

# LIST OF TABLES

# LIST OF FIGURES

# LIST OF SYMBOLS

| | |
|---|---|
| $\sigma$ | kinetic diameter (Å: Angstrom) |
| $\alpha$ | polarizability (Å$^3$: Angstrom$^3$) |
| $\mu$ | dipole moment (D: coulomb-metre) |
| $W_i$ | weight of the initial sample in g |
| $W_f$ | weight of the final dried sample in g |
| $W_c$ | weight of the crucible with lid in g |
| $W_a$ | weight of ash and crucible in g |
| $\lambda$ | wavelength of the X-ray (Å) |
| $\theta$ | diffraction angle (°) |
| $C_0$ | initial adsorbate ($H_2S$) concentration |
| $C_1$ | adsorbate ($H_2S$) concentration after purification at time t |
| $C_e$ | equilibrium adsorbate ($H_2S$) concentration |
| V | volume of solution |
| m | amount of adsorbent |
| $q_e$ | the amount of $H_2S$ adsorbed at equilibrium (mg g$^{-1}$) |
| $q_t$ | the amount of $H_2S$ adsorbed at time t (mg g$^{-1}$) |
| $k_1$ | pseudo first-order rate constant (min$^{-1}$) |
| $k_2$ | pseudo second-order rate constant (g mg$^{-1}$ min$^{-1}$) |
| $k_p$ | intraparticle diffusion rate constant (mg g$^{-1}$ min$^{-1/2}$) |
| C | the constant associated with the boundary layer effect (intercept) |
| $a_e$ | initial adsorption rate (mg g$^{-1}$ min$^{-1}$) |
| $b_e$ | the extent of surface coverage for the chemisorption (g mg$^{-1}$) |
| $R^2$ | linear regression correlation coefficient |
| $S^0$ | elemental sulphur |
| $A$ | fraction of $CO_2$ absorbed from the gas mixture after time t |
| $C_o$ | outlet $CO_2$ concentration (% v/v) after time t |
| $C_i$ | inlet $CO_2$ concentration (% v/v) |
| $k$ | absorption rate constant |
| $A_0$ | fraction of $CO_2$ absorbed from the gas mixture after τ |
| $\tau$ | characteristic absorption time when 50% absorption of $CO_2$ occurs (min) |

| | |
|---|---|
| $t$ | experimental time (min) |
| Ω | ohm |
| V | voltage (V) |
| I | current (A) |
| R | external resistance (ohm) |
| B | cumulative biogas production |
| P | maximum biogas production potential (ml) |
| $R_m$ | maximum biogas production rate (ml $d^{-1}$) |
| λ | lag phase (day) |
| t | retention time (day) |
| $e$ | Euler's function |

# LIST OF ABBREVIATIONS

| | |
|---|---|
| AAS | amino acid salts |
| ABD | anaerobic bioelectrochemical digestion |
| AC | activated carbon |
| AD | anaerobic digestion/ anaerobic digester |
| AD-MEA | anaerobic digester- membrane electrode assembly |
| AMP | 2-amino-2-methyl-1-propanol |
| APA | bis(3-aminopropyl)amine |
| ASTM | american society for testing and materials |
| ATBR | anaerobic trickle-bed reactors |
| BB | bamboo biochar |
| BCC | biochar-clay composite |
| BET | brunauer–emmett–teller |
| BPB | banana peel biochar |
| BPS | banana pseudostem |
| CAC | coconut shell activated carbon |
| CHP | combined heat and power |
| CI | compression ignition |
| C:N | carbon: nitrogen |
| CPVC | chlorinated polyvinyl chloride |
| CR | compression ratio |
| CSB | corn stover biochar |
| CSTR | continuous stirred tank reactor |
| CV | cyclic voltammetry |
| DEA | diethanolamine |

| | |
|---|---|
| DETA | diethylenetriamine |
| DGA | diglycolamine |
| DIET | direct interspecies electron transfer |
| EDX | energy dispersive x-ray spectroscopy |
| FC | fixed carbon |
| FESEM | field emission scanning electron microscopy |
| FT-IR | fourier transform infra-red spectroscopy |
| FVW | fruit and vegetable wastes |
| GC | gas chromatography |
| HCV | higher calorific value |
| HPP | hydrogen partial pressures |
| HRT | hydraulic retention time |
| IC | internal combustion |
| IHT | interspecies hydrogen transfer |
| L | litre |
| LCV | lower calorific value |
| M | moisture |
| MAP | musa acuminata peel |
| MB | maple wood biochar |
| MBP | musa balbisiana peel |
| MC | methane content |
| MCFC | molten carbonate fuel cell |
| mcrA | methyl-coenzyme M reductase A |
| MCW | maize cob waste |
| MDEA | methyldiethanolamine |
| MEA | membrane electrode assembly |

| | |
|---|---|
| *MEA* | monoethanolamine |
| MES | microbial electrosynthesis system |
| MFC | microbial fuel cell |
| MMMs | mixed matrix membranes |
| NBAS | natural base ash solution |
| NREL | national renewable energy laboratory |
| OCV | open circuit voltage |
| PAFC | phosphoric acid fuel cell |
| PDMS | polydimethylsiloxane |
| PEM | proton-exchange membrane |
| PEMFC | polymer electrolyte membrane fuel cell |
| PSA | pressure swing adsorption |
| PVC | polyvinyl chloride |
| PZ | piperazine |
| RAA | recovered aqueous ammonia |
| SD | standard deviation |
| SEM | scanning electron microscopy |
| SI | spark ignition |
| SOFC | solid oxide fuel cell |
| TCOD | total chemical oxygen demand |
| TEA | triethanolamine |
| TGA | thermogravimetric analysis |
| TRI-PE-MCM-41 | triamine-grafted pore-expanded mesoporous silica |
| VFA | volatile fatty acids |
| VM | volatile matter |

| | |
|---|---|
| XRD | X-ray diffraction |

# Chapter 1

## Introduction

# CHAPTER 1: INTRODUCTION

## 1.1 BACKGROUND AND MOTIVATION

Global demand for renewable energy is increasing rapidly due to the continuous increase in the population and also to control climate and environmental pollution owing to carbon emissions and toxic chemicals [Bansal et al., 2019]. Thus, various forms of renewable energy, such as wind, tidal wave, solar, and biomass, have received global attention in recent decades [Demirbas, 2010]. Solar photovoltaic systems are limited due to the high cost of production, while the use of wind, tidal, and wave energy is site-specific. The International Energy Agency reported that around 14.1% of the total global energy supply was contributed by renewable energy, of which approximately 9.4% comprised bioenergy (Fig. 1.1) [International Energy Agency].

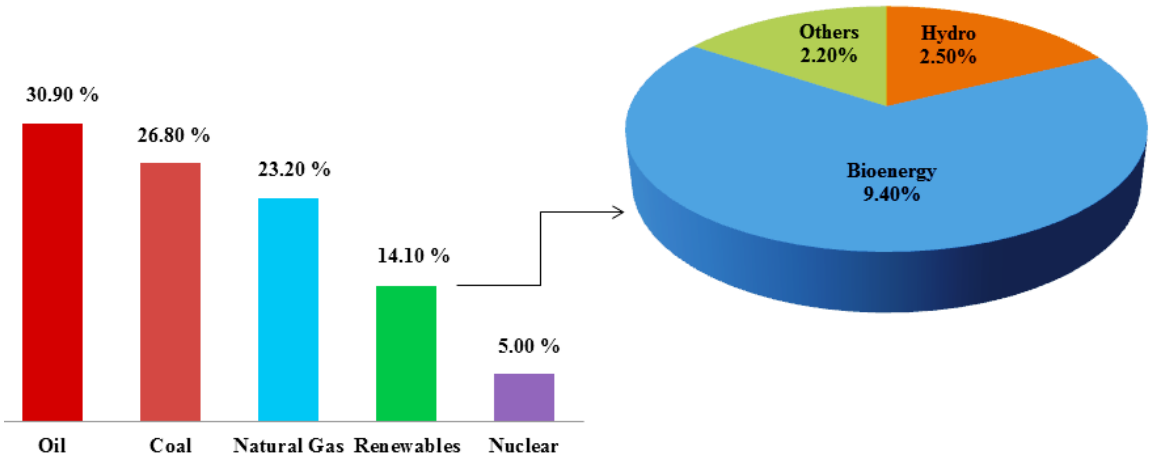


**Fig. 1.1** A glimpse of total global energy supply (2021)

Dry and wet biomass can be utilized for energy production by gasification and anaerobic digestions respectively. The advantage of biogas technology is the ease in production and sustainability [Sakar et al., 2009]. Many arable farmlands universally have now been implemented in constructing anaerobic digesters to produce small quantities of

biogas from organic waste such as kitchen waste, sludge and manure [Lo et al., 1994]. The widespread availability of the organic materials required for biogas synthesis is considered a potentially effective and sustainable energy source [Diaz et al., 2011]. But the presence of a high concentration of $CO_2$ and $H_2S$ limits the wider applicability of biogas and thus needs purification to enhance its efficiency and to reduce environmental problems.

Numerous basic mechanisms are employed to attain selective separation of $CO_2$ and $H_2S$ from biogas, such as physical or chemical absorption, adsorption on a solid surface, membrane separation, cryogenic separation, pressure swing adsorption (PSA), and so on [Ryckebosch et al., 2011]. Based on different biogas upgrading sites, all the biogas purification technologies have their own specific advantages and disadvantages. The accurate choice of an economically feasible purification technology strongly relies on the quality and quantity of the raw biogas, the biomethane quality to be attained, and its utilization.

The use of biogas in India has been running for several decades ranging from 1 to 6 $m^3$ (household) and 10 to 100 $m^3$ (farm), mainly existing in the rural areas and having animal manure and agricultural wastes as the major feedstocks. However, technology related to the purification of biogas for these small decentralized biogas plants needs proper attention due to high chemical costs, disposal of used scrubbing agents, and environmental concerns, thus demanding thorough research for locally available, cost-effective and environmentally friendly scrubbing agents. Hence the author was motivated to adopt a simple purification process for the removal of $CO_2$ and $H_2S$ from raw biogas to check the potential of locally available biomass-based scrubbing agents. Kinetic studies of $CO_2$ and $H_2S$ removal by different scrubbing agents are also important to evaluate their best-fitted mechanisms.

## 1.2 GLIMPSE OF BIOMASS AVAILABILITY IN INDIA

India is a rich country in terms of biomass, and the consumption of biomass energy has been in practise since ancient times. Biomass is organic matter that is available on a renewable basis and includes all plants and plant-derived materials. Harnessing energy from biomass is gaining popularity in developing countries due to the high availability of biomass and bio-waste. Various kinds of animal waste, lignocellulosic biomass, and municipal solid waste are abundantly available and are recognized as potential feed materials for different applications like landfilling, biogas, and biofuel production [Borah et al., 2016]. Lignocellulosic biomass also has scope to be used as a raw material for the production of feedstock for producing biochemicals, bio-sorbents and adsorbents, or enzymes and metabolites [Chen et al., 2010; Gupta and Suhas, 2009]. Figure 1.2 shows the various classifications of biomass available in India.

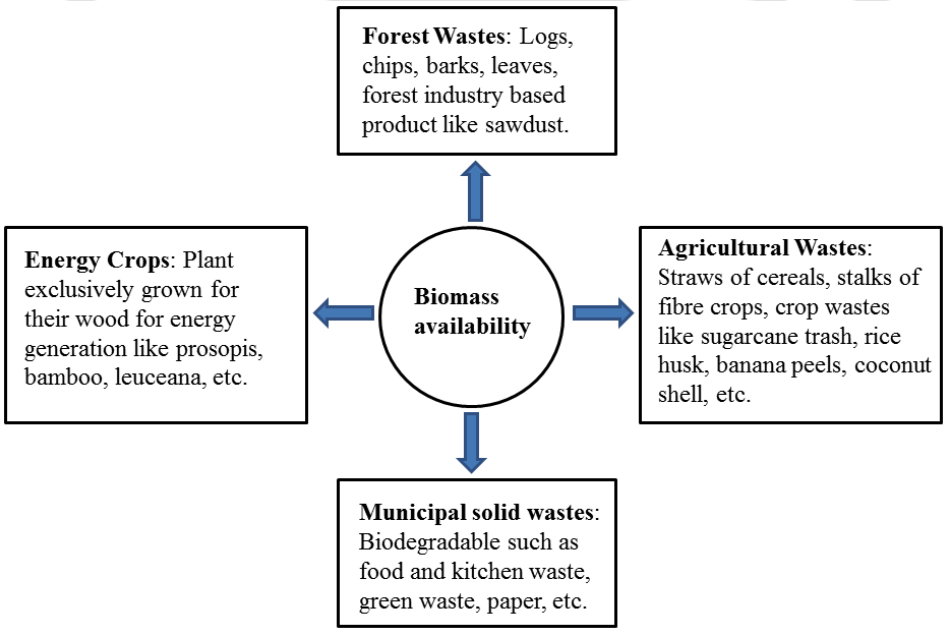


**Fig. 1.2** Classifications of biomass resources in India

They can be simply classified as grasses, woody plants, fruits, vegetables, and aquatic plants. These biomasses distinguish themselves by several parameters such as calorific value,

moisture content, carbon proportion, ash, mineral content, etc. These properties are substantial for wet and dry biomass, which enables them to consider biomass potentials like conversion into useful energy, biochemical, and adsorbents. Bio-chemical/biological and thermo-chemical are the two main processes for conversion of biomass to energy, biochemical, and adsorbents [Surra et al., 2019; Taherzadeh and Karimi, 2008].

## 1.3 PROCESS OF BIOGAS PRODUCTION: ANAEROBIC DIGESTION

Biogas is considered as one such clean and alternative renewable energy source produced by anaerobic digestion (AD) of organic matters in the absence of oxygen and the presence of anaerobic microorganisms [Awe et al., 2017; Mamun et al., 2016; Yadvika et al., 2004]. The digestion process takes place through various reactions and interactions among acetogens, methanogens, and substrates fed into the digester as input [Mahanta et al., 2005]. As depicted in Fig. 1.3, the anaerobic digestion process generally consists of four steps: hydrolysis, acidogenesis, acetogenesis, and methanogenesis [Gerardi, 2003; Takuwa et al., 2009].

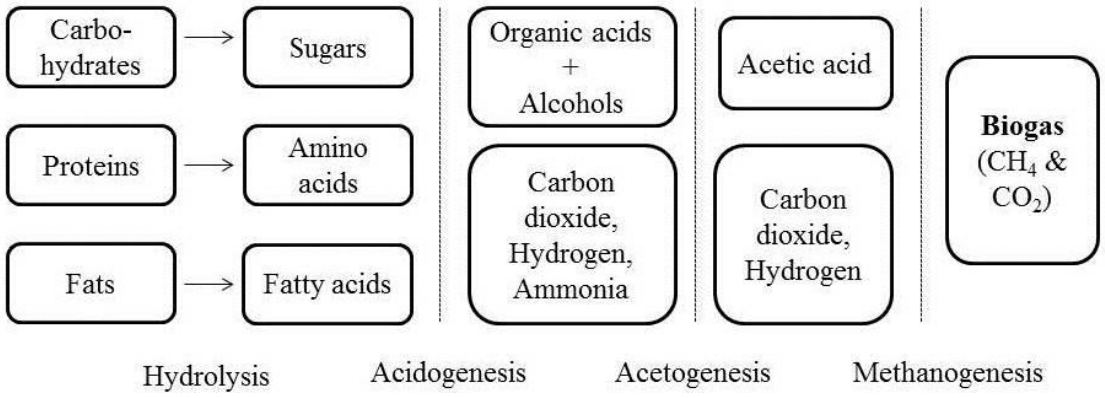


**Fig. 1.3** Breakdown of the anaerobic digestion process

The typical reactions during the process of anaerobic digestion are [Ostrem et al., 2004]:

$$C_6H_{12}O_6 \longrightarrow 2C_2H_5OH + 2CO_2 \quad (1.1)$$

$$2C_2H_5OH + CO_2 \longrightarrow CH_4 + 2CH_3COOH \quad (1.2)$$

$$CH_3COOH \longrightarrow CH_4 + CO_2 \quad (1.3)$$

$$CO_2 + 4H_2 \longrightarrow CH_4 + 2H_2O \quad (1.4)$$

The composition of biogas is typically a mixture of 45-60% methane ($CH_4$), 40-55% carbon dioxide ($CO_2$) and a trace amount of other gases like hydrogen ($H_2$), nitrogen ($N_2$), and hydrogen sulfide ($H_2S$) [Karki et al., 2005; Mann et al., 2009]. The variable composition of biogas is due to the variety of materials that can be used for its production. The production of biogas and the process's stability are entirely dependent on waste composition, such as the C:N ratio (25:1 to 30:1), process conditions, such as pH (6.8-7.2), operating temperature (35-37 °C), and the population of the microbial community in the system [Rasi et al., 2007]. The properties of biogas are shown in Table 1.1.

**Table 1.1** Properties of biogas [Hotta et al., 2019; Steinhauser 2008]

| **Properties** | **Biogas** |
|---|---|
| Composition | 55-60% $CH_4$, 40-45% $CO_2$ and traces of other gases |
| Energy value | 6.0-6.5 kW/$m^3$ |
| Fuel equivalent | 0.6-0.65 L oil/$m^3$ biogas |
| Explosion limits | 6-12% biogas in air |
| Ignition temperature | 650-750 °C |
| Critical pressure | 75-89 bar |
| Critical temperature | -82.5 °C |
| Normal density | 1.2 kg/$m^3$ |
| Flame speed | 25 cm/s |
| Odour | Bad eggs (the smell of $H_2S$) |
| Lower heating value | 17 MJ/kg |
| Heat of vaporization | 0.5 MJ/kg |

Hydraulic retention time (HRT) is normally inversely proportional to the process temperature and varies from place to place. The feed materials are generally animal by-products, which are fed to the digester. In recent times, co-digestion of lignocellulosic biomass with manure

has gained much attention in many countries since it increases the yield of biogas. But an initial pretreatment step prior to the AD process is of utmost importance in order to rupture the recalcitrant structure of the lignocellulosic biomass to release the cellulose and hemicellulose to the microbial consortia present in the digester, which in turn increases the rate of biomass degradation along with an increase in biogas yield [Zheng et al., 2014]. The digested residue after the AD process is transferred automatically to outlet tanks, which are typically covered with concrete to prevent methane leakage into the atmosphere. Digested residue has an added advantage of high nutrient value and can be reprocessed directly as fertilizer for agricultural fields.

## 1.4 BIOGAS DISADVANTAGES AND THE NEED FOR PURIFICATION

Methane in biogas is a highly valued energy source, although other constituents are impurities that pose key obstacles to the viable use of biogas [Abatzoglou and Boivin, 2008]. $CO_2$ through combustion has no energy yield and greatly diminishes the heating value per volume of biogas due to its high content. Biogas with $CO_2$ has a calorific value ranging from 18.7 to 26 MJ/$m^3$, while biogas without $CO_2$ has a calorific value ranging from 33.5 to 35.3 MJ/$m^3$ [Monnet, 2003]. Apart from $CO_2$, another major impurity is $H_2S$. It is always present in biogas, while concentrations differ with the feedstock [Wellinger and Lindeberg, 1999]. The concentration of hydrogen sulfide ($H_2S$) in biogas depends on the types of organic substrates and anaerobic digestion conditions and typically ranges between 10–5000 ppm [Fortuny et al., 2011; Kadam and Panwar, 2017]. $H_2S$ is a colorless, flammable, foul-smelling, toxic gas. The presence of high $H_2S$ concentrations in biogas often damages gas burners, gas storage tanks, compressors, engines and pipelines to transport due to its highly corrosive nature [Chen et al., 2017; Kapdi et al., 2005]. It also acts as strong poison for fuel cells and reformer catalysts. The odour of rotten eggs in $H_2S$ can be detected at even lower than 1 ppb concentration. Upon combustion, it also forms a risky pollutant, sulfur dioxide,

whose emissions can be subjected to regulations. Furthermore, extensive exposure to a concentration of 300 ppm of $H_2S$ in the air poses a severe health threat to the users [Janssen et al., 2001; Krischan et al., 2010; Rasi et al., 2011]. When it is emitted into the atmosphere, it is also considered a major air pollutant because $H_2S$ is not only malodorous but also a source of acid rain [Lee et al., 2006].

That is why to use biogas effectively it is very important to remove the $CO_2$ and $H_2S$ from it. Thus, removal of $CO_2$ and $H_2S$ from biogas will enhance the fuel efficiency which could serve as a source of immense energy that can be used effectively for different applications like cooking [Ray et al., 2016], vehicle fuel and powering of generators for electrical energy [Abushammala et al., 2016; Sun et al., 2015; Zhao et al., 2010]. After scrubbing, the biogas can be compressed and stored in gas cylinder and transported to the desired location for utilization. Additionally, the scrubbed biogas reduces greenhouse gas emissions [Monnet, 2003].

## 1.5 TECHNOLOGIES FOR BIOGAS PURIFICATION

Biogas upgrading to biomethane is a novel degree of gas purification. Splitting of minor impurities (moisture, $H_2S$, etc.) and especially $CO_2$, is an essential and critical operation. Removal of these impurities is necessary for all generally used gas applications like cooking, CHP engines, boilers, vehicles, or injection into the natural gas grid. The qualitative requirements for the removal of key constituents from biogas fitting its uses are mentioned in Table 1.2 [Ryckebosch et al., 2011].

**Table 1.2** Requirement of purification

| Applications | $H_2S$ | $CO_2$ | Moisture |
|---|---|---|---|
| Kitchen stoves | Yes | No | No |
| Boiler | Recommended | No | No |
| CHP engine | Yes | Recommended | No condensation |
| Vehicle fuel | Yes | Recommended | Yes |
| Natural gas grid | Yes | Yes | Yes |

Currently, a number of altered biogas upgrading technologies to fulfil the job of producing biomethane of sufficient quality are commercially available and have proven to be technically feasible. The major step comprises the drying of the raw biogas and the removal of $CO_2$, thereby enhancing the heating value of the produced gas. Various biogas upgrading techniques employed to remove $CO_2$ gas constituents from biogas are shown in Fig. 1.4 [Gomes and Hassan, 2001; Osorio and Torres, 2009; Yang et al., 2008].

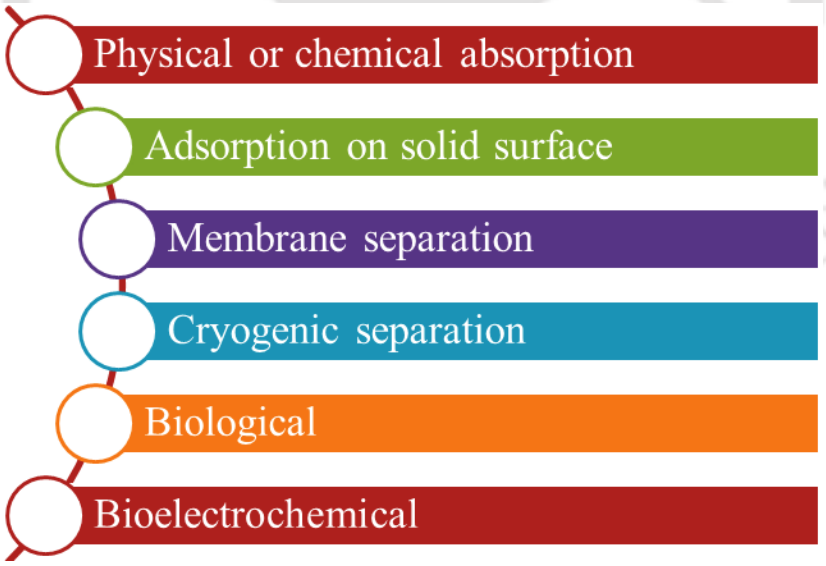


**Fig. 1.4** Various biogas upgrading techniques

Various techniques like physical and chemical absorption, adsorption on solid surfaces, selective catalytic oxidation, and metallic precipitation have been employed to remove $H_2S$ from biogas because of their simple and easy-to-control physicochemical properties

[Ramírez-Sáenz et al., 2009]. The types of solvent and the scrubber design are also equally important for achieving high $H_2S$ removal efficiencies. Chemical absorption with base and oxidant solutions is promising for increasing $H_2S$ solubility in the aqueous phase [Miltner et al., 2012]. However, inoculation of chemicals in the absorption process generally leads to disposal problems due to its toxic nature [Muthuraman et al., 2012]. Moreover, use of these solvents in rural areas for $H_2S$ removal has become impractical owing to technical and cost issues.

In recent times, integration of anaerobic digesters (AD) and microbial fuel cells (MFC) has been researched to increase the energy efficiency, minimize pollutants and recover inorganic nutrients in the end products of waste treatment [Premier et al., 2013]. AD effluents provide the necessary amount of electrochemically active microorganisms for anode reduction, thereby making the anode function stable during the process. Enrichment of methane in biogas can be done via two metabolic pathways. The first metabolic pathway implicates the role of hydrogenotrophic methanogens which convert $CO_2$ directly to $CH_4$. The other metabolic pathway selects an indirect path where homoacetogenic bacteria first convert $CO_2$ to acetate and then convert it to $CH_4$ by acetoclastic methanogens [Angelidaki et al., 2018].

## 1.6 AIM AND OBJECTIVES

The aim of the present work was to develop a cost-effective $CO_2$ and $H_2S$ scrubbing process for decentralized biogas plants installed in rural areas using locally available biomass-based scrubbing agents and also to develop a bio-electrochemical system for $CH_4$ enrichment.

**The objectives of this thesis were:**

1. Survey and selection of indigenous and easily available biomass for the preparation of scrubbing agents and adsorbents.

2. Characterization of selected biomass as adsorbents and scrubbing agents.
3. Performance evaluation of biomass-derived adsorbents using an adsorption method for the removal of $H_2S$ from biogas and their kinetic studies.
4. Experimental and kinetic studies of $CO_2$ scrubbing from biogas by absorption process using natural base ash solutions.
5. Integration of an anaerobic digester with a membrane electrode assembly for the co-generation of methane-enriched biogas and electricity: A comparison with a control system and kinetic analysis.

## 1.7 OUTLINE OF THE THESIS

The present thesis comprises of 7 (seven) chapters.

A detailed literature review on the important scientific findings on biogas scrubbing technologies for $CO_2$ and $H_2S$ using different scrubbing agents and experimental conditions is given in chapter 2. Chapter 3 provides a survey and detailed characterization of selected biomass as scrubbing agents and adsorbents for biogas purification. In Chapter 4, a study of $H_2S$ removal from biogas using biomass-derived naturally alkaline adsorbents along with their kinetics is presented. Chapter 5 presents $CO_2$ scrubbing from biogas by an absorption process using natural base ash solutions and its comparison with KOH. Chapter 6 describes an approach to an alternative pathway for simultaneous enrichment of methane in biogas and electricity generation using a hybridized bio-electrochemical system consisting of an anaerobic digester (AD) and a membrane electrode assembly (MEA). The performance and operation of the AD-MEA system for the co-generation of enriched biogas and electricity are evaluated. Conclusions of the present work and scopes for future work are summarized in chapter 7.

# Chapter 2

## Literature Review

# CHAPTER 2: LITERATURE REVIEW

## 2.1 INTRODUCTION

The present chapter deals with a literature review on various aspects and purification technologies of $CO_2$ and $H_2S$ removal from biogas. The subsequent sections discuss the applications of biogas and its purification standards, biogas scrubbing technologies for $CO_2$ and $H_2S$ with various effects of parameters like pressure, temperature, pH, flow rate, dimension, etc., along with kinetic studies. Emerging technologies for biogas upgradation and recent advances in AD technology with kinetic models based on biogas production are discussed in sections 2.4, 2.5, and 2.6. Subsequently, a research gap is discussed based on available literature and the scope of the present work is presented.

## 2.2 APPLICATION OF BIOGAS AND ITS PURIFICATION STANDARDS

Biogas can be used in different applications, such as household fuel for cooking, steam and electricity generation for domestic and industrial use, as a substrate in fuel cells, and can be further upgraded to vehicle fuel or for production of chemicals depending on the need for quality standards [Andriani et al., 2014]. It has been estimated that the application of upgraded biogas (> 90% $CH_4$) as vehicle fuel reduces 60-80% greenhouse gas emissions in comparison to gasoline. More than 90% of the biogas produced is used for electricity generation in Europe [IRENA, 2017]. The market for biogas is being deeply encouraged for cooking, heating, power generation and transport sectors and is anticipated to increase to 29.5 GW by 2022 [World Energy Council, 2013]. Thus, biogas has become a deep-rooted technology for producing bioenergy and is considered one of the most environmentally friendly processes for substituting fossil fuels [Jeihanipour et al., 2013]. But the end use of biogas determines its composition and the type of purification process it requires. $CO_2$ is non-combustible and its presence decreases the energy content per unit volume which lowers the

power output from the engine. The presence of $H_2S$ in biogas is both toxic and corrosive, causing substantial harm to the metallic parts of engines, stoves, pipes, and valve fittings, which reduces the lifespan of equipment [Chen et al., 2017]. Thus, an optimized purification process is required in terms of low energy consumption and high removal efficiencies of $CO_2$ and $H_2S$, giving a high methane content in the upgraded biogas [Zhao et al., 2010].

### 2.2.1 BIOGAS AS FUEL FOR BOILERS

Boilers generally have a high tolerance limit for biogas quality and can be used for combustion without upgrading. A large number of boilers equipped with flue gas desulphurization do not even require the removal of $H_2S$ [Sun et al., 2015]. However, most combined heat and power plants (CHP) require $H_2S$ removal below 250 ppm in order to avoid excessive corrosion of boilers and deterioration of lubricating oil [Weiland, 2010]. He also reported that biological desulphurization is often used to remove $H_2S$ from biogas for CHP boilers.

### 2.2.2 BIOGAS AS FUEL FOR COOKING

Biogas produced from decentralized biogas plants with a composition of 45-60% $CH_4$, 40–55% $CO_2$ and a trace amount of other gases like $H_2$, $N_2$ and $H_2S$ is directly used for cooking in rural areas [Mann et al., 2009]. As such, there is no need to upgrade biogas for cooking, but removal of $H_2S$ is especially required in order to reduce health issues, corrosion, and environmental problems [Kadam and Panwar, 2017]. For these types of plants, chemical absorption and adsorption on solid surfaces are the most suitable technologies for the removal of $H_2S$ from raw biogas.

### 2.2.3 BIOGAS AS FUEL FOR INTERNAL COMBUSTION ENGINES FOR PRODUCING ELECTRICITY

The physico-chemical properties of biogas justify its applicability as an alternate fuel for internal combustion (IC) engines. For both spark ignition (SI) and compression ignition (CI) engines, biogas provides a clean fuel. To use biogas effectively in SI engines, a higher compression ratio (CR) engine with magneto ignition and modification of the piston and carburettor is required, while in CI engines it can be employed efficiently in dual fuel mode with diesel as a pilot fuel. The actual calorific value of biogas mainly depends on $CH_4$ percentage, temperature, and absolute pressure and is a vital parameter for the performance of an engine [Chandra et al., 2011]. Internal combustion engines often require more than 30% $CH_4$ in the fuel to attain optimal combustion [Karim and Wierzba, 1992]. Moreover, the efficiency of IC engines can be enhanced by increasing the $CH_4$ concentration in the raw biogas. IC engines for combined heat and power generation perform well when $H_2S$ is maintained below 200 ppm [Sun et al., 2015].

### 2.2.4 BIOGAS AS FUEL FOR VEHICLES AND INJECTION INTO NATURAL GAS GRIDS

The quality of biomethane must be upgraded to a related standard for natural gas in order to be injected into natural gas grids and used in vehicles. However, the minimum acceptable standard range for gas quality varies in Europe and the USA. GASQUAL (gas quality measuring equipment provider company, Sweden) reviewed the present specifications and opted to change the future gas quality for member states of the EU-27 and tried to produce a harmonized European Standard for gas quality [Sun et al., 2015]. The interest in the use of upgraded biogas as vehicle fuel is growing worldwide, especially in Sweden [Persson, 2013]. A relatively higher $CH_4$ concentration is necessary for biogas to be used as vehicle fuel than to be injected into natural gas grids. However, a higher concentration of $H_2$ is allowed in vehicle fuel. Due to the requirement for high $CH_4$ purity, technologies of chemical absorption, pressure swing adsorption, membrane and cryogenic separation would be

appropriate. Methods of impregnated activated carbon and iron hydroxide/oxide are often used for $H_2S$ removal to meet the standards.

### 2.2.5 BIOGAS AS A SUBSTRATE FOR FUEL CELLS

Fuel cells are electrochemical devices that convert chemical energy of a fuel mixture into electricity [Tamta et al., 2020]. Biogas can be used in various types of fuel cells such as Polymer Electrolyte Membrane fuel cell (PEMFC), Phosphoric Acid Fuel cell (PAFC), Molten Carbonate Fuel Cell (MCFC) and Solid Oxide Fuel Cell (SOFC) [Appleby, 1996]. However, the sensitivity and tolerance limit of carbon dioxide and sulphur impurities varies with types of fuel cell. Removal of $CO_2$ is not mandatory, when $CH_4$ concentration in raw biogas is higher than 65%. SOFC is more suitable for biogas feed due to its low sensitivity towards sulphur impurities and also considered as electrically efficient due to reforming of $CH_4$ to $H_2$ within the cell at 750-1000 °C [Thiruselvi et al., 2021]. A few literatures have reported the relation between the $CH_4$ purity and the overall efficiency of fuel cells. Further research is needed for determination of optimal $CH_4$ concentration corresponding to the highest efficiency of fuel cells.

## 2.3 CONVENTIONAL BIOGAS SCRUBBING TECHNOLOGIES FOR $CO_2$ AND $H_2S$

A variety of processes are being used for removing $CO_2$ and $H_2S$ from natural gas and biogas in petrochemical and renewable industries. Several basic mechanisms are involved in achieving the selective separation of gas constituents. These may include physical or chemical absorption; adsorption on a solid surface; pressure swing adsorption; membrane separation; and cryogenic separation [Osorio and Torres, 2009]. Additionally, the $H_2S$ removal process can be classified into two general categories, namely the dry oxidation process and the liquid phase oxidation process [Wise, 1981]. Many factors, such as scrubber dimension, scrubbing agent nature, operating temperature, pressure, pH, mineral content, and

flow rate, all play a significant role and vary depending on the purification process. A brief discussion on different commercially available technologies for biogas upgradation is given below.

### 2.3.1 PRESSURE SWING ADSORPTION

Pressure swing adsorption (PSA) is an established and developed technology for biogas upgradation. The method is based on the specific adsorption behaviour of at least one gaseous component (adsorbate) on a solid surface (adsorbent) under elevated pressure**,** mainly as a result of physical, Van der Walls or electrostatic forces [Grande, 2012]. Materials such as activated carbon, zeolites, and molecular sieves play a crucial role in adsorption. Adsorbent materials are able to capture some gaseous components of a mixture by adsorption affinity and molecular size of the adsorbent. The physico-chemical properties of the gaseous components present in biogas are reported in Table 2.1.

**Table 2.1** Physico-chemical properties of biogas components [Kapoor et al., 2019]

| Gaseous component | σ (Å) | α (Å$^3$) | μ (D) |
|---|---|---|---|
| $CH_4$ | 3.80 | 2.448 | 0.000 |
| $CO_2$ | 3.40 | 2.507 | 0.000 |
| $H_2S$ | 3.60 | 3.630 | 0.970 |
| $N_2$ | 3.64 | 1.710 | 0.000 |
| $H_2O$ | 2.65 | 1.501 | 1.850 |

where, σ is the kinetic diameter (Å: Angstrom), α polarizability (Å$^3$: Angstrom$^3$) and μ dipole moment (D: coulomb-metre), respectively.

The size of $CO_2$ molecules is smaller than the size of $CH_4$ molecules. So, in the case of biogas, molecules of $CO_2$ are easily adsorbed on a selective adsorbent material, which later enriches the $CH_4$ content of biogas. Conventional PSA usually consists of four adsorption columns packed with adsorbents. One cycle typically has four basic steps: pressure build-up,

adsorption, depressurization, and regeneration. After building pressure, $CO_2$ is captured from raw biogas in the adsorbent and consequently leaves the adsorber as off-gas by a stepwise decrease in pressure. Enriched $CH_4$ leaves the column as a biomethane stream. Afterwards, the pressure is increased again with raw biogas or biomethane, and the adsorber is ready for the next sequence of loading. Biogas feeding and column pressurization are usually carried out at 4–10 bars to increase $CO_2$ adsorption inside the pores [Bauer et al., 2013]. $CH_4$ concentration in the raw biogas can be upgraded up to 96–98%, and up to 2-4% of $CH_4$ can be lost in the off-gas stream [Allegue and Hinge, 2012]. But, in an investigation of two PSA plants, 10–12% $CH_4$ losses were observed, though the equipment provider claimed that the losses should be below 2% [Patterson et al., 2011]. In general, more $CH_4$ loss occurs at higher purity [Cavenati et al., 2005]. Also, the vent gas requires proper treatment before being released into the atmosphere due to the high concentration of $CH_4$, for example, being burnt in a flox burner. Since adsorption of $H_2S$ is irreversible and harms the adsorbent material, an initial removal of $H_2S$ is required prior to PSA [Ryckebosch et al., 2011].

### 2.3.2 MEMBRANE SEPARATION

Separation by membrane is a mature, commercialized technology with a market share of 10%. It has emerged as an attractive process for biogas upgradation [Patterson et al., 2011]. The process is established on the principle of selective permeation of different components through a semi-permeable membrane (<1 mm) while others are retained. The carriage of each component is driven by a change in partial pressure over the membrane and is highly dependent on the permeability of the membrane material in the component [Scholz et al., 2013]. It is also determined by other factors, such as changes in temperature, concentration, and electric charges of various gases. Membranes for biogas upgradation are made of materials that are mainly permeable to $CO_2$, $H_2S$, and water, while $CH_4$ passes only to a very low extent [Bauer et al., 2013]. For high methane purity, the difference in permeability

between $CH_4$ and $CO_2$ must be high. Basically, for gas separation, there are three types of membranes used: inorganic, polymeric, and mixed matrix membranes (MMMs) [Basu et al., 2010].

Some of the polymeric and non-polymeric membrane materials for biogas upgrading are mentioned in Table 2.2.

**Table 2.2** Membrane constituents for biogas upgrading [Andriani et al., 2014; Basu et al., 2010]

| **Polymeric materials** | **Non-polymeric materials** |
|---|---|
| Polysulfane, polyethersulfone | Carbon molecular sieves |
| Cellulose acetate, cellulose triacetate | Non-porous carbon |
| Polyphenyleneoxide | Palladium alloys |
| Polycarbonate | Zeolites and non-zeolitic molecular sieves |
| Polyaramide | Mixed conducting perovskites |
| Polyimide, polyetherimide | Ultramicroporous amorphous silica |

The high pressure membrane separation process is usually operated at a pressure of less than 20 bars. Using high-pressure gas separation, the raw biogas can be filtered up to 94% $CH_4$ in one-stage performance, and it can be improved up to 96% $CH_4$ by using two or three-stage performance [Weiland, 2010]. The complicated fabrication process and higher cost of inorganic membranes limit their application at commercial scale. Improvement in the permeability of porous membranes is a challenge in the case of inorganic membranes [Chen et al., 2015]. On the other hand, polymeric membranes have lower fabrication costs and have the advantage of ease of scaling-up. However, under high pressure and high $CO_2$ concentration, the performance of polymeric membrane deteriorates due to phenomena like plasticization, compaction, and ageing [Zhang et al., 2013]. Also, removal of $H_2S$ and water is essential in order to avoid negative effects on the $CO_2$ separation performance.

### 2.3.3 CRYOGENIC SEPARATION

The cryogenic method of purification is based on the principle of separation of different gases by fractional condensations and distillations at low temperatures. As different gases liquefy at different temperatures and pressure domains, it is possible to separate gas components by cooling and compressing the biogas. The process has the advantage that it allows recovery of pure components in the form of a liquid, which can be transported conveniently [Andriani et al., 2014; Goffeng, 2013]. At 1 atm pressure, the boiling point of $CH_4$ is −161.5 °C, which is much lower than the boiling point of $CO_2$ (−78.2 °C), allowing $CO_2$ to be separated from biogas by liquefying $CO_2$ at very low temperatures [Green and Perry, 2008]. Removal of water and $H_2S$ from biogas is necessary in order to avoid freezing and other problems. However, gases like $N_2$ and $O_2$ can be condensed during $CH_4$ separation [Chen et al., 2015]. Cryogenic separation is carried out by first drying, followed by multistage compression of raw biogas with intermediate cooling. The pressurised biogas is cooled to −55 °C in stages to achieve $CO_2$ liquefaction before being expanded to 8–10 bars in a flash tank at −110 °C to facilitate biomethane purification via $CO_2$ solidification. Typically, the entire process is carried out at a very low temperature of −100 °C at a high pressure of 40 bars [Kadam and Panwar, 2017; Ryckebosch et al., 2011]. This method can upgrade raw biogas up to 97% with a $CH_4$ loss of less than 2%. However, the process requires a large number of equipment facilities and thus consumes high investment and a large amount of energy, which increases the final cost of biomethane production [Deublein and Steinhauser, 2010]. The operating cost and practical problems of clogging and freezing due to high concentrations of solid $CO_2$ or the presence of residual impurities limit the wider implementation of this technique [Biernat et al., 2011; Hagen and Polman, 2001]. The Los Angeles County Sanitation District and the Cryenco Engineering Company of Denver, Colorado attempted to apply the cryogenic process for the removal of $CO_2$ from digester gas but could not make it successful. Rather

complicated flow schemes got involved**,** and thermal efficiency became low. Capital costs and utility requirements were also very high in this process [Wise, 1981].

### 2.3.4 PHYSICAL ABSORPTION METHOD USING WATER AND ORGANIC SOLVENTS

Physical absorption employing water as a solvent for dissolving $CO_2$ and $H_2S$ is considered a simple method for biogas purification. This method is eco-friendly as well as economical in terms of the requirement for space and equipment. For biogas scrubbing, the physical absorption method is suitable even at a low flow rate of biogas from the reactor [Singhal et al., 2017]. In this case, the absorbed gas components are physically bound to the scrubbing agent. The absorption in water is employed because $CO_2$ and $H_2S$ have higher solubility in water than $CH_4$ and will therefore be dissolved to a greater extent, particularly at lower temperatures and higher pressures [Sun et al., 2015]. This method can tolerate $H_2S$ concentrations of around 300–2500 ppm, but higher $H_2S$ concentrations are detrimental to the scrubbing system as they lower the pH of the scrubbing liquid [Muñoz et al., 2015]. In this process, the raw biogas is compressed and fed into a packed bed column from the bottom; pressurized water is sprayed from the top, which flows downward. The process is thus a counter-current one. Purified biogas (biomethane) leaves the column at the top and dissolves $CO_2$ as well as $H_2S$ in water, which are collected at the bottom of the tower. In order to maintain the absorption performance, the scrubbing liquid has to be replaced by fresh liquid or regenerated in a separate step (desorption or regeneration step). The regenerated water is then pumped back to the absorber as fresh scrubbing liquid. In the case of a water recirculation system, $CO_2$ is released into the atmosphere as an off-gas, or stays in the water in the case of a single-pass system [Persson, 2003]. Any $CH_4$ dissolved in water is captured and recycled in the absorption column in order to alleviate methane losses.

Bhattacharya and Khai (1987) designed a water scrubbing system that provided 100% pure methane, but the actual percentage of methane in the upgraded biogas was dependent on some factors like the dimensions of the scrubbing tower, gas pressure, and composition of raw biogas, water flow rates, and purity of water used.

Dubey (2000) performed a similar experiment on three water scrubbers whose diameters were 150 mm (height: 15 m), 100 mm (height: 10 m) and 75 mm (height: 10 m) to absorb $CO_2$ (37-41%) present in the biogas and found that the $CO_2$ absorption depends upon the flow rates of gas and water rather than the different diameters of scrubbers.

Shyam, in 2002, designed a scrubbing tower of a height of 6 m, which is packed to a height of 2.5 m with spherical plastic balls of diameter 25 mm. Raw biogas compressed at a pressure of 5.88 bars was passed at a flow rate of 2 $m^3/h$ while water was circulating through the tower. The scrubbing tower could remove $CO_2$ content of up to 87.6% of the raw biogas. Table 2.3 presents some similar research done on $CO_2$ removal from biogas using water scrubbing systems by varying physical parameters such as scrubber dimension, gas pressure, and gas flow rates.

**Table 2.3** Literature on $CO_2$ removal from biogas using physical absorption process

| Authors | Purification process/ Solvent | Scrubber dimension | Gas pressure | Gas flow rate | Water flow rate | $CH_4$ enrichment | $CO_2$ removal |
|---|---|---|---|---|---|---|---|
| Viyaj et al., 2006 | Physical absorption (Water) | Diameter = 150 mm; Height = 3500 mm | 1.0 MPa | 1.5 $m^3$/h | 1.8 $m^3$/h | - | 99% |
| Ofori-Boateng and Kwofie, 2009 | Physical absorption (Water) | Diameter = 300 mm; Height = 9800 mm | 1.0 MPa | - | - | - | 93% |
| Xiao et al., 2014 | Physical absorption (Water) | Diameter = 50 mm; Height = 0.9 m | 0.8–1.2 MPa | 400–700 L/h | 100-200 L/h | | 34.6 - 94.2% |
| Singh and Dwivedi, 2019 | Physical absorption (Water) | Diameter = 0.5 m; Height = 5 m | 7.4 bar | 3.9 water to gas ratio | | 95.1% | - |

However, the physical absorption technique has the drawback of dissolving oxygen and nitrogen with the upgraded biogas during regeneration. This technology also uses organic solvent solutions (e.g., polyethylene glycol) instead of water as a scrubbing agent. The solubility of $CO_2$ in these solvents is higher than in water [Patterson et al., 2011]. As a result, less scrubbing liquid circulation is required for higher $CO_2$ absorption, and thereby smaller apparatus is needed for the same raw biogas upgradation. Some of the commercially available organic physical scrubbing agents used for biogas upgrading technologies are Genosorb®, Selexol® and Rektisol® [Allegue and Hinge, 2012]. However, the regeneration of solvent is processed at a higher temperature, which makes the process highly energy intensive [Niesner et al., 2013]. Also, before the process of absorption, separation of $H_2S$ is necessary as it is difficult to regenerate $H_2S$ from the solvent, which thereby significantly reduces the capacity for $CO_2$ absorption.

### 2.3.5 CHEMICAL ABSORPTION METHOD

The mechanism of chemical absorption is quite similar to that of a water scrubbing process where a chemical reaction takes place between scrubbing agent components and absorbed gas components within the liquid phase. But the conformation of chemical absorption is much simpler with improved performance because of higher $CO_2$ solubility at low pressure in highly reactive chemical absorbents [Andriani et al., 2014]. The separation principle of absorption is based on the different solubility of various gas constituents in a liquid scrubbing solution. As the process includes the development of reversible chemical bonds between the solute and the solvent, regeneration of the solvent involves the breaking of these bonds and requires a very high energy input [Petersson and Wellinger, 2009; Savery and Cruzon, 1972]. The most commonly used chemical solvents are diethanolamine (DEA), monoethanolamine (MEA), diglycolamine (DGA), triethanolamine (TEA), and methyldiethanolamine (MDEA), which can dissolve

significantly more $CO_2$ per unit volume of biogas than water. The general reactions involved in the absorption of $CO_2$ by amines are shown below [Kadam and Panwar, 2017].

$$RR'NH + CO_2 \rightarrow RR'NH^+COO^- \quad (2.1)$$

$$RR'NH^+COO^- + RR'NH \rightarrow RR'NCOO^- + RR'NH_2^+ \quad (2.2)$$

The overall reaction is

$$2RR'NH + CO_2 \rightarrow RR'NCOO^- + RR'NH_2^+ \quad (2.3)$$

$$RR'NCOO^- + H_2O \rightarrow RR'NH + HCO_3^- \quad (2.4)$$

Usually, amine scrubbing plants are operated at a slightly higher pressure, which is already available in the raw biogas, and no extra compression of the gas is required. The high selectivity and absorptivity of the amine solution have an advantage during absorption but turn out to be a hindrance during regeneration of the scrubbing solution. Due to its high absorption capacity for $CO_2$, MEA is the cheapest amine and it is the most commonly used as a scrubbing agent. Amine scrubbing agents can also absorb $H_2S$ from the raw biogas, but a higher temperature is needed during regeneration of the solution. Hence, it is advisable to remove this component prior to the amine scrubber. Sodium hydroxide (NaOH), potassium hydroxide (KOH), and calcium hydroxide $Ca(OH)_2$ are the most common inorganic solvents used in this process [Malla et al., 2016; Zhao et al., 2010]. The reactions occurring during $CO_2$ absorption into aqueous solutions of hydroxides can be expressed by the following equations [Gondal et al., 2015]:

$$CO_2\ (g) \leftrightarrow CO_2\ (l) \quad (2.5)$$

$$CO_2\ (l) + OH^- \leftrightarrow HCO_3^- \quad (2.6)$$

$$HCO_3^- \leftrightarrow CO_3^{2-} + H^+ \quad (2.7)$$

The solubility of $CO_2$ in NaOH is higher in comparison to amines [Abdeen et al., 2016]. Theoretically, to absorb 1 ton of $CO_2$, 1.39 tons of MEA will be required. When compared with NaOH, only 0.9 tons are required [Angelidaki et al., 2018]. Alkali hydroxides are more efficient, cost-effective, and easily available on the market as compared to amines. But regeneration of these hydroxides is complex and challenging because of the formation of thermally stable products such as $Na_2CO_3$, $K_2CO_3$ and $CaCO_3$ salts. A schematic diagram of physical and chemical absorption for the purification of biogas is shown in Fig. 2.1.

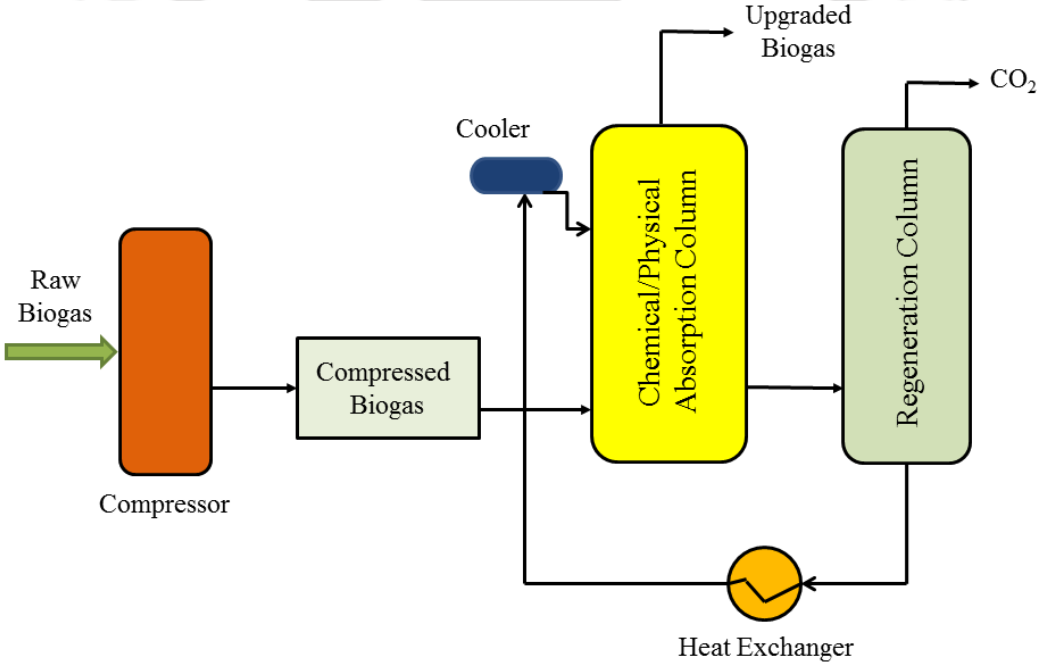


**Fig. 2.1** Schematic of physical/chemical scrubbing technology for biogas upgrading [Andriani et al., 2014; Ryckebosch et al., 2011]

Biswas (1977) developed a method of $CO_2$ scrubbing by passing biogas through a 10% aqueous solution of MEA in a column of 15 cm and a diameter of 5 cm, respectively, with an orifice. The

gas flow rate was 100 ml/min. The initial pressure of the gas was 10 cm of water column and the drop in pressure head was 5 cm of water column. With this method, the $CO_2$ content of biogas was reduced by 0.5-1%.

Yeh and Pennline (2001) studied a chemical absorption and desorption process in a packed column for the removal of $CO_2$. They also used MEA as a scrubbing agent in a conventional and structured packed column. Various areas were investigated, such as the gas-liquid contacting area, the type of reactant, and the dilution of the aqueous fraction with organic liquids. Significant improvements in $CO_2$ removal above 90% were obtained with structured packing.

Tippayawong and Thanompongchart (2010) investigated a method for $CH_4$ enrichment in a packed column using aqueous solutions of NaOH, $Ca(OH)_2$, and MEA for the chemical absorption of $CO_2$ and $H_2S$. Test results revealed that the aqueous solutions used were effective in reacting with $CO_2$ in biogas with over 90% removal efficiency, making $CH_4$ enriched fuel. The $CH_4$ enrichment is strongly dependent on the pH of the solutions and varies on $CO_2$ absorption with time. Saturation was reached in about 50 minutes for $Ca(OH)_2$, and in about 100 minutes for NaOH and MEA.

Farooq et al. (2012) investigated a biogas upgrading method in a pilot scale biogas plant using different absorbent solutions such as NaOH, $Ca(OH)_2$, and KOH. The results showed an increase in $CH_4$ (3-4%) and a decrease in $CO_2$ (4-5%) and $H_2S$ (40-45 ppm) after the chemical absorption method.

Xiao and Li (2014) investigated the removal of $CO_2$ from biogas using MEA solution as an absorbent. They studied the important parameters influencing $CO_2$ removal. The optimized $CO_2$ removal efficiency could be achieved at the MEA solution flow of 20 L $h^{-1}$ and the gas flow of

350 L $h^{-1}$ when the volume of $CO_2$ was 45%. The purity of biogas of the resulting gas could be as high as 97-100%. Moreover, the $CO_2$ removal efficiency was reduced with the increasing $CO_2$ content of the input gas. The pressure in the absorption tower varies from 0.05 MPa to 0.1 MPa and has no significant influence on $CO_2$ removal.

Osorio et al. (2014) analyzed the extraction of $CO_2$ from biogas by using three chemical absorption towers with MEA of 20% as the scrubbing agent. They tested the viability of a low-pressure process (1.250 bar) for treating biogas with a high $CO_2$ content (approximately 40%). The results obtained indicated the optimal amine quantity and scrubbing tower volume, as well as the temperature necessary to make the desorption process for amine regeneration most effectively. When this process was optimized, the outflowing biogas had a mean $CH_4$ concentration of more than 80% and a $CO_2$ concentration of 0.1%.

Tahir et al. (2015) investigated the biogas production and $CH_4$ enrichment for anaerobic digestion (AD) of fruit and vegetable waste (FVW). They pebbled raw biogas through water, NaOH, $Ca(OH)_2$, and TEA for biogas purification and $CH_4$ enrichment. The optimum pH range under mesophilic and thermophilic temperature conditions was found to be between 8.3 - 8.8. The addition of NaOH, $Ca(OH)_2$, and TEA to the mixture increased $CH_4$ enrichment by 5%, 9%, and 7%, respectively. The use of $Ca(OH)_2$ produced biogas with a 71% $CH_4$ content, a 28% reduction in $CO_2$, and a $H_2S$ content of 150 ppm.

Mel et al. (2016) studied an absorption method to purify both $CO_2$ and $H_2S$ gases by using 4%, 9%, and 14% w/v of NaOH in a column. The concentrations of NaOH were varied, as was the biogas flow rate. The highest $CO_2$ removal efficiency has been achieved at a 14% concentration of NaOH solution, where the $CH_4$ increment is about 54.9% of its original value.

Leonzio (2016) analyzed and compared the removal of $CO_2$ from biogas using a chemical absorption process with an aqueous solution of MEA, NaOH, and KOH through ChemCad 6.3® simulations. The results indicated that the solubility of $CO_2$ decreases with an increase in temperature, as shown in Fig. 2.2. This shows temperature plays a significant role in altering the effects of other process parameters.

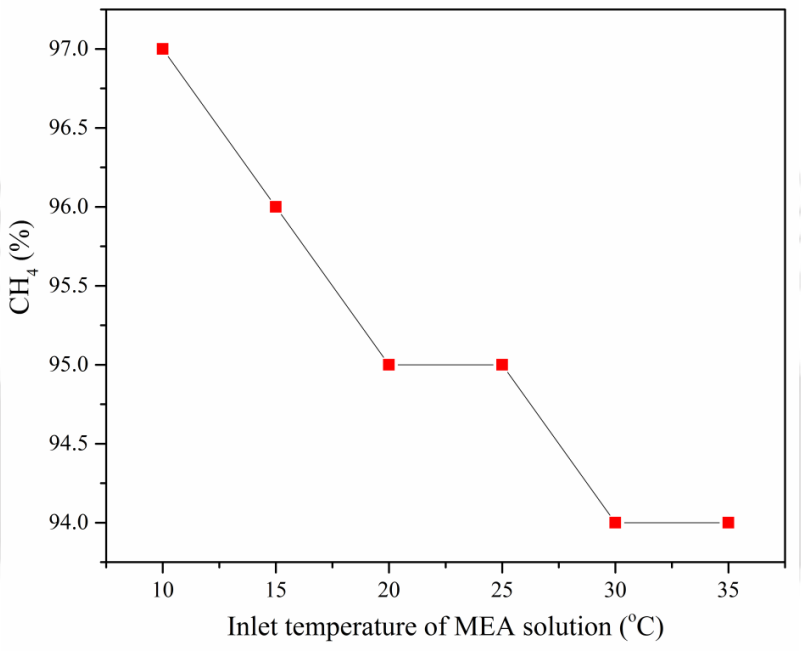


**Fig. 2.2** Outlet methane concentrations versus the inlet temperature [Leonzio, 2016]

He et al. (2018) investigated $CO_2$ capture from biogas using four novel renewable absorbents derived from biogas slurry by membrane contactors. Recovered aqueous ammonia (RAA) by vacuum membrane distillation showed the best performance for $CO_2$ absorption among the four types of renewable absorbents. Higher $CH_4$ content was achieved when the absorbent flow rate was increased from 10 to 50 ml/min, suggesting better performance in biogas upgrading. The highest 90% $CH_4$ content in the retentate was found when the biogas and solvent flow rates were 200 mL/min and 50 mL/min and then the $CO_2$ absorption decreased with an increase in biogas

flow rate as shown in Fig. 2.3. This shows that biogas and absorbent flow rates have substantial effects on biogas upgradation.

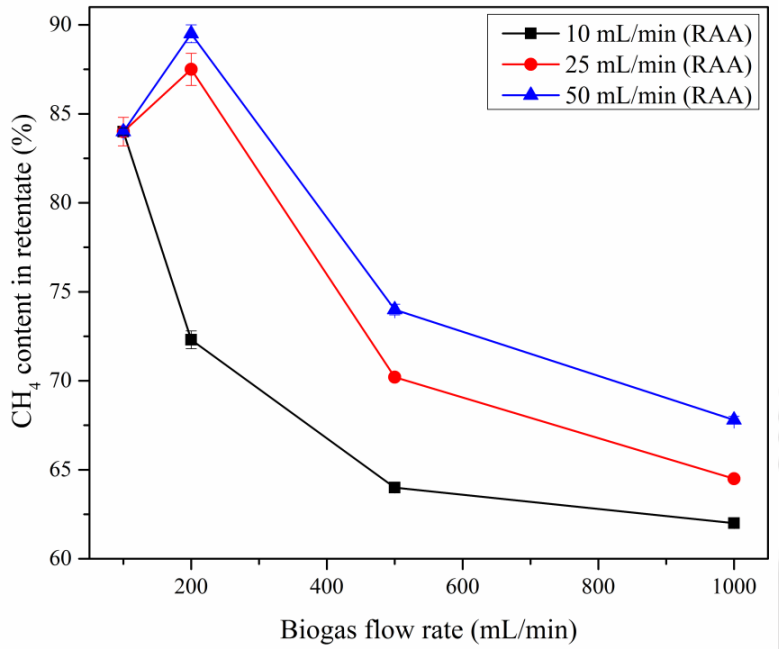


**Fig. 2.3** Biogas upgrading performance at various gas and liquid flow rates, Absorbent: 0.3 mol/L RAA, T=35 °C, $CO_2$ content = 40% [He et al., 2018]

Lee et al. (2020) studied the simultaneous absorption of $CO_2$ and $H_2S$ using 12 different N-methyldiethanolamine (MDEA) blended additives. A mixture gas of $CH_4$ (35%), $CO_2$ (15%), and $H_2S$ (50 ppm) balanced by $N_2$ was used for absorption and regeneration, and the temperatures were kept at 35 and 80 °C, respectively. $CO_2$ absorption capacity of the mixed gas was excellent in MDEA/diethylenetriamine (DETA), among the absorbents, but the $CO_2$ circulation capacity was the highest in the MDEA/bis(3-aminopropyl)amine (APA). The $H_2S$ absorption capacity was excellent in MDEA/APA, but the cyclic capacity was highest in MDEA/DETA. Thus, $CO_2$ absorption and regeneration rates were fastest in MDEA/piperazine (PZ), and the $H_2S$ absorption and regeneration rates were highest in MDEA/2-amino-2-methyl-1-propanol (AMP). From the

results, it was confirmed that MDEA/APA was superior for gas composition in the simultaneous absorption and regeneration of $CO_2$ and $H_2S$ and could be reused as an absorbent for continuous experiments.

### 2.3.6 PHYSICAL/CHEMICAL ADSORPTION ON SOLID SURFACE

Chemical adsorption on a solid surface is based on the different adsorption behaviour of various gas components on a solid surface under pressure and physico-chemical reactions. The adsorption process involves the transfer of solutes in the gas stream to the surface of a solid material, where they concentrate mainly as a result of physical or Vander wall forces. With an appropriate choice of adsorbent, the process is able to eliminate $CO_2$, $H_2S$, moisture, and other impurities either simultaneously or selectively from biogas [Tagliabue et al., 2009]. Solid adsorbents with a high surface area per unit volume are typically commercially available. Gas purification can also be performed using some form of activated carbon, alumina, silica, or silicates, which are also known as molecular sieves [Wise, 1981]. The efficiency of the adsorption process depends mainly on temperature, the pore size of the adsorbent and the partial pressure of the adsorbate. Adsorbents with a molecular sieve with a regular pore size of 3.7 are typically used to capture $CO_2$ (molecular size of 3.4 Å) while rejecting $CH_4$ molecules (molecular size of 3.8 Å) [Kapoor et al., 2019].

Belmabkhout et al. (2009) performed an experiment where they showed that triamine-grafted pore-expanded mesoporous silica (TRI-PE-MCM-41) exhibited a high adsorption capacity for $CO_2$ as well as high selectivity toward acid gases versus $CH_4$. Unlike physical adsorbents such as zeolites and activated carbons, the presence of moisture in the feed materials enhanced the $CO_2$ removal capability of TRI-PE-MCM-41. Thus, depending on the feed composition, $CO_2$ and

other acid gases may be removed over TRI-PE-MCM-41 simultaneously or sequentially. These findings are suitable for acid gas separation from $CH_4$ containing mixtures such as natural gas and biogas.

Mwandila et al. (2016) tested a laboratory experiment for the adsorption of $CO_2$ from raw biogas where they used a novel adsorbent made out of clay and burnt maize cob particles for the development of a low-cost biogas treatment technology. A novel adsorbent was impregnated with a hot natural alkaline solution of pH 10-10.5, degassed, and then activated at a temperature of 250 °C, thereby making it low cost. They studied the effect of pressure drops on $CO_2$ removal, the breakthrough curve, and the absorption isotherm. The maximum percentage of $CO_2$ removal was 87.8% at 102 Pa/m pressure drop and temperatures ranging from 20 to 28 °C.

Mamun et al. (2016) studied the biogas generated from vegetable, fruit, and cafeteria wastes for a duration of 30 days, with the average concentration for $CH_4$ and $CO_2$ being 62 and 34%, respectively. They treated the raw biogas with purifying agents such as solid CaO, CaO solution, and activated carbon. The highest percentage of $CH_4$ achieved by treating with solid CaO, CaO solution, and activated carbon was 89, 90, and 91%, respectively.

Sethupathi et al. (2017) investigated the adsorption of $CH_4$, $CO_2$, and $H_2S$ on biochars derived from perilla, Japanese and Korean oaks, and soybean stover in a fixed-bed adsorber. The obtained results demonstrated that $CO_2$ and $H_2S$ were successfully captured by the respective biochars and were associated with both surface adsorption and chemical reactions. The highest removal and breakthrough capacities of $CO_2$ and $H_2S$ were reported by perilla biochar, followed by soybean stover biochar, Korean oak and Japanese oak biochars, respectively. The results suggested that $H_2S$ adsorption was preferred over $CO_2$, due to the physical and chemical

properties of the biochars. Biochars can be a promising material for the purification of biogas as they are low-cost materials, sustainable, and can be prepared from renewable and waste biomass materials.

Pertiwiningrum et al. (2018) evaluated $CO_2$ adsorption from biogas mixtures using three different combinations of adsorbents, such as natural zeolite-natural zeolite (Z-Z), natural zeolite-chicken manure based biochar (Z-CM) and natural zeolite-biogas sludge based biochar (Z-BS). The experiment was carried out at room temperature and at a gas pressure of 5-7 bar. Raw and adsorbed biogas samples were analyzed using gas chromatography (GC) to determine the percentage of $CH_4$. Experimental results showed that the highest $CH_4$ enrichment was performed by Z-CM (28.92%), followed by Z-BS (5.12%).

A number of commercially available as well as conventional technologies for biogas upgradation have been studied meticulously. Table 2.4 summarizes the advantages and disadvantages of each biogas upgradation technique. Also, a comparative study on the discussed biogas upgradation technologies in terms of efficiency under varying experimental conditions is presented in Table 2.5.

**Table 2.4** A summary of the advantages and disadvantages of biogas upgradation processes

| **Upgradation Technologies** | **Advantages** | **Disadvantages** | **References** |
|---|---|---|---|
| Pressure swing adsorption | Established and developed technology, high $CH_4$ purity, good moisture removal capacities | High capital cost, high pressure is required, $CH_4$ losses when malfunctioning of valves, pre-treatment of $H_2S$ is required | Bauer et al., 2013; Allegue and Hinge, 2012; Cavenati et al., 2005; Ryckebosch et al., 2011 |
| Membrane separation | Fast installation and startup, high purity $CH_4$, production output is flexible | High cost membrane, consumes more energy | Weiland, 2010; Chen et al., 2015; Zhang et al., 2013 |
| Cryogenic separation | High purity $CH_4$, produce $CO_2$ in marketable form, such as dry ice, liquid $CH_4$ decreases gas volume, thus can be easily transported | Consumes relatively more electricity per unit of gas production, uses lots of process equipment | Andriani et al., 2014; Deublein and Steinhauser, 2010; Biernat et al., 2011 |
| Physical absorption | Simple process, can remove both $H_2S$ and $CO_2$ simultaneously, eco-friendly solvents, low cost to operate and maintain | Requires high pressure, need a larger column compare to chemical absorption | Singhal et al., 2017; Sun et al., 2015; Persson, 2003 |
| Chemical absorption | High purity $CH_4$, more efficient in low pressure, column volume is smaller than water scrubbing | Chemicals are corrosive in nature and expensive, higher energy require to regenerate the solvent | Andriani et al., 2014; Petersson and Wellinger, 2009; Zhao et al., 2010 |
| Physical/Chemical adsorption on solid surface | Simple scrubber design, economy in production with comparatively high purity, good moisture removal capacities | Chemicals are corrosive in nature and expensive, requires high energy during regeneration | Tagliabue et al., 2009; Ryckebosch et al., 2011; Zhao et al., 2010 |

**Table 2.5** Comparison of different $CO_2$ upgradation technologies

| Technologies | Gas pre-cleaning requirement | Temperature (°C) | Working pressure (bar) | Solvent/adsorbents/ membranes | Purity of $CH_4$ (%) in upgraded gas | References |
|---|---|---|---|---|---|---|
| Pressure swing adsorption | Required and recommended | 15–30 | 4–10 | Zeolites, activated carbon, molecular sieve | 96–98 | Allegue and Hinge, 2012; Bauer et al., 2013 |
| Membrane separation | Required and recommended | 25–60 | 8-10, usually < 20 | Cellulose acetate, carbon molecular sieves, polyimide, | 94–96 | Weiland, 2010; Andriani et al., 2014 |
| Cryogenic separation | Highly recommended | − 55 to – 100 | 8-40 | Glycol refrigerant | 97-99 | Kadam and Panwar, 2017; Biernat et al., 2011; Andriani et al., 2014 |
| Physical absorption | Not required | 20–30 | 4–10 | Water, organic solvents | 90–98 | Muñoz et al. 2015; Singh and Dwivedi, 2019; Sun et al., 2015 |
| Chemical absorption | Required and recommended | 25–35 | 1-5 | Amines (MEA, DMEA), alkali solutions such as NaOH, $Ca(OH)_2$ | 80-98 | Ryckebosch et al., 2011; Tippayawong and Thanompongchart, 2010; Osorio et al., 2014; Zhao et al., 2010 |
| Physical/ Chemical adsorption on solid surface | Required and recommended | 20–35 | 1–5 | Activated carbon, CaO, biochar, | 80–98 | Mamun et al., 2016; Sethupathi et al., 2017; Kapoor et al., 2019 |

### 2.3.7 DRY OXIDATION PROCESS FOR $H_2S$ REMOVAL

It can be used for the removal of $H_2S$ from gas streams by converting it either into sulfur or oxides of sulfur. This process is used where the sulfur content of gas is relatively low and high purity is required. Some of these methods are described below.

#### 2.3.7.1 INTRODUCTION OF AIR/OXYGEN INTO THE BIOGAS SYSTEM

A small amount of oxygen (2–6%) is introduced into the biogas system by using an air pump. As a result, sulfide in the biogas is oxidized into sulfur and $H_2S$ concentration is lowered.

$$2H_2S + O_2 \longrightarrow 2S + 2H_2O \qquad (2.8)$$

This is a simple and low-cost process. No special chemicals or equipment are required [Petersson and Wellinger, 2009]. Depending on temperature, reaction time, and the place where air is added, the $H_2S$ concentration can be reduced by 95% to less than 50 ppm. However, care should be taken to avoid overdosing of air, as biogas in air is explosive in the range of 6–12% depending on the methane content [Wellinger and Lindberg, 1999].

#### 2.3.7.2 ADSORPTION USING SOLID SURFACE

$H_2S$ reacts with iron hydro-oxides or oxides to form iron sulfide. Biogas is passed through iron oxide pellets to remove $H_2S$. When the pellets are completely covered with sulfur, they are removed from the tube for regeneration of sulfur. It is a simple method, but during regeneration a lot of heat is released. Also, dust packing contains a toxic component, and the method is sensitive to the high water content of biogas. Wood chips covered with iron oxide have a somewhat larger surface-to-volume ratio than plain steel. Roughly 20 g of $H_2S$ can be bound per 100 g of iron oxide chips. Application of wood chips is very popular, particularly in the USA. It

is a low-cost product; however, particular care has to be taken that the temperature does not rise too high while regenerating the iron filter [Wellinger and Lindeberg, 1999]. $H_2S$ can be adsorbed on activated carbon. The sulfur containing carbon can then be either replaced with fresh activated carbon or regenerated. It is a catalytic reaction, and carbon acts as a catalyst [Hagen and Polman, 2001]. Biochar is a fine-grained, porous, and carbon-rich adsorbent produced by the pyrolysis of biomass in oxygen-limited environments [Van-Zwieten et al., 2010]. Biochar derived from plant residues or agricultural wastes has been reported to be effective for sorbing pollutants and controlling contaminants in the environment [Inyang et al., 2012]. The carbon matrix structure of biochar with high surface area, porosity, mineral contents, high removal capacity, and low cost per unit volume of adsorber suggests that it can be used as an $H_2S$ adsorbent. Biochar has an added advantage as, after saturation with sulphurous compounds, it can be directly used as a soil amendment to improve retention of nutrients, soil fertility, and crop production [Akio et al., 2012; Creamer et al., 2014]. Also, biochar-based adsorbents are comparatively much cheaper than commercial-grade activated carbon.

Seredych et al. (2008) prepared adsorbents from sewage sludge and fly ashes by pyrolysis at 950 °C and used them for the removal of $H_2S$ from simulated dry digester gas mixtures or moist air. It was found that fly ash addition decreases the capacity of desulfurization in comparison with sewage sludge adsorbents; the degree of this decrease depends on the type of ash, its mineral content, and the composition of challenging gas. Also, the presence of $CO_2$ disables some adsorption sites to some extent depending on the sample composition; the addition of ashes makes the process more detrimental when the adsorbents remove hydrogen sulfide from air than from digester gas.

Hao et al. (2016) developed a photocatalytic reactor filled with zeolite/$TiO_2$ with the objective of selective $H_2S$ removal from synthetic gas as well as in-situ removal from raw biogas and its improvement of methane production. The $H_2S$ removal rate reached up to 98.1%, and no $SO_2$ was detected. Furthermore, $H_2S$ in-situ removal enhanced biogas production by 4.5% and bio-methane production by 16.1%, compared to the blank control.

Fernández-Delgado Juárez et al. (2018) investigated a study to purify biogas from small-scale biogas plants by removing $CO_2$ and $H_2S$ with regionally available biomass ash at an average input gas pressure of approximately 10 mbar. For the initial few hours, $CO_2$ was trapped, resulting in pure methane, but due to high filter rates, it is not economically feasible. However, the $H_2S$ removal was much longer-lasting up to 34 days, and it was found that the cumulative $H_2S$ uptake by the biomass ash ranged from 0.56 to 1.25 kg $H_2S$ per ton of ash. Therefore, in small and medium biogas plants, wood ash can be used as a scrubbing agent for the removal of $H_2S$ from biogas.

Sahota et al. (2018) investigated biochars for $H_2S$ removal from biogas prepared from leaf waste at different temperatures. Obtained results show that biochar prepared from leaf waste at 400 °C removes $H_2S$ from 1254 ppm to 201 ppm (84.2%) for 25 minutes in a continuous adsorption tower. It was attributed to the higher pH of the biochar, which increased the dissociation rate of $H_2S$ and conversion of elemental sulphur. Several factors, such as pH, carbonization temperature, surface area, and mineral elements present on the surface of biochar, played a significant role in $H_2S$ adsorption from the biogas.

Pelaez-Samaniego et al. (2018) studied the effect of thermochemical processing conditions of biochars derived from anaerobically digested fibrous solids (AD fiber) on their ability to adsorb

$H_2S$ from biogas. It was found that AD fiber pyrolyzed at temperatures of 600 °C for 60 min can be an effective material for $H_2S$ removal from biogas. An additional method consisting of impregnation with $Na_2CO_3$ prior to the $H_2S$ scrubbing process resulted in further $H_2S$ adsorption potential. The results also suggested that after the $H_2S$ sorption process, a portion of the S in the biochar exists as free or adsorbed S.

Surra et al. (2019) studied the assessment of activated carbons (ACs) on $H_2S$ removal prepared by physical activation and chemical activation of Maize Cob Waste (MCW) and named them MCW(PA)2h, MCW(PA)3h, MCW(LD) and CAR-MCW(LD). All of the ACs were characterised in order to study their textural and chemical properties before being used as adsorbents for $H_2S$ removal from real biogas samples. The ACs that were physically activated performed much better than the impregnated ones. The results showed that the $H_2S$ uptake capacities of MCW(PA)3h and MCW(PA)2h were 15.5 and 0.65 mg $g^{-1}$, while MCW(LD) and CAR-MCW(LD) showed values of 0.47 and 0.25 mg $g^{-1}$, respectively. Also, the oxygen content in MCW(PA)3h was found to be higher, which favoured the catalytic oxidation reaction of $H_2S$, enhancing its removal.

Choudhury and Lansing (2021) studied the removal of $H_2S$ from synthetic biogas using unmodified and (Fe)-impregnated biochar in a scrubbing column. Two biochar substrates, corn stover (CSB) and maple wood biochar (MB) with and without iron-impregnation, were synthesized for the comparison of $H_2S$ adsorption. Unmodified CSB and MB showed the highest $H_2S$ adsorption capacities of 3.3 and 6.1 mg $H_2S$ $g^{-1}$ biochar, whereas the Fe-impregnated CSB and MB showed 8.2 and 23.9 mg $H_2S$ $g^{-1}$ biochar.

### 2.3.8 LIQUID PHASE OXIDATION PROCESS FOR $H_2S$ REMOVAL

This process is primarily used for the treatment of gases containing a relatively low concentration of $H_2S$. It may be either: (a) physical absorption process or (b) chemical absorption process. In the physical absorption process, the $H_2S$ can be absorbed by the solvents, particularly at lower temperatures and higher pressures [Sun et al., 2015]. One of the solvents is water. But the consumption of water is too high for the absorption of a small amount of $H_2S$. This method has a tolerance limit of $H_2S$ concentrations of around 300–2500 ppm as a high concentration of $H_2S$ lowers the pH of the scrubbing liquid [Muñoz et al., 2015]. If some chemicals like NaOH are added to water, the absorption process is enhanced. It forms sodium sulfide or sodium hydrosulfide, which is not regenerated and poses problems with disposal.

Chemical absorption of $H_2S$ can take place with iron salt solutions like iron chloride. This method is extremely effective in reducing high $H_2S$ levels. The process is based on the formation of insoluble precipitates. $FeCl_3$ can be added directly to the digester slurry. In small anaerobic digester systems, this process is most suitable. All other methods of $H_2S$ removal are suitable and economically viable for large-scale digesters. By this method, the final removal of $H_2S$ is about 10 ppm.

Horikawa et al. (2004) studied the removal of hydrogen sulphide ($H_2S$) from biogas by using a chemical absorption method in an iron-chelated solution catalyzed by Fe/EDTA. When compared with physical absorption using pure water, it was found that the catalytic solution could remove a higher percentage of $H_2S$ under similar experimental conditions. Total removal of $H_2S$ depends on certain factors such as adequate gas-to-liquid ratio, flow rates, low gas

pressure, and ambient temperature. The advantage of this process is that it addresses $H_2S$ pollution by converting $H_2S$ into elemental sulphur (S).

Osorio and Torres (2009) investigated the purification of biogas coming from the anaerobic digestion of sludges in a wastewater treatment plant, in order to be used later as biofuel for vehicles. They focused on optimization of biogas desulphurization in a chemical way using NaOH. They also showed that the system worked best when the pH range in the basic tower was 10.5–11. Besides the scrubbing towers, the pilot plant used included filters of activated carbon at the end of the line. The $H_2S$ inflow concentrations were quite high, up to 3500 ppm. The effluent biogas from the scrubbing towers presented an $H_2S$ concentration of less than 1 ppm and zero or undetectable values were obtained for up to 58 analyzed trace elements.

Lin et al. (2013) established a pilot-scale chemical-biological process to remove $H_2S$ from biogas. Livestock biogas purification was conducted at various $H_2S$ loading rates for a consecutive 356 days. With an average inlet $H_2S$ concentration of 3542 ppm, 90–95% $H_2S$ removal efficiency was achieved under a gas retention time of 288 to 144 s where the biogas flow rate was kept between 50 and 100 LPM. Additionally, with an average of 59% $CH_4$, 28.3 kW h of power was generated by using a 30 kW biogas generator under a biogas flow rate of 300 LPM.

Nie et al. (2013) studied the feasibility of biogas upgrading with propylene carbonate as the absorbent. They also compared the absorption of propylene carbonate with that of water. They found that the capacity of biogas treated by propylene carbonate was 4−5 times higher than that of water. The propylene carbonate absorption showed better tolerance to the existence of $H_2S$. When the concentration of $H_2S$ in the feed gas increased to 4000 ppm, the $CH_4$ content in the

product gas decreased by 5.09% with water as the absorbent, while it decreased only 1.68% in the propylene carbonate absorption test. The results showed that the propylene carbonate absorption had high efficiency and an obvious advantage of energy conservation when applied for biogas upgrading.

Tilahun et al. (2018) conducted a study on $H_2S$ removal from biogas using a novel hybrid polydimethylsiloxane (PDMS) membrane bioscrubber. Parameters such as pH, DO concentration, and biogas flow rate on $H_2S$ removal efficiency and sulfide oxidation were investigated. Results obtained from experiments showed that almost complete $H_2S$ removal (> 97%) and half of the $CO_2$ were successfully removed when volumetric loading rate and DO concentration were kept below 148 g $H_2S/m^3d$ and 1 mg/l, respectively.

Ou et al. (2020) developed a simple bubbling scrubber fed with aerating wastewater for the removal of $H_2S$ in biogas. The volume of the scrubber was 2,000 L, in which aerated liquid was filled to a depth of 0.8–1 m. The operation conditions were as follows: influent liquid of pH 7.5–7.7, a flow rate of 23–25 L $min^{-1}$, influent biogas flow rates of 0.050–0.200 $m^3$ $min^{-1}$, and an inlet $H_2S$ concentration of 907 ± 212 ppm. Results showed that with a gas/liquid rate ratio of 2–8 $m^3$ $m^{-3}$ liquid and volumetric gassing intensities of 0.04–0.20 $m^3$ $m^{-3}$ liquid $min^{-1}$, the average $H_2S$ removal achieved was 86–71%. Absorption of $CO_2$ in the scrubbing liquid caused a decrease in the pH, consequently decreasing the $H_2S$ removal efficiency. Increasing the pH of the scrubbing liquid will enhance the $H_2S$ removal efficiency from biogas. Thus, it shows that pH plays an important role in removing $H_2S$ from biogas. Table 2.6 summarizes the advantages and disadvantages of physical and chemical techniques used for $H_2S$ removal from biogas.

**Table 2.6** Physical and chemical techniques used for $H_2S$ removal from biogas

| Technologies | Solvent/ adsorbents | $H_2S$ removal Efficiency (%) | Advantages | Disadvantages | References |
|---|---|---|---|---|---|
| In-situ $H_2S$ precipitation | Introduction of air/oxygen | 90-95% | - Effective in reducing high $H_2S$ concentration to (200-100 ppm)<br>- Simple and low cost process<br>- No chemicals required | - Difficulty in dossing<br>- Overdose leads to explosion<br>- Degree of desulfurization is difficult to control | Petersson and Wellinger, 2009; Wellinger and Lindberg, 1999 |
| Adsorption | Activated carbon, iron oxide, zeolites, metal-organic frameworks (MOF), biochars | 84-99% | - Simple process<br>- Fast oxidation kinetics<br>- Efficient to reduce high $H_2S$ concentrations | - Expensive operating costs (regeneration and replacement of the adsorbent Material)<br>- Reagent disposal | Sahota et al., 2018; Hagen and Polman, 2001; Ryckebosch et al., 2011; Hao et al., 2016 |
| Physical absorption | Water, organic solvents | 90-99% | -Cheap when water is available<br>-Not require additional compression | -Suitable for removal of low $H_2S$ concentrations<br>-High initial investment costs<br>- High water and energy consumption<br>- High pressure and low temperature | Muñoz et al., 2015; Ryckebosch et al., 2011; Sun et al., 2015; Tilahun et al., 2018 |
| Chemical absorption | Amines (MEA, DMEA), alkali solutions | 90-99% | -Can be used with medium or high $H_2S$ concentrations<br>-Can treated $H_2S$ with high load fluctuation<br>-Low electricity requirements | -Higher Specific Costs<br>-Needs proper chemicals handling<br>-Create a contaminated liquid stream | Miltner et al., 2012; Lin et al., 2013; Osorio and Torres, 2009 |

### 2.3.9 KINETIC MODELING STUDY

The kinetics of $CO_2$ and $H_2S$ removal from biogas are critical for understanding the performance of scrubbing agents and the size of the purification unit. It also helps in understanding the reaction mechanisms behind the removal of $CO_2$ and $H_2S$. Different kinetic models based on absorption and adsorption have been reported in the literature. It is interesting to note that most of the kinetic models reported were based on alkaline chemicals such as aqueous ammonia, MEA, NaOH, KOH, and adsorbents such as activated carbon, biochar, etc. Some of the selected models are discussed below.

#### 2.3.9.1 KINETIC MODELS BASED ON $CO_2$ ABSORPTION

Qin et al. (2010) studied the kinetics of $CO_2$ absorption in an unloaded aqueous ammonia solution. The zwitter ion mechanism and the termolecular mechanism were proposed to explain the reaction between primary amine and $CO_2$. From a statistical perspective, it was observed that the fitting results for the termolecular mechanism were more robust than those for the zwitter ion mechanism.

Yan et al. (2015) studied five green amino acid salts (AASs) for $CO_2$ removal from biogas using the typical absorption–regeneration screening method. Three kinetic equations were used to study the $CO_2$ absorption rates and evaluate the $CO_2$ absorption performance of biogas. Results showed that the $CO_2$ absorption rate increases up to a certain limit of $CO_2$ loading, but above that critical value, the absorption rate drops rapidly. This indicates that with the continuous rise in $CO_2$ loading, the large consumption of free absorbent molecules makes $CO_2$ absorption controlled by the kinetics of the chemical reaction.

Malla et al. (2016) studied the kinetics of $CO_2$ absorption in alkaline and amine solutions by developing a correlation for empirical modeling of the absorption process. Obtained results showed that in the initial phase, the solvents reacted rapidly, and the concentration of $CO_2$ was found to decrease gradually with time. But after a certain time, $CO_2$ started desorbing and evolving in the outlet gas stream, indicating the solvents had become completely saturated. Thus, the absorption of $CO_2$ purely depends on the pH, inlet $CO_2$ concentration, and other factors like the pressure, temperature, and ionic strength of the solution.

#### 2.3.9.2 KINETIC MODELS BASED ON $H_2S$ ADSORPTION

Shang et al. (2013) prepared three different biochars from camphor (SC), bamboo (SB), and rice hull (SR) at 400 °C by oxygen-limited pyrolysis and tested them for their hydrogen sulfide ($H_2S$) adsorption ability. Kinetic analyses of adsorption by biochars were obtained using the Michaelis–Menten-type equation to evaluate and compare the overall removal rate and the saturated constant of the respective biochars.

Kanjanarong et al. (2016) studied the kinetics of $H_2S$ adsorption onto the biochar using pseudo-first-order (eq. 2.9) and pseudo-second-order (eq. 2.10) kinetic models via a series of $H_2S$ breakthrough studies. A similar study was also reported by Chen et al., 2011.

$$\log(q_e - q_t) = log q_e - \frac{k_1 t}{2.303} \tag{2.9}$$

$$\frac{t}{q_t} = \frac{1}{k_2 q_e^2} + \frac{t}{q_e} \tag{2.10}$$

Where $q_e$ and $q_t$ (mg $g^{-1}$) are the adsorbed $H_2S$ amounts at equilibrium and time t (min), $k_1$ ($min^{-1}$) and $k_2$ (g $mg^{-1}$ $min^{-1}$) are the pseudo-first-order and pseudo-second-order rate constants,

respectively. The kinetic studies showed that the experimental data correlated well with the pseudo-second order kinetic model, with an $R^2 > 0.99$.

Han et al. (2020) prepared two macroalgae biochars through pyrolysis and used them to adsorb $H_2S$ from biogas. Sorption kinetics of $H_2S$ on two biochars was studied using three kinetic models, viz., pseudo-first-order, pseudo-second-order and Weber–Morris respectively. Results showed that the pseudo-first-order model could clearly describe the $H_2S$ adsorption process, which indicates that the external mass transfer process may be the dominant control step during $H_2S$ adsorption.

## 2.4 EMERGING TECHNOLOGIES FOR BIOGAS UPGRADATION

Though conventional technologies are promising in biogas' up-gradation, the market for upgrading is often characterized by stiffer competition with the establishment of new technologies. Biological technologies are one of the recent developments in biogas upgrading technology. Both conventional and emerging biogas upgrading technologies are currently being developed for enhanced performance, to increase $CO_2$ reduction efficiency, and to render them cost-effective to get a wider implementation network.

### 2.4.1 BIOLOGICAL $CO_2$ REMOVAL TECHNOLOGIES

Biological biogas up-gradation involves the employment of microbes for the conversion of $CO_2$ and $H_2$ into $CH_4$. In comparison with conventional technologies, the major advantage of biological technology is that the $CO_2$ is converted into other value-added products at atmospheric pressure and moderate temperature, contributing significantly to a sustainable bio-based and circular economy [Rachbauer et al., 2016]. Biological biogas upgrading consists of two types of metabolic pathways: The first metabolic pathway involves the role of hydrogenotrophic

methanogens, which convert $CO_2$ directly to $CH_4$. The other metabolic pathway uses an indirect route where homoacetogenic bacteria first convert $CO_2$ to acetate and then convert it to $CH_4$ by the acetoclastic methanogens [Angelidaki et al., 2018]. The former pathway is preferable as hydrogenotrophic methanogens (*Methanobacterium, Methanoculleus* and *Methanomicrobium*) are more abundant than acetoclastic methanogens such as *Methanosarcina* [Agneessens et al., 2017]. The biological biogas upgrading process is generally classified into two types:

(a) In situ biological methane enrichment and

(b) Ex situ biological methane enrichment

#### 2.4.1.1 IN SITU BIOLOGICAL METHANE ENRICHMENT

Biological in situ biogas upgradation implicates injection of $H_2$ inside the biogas digester in order to couple with endogenous $CO_2$ produced in the anaerobic digester to convert it into $CH_4$ by the action of autochthonous hydrogenotrophic methanogens [Kougias et al., 2017]. The process can enrich $CH_4$ up to nearly 99% if the operational parameters (e.g. pH, temperature, $H_2$ flow rate, etc.) are fully monitored and controlled [Wang et al., 2013]. Though in situ biogas upgrading is a cost-effective method, it also has some technical challenges with the increase of pH values above 8.5 due to the elimination of the key buffering agent, i.e. bicarbonate, thus leading to inhibition of methanogenesis [Liu and Whitman, 2008]. Therefore, 8.5 is measured as the threshold pH for the ideal biomethanation process in both conventional and emerging biogas production systems. In order to overcome this technical challenge, co-digestion of manure with acidic waste was anticipated to arrest the pH in an optimal range during the biogas upgrading process [Luo and Angelidaki, 2013]. Another challenge is that oxidation of volatile fatty acids (VFA) and alcohols is thermodynamically viable only if the partial pressure of $H_2$ is very low [Dolfing et al., 2008].

On the other hand, the addition of $H_2$ in the biogas digester increases the concentration of $H_2$ inside the digester, which inhibits the process of VFA oxidation [Batstone et al., 2002]. Due to this concern, the in situ methane enrichment process is limited to lab scale studies only and more process optimization is required to achieve a wider implementation worldwide.

#### 2.4.1.2 EX SITU BIOLOGICAL METHANE ENRICHMENT

The concept of ex-situ biogas upgradation came into existence to overcome the challenges incurred in in-situ biogas upgradation. Ex situ biogas upgradation implicates accumulation of $CO_2$ from biogas and $H_2$ from external sources in a separate anaerobic reactor having the hydrogenotrophic methanogenic archaea, resulting in their subsequent conversion to $CH_4$. In this process, $CO_2$ is utilized as a carbon source and $H_2$ as a reducing agent for the production of $CH_4$ [Kougias et al., 2017]. The efficiency of biogas upgradation strongly depends on the reactor type, partial pressure of $H_2$ and operating temperature inside the bioreactor, which can result in methane conversion from 79 to 98%. In comparison with mesophilic culture, the enriched thermophilic culture resulted in > 60% higher $H_2$ and $CO_2$ bioconversion in the batch assay [Lecker et al., 2017]. Various types of reactors that can address the challenges of gas–liquid mass transfer of $H_2$ are fixed-bed reactors, anaerobic trickle-bed reactors (ATBR), continuous stirred tank reactors (CSTR), and series up-flow reactors.

## 2.5 RECENT ADVANCES IN THE AD TECHNOLOGY

Anaerobic digestion (AD) technology is a deep-rooted technology for the renewable energy sector and for the utilization of organic wastes. The intricacy of the AD process is due to the interconnection of different processes such as chemical, microbiological, and operational aspects that are integrally dependent on each other [Hagelqvist and Granström, 2016]. However, recent

advances in AD systems to increase energy efficiency in the form of $CH_4$ have offered new hope for better understanding the mechanism of this technology. Thus, it requires optimization and technical modification of operating factors that support syntrophic interactions amongst different microorganisms in the digestion process. Some recent advances in AD technology include the design of a digester, the integration of AD with a microbial fuel cell (MFC), the integration of AD with a microbial electrosynthesis system (MES), and the use of non-biological conductive materials to improve AD and digestate [Chung et al., 2019; Li and Yu, 2016; Ni et al., 2017].

Zhao et al. (2012) demonstrated a microbial fuel cell (MFC) to investigate the possible generation of electricity from cattle dung. Stable electricity generation was observed after 30 days with a maximum volumetric power density of 0.220 $W/m^3$. The production of biogas continued for only 8 days, with a maximum production of 285 mL/d. After 120 days of operation, the total chemical oxygen demand (TCOD) removal and coulombic efficiency (CE) of the MFC reached 73.9 ± 1.8% and 2.79 ± 0.6%, respectively. Microbial community analysis showed that Proteobacteria (36.3%) and Firmicutes (24.2%) were the dominant phyla in the cattle dung sample. The archaea population was mainly hydrogenotrophic methanogens, which disappeared during the periods of stable power generation via acidogenesis.

Higgins et al. (2013) developed an electrogenic biofilm on a macroporous chitosan-carbon nanotube (CHIT-CNT) electrode under a constant potential and flow through conditions using the effluent from an anaerobic digester. After continuous inoculation for 125 days, the bioelectrode was able to demonstrate an open circuit potential and a current density of −0.62 V and 9.43 µA $cm^{-3}$ respectively. SEM images indicated the biofilm formed on the surface of the bioelectrode with a high density of bacterial nanowires ubiquitously connecting bacteria to

bacteria and bacteria to the electrode surface, suggesting the nanowires are electrically conductive and conduct direct electron transfer.

Chung et al. (2019) constructed a combined anaerobic digester (AD) and a microbial fuel cell (MFC) using rumen fluid dairy digester inoculum as an anode to convert cellulosic biomass (Avicel) at 2% (w/v) to produce biomethane and electricity. MFC power and current across an external resistor were measured regularly for 10 days, and on day 19, gas and liquid solutions from the anode chamber were analyzed for gas compositions and volatile fatty acids, respectively. The results indicated that with the addition of enriched rumen microorganisms, electricity generation was increased, and the average power density normalized to anode surface area was 36.0 $mW/m^2$, while control had 12.0 $mW/m^2$. Moreover, enriched rumen microorganisms increased cellulose digestibility in the anaerobic anode chamber and enhanced both $CO_2$ and methane production.

Nelabhotla and Dinamarca (2019) presented a practical approach through the integration of an anaerobic digester (AD) with a microbial electrosynthesis system (MES) to increase the biogas yield. The biocathode in MES was able to reduce carbon dioxide with the supplied electrons and protons ($H^+$) to produce biogas with over 90% methane. The optimum cathode potential was in the range of -0.70 V to -0.60 V and pH was around 7.0. A control experiment was also carried out to compare open circuit and MES methanogenesis. The control experiment revealed that an improvement of about 13.6% in methane production rate was achieved with electrochemical $CO_2$ reduction.

An et al. (2020) investigated a carbon-modified copper foam electrode in an anaerobic bioelectrochemical digestion (ABD) reactor using food waste for process stability,

electrochemical characterization and bioelectrochemical methane production, and the results were compared to a control reactor. The ultimate methane production from food waste in the ABD reactor reached 338.1 mL $CH_4$/L, which was almost two times higher than that of the control reactor (181.0 mL $CH_4$/L). It was confirmed by the cyclic voltammetry (CV) analysis, which showed higher redox peaks, thereby affirming the enrichment of electroactive bacteria. Therefore, it was attributed to the enriched and activated electroactive bacteria in the ABD reactor, which further activated the direct interspecies electron transfer (DIET) pathways for methane production.

## 2.6 KINETIC MODELS BASED ON BIOGAS PRODUCTION

Donoso-Bravo et al. (2010) used three mathematical models (Modified Gompertz equation, Logistic function, and Transference function) and one kinetic model (first-order equation) to study the effect of thermal and sonication pre-treatment on the anaerobic degradation of sewage sludge for biogas production. All the experimental data fitted well with the models, but the transference function presented the best agreement in the fitting process. Li et al. (2015) investigated the process of anaerobic digestion and kinetics of four livestock manures with different substrate concentrations under mesophilic conditions. They used three kinetic models, viz., first-order kinetics, Transference function model, and Cone model, to fit the methane production from four livestock manures. Among the three models, the Cone model best fitted the experimental data, and the evaluated parameters indicated that anaerobic digestion of manures at higher loading has a longer lag phase and a lower hydrolysis rate. Rajput et al. (2018) conducted a lab-scale batch experiment to study the effects of thermal pretreatment on the anaerobic digestion of wheat straw. They also fitted the experimental data of biogas production into a kinetic model using the modified Gompertz model, the Logistic function model, and the

Transference function. The results showed a modified Gompertz model was best fitted to the experimental biogas production data, followed by logistic and transference function models**.** However, all three models predicted an increase in biogas production rate and a decrease in lag phase time with an increase in thermal pretreatment temperature.

Thus, the maximum biogas production, maximum biogas production rate, and lag phase can be easily calculated for batch anaerobic digestion using these models.

## 2.7 LOCALLY AVAILABLE BIOMASS AS RAW MATERIALS

The banana, one of the world's most popular fruits, contributes to 16% of the world's total fruit production and is the second largest food produced in the world [www.fao.org/production/faostat]. At the time of harvesting, the average weight of a banana plant is about 100 kg, of which 50 kg corresponds to pseudo-stalks, 2 kg to rachis, 33 kg to fruits, and 15 kg to leaves. The percentage of product loss due to size, contamination, handling, transport, and storage is estimated at about 20% [Zhang, et al., 2005]. The proportion of the banana which is wasted as peel is estimated at 18–20%. After harvesting the fruit, the parts of the plant that are cut and wasted as pseudo stem amount to a few hundred metric tons in the plantations. The banana peel has been used as a bio-adsorbent of soluble contaminants such as phenolic compounds [Achak et al., 2009], metals [Memon et al., 2008], and dyes [Gupta and Suhas, 2009]. It has also been used in the production of ethanol [Brooks, 2008], biomass and metabolites of biotechnological interest, and for the production of pectin [Happi, et al., 2008].

A natural base ash solution (locally known as Kolakhar) made from pseudostem, rhizome, and peel is a traditional ingredient and a popular food additive in Assam, India. This process includes the production of antacid by filtering water through the ashes of a banana peel or pseudostem

(the name derived from the local term of banana-kol or kola). Khar, or base solution made from *Musa balbisiana* kola, has the best quality of all the variants present in the north-eastern region of India [Hemanta et al., 2014]. Other than its normal use as a food additive in cooking, kolakhar has been used to treat various diseases and disorders. The tradition of villagers using kolakhar as soap and detergent for washing clothes and shampooing hair has been practised for a long time. Farmers use kolakhar to kill leaches and prevent their attack while working in leech-infected fields [Deka and Talukdar, 2007]. Banana peels are natural sources of potassium, and the solutions prepared from their ash can have a very high pH. It has several advantages over other conventional bases. It is a naturally available alkali, milder and less corrosive than NaOH or KOH, is inexpensive, abundant, and environmentally friendly.

Another biomass, bamboo, is the one and only plant that grows faster than any other plant on Earth. Bamboos are a diverse group of evergreen perennial flowering plants in the subfamily Bambusoideae of the grass family Poaceae. Assam is the largest producer of bamboo in the entire country and more than 50 types of bamboo are found in Assam. The most common varieties include *Bambusa balcooa* (Bhaluka), *Bambusa tulda* (Jati) and *Dendrocalamus hamiltonii* (Koko) which can be seen in most of the households in the state [krishijagran.com]. Because of its uniqueness, culture, and role as a source of income for many families in Assam, India, the people of Assam have a close relationship with bamboo. Household products such as houses, ladders, baskets, mats, and hand-fans can be hand-crafted, and a lot of waste is generated while making these products.

## 2.8 RESEARCH GAP

The literature review shows that all biogas up-gradation technologies have their specific advantages and disadvantages and are different for different biogas upgrading sites. The correct choice of the economically feasible technology relies on the quality and quantity of the raw biogas, the biomethane quality to be attained, and its utilization. Pressure swing adsorption, membrane and cryogenic separation give high purity, but they are economically not viable for pilot plants as they are energy intensive and consume relatively more power per unit of gas produced [Bauer et al., 2013; Deublein and Steinhauser, 2010; Zhang et al., 2013]. Physical scrubbing of biogas using water is simple and one of the cheapest methods to remove $CO_2$ and $H_2S$ simultaneously. However, the requirement for high pressure and a lot of water for this process makes it impractical for areas with water scarcity [Sun et al., 2015]. Physico-chemical adsorption on a solid surface is practical and economical, has good moisture removal capacities, and is simple in design. Nevertheless, due to the compactness of the packing material, very high pressure for chemical regeneration is required. Chemical absorbents, compared, are considered to be more efficient as they do not require high pressure to act as absorbents. Besides, they store $CO_2$ permanently in a solid form by converting it into alkali metal carbonates. However, the only limitations are that the regeneration of the solvents requires relatively high energy input and that the chemicals used are not eco-friendly. Most biogas scrubbing experiments used chemical bases such as MEA, NaOH, $Ca(OH)_2$, and KOH [Leonzio, 2016; Tippayawong and Thanompongchart, 2010]. These are no doubt commonly available chemicals, but using these solvents in rural areas for biogas scrubbing becomes impractical due to technical and cost issues. However, limited literature has been found using naturally available biomass-based scrubbing agents for biogas purification.

Biomass is readily available in all geographic locations, which has enormous potential for conversion into scrubbing agents but has not yet been explored efficiently. Hence, detailed characterization of biomass is essential to ascertain its physico-chemical properties and be used as a scrubbing agent for biogas purification. There is a lot of literature on the characterization of biomass in terms of efficient biogas production. However, there is very little literature on biomass characterization as scrubbing agents, which requires additional research regarding potential and applicability.

Removal of $H_2S$ from raw biogas undergoes several desulphurization methods, such as in-situ $H_2S$ precipitation, physical/chemical absorption, and adsorption on solid surfaces. Similarly, each scrubbing technique has its own advantages and disadvantages. For instance, in-situ $H_2S$ precipitation using air or oxygen is risky as a high dose can lead to an explosion; chemical absorption produces harmful by products which need treatment before discharge; physico-chemical adsorption on solid surfaces is a convenient method for decentralized biogas plants in rural areas because adsorption techniques are highly efficient and preferable for the removal of low concentration $H_2S$ from biogas systems. So far, many researchers have reported different kinds of adsorbents such as zeolite [Hao et al., 2016], fly ash [Seredych et al., 2008], activated carbon [Surra et al., 2019], and impregnated biochar prepared from corn stover and maple wood [Choudhury and Lansing, 2021], respectively. It is understood that the abovementioned adsorbents give encouraging results for $H_2S$ adsorption. However, challenges remain in considering sustainable, eco-friendly, easy-to-prepare, and cost-effective adsorbents. However, very little research was found for the study on naturally alkaline biochar and clay composites for the removal of $H_2S$ from biogas. Continued research efforts are

necessary towards the synthesis of locally available biomass-based adsorbents with fewer disadvantages in all terms.

Integration of AD with MFC, MES and the use of non-biological conductive materials to improve AD and digestate are some of the recent advances made in AD technology. Several researchers have reported on recent advances in AD systems that improve energy efficiency in the form of $CH_4$ and electricity. But most of the work is in the initial stages and requires further research on technical modification to enhance the $CH_4$ yield, overall biogas production, and electricity.

## 2.9 SCOPE OF THE PRESENT WORK

Based on the extensive literature review and identification of subsequent pros and cons of the upgradation processes, the absorption and adsorption methods are found to be simple and efficient targets for the decentralized biogas plants installed in rural areas, especially for cooking and power generation. Thus, there is a need to develop a process which –

- Works at room temperature and pressure
- Uses locally available, and environmentally friendly scrubbing agents
- Is easy to operate
- Is affordable for rural communities
- Is highly efficient for $CH_4$ enrichment and $H_2S$ removal

Accordingly, it is proposed to identify and collect locally available biomass to check their potential as scrubbing agents for purification of biogas. A detailed characterization of biomass as a scrubbing agent is considered to understand its physico-chemical properties. Performance evaluation of the selected scrubbing agents and adsorbents for $CO_2$ and $H_2S$ removal from biogas

using absorption and adsorption is proposed as the key scope along with their kinetic studies. Furthermore, kinetic studies on the operation of an integrated bioelectrochemical system for co-generation of methane-enriched biogas and electricity are planned.

## 2.10 AIM AND OBJECTIVES

The aim of the present work is to develop a cost-effective $CO_2$ and $H_2S$ scrubbing process for decentralized biogas plants installed in rural areas using locally available biomass-based scrubbing agents and also to develop a bio-electrochemical system for $CH_4$ enrichment.

**The objective of this thesis is aimed at:**

1. Survey and selection of indigenous and easily available biomass for the preparation of scrubbing agents and adsorbents.
2. Characterization of selected biomass as adsorbents and scrubbing agents.
3. Performance evaluation of biomass-derived adsorbents using an adsorption method for the removal of $H_2S$ from biogas and their kinetic studies.
4. Experimental and kinetic studies of $CO_2$ scrubbing from biogas by absorption process using natural base ash solutions.
5. Integration of an anaerobic digester with a membrane electrode assembly for the co-generation of methane-enriched biogas and electricity: A comparison with a control system and kinetic analysis.

## 2.11 SUMMARY OF THE CHAPTER

The present chapter discusses a detailed literature review on applications of biogas and its purification standards, including conventional, emerging, and recent advances in biogas

purification technologies. Kinetic studies of $CO_2$ and $H_2S$ removal from biogas using absorption and adsorption techniques are also discussed. Accordingly, the research gap and scope of the present work are formulated based on available literature. The next chapter provides a detailed study on the survey and characterization of various selected biomass as scrubbing agents to be used for biogas purification.

# Chapter 3

## Biomass Characterization as Scrubbing Agents and Adsorbents

# CHAPTER 3: BIOMASS CHARACTERIZATION AS SCRUBBING AGENTS AND ADSORBENTS

## 3.1 INTRODUCTION

There are numerous applications for lignocellulosic biomass as a raw material for the production of biochemicals, bio-sorbents, adsorbents, and metabolites [Chen et al., 2010; Gupta and Suhas, 2009]. They differentiate themselves by several physico-chemical parameters such as calorific value, moisture content, carbon proportion, ash, mineral content, and pH. Characterization of biomass is necessary to understand the physico-chemical properties for selecting them as scrubbing agents for $CO_2$ and $H_2S$ removal from biogas. Therefore, as both the components $CO_2$ and $H_2S$ are acidic in nature, they require basic components in order to remove them through certain physico-chemical reactions. Hence, the present chapter is an attempt to select and characterize locally available biomass to be used as scrubbing agents for biogas purification based on their physico-chemical properties.

## 3.2 MATERIALS AND METHODS

### 3.2.1 SURVEY OF BIOMASS

Some of the easily available biomass includes leaf waste, duckweed, grasses, woody plants, banana plants, and bamboo. The physico-chemical properties enable them to be considered as potential biomass for conversion into useful biochemicals and adsorbents. All biomass varies significantly in elemental composition, and even the same kind of biomass can change in composition based on climatic conditions and seasonal deviation. Based on a local survey and availability, the following biomass, as shown in Table 3.1, were selected for initial characterization using proximate analysis and pH.

**Table 3.1** Initial selection of biomass based on a survey

| Absorption | Adsorption |
|---|---|
| Duckweed | Leaf waste |
| *Musa balbisiana* peel | Bamboo (*Bhaluka*) |
| Banana pseudostem | Banana peel |
| Pine saw dust | Clay composite |
| *Musa acuminata* peel | Areca nut |

### 3.2.2 PREPARATION OF SAMPLES

The selected biomass was collected from a nearby local village of IIT Guwahati, Assam, and air-dried for a week. Collected biomass was cleaned under tap water to remove any attached contaminants and incubated in a hot air oven at 60 °C for 24 hours. The biomass samples chosen for absorption were then burned to ashes and ground into powder in a grinder. For adsorption, the biomass samples were carbonized under an oxygen-poor atmosphere in a furnace at 500°C for 3 hours. Additionally, a clay composite was prepared by mixing clay and banana peel in a 1:1 ratio at 500 °C for 3 hours. The composite thus prepared was impregnated with a banana peel ash solution and oven-dried at 80 °C for 24 hours. Thus, the synthesized samples (ash and biochar) were cooled and stored in an inert condition for further analysis.

### 3.2.3 TECHNIQUES AND INSTRUMENTS USED FOR CHARACTERIZATION

Biomass, their ashes, and biochars were characterized by proximate analysis, pH, thermogravimetric analysis (TGA), elemental analysis by energy dispersive X-ray spectroscopy (EDX), and flame photometry, topographical analysis by field emission scanning electron microscopy (FESEM) and Brunauer–Emmett–Teller (BET) surface area. Additionally, Powder

X-ray diffraction (PXRD) and Fourier Transform Infra-red (FT-IR) spectroscopy were carried out to elucidate the structural differences of biochars before and after treatment for biogas purification, which is discussed in chapter 4.

### 3.2.3.1 PROXIMATE ANALYSIS

By proximate analysis, the moisture, volatile matter, ash, and fixed carbon content of the biomasses were calculated. The procedure to estimate the amount of moisture and ash content was adopted from the National Renewable Energy Laboratory (NREL) protocol. For volatile matter determination, the American Society for Testing and Materials (ASTM) D 271-48 was followed.

**Moisture content:** The moisture content of the biomass sample was determined as follows: A digital electronic balance was used to weigh approximately 1 g of the sample before placing it in a pre-weighed porcelain crucible. The sample was placed in a muffle furnace at 105±3°C for 8 hours. After that, the sample was transferred to a desiccator for cooling to room temperature. The final weight of the dried sample with a pre-weighed crucible was recorded. The percentage of moisture in the biomass sample was then calculated using the following relation (3.1).

$$Moisture\ \% = \frac{W_i - W_f}{W_i} \times 100\ \% \qquad (3.1)$$

where

$W_i$ = weight of the initial sample in g

$W_f$ = weight of the final dried sample in g

**Volatile matter content:** Approximately 1 g of the dried sample used for moisture content was further volatilized at 950±20°C for 7 minutes in a pre-weighed porcelain crucible with a lid. After cooling the samples in a desiccator to room temperature, the final weight of the cooled crucibles with a lid containing the remaining burnt sample was recorded. The volatile matter content of the sample was calculated by the following equations (3.2 & 3.3).

$$Weight\ loss\ \% = \frac{W_i - W_f}{W_i - W_c} \times 100\% = A \tag{3.2}$$

where

$W_c$ = weight of the crucible with lid in g

$W_i$ = initial weight in g

$W_f$ = final weight in g

$$Volatile\ matter\ \% = A - B \tag{3.3}$$

where

A = weight loss %

B = moisture %

**Ash content:** Approximately 1 g of the dried sample used for moisture content was further allowed to ignite completely to ash at 625±25°C for 3 hours in a pre-weighed porcelain crucible. After cooling the samples in a desiccator to room temperature, the final weight of the cooled crucible containing the remaining burnt sample was recorded. Ash content of the sample was calculated by the following equation (3.4).

$$Ash\ \% = \frac{W_a - W_c}{W_i - W_c} \times 100\% \quad (3.4)$$

where

$W_a$ = weight of ash and crucible in g

$W_c$ = weight of the empty crucible in g

$W_i$ = initial weight of 105°C dried sample and crucible in g

**Fixed Carbon content:** Fixed carbon is a calculated value. It is the summation of moisture, volatile matter, and ash percentage, subtracted from 100.

Fixed carbon % = 100 – (Moisture % + Ash % + Volatile matter %) (3.5)

### 3.2.3.2 MEASUREMENT OF pH

pH is a scale range from 0-14 used to specify the acidity or basicity of an aqueous solution. It is approximately the negative of the base 10 logarithms of the molar concentration, measured in units of moles per liter of hydrogen ions. The pH of the prepared base solutions and adsorbents before and after treatment was measured with the help of a digital pH meter (*Make: Mettler Toledo, Model: 30266889*).

### 3.2.3.3 THERMOGRAVIMETRIC ANALYSIS

Thermogravimetry delivers a rapid method for determining the temperature-assisted decomposition profile of a material and the kinetics of its thermal decomposition. Thermogravimetric experiments were performed in an STA 7200 Integrated Thermal Gravimetric Analyzer (Hitachi, Japan), with high purity nitrogen (99.999%) as carrier gas at a flow rate of 100 mL/min. Each time, about 5 mg of the prepared sample was put in a platinum

pan and the sample was heated between 35 °C and 800 °C at a rate of 15 °C $min^{-1}$. Calculated thermogravimetric rate data was automatically obtained from the system using computer software. The average size of all samples was below 0.5 mm, so the mass loss of the samples was under the control of the kinetic reaction.

### 3.2.3.4 ELEMENTAL ANALYSIS BY ENERGY DISPERSIVE X-RAY SPECTROSCOPY

EDX is an analytical technique used for the elemental analysis or chemical characterization of a sample. With the help of EDX, all alkali, alkaline earth, and transition metals can be detected with composition percentage on a weight basis. The natural base powder ash samples and biochars before and after $H_2S$ sorption were characterized with the help of an EDX equipped with a scanning electron microscope *(Make: Zeiss, Model: Sigma)* to study their elemental compositions. Before analysis, samples were oven-dried at 100 °C for 8 hours and then placed in a desiccator to cool to room temperature for further analysis. The samples were mounted on a stub using double-sided conductive carbon tape. Double gold coating was done on the surface of the sample in a vacuum coating unit called a Gold Sputter Coater to make the sample electrically conductive.

### 3.2.3.5 FIELD EMISSION SCANNING ELECTRON MICROSCOPY

FESEM (*Make: Zeiss, Model: Sigma*) was conducted to study the difference in surface morphology of the raw biomass samples, their ashes, and biochars before and after $H_2S$ sorption. The samples were exactly prepared according to the procedure followed for EDX. The images were captured at 3 kV EHT for visualization of surface morphology and structural changes in the respective samples.

### 3.2.3.6 ELEMENTAL ANALYSIS BY FLAME PHOTOMETRY

A photoelectric flame photometer is a device used in chemical analysis to determine the concentration of inorganic metal ions such as sodium, potassium, and calcium. Flame photometry (*Make: Systronics, Model: 128*) was used for the estimation of the concentration of inorganic metal ions ($Na^+$, $K^+$, and $Ca^{2+}$) in the biomass ashes. The desired metal ions for this work belong to Group 1 and Group 2 of the periodic table, which are quite sensitive to flame photometry due to their low ionization enthalpies.

The following standards were prepared for the analysis of the concentration of $K^+$, $Na^+$, and $Ca^{2+}$ of the respective samples.

*Standards:*

KCl- 10 ppm, 10 mg of KCl in 1000 ml of distilled water

$CaCl_2$- 100 ppm, 100 mg of $CaCl_2$ in 1000 ml of distilled water

NaCl- 10 ppm, 10 mg of NaCl in 1000 ml of distilled water

Samples- 1g ash of the respective sample in 1000 ml distilled water

The sample for Flame Photometry was prepared by diluting 100 times its original volume by taking 5 ml of the sample solution in a 500 ml volumetric flask and making volume up to the mark with distilled water.

### 3.2.3.7 POROSITY AND BRUNAUER–EMMETT–TELLER SURFACE AREA

BET surface area, pore-volume, and the average pore diameter of the adsorbent samples were measured using an $N_2$ adsorption/desorption pattern on a surface area analyzer (Make: M/s

Micromeritics, USA; Model No.: Tristar II) at –196 °C. Prior to the analysis, the samples were degassed under a vacuum at 150 °C for 6 hours.

#### 3.2.3.8 POWDER X-RAY DIFFRACTION

XRD is a powerful tool for biochar and clay characterization. It is a non-destructive test method used to analyze the structure of crystalline materials. Here it is used to elucidate the patterns of adsorbent samples before and after $H_2S$ sorption with Cu-Kα radiation at λ=1.5406 Å (model TTRAX III, Rigaku). The diffraction patterns were recorded between 5° and 80° scanning range (2θ) at 50 kV and 100 mA with a scan speed of 4° $min^{-1}$. A microscope slide was used as the sample holder, which was then placed in the XRD sample compartment to obtain the diffractograms.

#### 3.2.3.9 FOURIER TRANSFORM INFRA-RED SPECTROSCOPY

FT-IR spectra of the adsorbents before and after $H_2S$ sorption were recorded to study the difference in their surface functional groups. The FT-IR spectra were identified using a PerkinElmer Spectrum Two FT-IR spectrometer ($\lambda_{max}$ in $cm^{-1}$) in the wavenumber range of 4000-400 $cm^{-1}$.

## 3.3 RESULTS AND DISCUSSION

### 3.3.1 PROXIMATE ANALYSIS OF BIOMASS SAMPLES

Table 3.2 shows the proximate analysis data of the raw dried biomass samples. The analysis was carried out for moisture, volatile matter, ash, and fixed carbon content.

**Table 3.2** Proximate analysis of raw dried biomass samples. The abbreviation M denotes moisture, VM denotes volatile matter and FC denotes fixed carbon. Each value is the Mean ± SD of three replicates.

| Biomass sample | M (%) | VM (%) | Ash (%) | FC (%) |
|---|---|---|---|---|
| Duckweed | 10.71 ± 0.95 | 83.24 ± 1.07 | 3.88 ± 0.76 | 2.17 ± 0.91 |
| *Musa balbisiana* peel | 7.42 ± 0.13 | 77.60 ± 1.20 | 11.27 ± 0.13 | 3.71 ± 1.40 |
| Banana pseudostem | 11.46 ± 0.43 | 73.62 ± 1.04 | 9.79 ± 0.08 | 5.13 ± 1.46 |
| Pine saw dust | 8.24 ± 0.87 | 77.25 ± 1.05 | 9.01 ± 0.04 | 5.50 ± 1.88 |
| *Musa acuminata* peel | 13.62 ± 0.08 | 75.63 ± 0.22 | 8.56 ± 0.13 | 2.19 ± 0.3 |
| Leaf waste | 6.57 ± 0.33 | 81.18 ± 0.32 | 5.94 ± 0.65 | 6.31 ± 0.93 |
| Bamboo (*Bhaluka*) | 9.78 ± 0.15 | 75.02 ± 0.65 | 9.85 ± 0.20 | 5.35 ± 0.61 |
| Areca nut | 10.48 ± 0.47 | 77.75 ± 0.77 | 4.52 ± 0.38 | 7.25 ± 1.15 |

The ash content of duckweed, *Musa balbisiana* peel, banana pseudostem, pine saw dust, *Musa acuminata* peel, leaf waste, bhaluka bamboo dust, and areca nut was found to be 3.88 ± 0.76%, 11.27 ± 0.13%, 9.79 ± 0.08%, 9.01 ± 0.04%, 8.56 ± 0.13%, 5.94 ± 0.65%, 9.85 ± 0.20% and 4.52 ± 0.38% respectively. *Musa balbisiana* peel has a higher ash content compared to other biomass, which indicates the presence of more inorganic compounds. A high content of ash indicates the presence of inorganic metals, which may be one of the reasons for making the surface alkaline [Guo et al. 2015]. Duckweed has higher volatile content (83.24 ± 1.07%) and lower ash content (3.88 ± 0.76%) as compared to other biomasses, which indicates higher gaseous components and is anticipated as a potential candidate for biogas production.

### 3.3.2 pH OF ASH AND BIOCHARS

An experiment was conducted to assess the effect of ash concentration on the pH of the prepared solutions. 100 ml of distilled water was taken in a conical flask to which 1 g of ash was added and mixed properly. The initial average pH of the respective ash solutions was recorded as 8.23 (duckweed), 11.39 (*Musa balbisiana* peel), 10.96 (banana pseudostem), 8.94 (pine saw dust), and 11.04 (*Musa acuminata* peel). The process was repeated by adding 1 g consecutively until the pH stabilized. The solution was kept in a shaker at 150 rpm for 45 minutes at ambient temperature for proper mixing of the ashes. Fig. 3.1 shows the values recorded for all the instances. From the graphs, it was observed that the pH increased with an increase in ash concentration (g) and stabilized at a certain level. Amongst all, the highest average pH was recorded for *Musa balbisiana* peel (12.77) followed by *Musa acuminata* peel (11.63), banana pseudostem (11.48), pine saw dust (10.04), and duckweed (9.16) respectively.

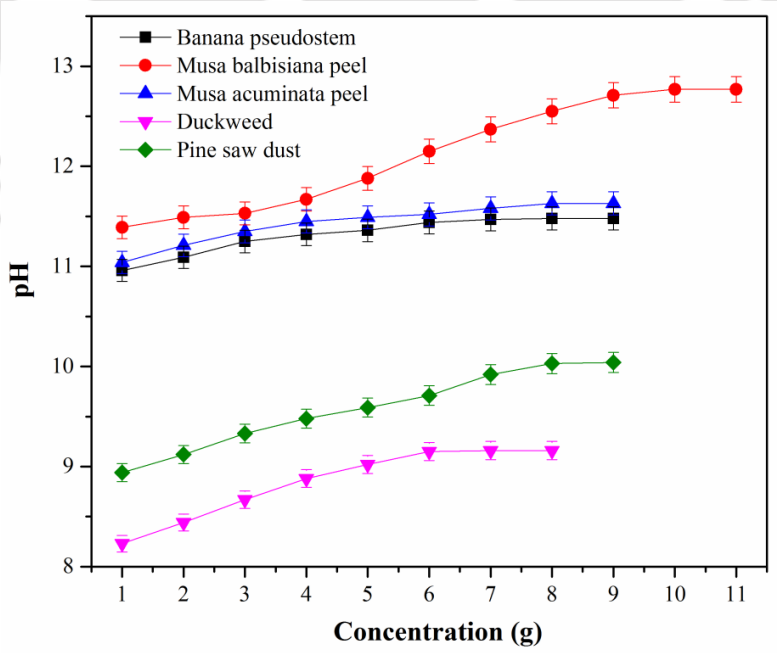


**Fig. 3.1** Comparison of pH versus concentrations of ash samples

The pH determines the average acidity/basicity of the sorbents. The pH was measured by adding 1 g of biochar samples to 50 mL of distilled water and then stirring to mix uniformly using a magnetic stirrer for 45 min. Table 3.3 shows the respective surface pH of the biochar samples.

**Table 3.3** Surface pH of biochars. Each value is the Mean ± SD of three replicates.

| Adsorbents | pH |
|---|---|
| Leaf waste biochar | 9.89 ± 0.04 |
| Bamboo biochar | 10.67 ± 0.03 |
| Banana peel biochar | 10.95 ± 0.03 |
| Areca nut biochar | 8.85 ± 0.03 |
| Biochar clay composite | 9.96 ± 0.05 |

The average pH of the respective biochars was recorded as 9.89 (leaf waste biochar), 10.67 (Bhaluka bamboo dust biochar), 10.95 (banana peel biochar), 8.85 (areca nut biochar), and 9.96 (biochar clay composite) respectively. The high pH recorded may be due to the formation of hydroxides, carbonates of alkali, and alkaline earth metals. The alkaline nature of biochar or higher pH plays a significant role in the sorption of acidic components such as $CO_2$ and $H_2S$ [Sahota et al., 2018; Seredych et al., 2008].

### 3.3.3 SELECTION OF BIOMASS BASED ON SURVEY, ASH CONTENT, AND pH FOR FURTHER ANALYSIS

A sufficient quantity of single biomass may not be available throughout the year or may change geographically. Thus, depending on the availability of biomass, the scrubbing process may require a change of scrubbing agents at different periods of the year. It may not be feasible or practical to conduct a comprehensive assessment for each of the biomass types used as a

scrubbing agent. Therefore, it is necessary to have a preliminary estimate of the alterations in the quality of the biomass as scrubbing agents in terms of pH and ash content. Based on the availability and physico-chemical properties, the following biomasses were selected for further characterization as shown in Table 3.4.

**Table 3.4** Selection of biomass as scrubbing agents and adsorbents for further characterization

| **Absorption** | **Adsorption** |
|---|---|
| Banana pseudostem (BPS) ash solution | Bamboo biochar (BB) |
| *Musa balbisiana* peel (MBP) ash solution | Banana peel biochar (BPB) |
| *Musa acuminata* peel (MAP) ash solution | Biochar-clay composite (BCC) |

Furthermore, as discussed in Chapter 2, many publications have reported biomass-derived biochars derived from leaf waste and woody plants, whereas there is very little literature on various parts of banana peels, bamboo, and clay composites. A natural base ash solution (locally known as Kolakhar) prepared from *Musa balbisiana* peel, *Musa acuminata* peel, and banana pseudostem is a traditional ingredient and a popular food additive in Assam, India. Banana peels and pseudostem are natural sources of potassium and the solutions prepared from their ash can have a very high pH. The potential of applying natural base ash solution and biomass-derived biochars for $CO_2$ and $H_2S$ removal from biogas is greatly dependent on its physico-chemical properties [Siddique, 2012].

### 3.3.4 THERMOGRAVIMETRIC ANALYSIS OF BIOMASS SAMPLES

Fig. 3.2 shows the TGA plot of MAP, MBP, and BPS, and Fig. 3.3 shows the TGA plot of banana peel and bamboo. The temperature range of 100 to 150 °C is related to weight loss due to

dehydration, i.e., the vaporisation of water molecules adsorbed on the surface of the biomass sample and those bonded within the inner cells [Lim and Wu, 2015]. Following the dehydration stage, the second stage covers a wide temperature range from 150 to 370 °C, respectively, indicating a major pyrolysis stage, which corresponds to the decomposition of hemicellulose and cellulose [Meszaros et al., 2004]. The maximum weight loss observed between 210 and 340 °C indicates hemicellulose volatilization, which occurs when the chemical bonds linking various bio-polymers begin to break. The specific temperature of bond breakage, however, depends on the thermal stability of the compounds, wherein less thermally stable compounds decompose at an early stage. The plot for cellulose decomposition normally starts at 350 °C and extends up to 380 °C and may overlap with that of hemicellulose, thereby shifting the range of temperature between 320 and 390 °C [Skodras et al., 2006]. At 500 °C onwards, a long tail of devolatilization was observed for all biomass, which indicates the loss of lignin and the formation of char [Meszaros et al., 2004].

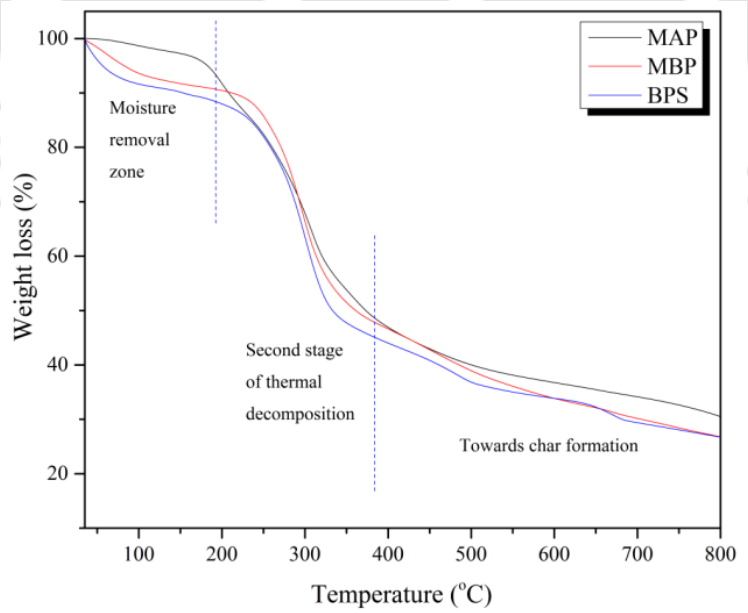


**Fig. 3.2** TGA profile of raw biomass samples (MAP, MBP and BPS)

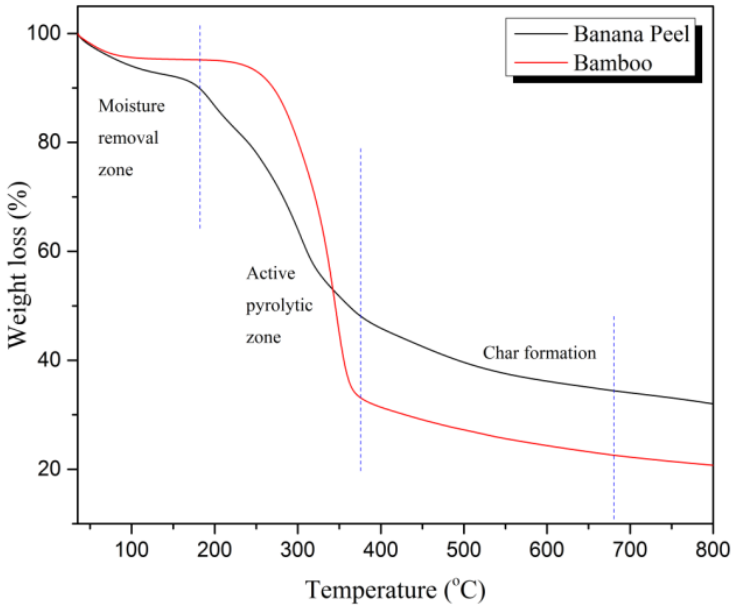


**Fig. 3.3** TGA profile of raw biomass samples (Banana peel and bamboo)

### 3.3.5 ELEMENTAL COMPOSITION OF ASH AND BIOCHAR SAMPLES (WT%) BY EDX

The composition of elements present in the ash samples (BPS, MBP, and MAP) and biochars (BB, BPB, and BCC) was determined with the help of Energy dispersive X-ray Spectroscopy (EDX), and the results are summarized in Table 3.5.

**Table 3.5** Elemental analysis of ash samples (BPS, MBP, and MAP) and adsorbents (BB, BPB, and BCC) using EDX

| | For Absorption | | | For Adsorption | | |
|---|---|---|---|---|---|---|
| **Components** | **BPS (wt%)** | **MBP (wt%)** | **MAP (wt%)** | **BB (wt%)** | **BPB (wt%)** | **BCC (wt%)** |
| K | 31.8 | 38.4 | 34.2 | 8.5 | 31.7 | 3.8 |
| C | 11.2 | 13.4 | 16.2 | 45.4 | 24.1 | 19.7 |
| O | 44.2 | 39.2 | 38.7 | 34.9 | 36.9 | 47.5 |
| Ca | 4.4 | 1.3 | 1.7 | 1.9 | 4.7 | - |
| P | 2.7 | 2.0 | 2.0 | 1.5 | - | - |
| Mg | 1.4 | 1.5 | 2.1 | 2.3 | 1.3 | - |
| Si | 1.0 | 1.4 | 1.5 | 5.1 | 1.1 | 10.7 |
| Mn | - | - | 0.2 | - | - | - |
| Al | - | - | 0.1 | - | - | 11.6 |
| Zn | 0.1 | - | 0.1 | - | - | - |
| Fe | 0.1 | - | - | - | - | 6.7 |

The major elements detected in the ash samples are O, K, and C, followed by small amounts of Ca, P, Mg, and Si. MBP ash has the highest potassium content (38.4 wt%), followed by MAP ash (34.2 wt%) and BPS (31.8 wt%). A high concentration of potassium is expected to increase the pH of the base solutions [Juárez et al., 2018]. The percentage weight of calcium in the biomass ash samples is very low as compared to potassium; 4.4%, 1.3%, and 1.7% for BPS, MBP, and MAP, respectively. However, the percentage of calcium (4.4 wt%) and phosphorous (2.7 wt%) was higher in BPS ash compared to MAP and MBP ashes. Other elements like P, Mg, Si, S, Mn, Al, Zn, and Fe are also present but in trace amounts.

C, O, K, Si, Mg, Ca, and P are the major elements found in BB and BPB. The elements detected in BCC are C, O, K, Si, Al, and Fe. The potassium content of BPB (31.7 wt%) is the highest amongst all biochars, followed by BB (8.5 wt%) and BCC (3.8 wt%). It was noticed that in the case of BCC, the percentages of Al and Fe are 11.6 and 6.7 wt%, whereas there is no detection of Al and Fe in BB and BPB. The percentage of silicon (10.7 wt%) in BCC is found to be higher as compared to BB (5.1 wt%) and BPB (1.1 wt%). The higher percentage of silicon in BCC indicates quartz as the major component of the clay material. The presence of a high concentration of inorganic metal oxides such as potassium, calcium, silicon, and magnesium in all samples is anticipated to react with water to form hydroxides, which in turn would help to remove $CO_2$ and $H_2S$ from biogas through physico-chemical reactions [Andersson and Nordberg, 2017].

### 3.3.6 FIELD EMISSION SCANNING ELECTRON MICROSCOPE IMAGES OF RAW BIOMASS AND THEIR ASHES

Figures 3.4, 3.5, and 3.6 show the FESEM images of the raw biomass samples and their ashes of BPS, MBP, and MAP. From the micrograph, it can be observed that the raw biomass samples have packed structures, whereas, on conversion to their ashes, the surface area and porosity of the samples increase due to the breakage of the structures and release of inorganic metal compounds.

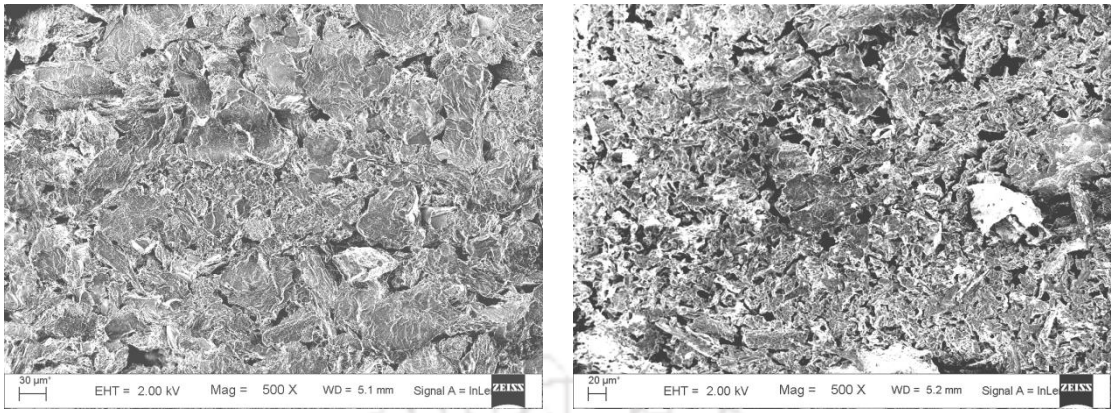


**Fig. 3.4** FESEM images of raw (left) and ash (right) samples of BPS

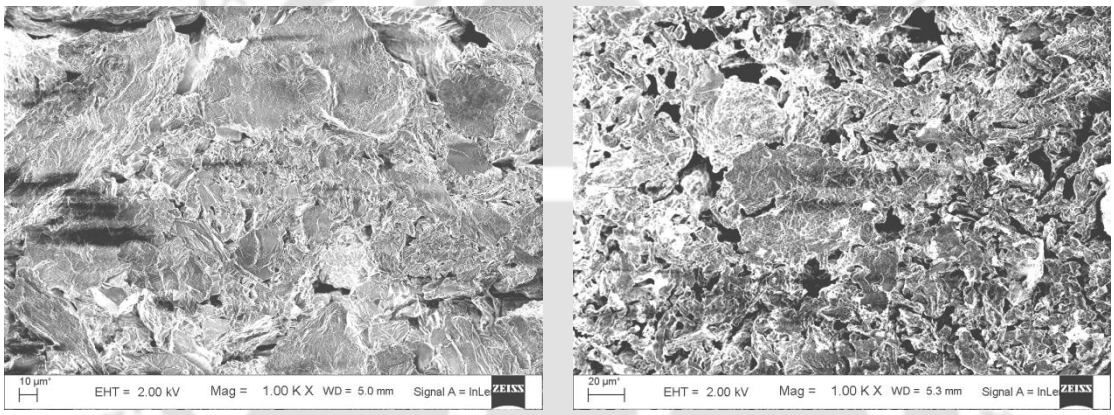


**Fig. 3.5** FESEM images of raw (left) and ash (right) samples of MBP

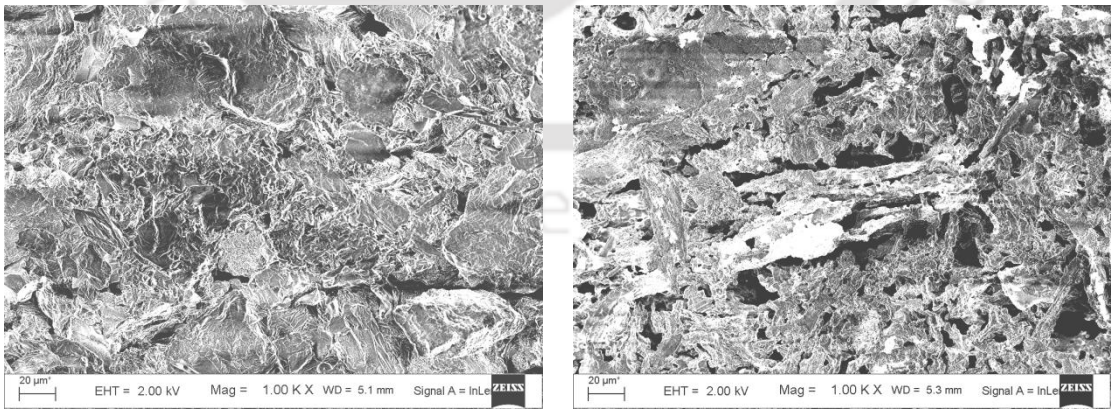


**Fig. 3.6** FESEM images of raw (left) and ash (right) samples of MAP

On the other hand, Figures 3.7, 3.8, and 3.9 show the FESEM images of BB, BPB, and BCC at a magnification of 10.00 KX respectively. From the micrograph, it can be observed that the porosity and the surface area of BPB and BB are comparatively higher than those of BCC. The formation of the porous cylindrical structures is attributed to the formation and subsequent expulsion of volatile components [Yin et al., 2013]. However, in Figure 3.9, the clay particles can be seen as small lumps. It is anticipated that the presence of rough surfaces and porous structures in the respective ash and biochar samples facilitates the sorption of $CO_2$ and $H_2S$ from biogas through certain physico-chemical reactions on the surface and pores.

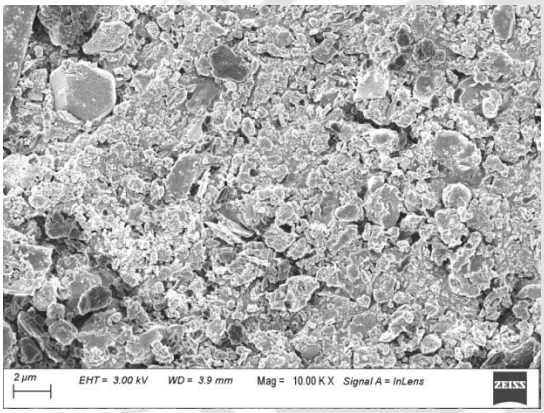


**Fig. 3.7** FESEM image of BB

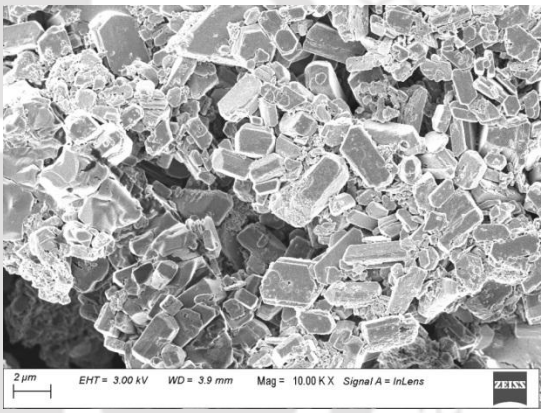


**Fig. 3.8** FESEM image of BPB

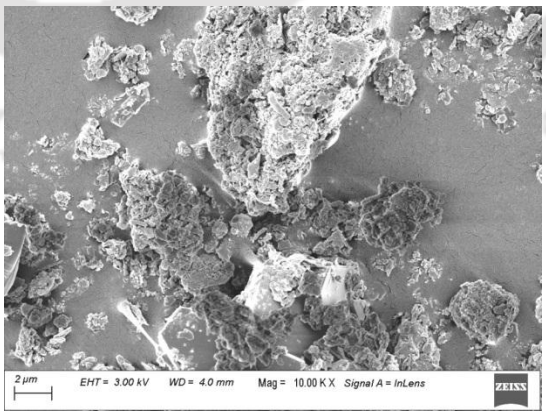


**Fig. 3.9** FESEM image of BCC

### 3.3.7 ANALYSIS OF ELEMENTS IN ASH SOLUTIONS

The concentration (mg $g^{-1}$) of alkali and alkaline earth metals present in BPS, MBP, and MAP ash solutions was determined with the help of a flame photometer. As indicated by EDX analysis, flame photometry confirms potassium as the major cationic constituent in all three samples (Table 3.6).

**Table 3.6** Elemental analysis of ash samples using a flame photometer. Each value is the Mean ± SD of three replicates.

| Samples | $K^+$ (mg $g^{-1}$) | $Na^+$ (mg $g^{-1}$) | $Ca^{2+}$ (mg $g^{-1}$) |
|---|---|---|---|
| BPS | 189.64 ± 1.77 | 0.66 ± 0.0700 | 1.97 ± 0.08 |
| MBP | 228.40 ± 1.04 | 0.0045 ± 0.0007 | 0.43 ± 0.02 |
| MAP | 209.72 ± 2.29 | 0.0017 ± 0.0002 | 1.34 ± 0.14 |

The average potassium quantity in MBP ash is found to be slightly higher (228.40 mg $g^{-1}$) than in MAP ash (209.72 mg $g^{-1}$) and BPS (189.64 mg $g^{-1}$). The finding is very encouraging as the presence of alkali (K) and alkaline earth metals (Ca) in higher quantities would contribute towards increasing the pH of the natural base solutions. However, as expected, the concentration of sodium and calcium was relatively low as compared to potassium.

### 3.3.8 POROSITY AND BET SURFACE AREA OF ADSORBENTS

Table 3.7 shows the BET surface area, pore volume, and adsorption average pore diameter of the adsorbent samples. Among all the adsorbents, the highest BET surface area for BPB was measured at 9.32 $m^2/g$, followed by BB (7.53 $m^2/g$) and BCC (3.36 $m^2/g$).

**Table 3.7** BET surface area, pore volume and adsorption average pore diameter of adsorbents

| Biochar Sample | BET Surface Area ($m^2/g$) | Pore Volume ($cm^3/g$) | Micropore volume ($cm^3/g$) | Adsorption average pore diameter (nm) |
|---|---|---|---|---|
| BB | 7.53 | 0.0242 | 0.0006 | 12.8 |
| BPB | 9.32 | 0.0399 | 0.0009 | 17.1 |
| BCC | 3.36 | 0.0093 | 0.0013 | 11.1 |

Though the BET surface areas for the biochars were low, they are within the general range (2–200 $m^2/g$) of biochars produced from various biomasses [Shinogi and Kanri, 2003]. Likewise, the pore volume of BPB was measured as 0.0399 $cm^3/g$, which is higher than BB (0.0242 $cm^3/g$) and BCC (0.0093 $cm^3/g$) respectively. Interestingly, the low BET surface area and porosity of the adsorbents assume the occurrence of structural collapse during carbonization due to the catalytic effect of the alkali and alkaline earth metals that were present in very high concentrations [Surra et al., 2019]. Carbonization temperature also plays an important role in enhancing biochar properties and, thus, the formation of micro-and mesopores. Moreover, the BJH pore size distribution curves of all the adsorbents are shown in Annexure A (Figures A1, A2, and A3). Figures 3.10, 3.11, and 3.12 show the $N_2$ adsorption-desorption isotherms of BB, BPB, and BCC. It is evident from the $N_2$ adsorption-desorption isotherms of adsorbents that BPB has the highest adsorption capacity of 29 $cm^3/g$, followed by BB (18 $cm^3/g$) and BCC (7 $cm^3/g$), which may be attributed to their hydrophilic nature, respective surface area, and pore volume.

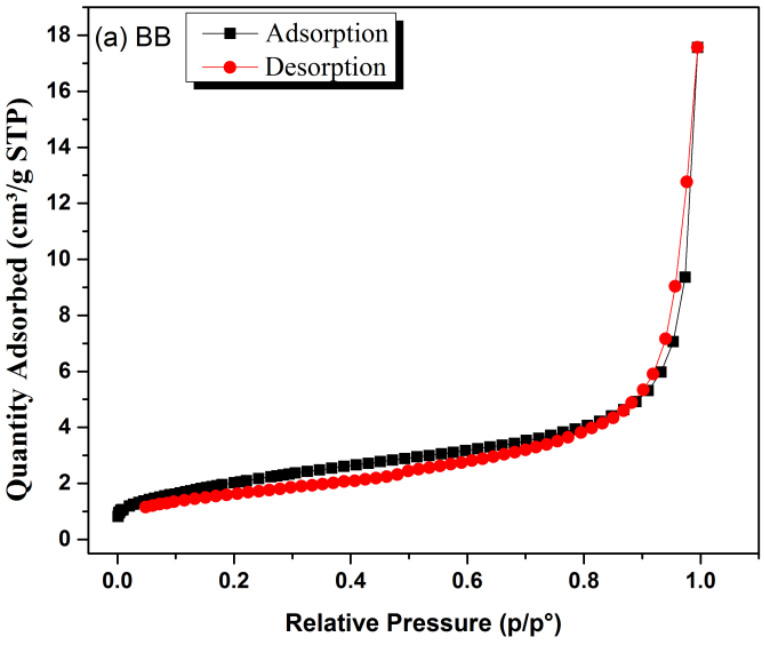


**Fig. 3.10** $N_2$ adsorption-desorption isotherms of BB

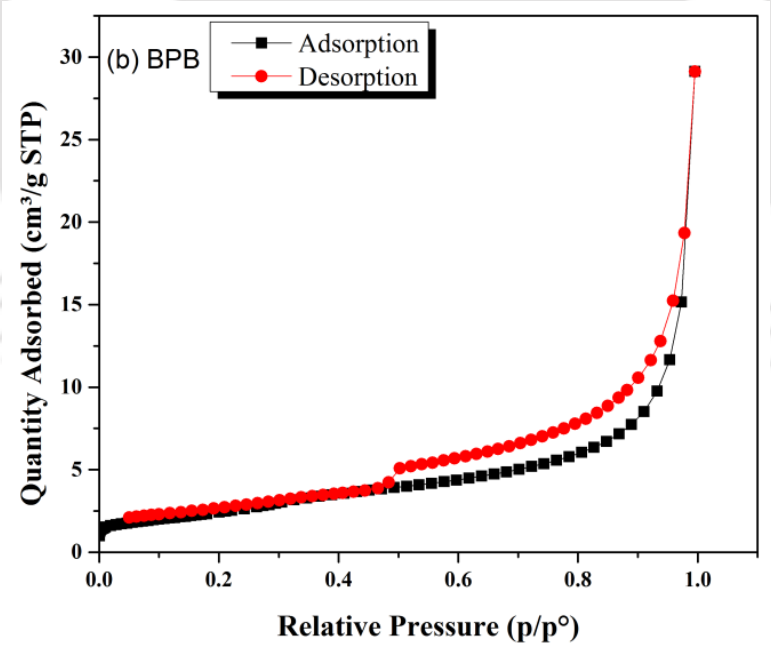


**Fig. 3.11** $N_2$ adsorption-desorption isotherms of BPB

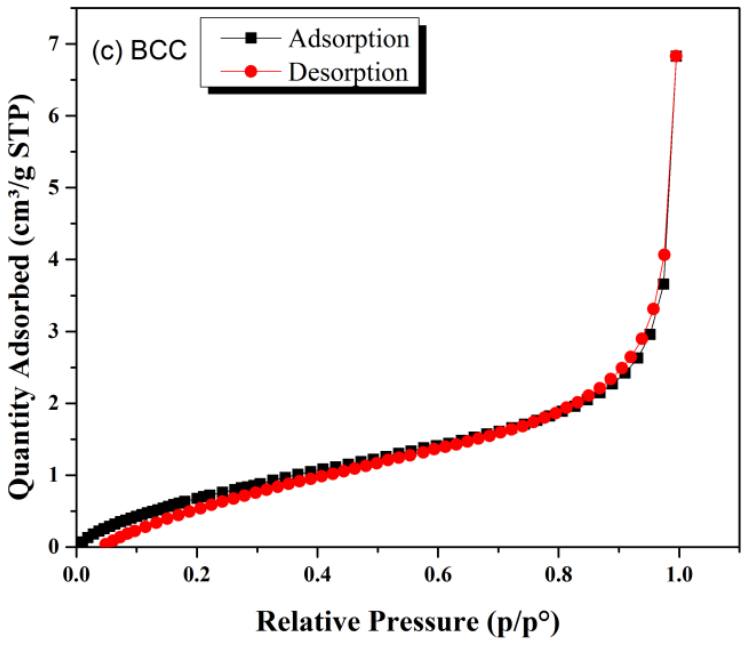


**Fig. 3.12** $N_2$ adsorption-desorption isotherms of BCC

It has been reported that the efficiency of $H_2S$ adsorption increases with biochars having a higher BET surface area and pore volume. Accordingly, the order of potential of the three adsorbents for $H_2S$ adsorption should be highest for BPB, followed by BB and BCC.

### 3.3.9 SELECTION OF BIOMASS AS SCRUBBING AGENTS FOR ABSORPTION AND ADSORPTION

Finally, the following biomasses: Banana pseudostem, *Musa balbisiana* peel, *Musa acuminata* peel, *Bambusa balcooa* (Bhaluka bamboo) and clay were chosen for the preparation of scrubbing agents based on the following criteria as discussed in Table 3.8.

**Table 3.8** Criteria for selecting biomass as scrubbing agents

| **Absorption** | **Adsorption** |
|---|---|
| Availability and high production of biomass | |
| Physico-chemical properties of ash like pH and elemental compositions | Physico-chemical properties of biochar like pH, elemental compositions, surface area, and porosity |
| Inexpensive and easily accessible | |

Thus, out of five scrubbing agents, BPS, MBP, and MAP were selected for the process of $CO_2$ absorption, and similarly, BB, BPB, and BCC were selected amongst the five adsorbents for further analysis based on physico-chemical properties like ash content, pH, elemental compositions, and porosity. Also, hardly any literature was found on biogas purification from these selected scrubbing agents and adsorbents. Application of natural base scrubbing agents and biomass-derived adsorbents is envisioned to be advantageous, especially for small decentralized biogas plants (1-10 $m^3$) installed in rural areas, over other conventional chemicals used for purification of biogas because the source materials are abundantly available, have a low production cost, and the process of preparation is easy and can be easily adopted.

## 3.4 SUMMARY OF THE CHAPTER

Based on the survey, available literature, and preliminary analysis, six types of biomass-based scrubbing agents and adsorbents, viz., BPS, MBP, MAP, BB, BPB, and BCC, were characterized in detail by using different techniques such as proximate, TGA, pH, EDX, flame photometry, FESEM, and BET. The physico-chemical properties of all the selected scrubbing agents showed that they are rich in mineral content and have a very high pH, which makes them naturally

alkaline. FESEM images and BET showed the presence of rough surfaces and porous structures in the ash and biochar samples, respectively. Thus, the findings indicate that biomass-derived scrubbing agents and adsorbents can be utilized for the removal of $CO_2$ and $H_2S$ from raw biogas.

The next chapter discusses the observations of experimental analysis, mechanisms, and kinetics of $H_2S$ adsorption from raw biogas using the selected adsorbents.

# Chapter 4

## $H_2S$ Removability from Biogas using Naturally Alkaline Adsorbents derived from Biomass

# CHAPTER 4: $H_2S$ REMOVABILITY FROM BIOGAS USING NATURALLY ALKALINE ADSORBENTS DERIVED FROM BIOMASS

## 4.1 INTRODUCTION

The presence of a high concentration of $H_2S$ in biogas needs special attention for both direct combustion for cooking and power generation as well as up-gradation to bio-methane due to its foul-smelling odor, toxicity, corrosion, health issues, regeneration, and environmental problems [Chen et al., 2017; Rasi et al., 2011]. The removal of $H_2S$ from raw biogas is necessary prior to using biogas efficiently in any commercial application or biogas upgrade. Thus, in this context, the present chapter is an attempt to study the suitability and applicability of the selected adsorbents based on their characterization for $H_2S$ removal from raw biogas by the process of adsorption.

## 4.2 MATERIALS AND METHODS

### 4.2.1 COLLECTION OF BIOMASS AND PROCESSING TO ADSORBENTS

The solid waste banana peel (*Musa balbisiana* peel) and waste dry bamboo (*Bhaluka*) were collected from a local village situated near the Indian Institute of Technology Guwahati (IITG), Guwahati, Assam-781039, India. Collected biomass was washed with tap water many times to ensure the complete removal of dust particles. The samples were cut into small pieces and kept in a hot air oven at 60 °C for 24 hours. The dried pieces were ground into small pieces using a crusher. After this, the biomass was carbonized under an oxygen-poor atmosphere in a furnace at 500°C for 3 hours. The carbonization temperature of biochar plays a significant role in imparting the adsorption capacity of biochar and is likely to depend on the biomass substrate. Sahota et al.

(2018) reported a maximum of 84.22% of $H_2S$ removal using leaf waste biochar carbonized at 400 °C. Pelaez-Samaniego et al. (2018) discovered that at 300 and 400 °C, biochar made from anaerobically digested dairy fibre had a lower $H_2S$ scrubbing capacity. However, biochar produced at 500 and 600 °C temperatures had a higher $H_2S$ removal efficiency from biogas. Therefore, we focused on carbonization temperature up to 500 °C for 3 hours and also our selected biomass is lignocellulosic in nature which requires higher temperature to convert it completely into char [Tan et al., 2017].

Clay was procured from a local pottery vendor, which was mixed with solid waste banana peel after cleaning under tap water, in a 1:1 mass ratio, and was kept in a furnace at 500 °C for 3 hours to form a mixture sample. The composite thus prepared was impregnated with banana peel ash solution and oven-dried at 80 °C for 24 hours. Biochars and biochar-clay composites with a particle size of approximately <0.5 mm, obtained by sieving through standard sieves (mesh no. 40), were used as adsorbents. The three adsorbents prepared, *viz.*, bamboo biochar (BB), banana peel biochar (BPB), and biochar-clay composite (BCC), were stored in an inert condition and used to remove $H_2S$ from raw biogas.

### 4.2.2 EXPERIMENTAL PROCEDURE FOR $H_2S$ ADSORPTION

A fabricated portable scrubber made of CPVC cylindrical pipe having two ends for inlet and outlet, respectively, was used as a scrubber for $H_2S$ removal from raw biogas. The height of the packed scrubber was 180 mm, with an internal diameter of 25 mm. A perforated sheet of approximately <0.25 mm pore size was fixed at both ends of the scrubber to support the loaded adsorbents. Each experiment for the adsorbents was performed at ambient temperature (25–30 °C) in triplicate, and the biogas pressure was kept slightly higher than the atmospheric pressure

(gauge pressure of nearly 20 kPa) with the help of a micro pressure gauge. 9 g of each biochar (BB and BPB) and 20 g of BCC were loaded into the packed bed scrubber, which was connected to a 3 $m^3$ Deenbandhu model biogas plant situated at Aaoniati Satra near IIT Guwahati (26°11'27.8"N, 91°43'17.3"E). Live experiments were performed to evaluate the applicability and suitability of biochars and biochar-clay composites as adsorbents for $H_2S$ removal from raw biogas. A process flow diagram of the experimental setup for the removal of $H_2S$ is shown in Fig. 4.1.

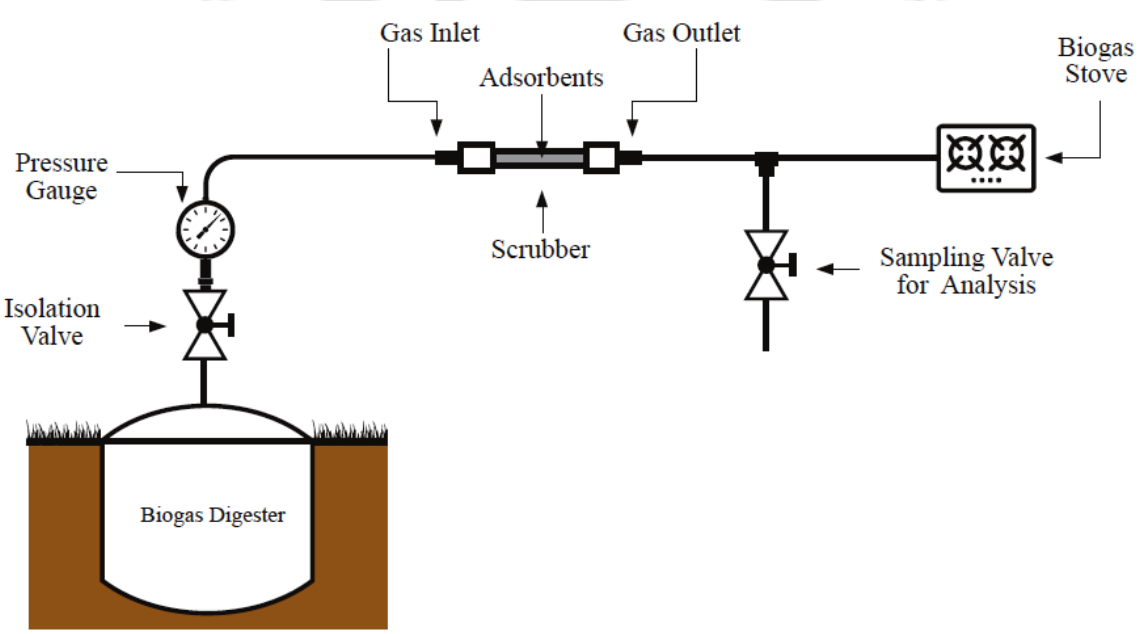


**Fig. 4.1** Process flow diagram of the experimental setup for $H_2S$ adsorption

### 4.2.3 REMOVAL EFFICIENCY AND $H_2S$ ADSORPTION CAPACITY OF ADSORBENTS

The removal efficiency and $H_2S$ adsorption capacity of the adsorbents were evaluated using Eqs. 4.1 and 4.2 [Mulu et al., 2021; Pan et al., 2017].

$$\text{Removal efficiency (\%)} = \frac{C_0 - C_1}{C_0} \text{ x } 100\% \quad (4.1)$$

$$\text{Adsorption capacity, } q_e = \frac{C_0 - C_e}{m} V \quad (4.2)$$

where $C_0$ is the initial adsorbate ($H_2S$) concentration, $C_1$ is the adsorbate ($H_2S$) concentration after purification at time t, and $C_e$ is the equilibrium adsorbate ($H_2S$) concentration, V is the volume of solution, m is the amount of adsorbent and $q_e$ is the equilibrium adsorption capacity.

### 4.2.4 DETAILED CHARACTERIZATION OF ADSORBENTS BEFORE AND AFTER TREATMENT

A comparison of the detailed characterization of adsorbents before and after treatment was carried out to understand the mechanisms behind the removal of $H_2S$. The techniques and instruments used for the study were discussed in chapter 3 under subsection 3.2.3.

### 4.2.5 $H_2S$ ANALYSIS BY HANDHELD BIOGAS ANALYZER

The treated and untreated biogas samples were collected in tedlar bags at 5 minutes' time interval and were analyzed for $H_2S$ concentration by a handheld biogas analyzer *(Make: Gas Data Ltd., Model: GFM416)* with a detection range of 0–5000 ppm.

### 4.2.6 KINETICS OF $H_2S$ ADSORPTION ON ADSORBENTS

The kinetics of $H_2S$ adsorption on BB, BPB, and BCC were studied using four widely used kinetic models, viz., pseudo first-order, pseudo second-order, intraparticle diffusion, and Elovich models. The following kinetic equations are described as follows [Chen et al., 2011; Han et al., 2020; Pan et al., 2017]:

Pseudo first-order equation: $$\ln(q_e - q_t) = lnq_e - k_1 t \quad (4.3)$$

Pseudo second-order equation: $$\frac{t}{q_t} = \frac{1}{k_2 q_e^2} + \frac{t}{q_e} \quad (4.4)$$

Intraparticle diffusion equation: $$q_t = k_p t^{1/2} + \mathrm{C} \quad (4.5)$$

where $q_e$ and $q_t$ (mg $g^{-1}$) is the amount of $H_2S$ adsorbed at equilibrium and time t (min), $k_1$ ($min^{-1}$) and $k_2$ (g $mg^{-1}$ $min^{-1}$) are the pseudo first-order and pseudo second-order rate constants respectively; $k_p$ (mg $g^{-1}$ $min^{-1/2}$) is the intraparticle diffusion rate constant, and C is the constant (intercept) associated with the boundary layer effect.

Elovich equation: $$q_t = \frac{\ln(a_e b_e)}{b_e} + \frac{1}{b_e}\ln \mathrm{t} \quad (4.6)$$

The parameter $a_e$ (mg $g^{-1}$ $min^{-1}$) denotes the initial adsorption rate, and $b_e$ (g $mg^{-1}$) represents the extent of surface coverage for the chemisorption. For the various models, the kinetic constants of adsorption were calculated, and the linear regression correlation coefficient ($R^2$) values were compared to evaluate the best-fit model.

## 4.3 RESULTS AND DISCUSSION

### 4.3.1 $H_2S$ REMOVAL BY ADSORBENTS

The $H_2S$ concentration in raw biogas may vary in the range of 10 to 5000 ppm and is fully dependent on the feed materials used in anaerobic digesters for the production of biogas [Mann et al., 2009]. For the experimental purpose, only cattle dung was used as feed material in the biogas digester. The $H_2S$ content in the raw biogas was found to be approximately 398±12 ppm. The other main components present in the raw biogas were 56% $CH_4$, 43% $CO_2$, <1% $N_2$, moisture, and a trace amount of $O_2$. Biogas produced from an anaerobic digestion system is

naturally saturated with moisture. Due to the hydrophilic nature of biochar, the moisture present in the raw biogas maintains the moisture content of the biochar, which facilitates $H_2S$ adsorption over the biochar surface. Moreover, the surface chemistry also plays a key role in $H_2S$ oxidation, due to the catalytic reactions. Trace oxygen present in the biogas or oxygen groups at the surface of the biochar act as catalysts in the $H_2S$ oxidation reaction to yield elemental sulphur ($S^0$) and other sulphurous compounds [Adib et al., 2000; Sitthikhankaew et al., 2014]. Periodic changes in $H_2S$ concentration with time after treatment with BB, BPB, and BCC are shown in Fig. 4.2. When treated with adsorbents, the $H_2S$ content in the purified biogas decreased to 49±2, 43±5 and 86±5 ppm when subjected to the scrubber packed with BB, BPB, and BCC, respectively.

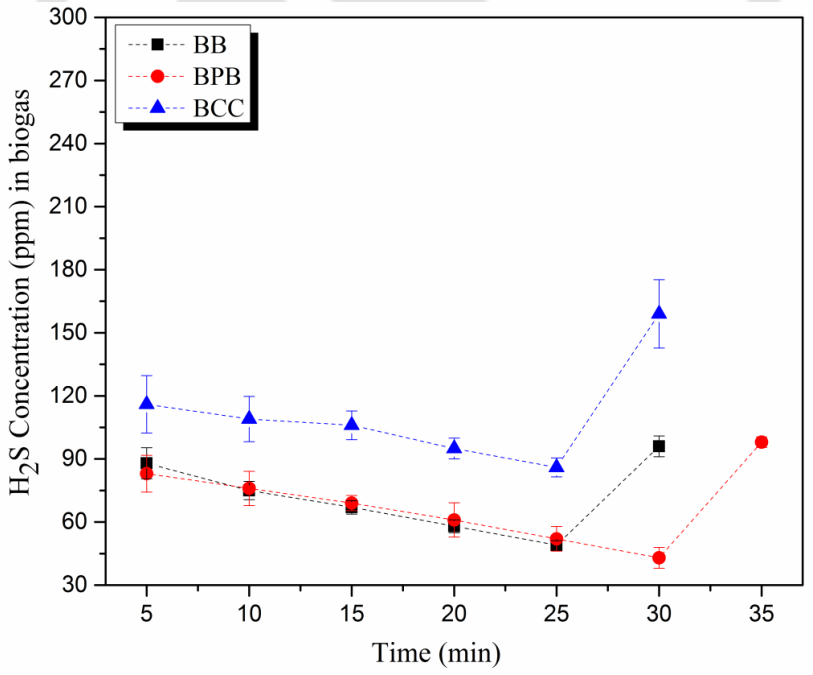


**Fig. 4.2** Time-dependent variation in the concentration of $H_2S$ in the outlet

The highest $H_2S$ adsorption capacities for BB, BPB, and BCC observed from the breakthrough experiments were 3.42, 3.48, and 1.37 mg $H_2S$ $g^{-1}$ biochar, respectively. The average $H_2S$

removal efficiency was calculated for all the adsorbents, with the highest reduction of up to 87.7% (BB) in 25 min, 89.2% (BPB) in 30 min, and 78.4% (BCC) in 25 min, respectively (Fig. 4.3). It was noticed from the results that after these equilibrium positions, the outlet $H_2S$ concentration started increasing till complete saturation of the adsorbents. The results indicate that the adsorption capacity of BB and BPB for $H_2S$ is at its maximum at the initial 25–30 minute interval, which then gradually decreases and reaches 50% saturation after approximately 45 minutes.

On the other hand, the graph for BCC showed maximum adsorption capacity at the initial 25 minutes and reached 50% saturation after 30 minutes of operation. This shows the saturation of the respective adsorbents and their need to be replenished with fresh adsorbents. Therefore, fresh and saturated adsorbent samples were characterized in order to distinguish the difference in characteristics and to study the $H_2S$ adsorption mechanisms. It has been reported that $H_2S$ adsorption takes place both on the surface as well as in the pores of biochar [Seredych et al., 2008]. The difference in $H_2S$ adsorption capacity amongst the adsorbents may be attributed to their surface pH, morphology, inorganic metal compositions, and pore dimensions. Hence, the next sections compare the surface pH, porosity, morphology, and elemental composition of the fresh and $H_2S$ saturated adsorbents to better understand the adsorption mechanism.

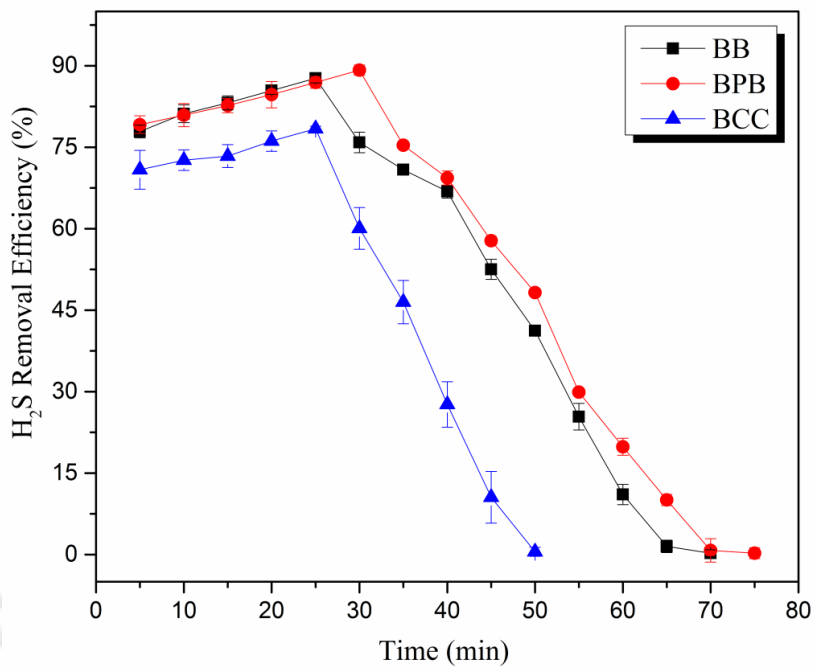


**Fig. 4.3** $H_2S$ removal efficiency of adsorbents with respect to time

### 4.3.2 pH OF ADSORBENTS

pH plays an important role in the sorption of $H_2S$ because with an increase in pH, the chemical equilibrium favours mass transfer towards the formation of more soluble species, such as hydrosulfide ($HS^-$) or sulfide ($S^{2-}$) [Dean, 1999; Laplanche et al., 1994]. Hence, the surface pH of the respective adsorbents before and after treatment was determined. The pH of the adsorbents BB, BPB, and BCC before adsorption was measured as 10.67, 10.95, and 9.96, respectively, which renders the biochars and BCC as potential $H_2S$ adsorbers, as the first and second dissociation constants of $H_2S$ are reported as 6.9 and 12.75, respectively [Dean, 1999]. The high pH of the adsorbents is due to the formation of alkaline species at higher preparation temperatures, as verified by EDX and XRD analysis. The initial $H_2S$ sorption from raw biogas by the adsorbents can be represented by equations 4.7 and 4.8.

$$H_2S_{(gas)} \rightarrow H_2S_{(ads)} \rightarrow H_2S_{(ads-liq)} \qquad (4.7)$$

$$H_2S_{(ads-liq)} + OH^- \rightarrow HS^-_{(ads)} + H_2O \quad (4.8)$$

$$HS^-_{(ads)} + OH^- \rightarrow S^{2-} + H_2O \quad (4.9)$$

$$HS^-_{(ads)} + O_2 \rightarrow S^0 \quad (4.10)$$

$$HS^-_{(ads)} + O_2 + H_2O \rightarrow SO_4^{2-} \quad (4.11)$$

where $H_2S_{(gas)}$, $H_2S_{(ads)}$ and $H_2S_{(ads-liq)}$, refer to the $H_2S$ in the gas, adsorbed, and liquid phases, respectively.

There are several basic mechanisms through which the removal of $H_2S$ from raw biogas may take place. However, the overall mechanism for $H_2S$ removal from raw biogas remains almost the same: $H_2S$ adsorption and $H_2S$ oxidation, as shown in equations 4.7–4.11 [Fernández-Delgado Juárez et al., 2018; Xu et al., 2014].

The average pH of the saturated adsorbents BB, BPB, and BCC was reduced significantly to 8.41, 8.59, and 8.81, respectively (Table 4.1), owing to the acid gas dissociation when $H_2S$ comes into contact and gets adsorbed on the surface of the alkaline adsorbents (Eq. 4.8). Although the pH range was well within the two dissociation constants of $H_2S$, no further $H_2S$ sorption was observed. This could be due to the blockage of the active site on the surface of the adsorbents by $H_2S$ molecules through physicochemical reactions.

**Table 4.1** Comparison of pH of biochars before and after adsorption. Each value is the Mean ± SD of three replicates.

| Adsorbents | Before adsorption | After adsorption |
|---|---|---|
| | pH | pH |
| BB | 10.67 ± 0.03 | 8.41 ± 0.02 |
| BPB | 10.95 ± 0.03 | 8.59 ± 0.04 |
| BCC | 9.96 ± 0.04 | 8.81 ± 0.05 |

Further, the pore size of the adsorbents also plays a significant role, as described in chapter 3 under sub section 3.3.8.

### 4.3.3 MORPHOLOGY OF ADSORBENTS

Figure 4.4, 4.5, and 4.6 show the comparison of FESEM images of the three adsorbents before and after $H_2S$ sorption. From images 4.4 and 4.5, it is clearly evident that $H_2S$ adsorption leads to agglomerate formation amongst the biochar particles for both BB and BPB. However, in the case of BCC (Fig. 4.6), a decrease in agglomerates is visible after $H_2S$ sorption. This may be attributed to the disintegration of structural continuity of the biochar clay particles on $H_2S$ penetration and adsorption. The pyrolysis temperature of the biochar plays an important role in increasing the surface area and mineral and metal content [Pelaez-Samaniego et al., 2018]. All the biochars have heterogeneous morphology with a rough surface, scattered micropores, and the brighter areas show the presence of inorganic matter. The rough surfaces with micropores along with the high surface pH could be the reason as a binding site for $H_2S$ adsorption where they undergo various physio-chemical reactions.

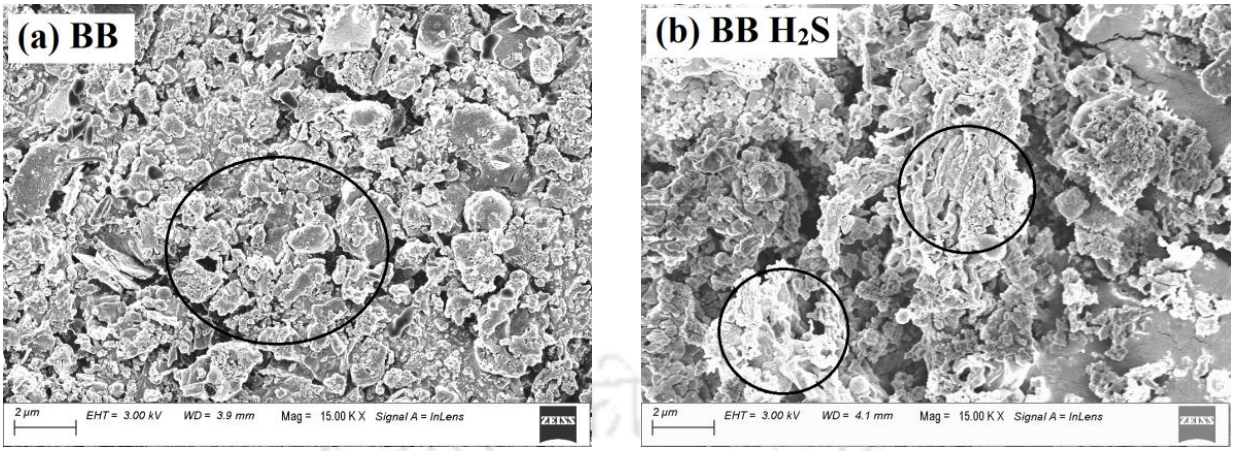


**Fig. 4.4** FESEM images of BB (a) before $H_2S$ sorption and (b) after $H_2S$ sorption

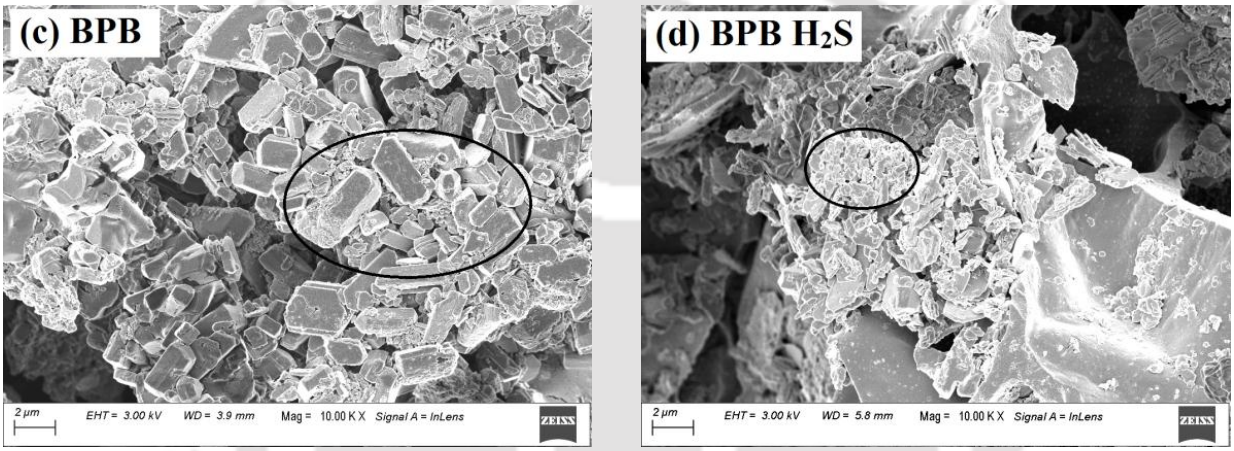


**Fig. 4.5** FESEM images of BPB (c) before $H_2S$ sorption and (d) after $H_2S$ sorption

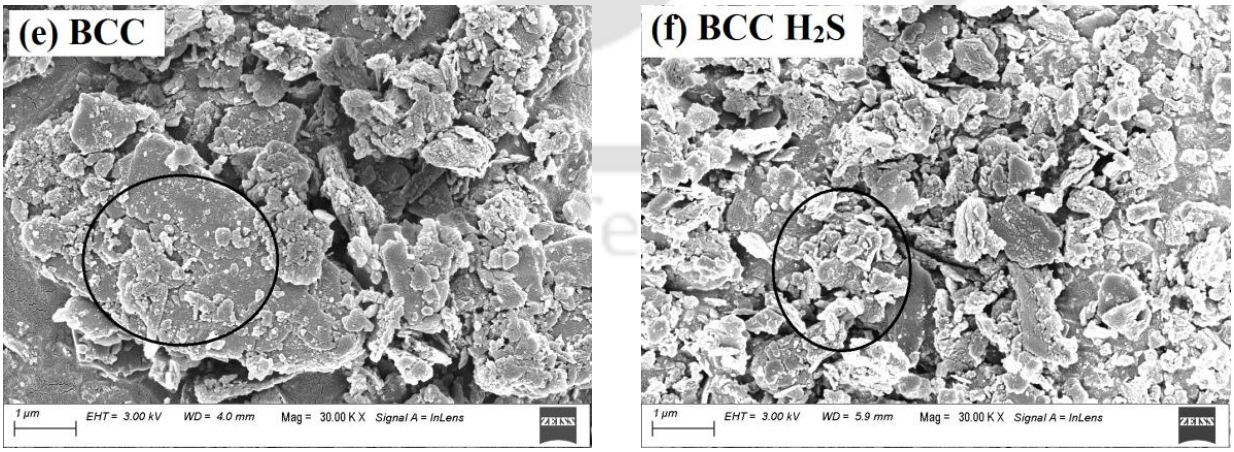


**Fig. 4.6** FESEM images of BCC (e) before $H_2S$ sorption and (f) after $H_2S$ sorption

### 4.3.4 ELEMENTAL COMPOSITION OF ADSORBENTS

Elemental compositions of BB, BPB, and BCC samples before and after $H_2S$ sorption, determined using EDX, are shown graphically in Figs. 4.7, 4.8, and 4.9 (mean of three replicate values). However, the SEM with EDX images of the three adsorbents may be seen in annexure D (Figs. D1, D2, D3, D4, D5, and D6 respectively). The presence of minerals such as K, Ca, Al, and Mg plays an important role as it can enhance the catalytic behaviour of a carbonaceous material for converting $H_2S$ into elemental sulfur and sulfates [Castrillon et al., 2016; Zhang et al., 2015].

EDX spectra of the adsorbents indicate that they are a mixture of scattered carbon particles with a combination of various minerals. The contents of C and O ranged from 10 to 45 wt% and 34–47 wt%, respectively, in fresh and saturated adsorbent samples. The presence of alkali and alkaline earth metals contributes to a higher surface pH. The highest K content was determined for BPB (31.7 wt%), followed by BB (8.5 wt%) and BCC (3.8 wt%). From the EDX analysis, it is evident that S was absent in the fresh adsorbent samples, but after treatment with the raw biogas, the saturated adsorbents exhibited the presence of S of about 2.2 wt% in BB, 2.6 wt% in BPB, and 0.5 wt% in BCC. This suggests the sorption of $H_2S$ by the respective adsorbents through certain physio-chemical reactions. The results indicate that the surface roughness, porosity, oxygen, and other alkaline mineral contents determine the removal efficiency of $H_2S$ from raw biogas. Thus, the sorption and conversion rate of $H_2S$ to $S^0$ and other sulphurous compounds is comparatively higher for BPB than for BB and BCC.

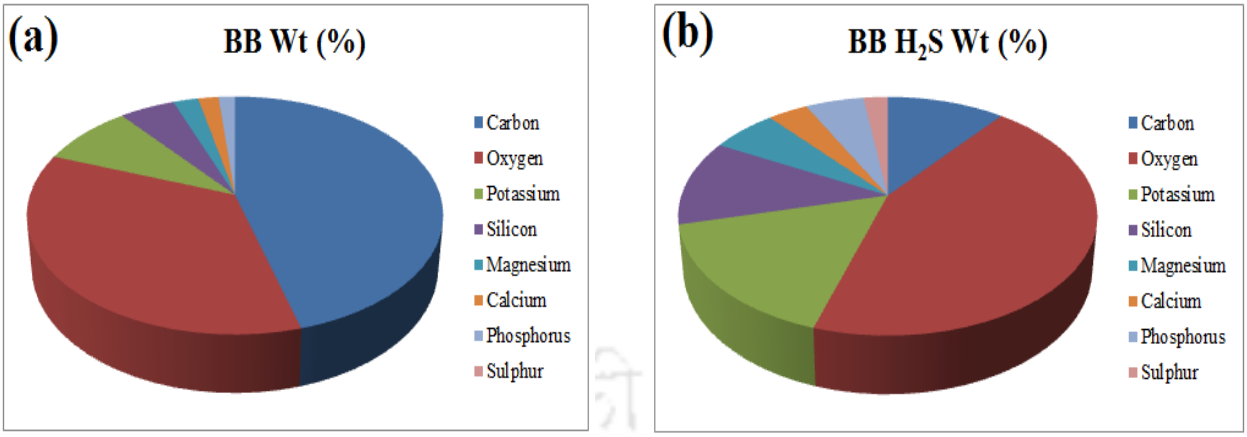


**Fig. 4.7** EDX analysis of BB (a) before $H_2S$ sorption and (b) after $H_2S$ sorption

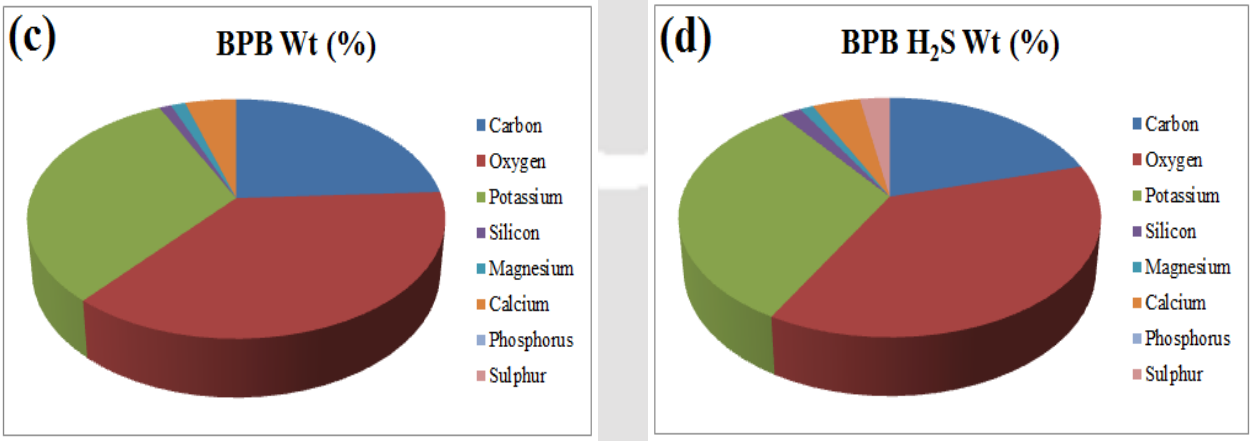


**Fig. 4.8** EDX analysis of BPB (c) before $H_2S$ sorption and (d) after $H_2S$ sorption

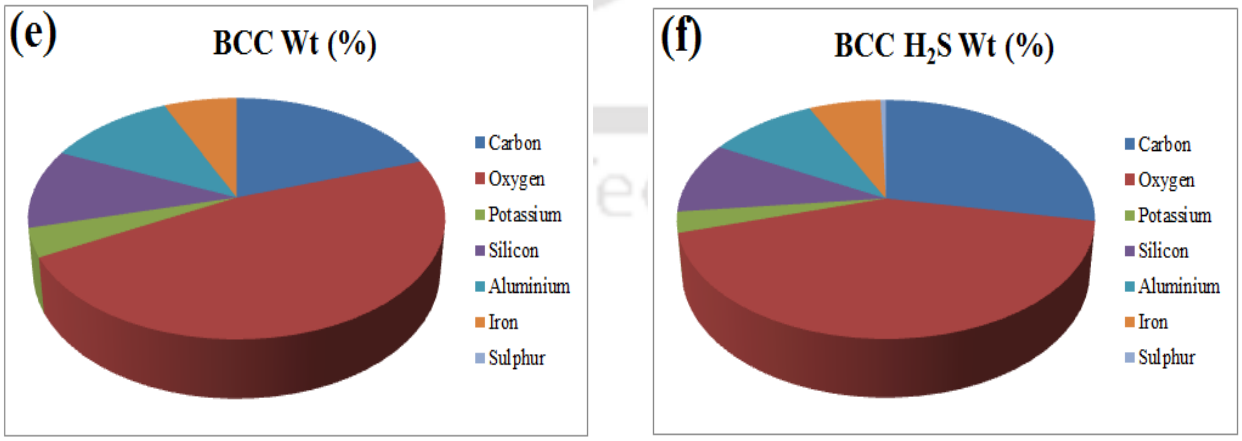


**Fig. 4.9** EDX analysis of BCC (e) before $H_2S$ sorption and (f) after $H_2S$ sorption

### 4.3.5 POWDER X-RAY DIFFRACTION OF ADSORBENTS

To elucidate the difference in the composition of minerals, XRD analysis was performed on the adsorbents before and after the sorption of $H_2S$ from raw biogas. The comparison of XRD patterns of adsorbents BB, BB $H_2S$; BPB, BPB $H_2S$; and BCC, BCC $H_2S$ is shown in Figs. 4.10, 4.11, and 4.12, respectively. XRD patterns were observed for freshly prepared and saturated adsorbents that are almost similar except for a few additional peaks in the $H_2S$ saturated adsorbents. The observed results indicated the presence of $K_2CO_3$, Quartz ($SiO_2$), and Calcite ($CaCO_3$) in both BB and BPB. Additionally, $(Ca,Mg)_3(PO_4)_2$ is the other compound present in BB. On the other hand, BCC contains Quartz ($SiO_2$), Alumina ($Al_2O_3$), Hematite ($Fe_2O_3$) and $K_2CO_3$ as the initial compounds. The diffraction data of adsorbents after $H_2S$ sorption (BB, BPB, and BCC) shows the presence of additional compounds like $CaSO_4.2H_2O$ (gypsum), $K_2SO_4$, and elemental sulphur ($S^0$). The XRD analysis showed the peak of $CaSO_4.2H_2O$ at $2\theta = 30.9°$, $K_2SO_4$ at $2\theta = 36.5°$ and $S^0$ at $2\theta = 23.6°$, 26.6°, 26.8°, and 28.1°. Thus, various diffraction peaks of elemental sulphur and other sulphur-related compounds were observed only after $H_2S$ sorption from raw biogas, as discussed in equations 4.10 to 4.13.

$$Ca^{2+} + SO_4^{2-} + 2H_2O \rightarrow CaSO_4.2H_2O \quad (4.12)$$

$$2K^{+} + SO_4^{2-} \rightarrow K_2SO_4 \quad (4.13)$$

No strong peaks were detected for elemental sulphur ($S^0$) and other sulphur-related compounds in the fresh adsorbents. The EDX results are also in agreement with the XRD profile of the adsorbents, showing the composition of elements forming the respective compounds in a stoichiometric manner before and after $H_2S$ sorption. Many authors reported that when exposed to excessive amounts of $O_2$, elemental sulphur ($S^0$) formed on the surface is further oxidized to

sulphur-related compounds ($SO_4^{2-}$), whereas due to limited $O_2$ diffusion, only elemental sulphur is formed in the pores of adsorbent particles [He et al., 2011; Sahota et al., 2018; Xu et al., 2014]. Also in the literature, the $H_2S$ adsorption capacities depend on various factors, such as high BET surface area, high mineral content, and the alkaline nature of the biochar, with different ranges of adsorption. The XRD profile after $H_2S$ sorption provided evidence of the speciation of $SO_4^{2-}$ ions generated on the surface of the biochar reacted with $K^+$ and $Ca^{2+}$ to form $K_2SO_4$ and $CaSO_4.2H_2O$, respectively, while elemental $S^0$ was formed in the pores.

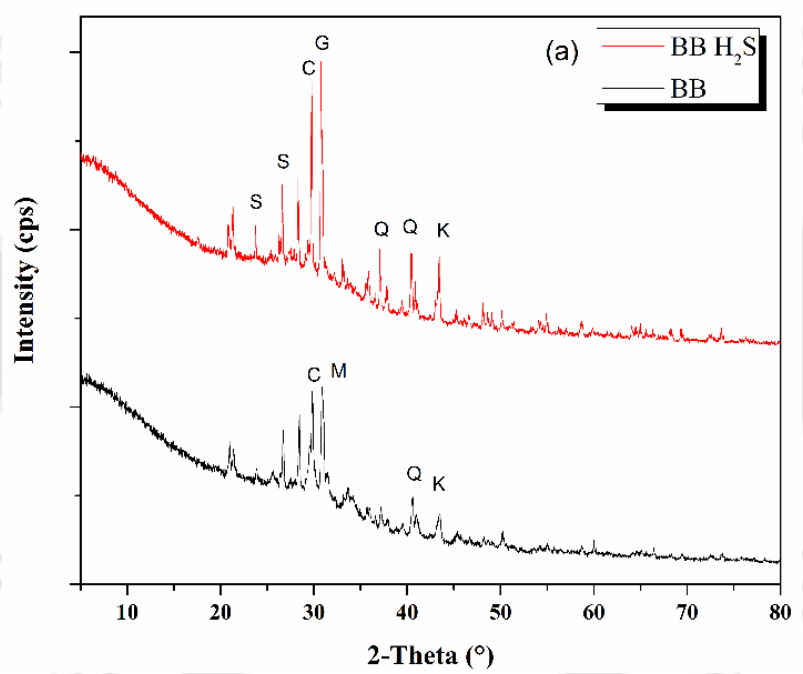


**Fig. 4.10** XRD patterns of BB, before and after $H_2S$ sorption

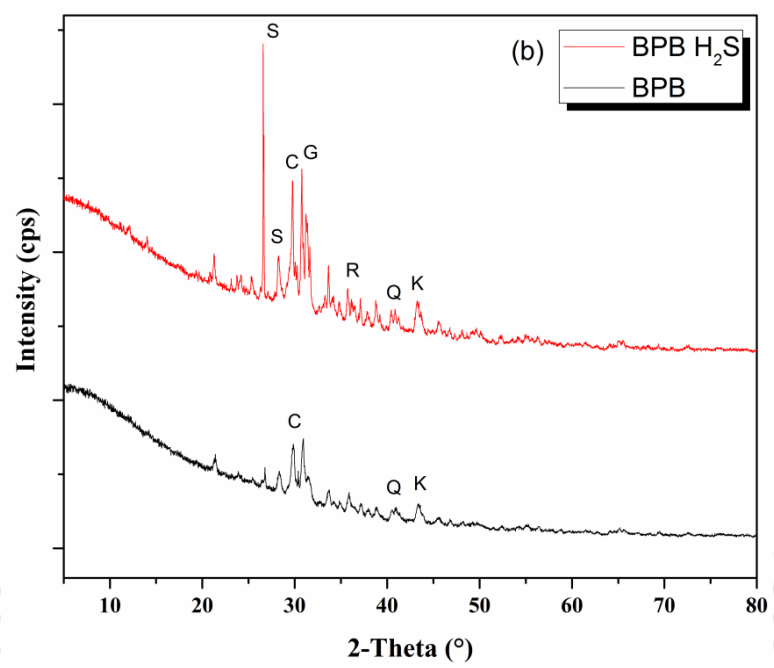


**Fig. 4.11** XRD patterns of BPB, before and after $H_2S$ sorption

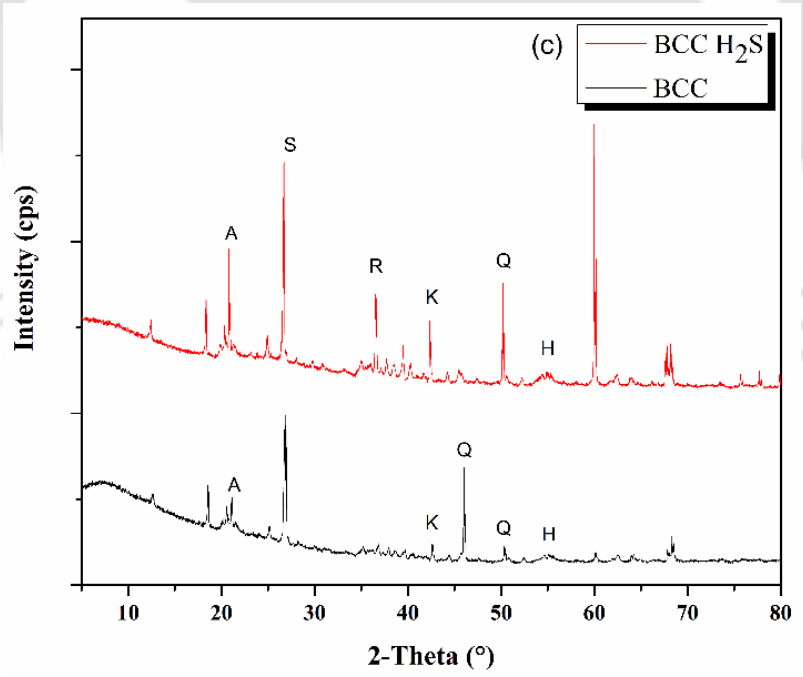


**Fig. 4.12** XRD patterns of BCC, before and after $H_2S$ sorption

Where, A, $Al_2O_3$; C, $CaCO_3$; G, $CaSO_4.2H_2O$; H, $Fe_2O_3$; K, $K_2CO_3$; M, $(Ca,Mg)_3(PO_4)_2$; Q, $SiO_2$; R, $K_2SO_4$; S, elemental $S^0$

Thus, the conversion of $H_2S$ into $S^0$ and $SO_4^{2-}$, and thereby formation of resulting compounds purely depends on various physico-chemical parameters such as surface area, pore size, pH, oxygen and other alkaline mineral elements. Usually, in the case of activated carbons, the byproduct of $H_2S$ removal is $H_2SO_4$, which would reduce the adsorption capacity by increasing the acidity. Therefore, in view of environmental concerns, the complete conversion of $H_2S$ into $SO_4^{2-}$ by biochar is preferable as it is less harmful than dilute $H_2SO_4$ [Bagreev and Bandosz, 2001; Bandosz, 2006].

### 4.3.6 FOURIER TRANSFORM INFRA-RED SPECTROSCOPY OF ADSORBENTS

FT-IR analysis was done to study the difference in surface functional groups on the adsorbents before and after $H_2S$ sorption (Fig. 4.13, 4.14, and 4.15). The IR band at around 1432 $cm^{-1}$ (BB), 1426 $cm^{-1}$, and 1437 $cm^{-1}$ (BPB) confirms the presence of $CO_3^{2-}$ in the biochars before and after treatment. The saturated biochar samples BPB $H_2S$ and BB $H_2S$, show high intensity peaks of elemental sulphur, (S–S) at 605 $cm^{-1}$ and 600 $cm^{-1}$ whereas BCC $H_2S$ shows a very low intensity peak of elemental sulphur at 639 $cm^{-1}$. This shows a clear figure on the sorption of $H_2S$ on the surface of adsorbents through various physico-chemical reactions. Further, the peak at 1127 $cm^{-1}$ of BPB $H_2S$ signifies the S–O bending vibrations. The bands at 775 $cm^{-1}$, 776 $cm^{-1}$, and 787 $cm^{-1}$ of the adsorbent samples represent the Si–O of quartz, and the band at 535 $cm^{-1}$ of BCC is related to the stretching vibration mode of Fe-O of hematite. The bands assigned to the O–H (3400–3600 $cm^{-1}$) and aliphatic C–H stretching (~2100 $cm^{-1}$) vibration are absent in both fresh and $H_2S$ adsorbed biochars and BCC, which might be due to the increase in pyrolysis temperature (500 °C), which also indicates the diminution of labile aliphatic compounds in biochars and BCC [Jakab et al., 1997; Sharma et al., 2004].

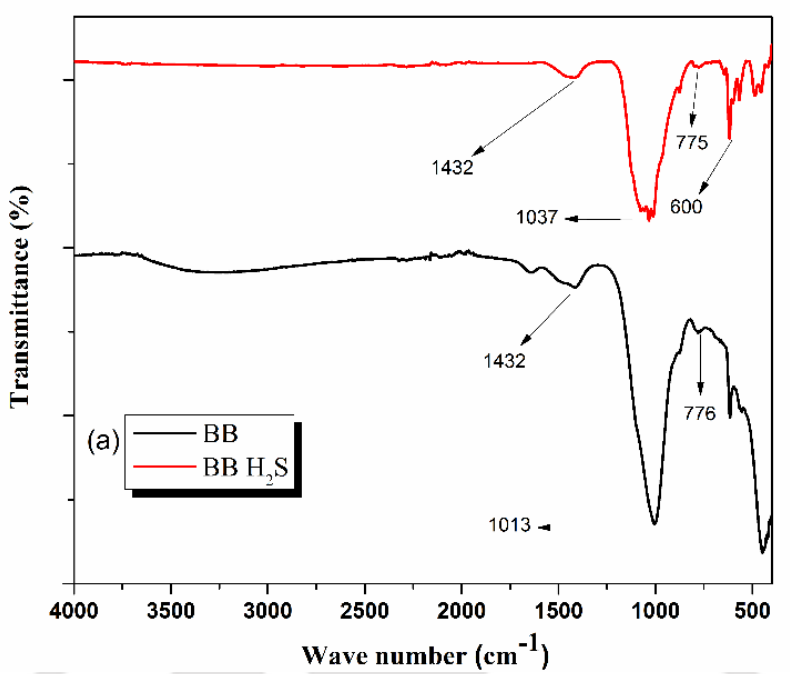


**Fig. 4.13** FT-IR spectra of BB, before and after $H_2S$ sorption

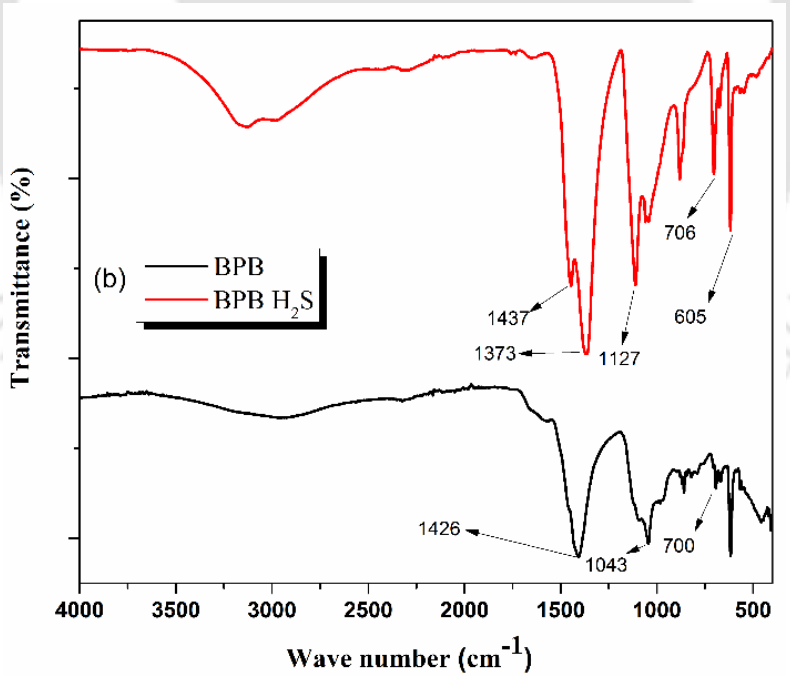


**Fig. 4.14** FT-IR spectra of BPB, before and after $H_2S$ sorption

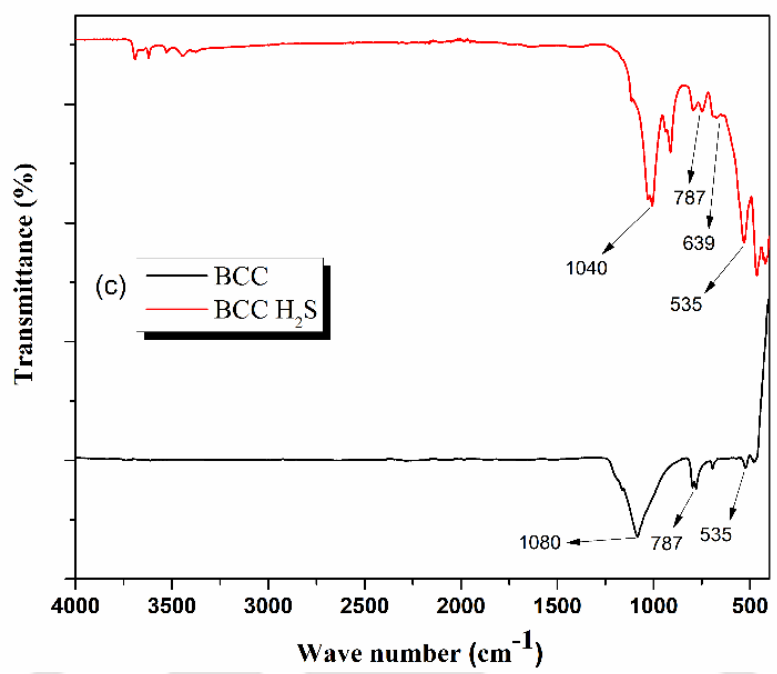


**Fig. 4.15** FT-IR spectra of BCC, before and after $H_2S$ sorption

Overall, noticeable differences were observed in the functional groups present in the biochars before and after $H_2S$ sorption, especially the presence of high intensity peaks of elemental sulphur (S–S) at 605 and 600 $cm^{-1}$, which show the ability of biochars to adsorb $H_2S$ and convert it into elemental sulphur and other S-related compounds due to high pH and the presence of supported K, Ca, and other compounds present on the surface of biochars.

### 4.3.7 ADSORPTION KINETICS OF $H_2S$ ON ADSORBENTS

Four widely used kinetic models, *viz.* pseudo-first-order, pseudo-second-order, intraparticle diffusion, and Elovich models, were fitted to evaluate the kinetics of $H_2S$ adsorption on BB, BPB, and BCC, respectively, as discussed in sub-section 4.2.6.

The pseudo-first-order model is typically applied to define the external mass transfer between the gas-phase material and the adsorption sites on the external surface. The pseudo-second-order model is applied to study the chemical sorption process of the active sites inside the adsorbent

and is considered one of the prominent reasons for the whole sorption process [Han et al., 2020; Vasanth, 2006]. The intraparticle diffusion model is usually adopted to understand the phases of diffusion. The Elovich kinetic model is used to describe the second-order kinetic equation, assuming the chemical adsorption processes on heterogeneous solid surfaces [Mezenner and Bensmaili, 2009]. Values of $k_1$ and $q_e$ for the pseudo-first-order model were obtained from the slope and intercept by plotting $\ln(q_e - q_t)$ versus t (min) as shown in Fig. 4.16. Similarly, values of $k_2$ and $q_e$ for the pseudo-second-order model were calculated from the slope and intercept of the plot of $\frac{t}{q_t}$ against time t (Fig. 4.17). The parameters $k_p$ and C of the intraparticle diffusion kinetic model were obtained from the slope and intercept of $q_t$ versus $t^{1/2}$ plot (Fig. 4.18). Lastly, $a_e$ and $b_e$ were obtained from the intercept and slope of $q_t$ versus ln t plot (Fig. 4.19).

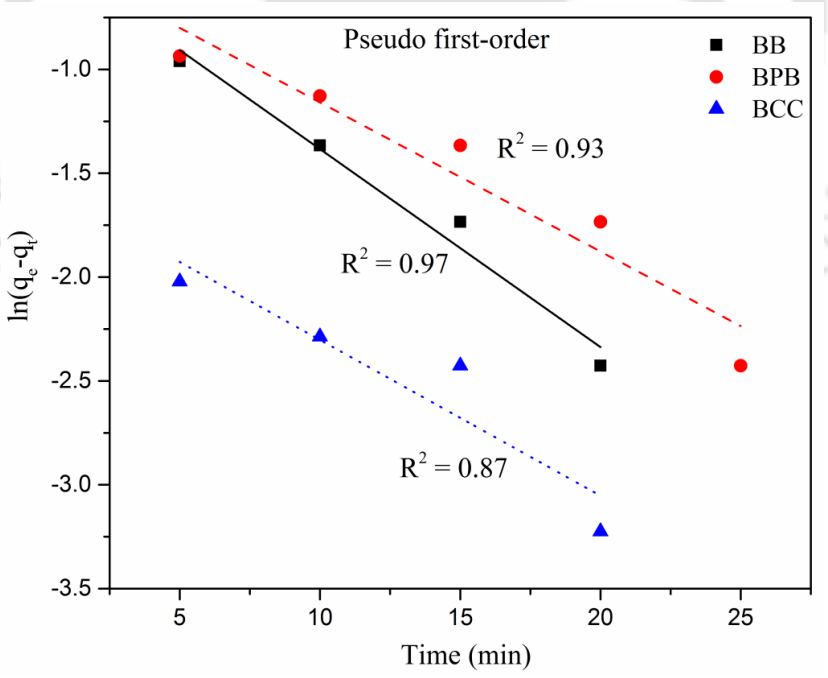


**Fig. 4.16** Pseudo-first-order model for the adsorption of $H_2S$ on BB, BPB, and BCC

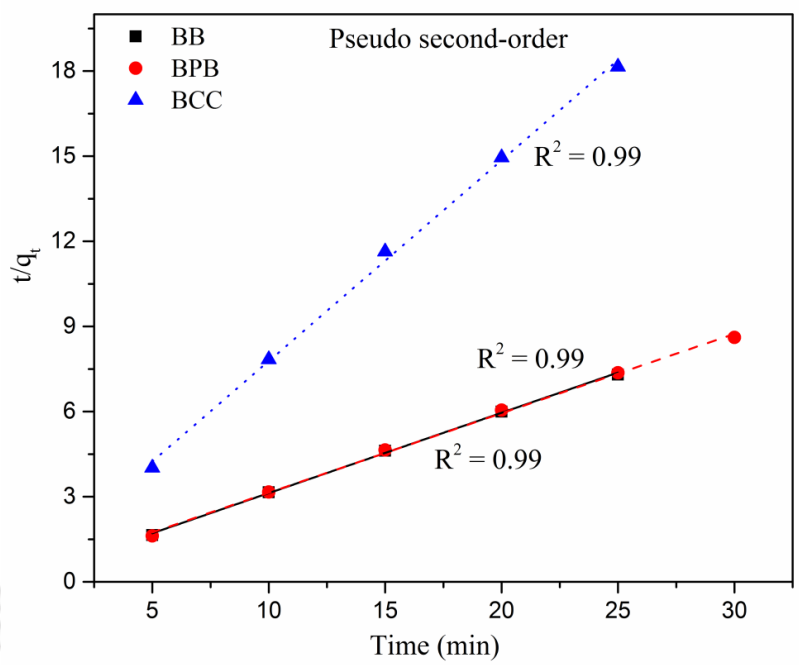


**Fig. 4.17** Pseudo-second-order model for the adsorption of $H_2S$ on BB, BPB, and BCC

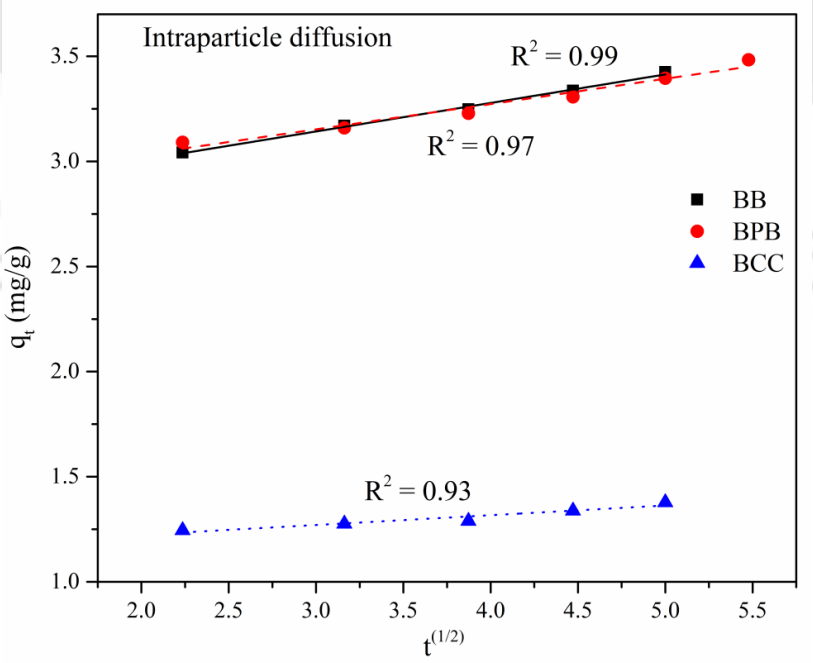


**Fig. 4.18** Intraparticle diffusion model for the adsorption of $H_2S$ on BB, BPB, and BCC

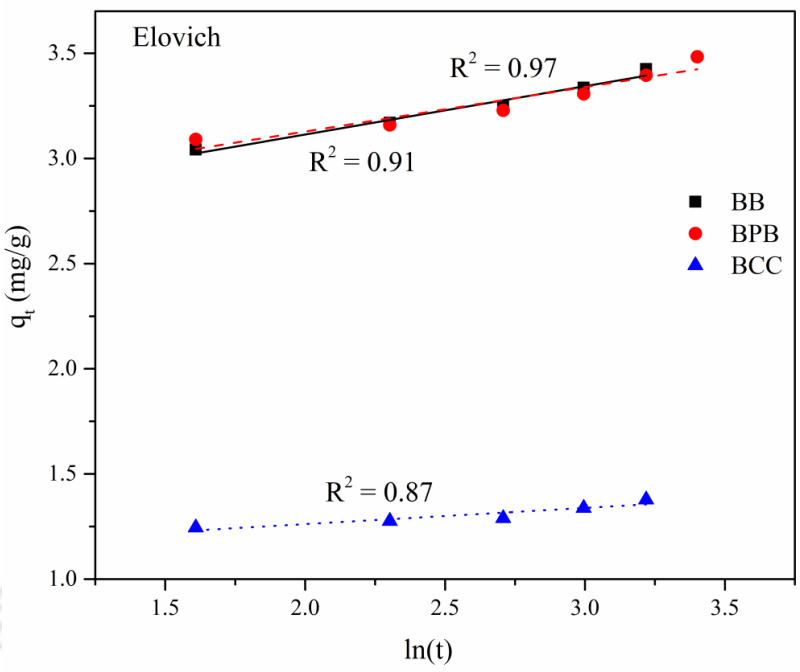


**Fig. 4.19** Elovich model for the adsorption of $H_2S$ on BB, BPB, and BCC

**Table 4.2** Kinetic parameters of pseudo-first-order, pseudo-second-order, intraparticle diffusion, and the elovich model for adsorption of $H_2S$ on BB, BPB, and BCC

| **Adsorbents** | **Pseudo-first-order** | | | **Pseudo-second-order** | | | **Intraparticle diffusion** | | | **Elovich** | | |
|---|---|---|---|---|---|---|---|---|---|---|---|---|
| | $k_1$ ($min^{-1}$) | $q_e$ (mg $g^{-1}$) | $R^2$ | $k_2$ (g $mg^{-1}$ $min^{-1}$) | $q_e$ (mg $g^{-1}$) | $R^2$ | $k_p$ (mg $g^{-1}$ $min^{-1/2}$) | C | $R^2$ | $a_e$ (mg $g^{-1}$ $min^{-1}$) | $b_e$ (g $mg^{-1}$) | $R^2$ |
| BB | 0.095 | 0.650 | 0.97 | 0.270 | 3.53 | 0.99 | 0.136 | 2.7354 | 0.99 | 23979.66 | 4.35 | 0.97 |
| BPB | 0.072 | 0.643 | 0.93 | 0.227 | 3.57 | 0.99 | 0.120 | 2.7915 | 0.97 | 76420.78 | 4.73 | 0.91 |
| BCC | 0.075 | 0.212 | 0.87 | 0.711 | 1.41 | 0.99 | 0.047 | 1.131 | 0.93 | 138936.55 | 13.00 | 0.87 |

**Table 4.3** Experimental $q_e$ of adsorbents

| Adsorbents | BB | BPB | BCC |
|---|---|---|---|
| $q_e$ (experimental) | 3.42 mg $g^{-1}$ | 3.48 mg $g^{-1}$ | 1.37 mg $g^{-1}$ |

The relative kinetic parameters of the pseudo-first-order, pseudo-second-order, intraparticle diffusion and elovich models are shown in Table 4.2. The experimental $q_e$ of adsorbents are shown in Table 4.3. From the adsorption kinetics, it can be seen that the pseudo-first-order model seems to be less preferable over the pseudo-second-order model for the adsorption of $H_2S$ on BB, BPB, and BCC due to its lower $R^2$ value and large difference between $q_{e,\,exp}$ and $q_{e,\,cal}$. As seen from the table, the calculated equilibrium adsorption value ($q_e$) obtained from the pseudo-second-order model (BB, $q_{e\ cal}$ = 3.53 mg $H_2S$ $g^{-1}$ biochar; BPB, $q_{e\ cal}$ = 3.57 mg $H_2S$ $g^{-1}$ biochar; and BCC, $q_{e\ cal}$ = 1.41 mg $H_2S$ $g^{-1}$ biochar) was best fitted for all the adsorbents with the experimental data (BB, $q_{e\ exp}$ = 3.42 mg $H_2S$ $g^{-1}$ biochar; BPB, $q_{e\ exp}$ = 3.48 mg $H_2S$ $g^{-1}$ biochar; and BCC, $q_{e\ exp}$ = 1.37 mg $H_2S$ $g^{-1}$ biochar) with correlation coefficient of $R^2$ = 0.99. This demonstrates that the pseudo-second-order model can clearly describe the $H_2S$ adsorption process, and it can be concluded that the chemical sorption process on the adsorbent is the dominant control step during the whole sorption process. Except for BCC ($R^2$ = 0.87), the elovich model was linear fitted for BB with $R^2$ = 0.97 and BPB with $R^2$ = 0.91, which also indicated the influence of chemical adsorption. The obtained $R^2$ value of the intraparticle diffusion model (BB, $R^2$ = 0.99; BPB, $R^2$ = 0.97; and BCC, $R^2$ = 0.93) of BB is found to be similar to the pseudo-second-order model, which indicates the intraparticle diffusion model can also express $H_2S$ adsorption on BB very well.

### 4.3.8 COMPARISON OF PRESENT WORK WITH LITERATURE

Comparison of $H_2S$ adsorption results from the present work with some of the selected literature is shown in Table 4.4. Zulkefli et al. (2019) showed that raw coconut shell activated carbon (Raw CAC) with a BET surface area of 901.04 $m^2/g$ had an $H_2S$ adsorption capacity of 0.528 mg/g, while on impregnation with KOH and $ZnAc_2$, the BET surface area decreased to 805.45

and 656.75 $m^2/g$ but the $H_2S$ adsorption capacity increased to 0.878 and 1.293 mg/g, respectively. In another study, Choudhury and Lansing (2021), reported the removal of $H_2S$ from synthetic biogas using unmodified corn stover biochar (CSB) and (Fe)-impregnated corn stover biochar in a scrubbing column. They showed that unmodified CSB and CSB-Fe with surface areas of 23.5 and 34.9 $m^2/g$ had $H_2S$ adsorption capacities of 3.3 and 8.2 mg/g, respectively. It is clearly indicated that the $H_2S$ adsorption capacity depends on the nature of the adsorbent rather than the BET surface area. In the present work, the BET surface area of the adsorbents was low, but it is well within the general range (2–200 $m^2/g$) of biochars produced from various biomasses [Shinogi and Kanri, 2003]. The alkaline nature, porosity, and high mineral concentrations of the biochars are the key factors, as discussed in the above sub sections, for $H_2S$ sorption from raw biogas.

**Table 4.4** Comparison of $H_2S$ adsorption results between the present work and literature

| Adsorbents | BET Surface area ($m^2/g$) | pH | Experimental Temperature (°C) | Experimental Pressure | Composition of inlet gases | Biogas type | $H_2S$ removal efficiency (%) | Adsorption capacity (mg/g) | Reference |
|---|---|---|---|---|---|---|---|---|---|
| Leaf waste biochar (LWB400) | 13.59 | 10.23 | Room temperature | - | $CH_4$: 65%, $CO_2$: 35%, $N_2$: <1%, Moisture: 4–5%, $O_2$ and $H_2S$: 500–1300 ppm | Natural | 84.22% | - | Sahota et al., 2018 |
| Corn stover biochar (CSB) | 23.5 | 10.2 | Room temperature (25 °C) | - | $CH_4$: 59.9% $CO_2$: 40% $H_2S$: 1000 ppm | Synthetic | - | 3.3 | Choudhury, and Lansing, 2021 |
| Fe-impregnated CSB (CSB-Fe) | 34.9 | 2.80 | Room temperature (25 °C) | - | $CH_4$: 59.9% $CO_2$: 40% $H_2S$: 1000 ppm | Synthetic | - | 8.2 | |
| $Fe_2O_3$ powder | 105 | | 25 °C | Atmospheric pressure | Mixture of three gases- 1000 ppm $H_2S$ in $N_2$, Air and $N_2$ | Synthetic | - | 3.9 | Costa et al., 2020 |
| Commercial ZnO | | | 25 °C | Atmospheric pressure | Mixture of three gases- 1000 ppm $H_2S$ in $N_2$, Air and $N_2$ | Synthetic | - | 2.4 | |
| Coconut shell activated carbon (Raw CAC) | 901.04 | | Ambient | 1 bar (gauge) | $H_2S/N_2/CO_2$ (1000 ppm $H_2S$ with 49.5% $N_2$ and balanced $CO_2$) | Synthetic | - | 0.528 | Zulkefli et al., 2019 |
| KOH–CAC | 805.45 | | Ambient | 1 bar (gauge) | $H_2S/N_2/CO_2$ (1000 ppm $H_2S$ with 49.5% $N_2$ and balanced $CO_2$) | Synthetic | - | 0.878 | |
| $ZnAc_2$-CAC | 656.75 | | Ambient | 1 bar (gauge) | $H_2S/N_2/CO_2$ (1000 ppm $H_2S$ with 49.5% $N_2$ and balanced $CO_2$) | Synthetic | - | 1.293 | |
| BB | 7.53 | 10.67 | Ambient | 1.2 bar | $CH_4$: 56%, $CO_2$: 43%, $N_2$: <1%, moisture, $O_2$ and $H_2S$: 398±12 ppm | Natural | 87.7% | 3.42 | Present work |
| BPB | 9.32 | 10.95 | | | | | 89.2 % | 3.48 | |
| BCC | 3.36 | 9.96 | | | | | 78.4 % | 1.37 | |

## 4.4 SUMMARY OF THE CHAPTER

This work reported the use of a biogas scrubber filled with adsorbents (BB, BPB, and BCC) to remove $H_2S$ from a 3 $m^3$ deenbandhu model biogas plant by the process of adsorption. The adsorbents, both fresh and $H_2S$ adsorbed, were characterized in detail with the help of XRD, FT-IR, FESEM, and EDX to elucidate the structural differences and mechanisms of $H_2S$ adsorption. BPB showed the highest $H_2S$ removal efficiency of 89.2%, followed by BB (87.7%) and BCC (78.4%). Furthermore, the kinetics of $H_2S$ adsorption on adsorbents was studied using pseudo-first-order, pseudo-second-order, intraparticle diffusion, and elovich models, respectively. Application of bamboo biochar, banana peel biochar, and biochar clay composite as $H_2S$ adsorbents will be advantageous for small-scale decentralized biogas plants installed in rural areas.

Results obtained on treating raw biogas for $CO_2$ removal using the selected scrubbing agents based on absorption and their kinetic studies are discussed in the next chapter.

# Chapter 5

## $CO_2$ Absorption from Biogas using Natural Base Ash Solutions and Comparison with KOH

# CHAPTER 5: $CO_2$ ABSORPTION FROM BIOGAS USING NATURAL BASE ASH SOLUTIONS AND COMPARISON WITH KOH

## 5.1 INTRODUCTION

Methane in biogas is measured as a highly valued source of energy, while $CO_2$ has zero energy yield through combustion and significantly reduces the overall heating value due to its high concentration per volume of biogas [Abatzoglou and Boivin, 2008]. Further $CO_2$ emissions increase greenhouse gas emissions, which contribute to global warming [Monnet, 2003]. Biogas with $CO_2$ has a calorific value ranging from 18.7 to 26 MJ/$m^3$, while biogas without $CO_2$ has a calorific value ranging from 33.5 to 35.3 MJ/$m^3$ [Monnet, 2003]. So, the removal of $CO_2$ from biogas enhances the fuel efficiency, which could serve as a source of immense energy that can be used effectively for different applications like vehicular fuel and power generation [Abushammala et al., 2016; Sun et al., 2015]. Monoethanolamine (MEA), sodium hydroxide (NaOH), potassium hydroxide (KOH), and calcium hydroxide ($Ca(OH)_2$ are the most commonly used chemical solvents [Kadam and Panwar, 2017; Malla et al., 2016; Zhao et al., 2010]. However, inoculation of chemicals in the absorption process generally leads to disposal problems due to its toxic nature and also becomes impractical for rural areas due to its higher cost [Muthuraman et al., 2012]. Hence, in this context, this work proposes the use of natural base ash solutions (NBAS) prepared from banana pseudostem (BPS), *Musa balbisiana* peel (MBP) and *Musa acuminata* peel (MAP) for $CO_2$ scrubbing from biogas. Also, to assess the potential of the NBAS as a $CO_2$ absorbent, the performance results have been compared with potassium hydroxide (KOH) of varying molar concentrations.

## 5.2 MATERIALS AND METHODS

### 5.2.1 BIOMASS COLLECTION AND PROCESSING FOR SCRUBBING AGENTS

Different parts of solid waste banana plant *viz. Musa acuminata* peel (MAP), *Musa balbisiana* peel (MBP) and banana pseudostem (BPS) were collected from a nearby local village of IIT Guwahati, Assam and air dried for a week, till they lost their yellow colour. The biomass was cleaned under tap water to remove any attached contaminants and was incubated in a hot air oven at 60 °C for 24 hours to remove the moisture. The peels and pseudostem were then burnt to ashes in a traditional way. The ash formed thereafter was crushed in a grinder into powder form and stored in an airtight container for further analysis.

Natural base ash solutions (NBAS) were prepared by mixing each type of ash with distilled water followed by measuring pH using a digital pH meter *(Make: Mettler Toledo, Model: 30266889).* The addition of ash at a 5 minute time interval was continued till no further increase in pH was observed even after the addition of ash. The solution was kept in a shaker at 150 rpm for 45 minutes at ambient temperature for proper mixing of the ashes. Thereafter, the final pH of the prepared natural base ash solution was recorded and used for further experimental investigations. A similar procedure was followed for the preparation of all the base solutions.

### 5.2.2 BASE SOLUTIONS FOR $CO_2$ SCRUBBING THROUGH THE ABSORPTION PROCESS

Five different molar concentrations of potassium hydroxide (KOH) solutions of 0.1, 0.3, 0.5, 0.7, and 1.0 M with pH of 12.68, 13.14, 13.30, 13.34, and 13.42 were prepared. Accordingly, the three natural base ash solutions with saturated pH of 11.48, 12.77, and 11.63 were prepared from BPS, MBP, and MAP, respectively. These eight types of base solutions were used for $CO_2$

scrubbing from biogas, and the performance of natural base ash solutions was compared with different molar concentrations of KOH.

### 5.2.3 DESCRIPTION OF THE SCRUBBER AND EXPERIMENTAL PROCEDURE FOR $CO_2$ SCRUBBING BY ABSORPTION PROCESS

The scrubber was fabricated using a PVC bottle having a dimension of 88 mm inner diameter and a height of 328 mm with a volume of 2 L. The gas inlet was connected to the bottom of the scrubber for feeding of the raw biogas, while the gas outlet was placed at the top for emission of the scrubbed biogas. Another opening with a seal was located at the top of the scrubber for feeding and extraction of the saturated scrubbing agent, respectively. The scrubber was filled with each type of scrubbing agent, and the biogas was directly fed from a $3m^3$ biogas plant (deenbandhu model) installed at Aaoniati Satra near IIT Guwahati, Assam, India (26°11'27.8"N, 91°43'17.3"E) (Fig. 5.1). Cattle dung was only used as the feed material in the biogas plant. The composition of biogas purely depends on the feedstock and reaction conditions and may vary with feedstocks. The flow rate was controlled at around 200 ml/min in order to measure the $CO_2$ absorption and saturation rates of the scrubbing agents. The treated and untreated biogas samples were collected in tedlar bags at a 5-minute time interval and analyzed for $CH_4$ and $CO_2$ concentration. All experiments were conducted at ambient temperature (25-30 °C) and the biogas pressure was maintained slightly above the atmospheric level (gauge pressure of nearly 20 kPa) throughout the experiment with the help of a micro pressure gauge. The pH of the solutions was measured at regular time intervals using a digital pH meter.

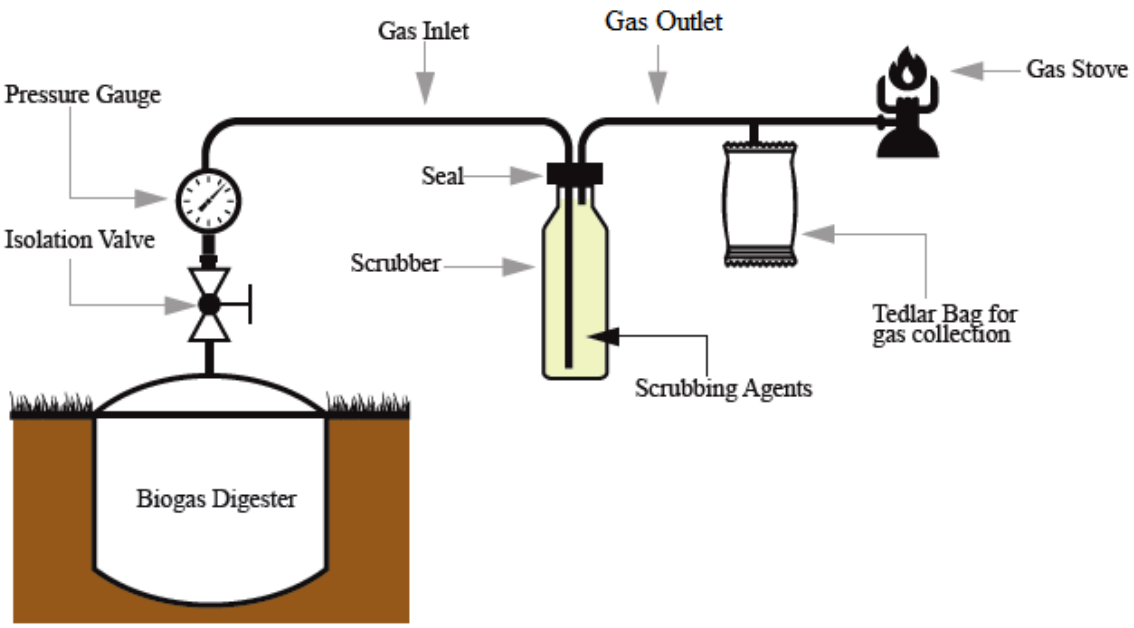


**Fig. 5.1** Process flow diagram of the experimental setup for $CO_2$ removal by absorption process

### 5.2.4 BIOGAS ANALYSIS BY GAS CHROMATOGRAPHY

The raw biogas samples and those treated with different scrubbing agents were collected in Tedlar® bags and immediately analyzed for $CH_4$ and $CO_2$ concentration in a Gas chromatograph (*Thermo Fisher Scientific Trace GC 1110 Gas Chromatograph, USA*). The GC was coupled with a thermal conductivity detector, using helium as a carrier gas at a makeup flow of 20 mL/min. The oven and detector temperatures were maintained at 45 and 180 °C, respectively.

### 5.2.5 $CO_2$ ABSORPTION KINETICS IN BASE SOLUTIONS

The rate of $CO_2$ absorption in the base solution is obtained as per the procedure reported by Tippayawong and Thanompongchart (2010). The fraction of $CO_2$ in biogas that is absorbed by the base solution at time t is represented by equation 5.1.

$$A = 1 - \frac{C_o}{C_i} \qquad (5.1)$$

where, A = fraction of $CO_2$ absorbed from the gas mixture after time t

$C_o$ = outlet $CO_2$ concentration (% v/v) after time t

$C_i$ = inlet $CO_2$ concentration (% v/v)

The removal rate of $CO_2$ from biogas is momentary for this particular scrubbing setup. The rate of declining $CO_2$ absorption is assumed to be proportional to the $CO_2$ fraction that was absorbed in the scrubbing column and the $CO_2$ fraction that passed through. It is expressed using the following equations reported by the authors [Tippayawong and Thanompongchart, 2010; Leonzio, 2016; Aboudheir, et al., 2003].

$$\frac{dA}{dt} = -kA(1 - A) \qquad (5.2)$$

After integration the above equation:

$$\ln\left(\frac{A(1 - A_0)}{A_0(1 - A)}\right) = k(\tau - t) \qquad (5.3)$$

After rearranging equation 5.3, we get:

$$t = \frac{1}{k}\ln\left(\frac{C_o}{C_i - C_o}\right) + \tau \qquad (5.4)$$

where, $k$ = absorption rate constant

$A_0$ = fraction of $CO_2$ absorbed from the gas mixture after $\tau$

$\tau$ = characteristic absorption time when 50% absorption of $CO_2$ occurs. This indicates that the solutions in the scrubbing column should be completely saturated after an elapsed time of $2\tau$.

$t$ = experimental time

### 5.2.6 CALORIFIC VALUE ANALYSIS METHOD

Higher calorific values (HCV) and lower calorific values (LCV) of enriched biogas were calculated according to the formula reported by Li, et al. (2017).

$$HCV_{biogas} = 0.3989 \text{ x } MC + 0.0213 \ (R^2 = 1) \qquad (5.5)$$

$$LCV_{biogas} = 0.3593 \text{ x } MC + 0.0192 \ (R^2 = 1) \qquad (5.6)$$

where MC is the methane content in biogas (%) and $R^2$ is the square of the correlation. The HCV and LCV of pure methane were 39.82 and 35.87 MJ/$m^3$ respectively [Li, et al., 2014].

## 5.3 RESULTS AND DISCUSSION

### 5.3.1 $CO_2$ ABSORPTION CAPACITY OF THE BASE SOLUTIONS

The experiment was first started with different molar concentrations of KOH to understand the basic mechanisms of $CO_2$ absorption. The $CO_2$ absorption capacity of different molar concentrations of KOH with respect to pH is shown in Fig. 5.2. The molar concentration of KOH ranging from 0.5 M to 1.0 M showed some similar trends of absorption, although their molar concentration was different. Hence, 0.5 M KOH is considered the optimum concentration for the comparison with NBAS.

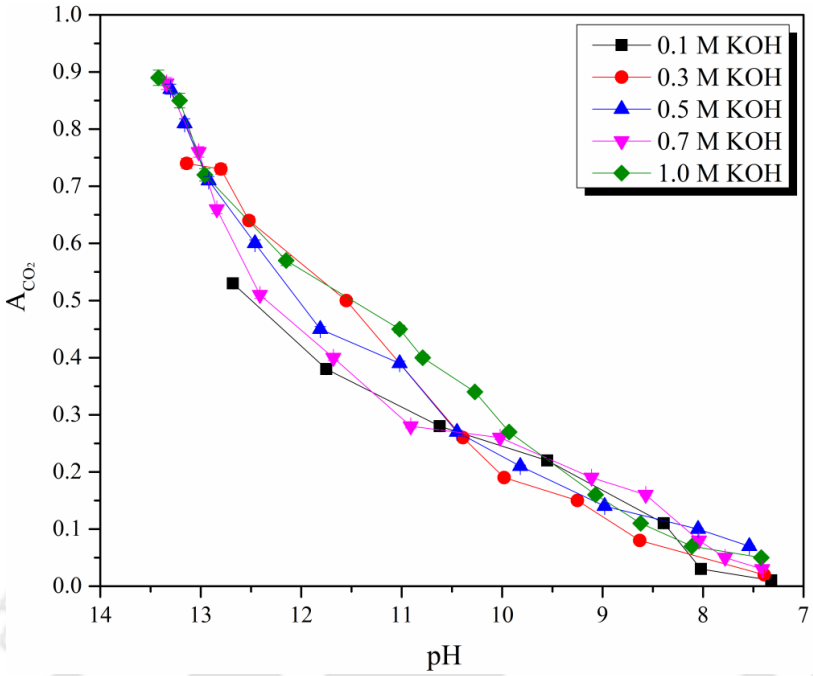


**Fig. 5.2** $CO_2$ absorption capacity of different molar concentrations of KOH with respect to pH

The addition of water to the ash mixture hydrates the oxides to form hydroxides, which react with $CO_2$ to form carbonates. During the process of carbonation, some $CO_2$ may directly adsorb on the surface of the ash particles. Thus, the wet sorption process involves the reaction of adsorbates in gaseous form with other species in the slurry. So, as the process involves both physical and chemical adsorption as well as absorption, it may be referred to as the sorption process [Ben-Mansour et al., 2016].

Figure 5.3 shows the comparison of the $CO_2$ absorption capacity of NBAS with 0.5 M KOH. It is observed from the results that the absorption capacity of the scrubbing agent is a function of its pH value. The higher the pH value of the solvent, the greater its $CO_2$ absorption capacity. Hence, the results show that the concentration of scrubbing agent has a significant impact on $CO_2$ absorption.

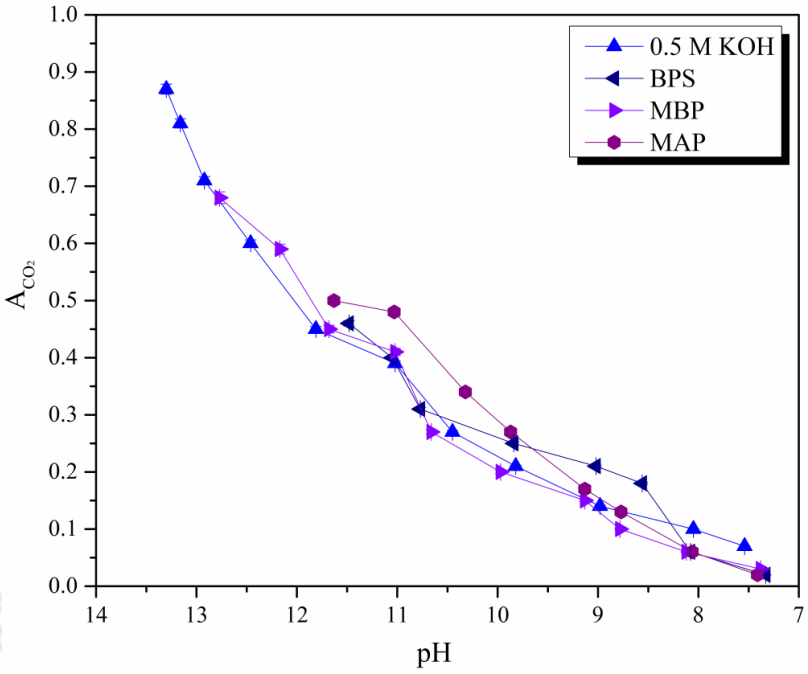


**Fig. 5.3** Comparison of the $CO_2$ absorption capacity of NBAS with 0.5 M KOH

As described below, the pH of the solvent decreased on $CO_2$ absorption, which may be attributed to the increase in concentration of $H_2CO_3$ and $K_2CO_3$ in the absorption system due to chemical reactions that take place during the absorption of $CO_2$ with base solutions.

$$H_2O\ (aq) + CO_2\ (g) \leftrightarrow H_2CO_3\ (aq) \qquad (5.7)$$

$$2KOH\ (aq) + CO_2\ (g) \leftrightarrow K_2CO_3\ (aq) + H_2O \qquad (5.8)$$

From the graph, it is observed that base solutions with a pH of 11 and above had a capacity of more than 40% $CO_2$ scrubbing from the fed raw biogas.

### 5.3.2 VARIATION OF $CO_2$ AND $CH_4$ CONTENT IN TREATED BIOGAS WITH TIME

A comparison of the outlet $CO_2$ concentrations in the biogas samples after passing through various scrubbing agents with respect to time is shown in Fig. 5.4. The increase in $CO_2$

concentration in the treated biogas samples with time was due to the steady saturation of the scrubbing agent, which also increases the solution viscosity, which simultaneously decreases the diffusion coefficient and hence the absorption rate [Zanfir and Gavriilidis, 2005].

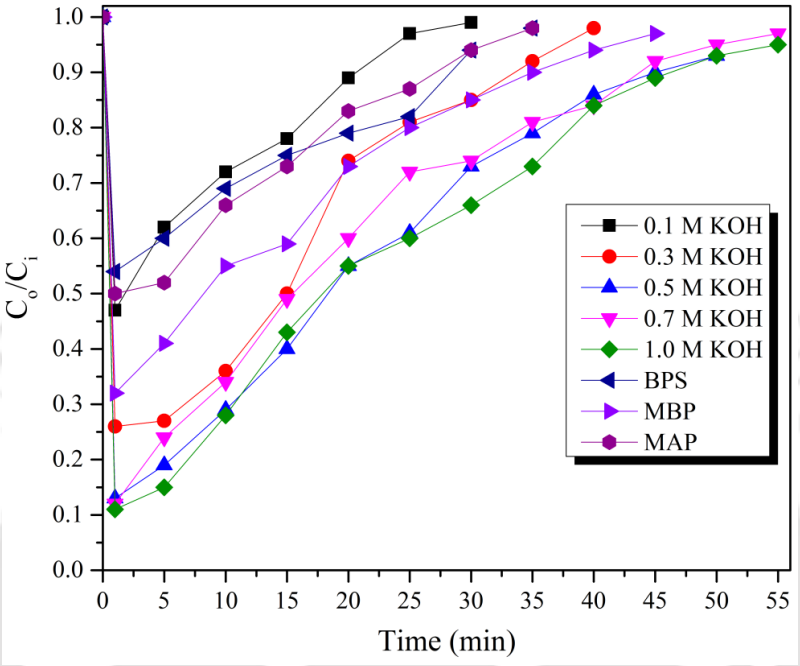


**Fig. 5.4** Outlet $CO_2$ concentrations with respect to time

For every solvent, after the respective saturation point, $CO_2$ started desorbing and evolved in the outlet gas stream. It is observed from the graph that amongst the chemical bases, 0.5 M, 0.7 M, and 1.0 M KOH solutions were able to reduce the $CO_2$ concentration of the inlet biogas by approximately similar amounts (~88%) followed by 0.3 M KOH (74%) and amongst the natural bases, MBP could reduce the maximum amount of $CO_2$ by 68% approximately. At lower concentrations of scrubbing agents (especially 0.1 M KOH, MAP, and BPS), the ability to absorb $CO_2$ is less and hence the outlet $CO_2$ concentration ($C_o/C_i$) is found more. It should be noted that the data presented here is an average value.

Figures 5.5 and 5.6 show the variation of $CH_4$ content in the treated biogas samples and the pH variation of the scrubbing agents with respect to time. It was observed that with an increase in KOH concentration and at a higher pH value, the ability of the scrubbing agents to absorb $CO_2$ increases, thereby enriching the $CH_4$ content in the outlet during the initial period of time.

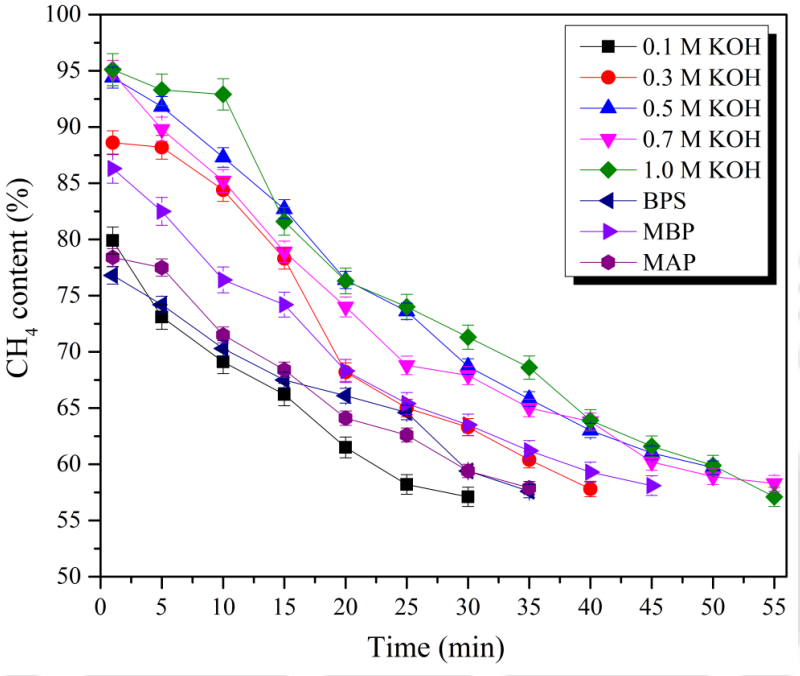


**Fig. 5.5** Variation of $CH_4$ content with respect to time

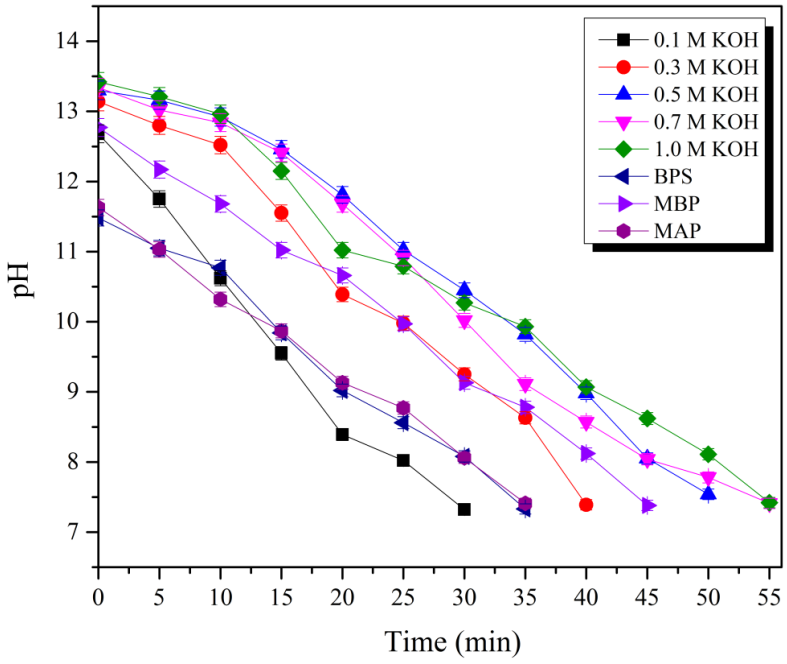


**Fig. 5.6** Variation of pH with respect to time

The experiment was stopped when the scrubbing agents became completely saturated or neutralized (pH 7-8). In this investigation, the fast saturation of the scrubbing agents with time may be attributed to the very high concentration of $CO_2$ (43%) present in the raw biogas. The process performance is fully reliant on factors such as dimensions of the scrubber, concentration of scrubbing agents, raw biogas composition, gas pressure, and flow rates. Accordingly, depending on the need, one can calculate the replenishment time of the scrubbing agent, the number of cycles the biogas needs to pass through, or the volume of the scrubbing agent required to attain the desired $CH_4$ content.

### 5.3.3 KINETICS OF $CO_2$ ABSORPTION BY DIFFERENT SOLVENTS

The graph of absorption time versus dimensionless biogas concentration ($\ln[C_o/(C_i-C_o)]$) for $CO_2$ absorption by chemical and natural base ash solutions is shown in Figure 5.7.

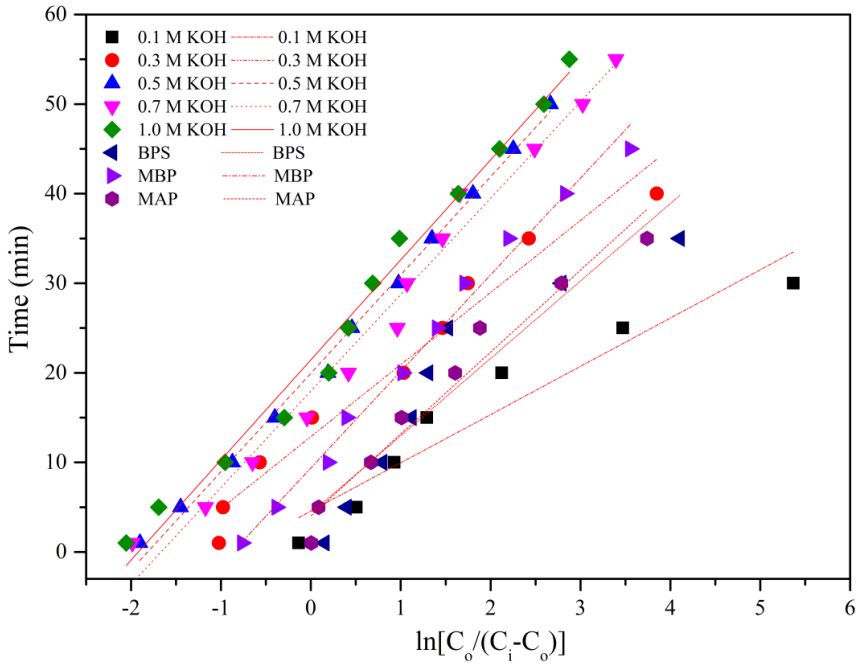


**Fig. 5.7** Kinetics of $CO_2$ absorption by varying molar concentrations of KOH and natural base ash solutions

Equation 3.9 has been used for the approximation of the curves to straight lines. The reaction rate constant *k* for MBP (10.67) was nearly equivalent to that of 0.5 M (10.88) and 0.7 M (10.68) KOH, which is very encouraging. However, the time for 50% saturation of the base solutions ($\tau$) varied; 0.5, 0.7, and 1.0 M KOH nearly had similar τ values. The τ value for MBP (9.61) was the highest amongst the three natural base ash solutions, which was also in agreement with the experimental value. It was observed that scrubbing agents with a lower pH range appeared to become saturated more rapidly than the other solvents. Table 5.1 shows the model parameters for both the chemical and natural base solutions and also the correlation coefficient $R^2$ of each linear approximation.

**Table 5.1** Kinetic parameters for $CO_2$ absorption by varying molar concentrations of KOH and natural base ash solutions

| Scrubbing agent | $k$ (min$^{-1}$) | $\tau$ (min) | $R^2$ |
|---|---|---|---|
| 0.1 M KOH | 5.29 | 4.89 | 0.91 |
| 0.3 M KOH | 7.96 | 13.06 | 0.96 |
| 0.5 M KOH | 10.88 | 20.07 | 0.99 |
| 0.7 M KOH | 10.68 | 18.12 | 0.98 |
| 1.0 M KOH | 11.08 | 21.57 | 0.98 |
| BPS | 8.53 | 4.62 | 0.87 |
| MBP | 10.67 | 9.61 | 0.99 |
| MAP | 9.03 | 4.32 | 0.96 |

Amongst the eight scrubbing agents, an $R^2$ value of 0.99 for 0.5 M KOH and MBP indicates a higher capacity for $CO_2$ absorption. All the chemicals as well as natural base solutions, except for 0.1 M KOH and BPS, exhibited $R^2$ values of greater than 0.95 and thereby reflected good linear relationships.

### 5.3.4 METHANE ENRICHMENT BY CHEMICAL AND NATURAL BASE SOLUTIONS

The volume percentage of methane content (%) after every five-minute time interval was analyzed with the help of a Gas Chromatograph. Figure 5.8 compares the methane enrichment that could be achieved with natural base ash solutions and different molar concentrations of KOH.

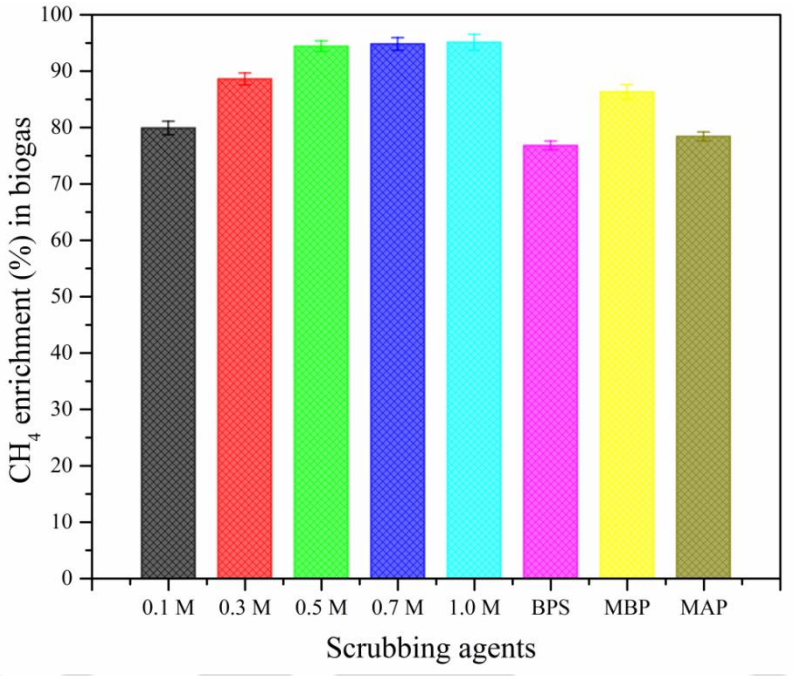


**Fig. 5.8** Methane enrichment in biogas by scrubbing agents

The methane content of the untreated biogas was 56.9%. 0.5 M KOH could enrich the methane content up to 94.4%, followed by 0.3 M KOH (88.6%), MBP (86.3%), 0.1 M KOH (79.9%), MAP (78.4%) and BPS (76.8%). When compared with the raw biogas sample, the treated biogas samples exhibited 19.9%, 29.4%, and 21.5% enrichment in methane when passed through base solutions prepared from BPS, MBP, and MAP, respectively. The high removal capacity of $CO_2$ by the respective scrubbing agents is attributed to their morphology, high pH, and inorganic metal compositions.

The findings clearly indicate that natural base ash solutions have almost equivalent potential to chemical base solutions for the scrubbing of $CO_2$ from biogas.

### 5.3.5 HCV AND LCV OF ENRICHED BIOGAS

The HCV and LCV of inlet biogas (raw) and enriched biogas were theoretically calculated using equations 5.5 and 5.6, respectively. Table 5.2 shows the calorific value of raw and enriched biogas treated with different scrubbing agents.

**Table 5.2** Calorific value of raw and enriched biogas treated with scrubbing agents

| Scrubbing agents | HCV ($MJ/m^3$) | LCV ($MJ/m^3$) |
|---|---|---|
| Raw | 22.72 | 20.46 |
| 0.1 M KOH | 31.89 | 28.73 |
| 0.3 M KOH | 35.36 | 31.85 |
| 0.5 M KOH | 37.68 | 33.94 |
| 0.7 M KOH | 37.84 | 34.08 |
| 1 M KOH | 37.96 | 34.19 |
| BPS | 30.66 | 27.61 |
| MBP | 34.45 | 31.03 |
| MAP | 31.29 | 28.19 |

The HCV (22.72 $MJ/m^3$) and LCV (20.46 $MJ/m^3$) of untreated biogas were significantly lower before the treatments. The HCV and LCV of scrubbed biogas obtained after passing through KOH solutions of 0.5, 0.7, and 1.0 M concentrations have almost equivalent HCV and LCV of 37.82 $MJ/m^3$ and 34.06 $MJ/m^3$ respectively. However, with the natural base solutions, the scrubbed biogas obtained after passing through MBP had the highest HCV of 34.45 $MJ/m^3$ and LCV of 31.03 $MJ/m^3$.

## 5.4 SUMMARY OF THE CHAPTER

An investigation was carried out into the potential of natural base ash solution (NBAS) prepared from banana pseudostem (BPS), *Musa balbisiana* peel (MBP), and *Musa acuminata* peel (MAP) for $CO_2$ scrubbing from biogas by the process of absorption and its comparison with KOH. MBP could enrich methane content up to 86.3%, which is nearly equivalent to 0.3 M KOH. The kinetic study showed that the reaction rate constant *k* for MBP (10.67) was nearly equivalent to that of 0.5 M (10.88) and 0.7 M (10.68) KOH. The high removal capacity of $CO_2$ by the respective scrubbing agents is attributed to their morphology, high pH, and inorganic metal compositions. Application of NBAS for $CO_2$ scrubbing from biogas is envisioned to be advantageous over other conventional chemicals because the source material is abundantly available, has low production cost, process of preparation is easy and can be easily adopted in the rural areas.

An approach to an alternative pathway for simultaneous enrichment of methane in biogas and electricity generation using a hybridized bio-electrochemical system consisting of an anaerobic digester (AD) and a membrane electrode assembly (MEA) is presented in chapter 6.

# Chapter 6

## Hybridized Anaerobic Digester-Membrane Electrode Assembly for Co-generation of Methane-Enriched Biogas and Electricity

# CHAPTER 6: HYBRIDIZED ANAEROBIC DIGESTER-MEMBRANE ELECTRODE ASSEMBLY FOR CO-GENERATION OF METHANE-ENRICHED BIOGAS AND ELECTRICITY

## 6.1 INTRODUCTION

Anaerobic digestion (AD) is a highly promising technology for the conversion of organic solid wastes into biogas, and has received great recognition worldwide [Mata-Alvarez et al., 2000]. Biogas as a renewable energy source has an added advantage in the reduction of greenhouse gas emissions and conventional fuel consumption. The decomposition of organic matter in the anaerobic digestion process is assisted by a group of microorganisms present in each stage of the digestion process [Chen et al., 2008]. Biogas has variable calorific value and it depends on the composition and volume percentage of $CH_4$ and $CO_2$. The $CH_4$ in biogas is regarded as an immense source of energy because of its high calorific value, while $CO_2$ has no energy and significantly reduces the overall heating value during combustion due to its high percentage [Abatzoglou and Boivin, 2008]. Therefore, biogas upgradation is resorted to, which is achieved either by scrubbing of $CO_2$ or conversion of $CO_2$ to $CH_4$. Thus, the reduction of $CO_2$ and other impurities from biogas enriches the fuel efficiency, which could be used efficiently for various applications like cooking, vehicular fuel, and power generation [Ray et al., 2016; Sun et al., 2015].

On the other hand, microbial fuel cells (MFC) are a technology for both environmental protection and energy production by treating organic waste and generating electricity simultaneously. The use of MFC technology has been studied for many applications, such as the wastewater treatment of domestic sewage [Logan et al., 2006]. An MFC is a bioelectrochemical

reactor that converts organic material directly into electricity by electrochemical microbial activity on the anode [Berk and Canfield, 1964; Logan and Regan, 2006]. At an MFC anode, facultative anaerobic bacteria oxidize organic compounds as substrates to generate electrons and protons. The exoelectrogens deposit electrons on an anode, from which the electrons move towards the cathode across a resistor and through an external circuit [Kondaveeti et al., 2014]. At the cathode, the generated, electrons and protons combine with oxygen, usually in the form of air, to form water. Hence, the bio-potential developed between the bacterial metabolic activity and electron acceptor conditions leads to the generation of bioelectricity in MFC [Rahimnejad et al., 2010]. The MFC's voltage is measured as the potential difference between the anode and the cathode [Srivastava et al., 2015]. In a typical dual-chamber set-up, a proton-exchange membrane (PEM) is used between the anode and cathode chambers to complete the circuit. This PEM acts as the separator between the cathode and the anode. It is also one of the significant parts of MFC that physically separates the cathodic and anodic biological reactions [Harnisch and Schröder, 2009; Kim et al., 2007]. The PEM also allows access to excess positive charge (protons) in the anode to migrate to the cathode [Oh et al., 2004]. Using a wide variety of substrates, including acetate, glucose, and wastewater, MFCs have led to the successful generation of electrical current. In particular, MFCs are always preferred for sustainable and long-term power applications, with potential health and safety issues [Du et al., 2007]. Until now, the primary goal of MFC has been to generate a suitable current and power for use in small electrical devices [Rahimnejad et al., 2012].

More recently, the integration of AD and MFC has been studied to improve energy efficiency, reduce pollutants, and recover inorganic nutrients in waste treatment end products [Premier et al., 2013]. AD effluents provide the necessary amount of electrochemically active microorganisms

for anode reduction, thereby making the anode function stable during the process. In the case of cellulosic material, prior to biomethane production from AD, pretreatment is required to degrade it into glucose or lower molecular compounds [Fradler et al., 2014; Kim et al., 2015]. The integration of microbial processes to yield biofuels and value-added bioproducts has been proposed to be more advantageous due to the overall economy and efficiency when compared to a single-stage system [Nordi et al., 2017; Patel et al., 2015].

Furthermore, electricity generation by an MFC utilizing renewable carbon sources can offer an alternate route to fossil fuels [Rabaey et al., 2008]. Cattle dung can be utilized by several fermentable bacteria and electricity-producing microorganisms as it contains numerous easily degradable substrates [Zhao et al., 2012].

An example of a substrate for an electrode reaction with acetate is as follows:

$$CH_3COO^- + 2H_2O \longrightarrow 2CO_2 + 7H^+ + 8e^- \quad (6.1)$$

Instigation of methane production can be done through two types of metabolic pathways in the presence of acetate, carbon dioxide, and hydrogen. The first metabolic pathway implicates the role of hydrogenotrophic methanogens, which convert $CO_2$ directly to $CH_4$. The other metabolic pathway selects an indirect path where homoacetogenic bacteria first convert $CO_2$ to acetate and then convert it to $CH_4$ by the acetoclastic methanogens [Angelidaki et al., 2018].

$$C_2H_4O_2 \longrightarrow CH_4 + 2CO_2 \quad (6.2)$$

$$4H_2 + CO_2 \longrightarrow CH_4 + 2H_2O \quad (6.3)$$

The first one is preferable as hydrogenotrophic methanogens (*Methanobacterium, Methanoculleus* and *Methanomicrobium*) are more abundant than acetoclastic methanogens such as *Methanosarcina* [Agneessens et al., 2017].

Hence, an alternative pathway for the simultaneous conversion of raw biogas products to biomethanation and electricity is needed. In this work, we developed a single chamber, above-ground, portable anaerobic digester (AD) hybridized with a membrane electrode assembly (MEA) for co-generation of biogas and electricity. The AD-MEA system utilizes cattle dung that has the ability to serve as a substrate for anaerobic digestion as well as a substrate for oxidation to be acted upon by exoelectrogens. The objective of this study is to demonstrate that hybridization of an AD-MEA system supports syntrophic interactions among methanogens and exoelectrogens for the simultaneous generation of methane-enriched biogas and electricity as a by-product.

## 6.2 MATERIALS AND METHODS

### 6.2.1 MATERIALS USED IN THE EXPERIMENTAL SETUP

Materials in the fabrication of the AD-MEA system involved the use of ISO-molded graphite plates, carbon cloth (Graphite Store, USA), and a proton exchange membrane, *viz.*, Nafion® 117 (Fuel Cell Store, USA). The electrical connection of the electrodes with the copper wire (electrode terminal wires) was established with silver conductive epoxy (MG Chemicals, USA). To eliminate the effect of silver in the anodic and cathodic reactions, the silver was covered with non-conductive epoxy. Other chemicals such as $H_2O_2$, $H_2SO_4$ (Himedia) were used for the activation of the Nafion® 117 membrane.

### 6.2.2 FABRICATION OF THE AD-MEA SYSTEM

A carbon cloth with a dimension of 6 cm × 6 cm and an ISO-molded graphite plate with a dimension of 6 cm × 6 cm × 0.3 cm were prepared to be used as the anode and the cathode, respectively. These two electrodes were separated by a Nafion® 117 membrane. The Nafion membrane was activated prior to use in the membrane electrode assembly. Initially, the membrane was treated with a 3% $H_2O_2$ solution at 100 $^0$C for two hours to remove any debris from the surface of the membrane. This step was followed by treatment of the membrane with a 5% $H_2SO_4$ solution to activate the membrane. The membrane was rinsed with Milli Q water after each and every treatment process. Copper wires were attached to the electrodes with silver conductive epoxy to establish the electrical connections of the electrodes with an external load. The exposed area of the silver conductive epoxy was covered with non-conductive epoxy to eliminate the effect of silver in the fuel cell operation. Thus, the MEA (Fig. 6.1) was fabricated by placing the proton exchange membrane, Nafion® 117, in between the anode and cathode, followed by hot pressing at a temperature of 120 °C and pressure of 70 kg/cm$^2$ for 3 min.

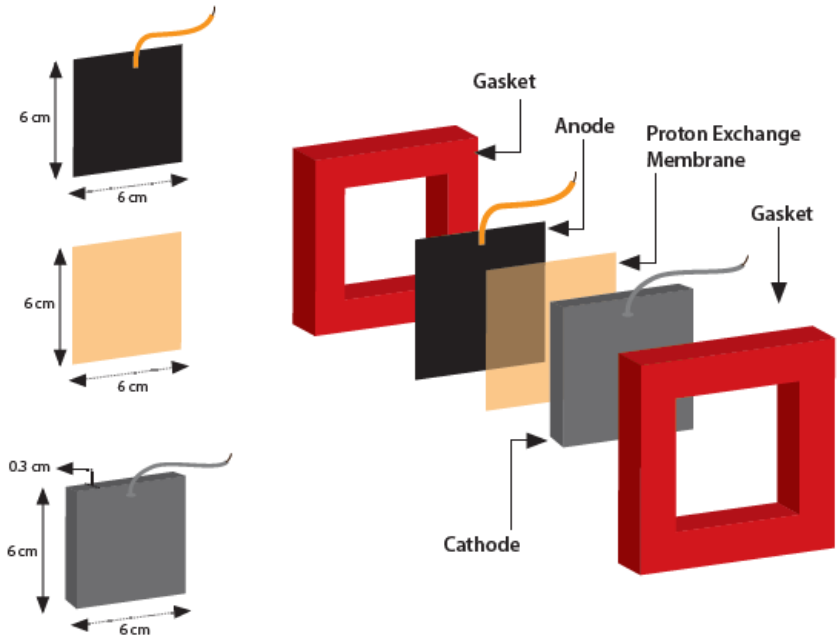


**Fig. 6.1** Schematic of the membrane electrode assembly

A batch-type lab-scale anaerobic digester was made using a container of 5L volume having a diameter of 14 cm and a height of 30 cm. The cap of the anaerobic digester was provided with an inlet for introducing the fresh cattle dung slurry and an outlet for the emission of biogas generated within the AD. A 6 cm × 6 cm square hole was created on one side of the container to attach to the MEA. The MEA was then fixed to the wall of the AD, which had an area of 36 $cm^2$ to function as the working area of the electrode.

As shown in Fig. 6.2, the anode side was placed towards the hole of the container so that the anode remains in contact with the organic waste. The cathode of the MEA remains exposed to the air in order to receive atmospheric oxygen. The complete MEA was supported on the side of the container with silicon gaskets and high-quality adhesives. Gas produced from the digester was measured by the liquid (acidified water) displacement method using a liquid container and a

graduated flask. The produced biogas was collected in a tedlar bag for biogas analysis with the help of gas chromatography (GC).

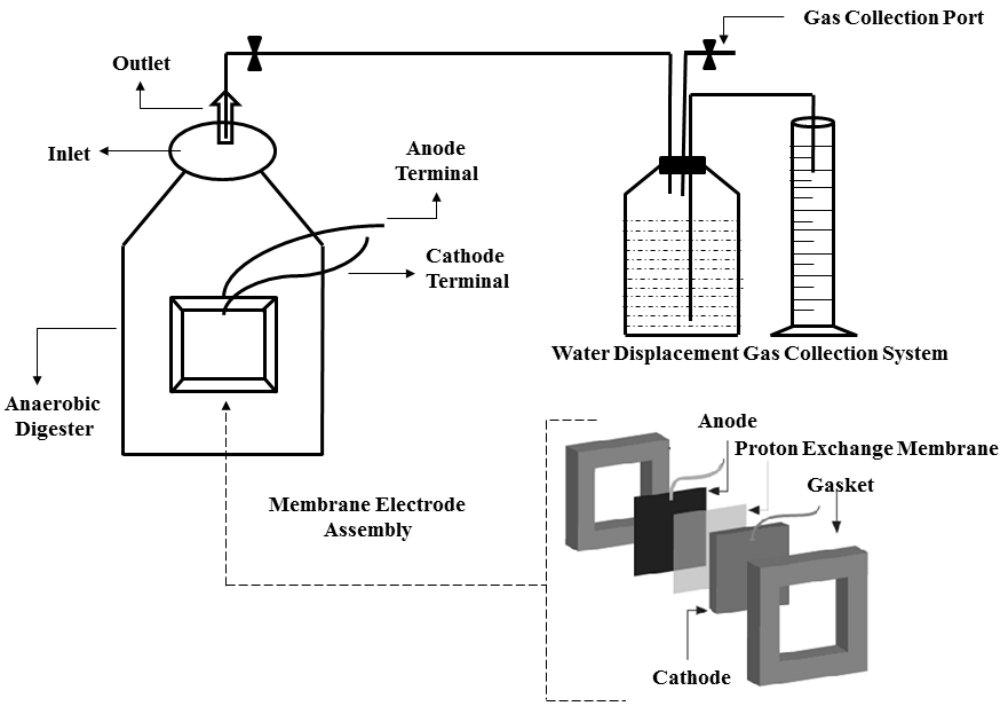


**Fig. 6.2** Schematic of the anaerobic digester hybridized with a membrane electrode assembly

Teflon tape was used to seal all the joints and to make the AD airtight. The digester was wrapped with black paper to avoid light in order to prevent photochemical reactions. The construction of the AD-MEA setup utilizes polymer containers, silicone tubes, carbon cloth, graphite plate, Nafion® 117 membrane, and conducting wires, which are robust in nature and can be re-utilized innumerable times for re-generation of the AD-MEA setup.

### 6.2.3 OPERATION OF THE HYBRIDIZED AD-MEA SYSTEM

The quality of biogas can be enhanced by reducing the inhibitory effects of substances and increasing the syntrophic interaction between different microorganisms in the anaerobic

digestion process [Amani et al., 2010, Werner et al., 2011]. Many research efforts have been made to identify factors that inhibit the anaerobic digestion processes as well as to propose an alternate pathway that could stimulate syntrophic interactions among co-existing microorganisms and their chemical reactions in the digestion process. Microbial activity in the AD system can be increased by electrical connections between microorganisms that occur as a result of feedstock aggregation, which enhances methanogenic reactions [Barua and Dhar, 2017]. An approach has been made to accelerate microbial metabolism in anaerobic digestion processes by using a non-biological conductive surface, i.e., carbon cloth, and to hybridize AD with MEA in order to stimulate interspecies hydrogen transfer (IHT) and hydrogen partial pressures (HPP) for electron transfer. Because of its high surface area and electrical conductivity, carbon cloth is used as the anode in MEA.

The AD and MEA were constructed separately, and then the MEA was integrated with the AD for the construction of the complete setup. Fresh cattle dung used in the AD-MEA setup was collected from Auniati Xatra, near IIT Guwahati, Assam, India (26°11'27.8"N, 91°43'17.3"E). The cattle dung was uniformly mixed with water at a ratio of 1:1 to form homogenous slurry and was introduced into the AD-MEA system. The digester was filled with the slurry up to 60% of its total volume to accommodate the gas volume and expansion of the slurry during the fermentation process. The AD-MEA setup was operated in a batch mode at an ambient temperature ranging from 26 °C to 35 °C under dark conditions with a hydraulic retention time (HRT) of 50 days with occasional manual stirring. After loading the cattle dung slurry into the AD-MEA setup, an airtight condition was maintained to avoid any interference of atmospheric oxygen. A similar volume of AD with cattle dung as feed material was also installed in batch mode, maintaining all conditions similar to the AD-MEA, which was kept as control.

Oxidation of organic matter is brought about by the action of microorganisms in the anodic chamber, and the aerobic cathode supports the reduction reaction. Also, the carbon cloth placed in the anode chamber accepts the electrons produced by the exoelectrogens as a terminal electron acceptor, and the nafion membrane, which acts as the proton exchange membrane, facilitates the proton flow to the cathode side. The electron and the proton cloud at the anode and the cathode surfaces produce the anode and the cathode potentials, respectively, and these two potentials give rise to the overall cell potential. When a load is connected across these electrodes, electrons flow from the anode towards the cathode and reduce oxygen at the surface of the cathode. This flow of electrons from the anode towards the cathode produces the current from the cathode to the anode [Kim et al., 2006; Kim et al., 2008].

### 6.2.4 ANALYSES AND CALCULATIONS

#### 6.2.4.1 PROXIMATE ANALYSIS AND pH

Moisture content was calculated for the fresh cattle dung sample, while volatile matter, ash, and fixed carbon content were calculated using oven-dried cattle dung samples. The amount of moisture and ash content were estimated using the procedure adopted by the National Renewable Energy Laboratory (NREL). For the determination of volatile matter, American Society for Testing and Materials (ASTM) D 271-48 was followed. Fixed carbon was calculated by the difference between the summation of moisture, volatile matter, and ash content. The initial pH of the fresh cattle dung slurry before anaerobic digestion was measured using a digital pH meter *(Make: Mettler Toledo, Model: 30266889)*.

### 6.2.4.2 GAS CHROMATOGRAPHY

Biogas samples were collected in Tedlar® bags and were analyzed for $CH_4$ and $CO_2$ concentrations in a Gas Chromatograph (*Thermo Fisher Scientific Trace GC 1110 Gas Chromatograph, USA*) coupled with a thermal conductivity detector using helium as a carrier gas at a makeup flow of 20 mL/min. The oven and detector temperatures were maintained at 45 and 180 °C, respectively.

### 6.2.4.3 CALORIFIC VALUE ANALYSIS METHOD

The formula reported by Li et al. (2017) was used to calculate the higher calorific values (HCV) and lower calorific values (LCV) of raw and enriched biogas generated from the control and AD-MEA setup [Li et al., 2017].

$$HCV_{biogas} = 0.3989 \times MC + 0.0213 \ (R^2 = 1) \quad (6.4)$$

$$LCV_{biogas} = 0.3593 \times MC + 0.0192 \ (R^2 = 1) \quad (6.5)$$

where MC is the methane content in biogas (%) and $R^2$ is the square of the correlation. The HCV and LCV of pure methane were 39.82 and 35.87 MJ/$m^3$, respectively [Li et al., 2014].

### 6.2.4.4 FIELD EMISSION SCANNING ELECTRON MICROSCOPY

The morphological characterization of biofilm formed on the anode was studied through FESEM (*Make: Zeiss, Model: Sigma 300*). FESEM at 3 kV was used to capture the images of blank carbon cloth and the biofilm formed on the surface of the anode. After 50 days of operation, FESEM analysis of the anode from the MEA set up was performed. The anode surface was thoroughly washed with a 0.1 M PBS solution to remove all the debris from the surface. Once the surface was cleaned, it was air dried for 1-hour, followed by the layering of glutaraldehyde

solution over the entire surface of the electrode and air dried. This step was further followed by cleaning of the surface with 0.1M PBS and again was left for air drying. At the end, the surface was rinsed with 30%, 50%, 60%, 80%, 90%, and 100% ethanol solutions, respectively. The sample was mounted on a stub using double-sided conductive carbon tape. A single gold coating on the surface of the sample was done in a vacuum coating unit called Gold Sputter Coater, which makes the sample electrically conductive.

#### 6.2.4.5 AD-MEA CALCULATION

The constructed AD-MEA was observed for monitoring the open circuit voltage (OCV) for the duration of 50 days of operation since day 1. The OCV of the AD-MEA was documented using a digital multimeter (Fluke 87V MAX True-rms Digital Multimeter, Fluke Corporation) on a daily basis. During this period of operation, when the OCV of the AD-MEA seemed to be stable, the AD-MEA system was polarized by connecting different values of resistors between the anode and cathode terminals of the system. Different resistor values ranging from as high as 1MΩ to a low value of 100Ω were chosen for the polarization of the AD-MEA setup. The respective polarization values, such as the current and voltage, were monitored using an Arduino UNO microcontroller board and the recorded values were extracted into an excel sheet for further calculation of the current and power densities as well as the I-V characteristics of the system. The current through resistors and power dissipation were calculated using Ohm's law and the power equation, respectively.

Ohm's law, $I = V/R$ (6.6)

Power equation, $P = VI$ (6.7)

Current and power densities were calculated by dividing the current and power values by the total surface area of the anode. Where, V (V) is voltage, I (A) is the current, and R (ohm) is the external resistance.

The electrochemical studies, including cyclic voltammetry on the anode electrode, were performed using a potentiostat (Autolab PGSTAT-302N, Metrohm). The results obtained during the above observations are discussed in the following sections.

## 6.3 RESULTS AND DISCUSSION

### 6.3.1 PROXIMATE ANALYSIS AND pH OF CATTLE DUNG

The results of the proximate analysis and pH of cattle dung are shown in Table 6.1. During anaerobic digestion of organic matter, volatile solids break through various chemical reactions led by microbes are a vital factor for deciding the amount of biogas generation [Yadav et al., 2017]. Cattle dung is used as a primary substrate in many small and large-scale biogas plants due to its higher digestibility rate of labile compounds.

**Table 6.1** Proximate analysis and pH of the fresh cattle dung samples. Each value is the Mean ± SD of three replicates.

| Feedstock sample | Fresh cattle dung (%) | | Proximate analysis (%), Dried basis | | | pH (Cattle dung slurry) |
|---|---|---|---|---|---|---|
| | Moisture | Total solid | Volatile matter | Ash | Fixed carbon | |
| Cattle dung | 90.6 ± 0.4 | 9.4 ± 0.4 | 67.5 ± 0.6 | 19.4 ± 0.6 | 13.1 ± 0.2 | 7.1 ± 0.1 |

The moisture content of the fresh cattle dung was 90.6 ± 0.4%, while the volatile matter was calculated for the oven-dried sample and was found 67.5 ± 0.6%. The initial pH of the cattle

dung mixed with water in a 1:1 ratio was measured at 7.1 ± 0.1. pH can be high or low depending upon the feedstock compositions and is a significant parameter in evaluating the quality of manure as it determines the microbial activity, nutrients, and physical conditions.

### 6.3.2 BIOGAS PRODUCTION AND METHANE ENRICHMENT IN HYBRIDIZED AD-MEA SYSTEM

A control system with similar volume and dimensions was also installed to compare the gas production and percentage of $CH_4$ concentration with the developed AD-MEA system. Figure 6.3 shows the comparison of daily biogas production (ml) of the control and the developed AD-MEA system. Biogas is produced from anaerobic fermentation of organic substrates, and it was observed that biogas production is enhanced by the hybridization of AD with MEA.

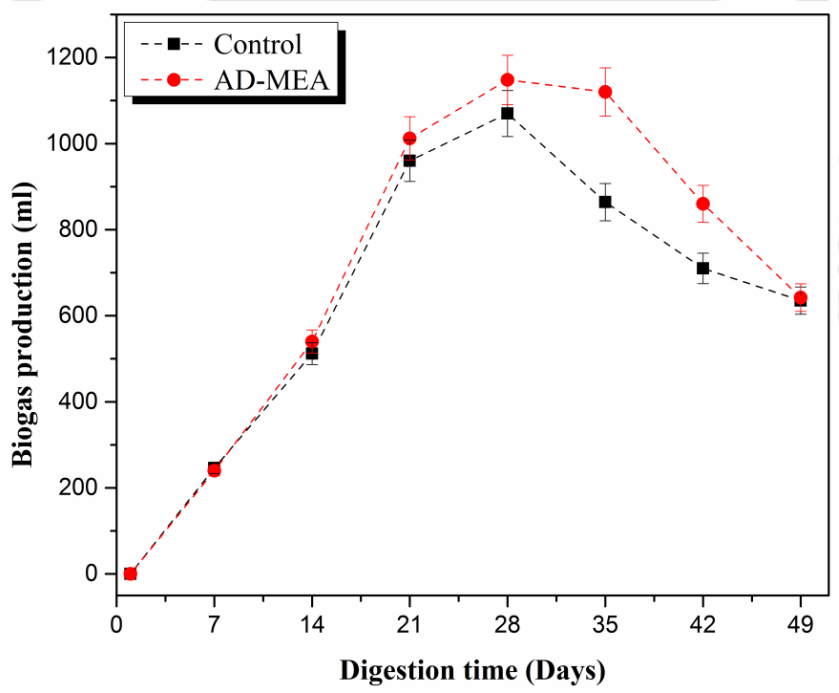


**Fig. 6.3** Daily biogas production of control and AD-MEA system

The initial biogas production was started within 7 days of incubation for both the control and AD-MEA systems. This may be due to the use of fresh cattle dung, which could be easily hydrolysed by acidogenic and acetogenic bacteria, which further provides the substrate to the methanogenic bacteria for methanogenesis [Seppala et al., 2013]. The maximum yield of biogas production of control and AD-MEA systems was measured and their peak values were 1070±53 ml and 1148±57 ml on the 28$^{th}$ day, respectively. It was seen from the results that the biogas production for control started decreasing after the 28$^{th}$ day, whereas for the AD-MEA system, it started decreasing after the 35$^{th}$ day. This could be due to the integration of AD with the MEA, which maintained syntrophic interactions among exoelectrogens and methanogens for further production of biogas.

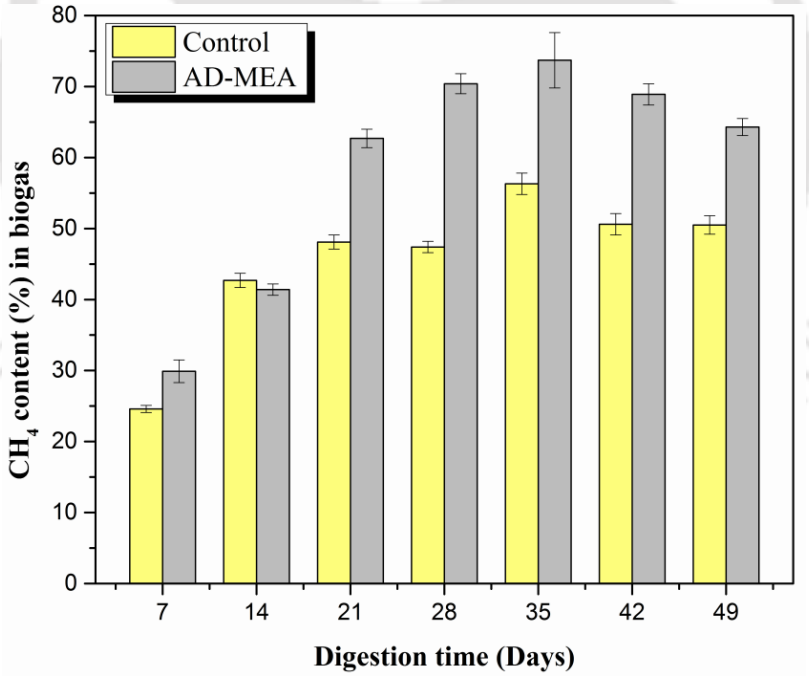


**Fig. 6.4** Methane content (%) of control and AD-MEA system

Figure 6.4 represents the methane content profile of biogas for control and AD-MEA systems. The highest concentration of $CH_4$ and $CO_2$ in control was 56.3±1.5% and 43.7±0.9%

respectively. On hybridization of the AD with MEA, the highest concentration of $CH_4$ and $CO_2$ was 73.7±3.9% and 26.3±0.5% respectively. This shows that there is an increase in the concentration of $CH_4$ from 56.3% to 73.7%, with an increment of 17.4% on the 35$^{th}$ day. The increased rate of methane production is anticipated owing to the presence of a conductive carbon surface, which serves as the anode electrode of the MEA.

MEA has the ability to transfer electrons extracellular through exoelectrogens, which on hybridization with AD, intimates collaboration with acetoclastic and hydroclastic methanogens, thereby improving the efficiency of the overall $CH_4$ yield [Premier et al., 2013; Wang et al., 2015]. The results also showed that the hybridization of the MEA with the anaerobic digester simultaneously enhances the production and enriches the quality of biogas when incubated in dark conditions. Organic waste like cattle dung contains numerous easily degradable substrates that can be utilized by a number of fermentable bacteria and electrogenic microorganisms. As reported by Singh et al. (2011), in a fresh cattle dung methyl-coenzyme M reductase A (mcrA) library, 93.5% of the clones belonged to the hydrogenotrophic methanogens, while 6.5% of the total clone diversity represented the acetoclastic methanogens [Singh et al., 2011]. In the absence of oxygen, electrogenic microbes decompose organic matter and produce electrons and protons simultaneously. As the anode chamber is anaerobic, the hydrogenotrophic methanogens combine electrons, protons and the excess $CO_2$ to produce $CH_4$ through direct interspecies electron transfer (DIET), which is the second route of methane generation in this setup and is shown in Eq. 6.8.

$$CO_2 + 8H^+ + 8e^- \longrightarrow CH_4 + 2H_2O \qquad (6.8)$$

The rate of $CO_2$ conversion to methane by this route is governed by the size of the electrode. The larger the size of electrode, the greater is the $CO_2$ reduction [Garg et al., 2020; Kato et al., 2012].

### 6.3.3 CALORIFIC VALUE OF PRODUCED BIOGAS

The HCV and LCV of biogas produced from the control and AD-MEA setups were theoretically calculated using equations 6.4 and 6.5, respectively, and are shown in Figs. 6.5 and 6.6. The HCV (22.48 MJ/$m^3$) and LCV (20.24 MJ/$m^3$) of biogas produced in the control were significantly less than the HCV (29.42 MJ/$m^3$) and LCV (26.491 MJ/$m^3$) of biogas obtained from the AD-MEA setup. The HCV and LCV values purely depend on the methane content in biogas and may change with the variation of the concentration of biogas.

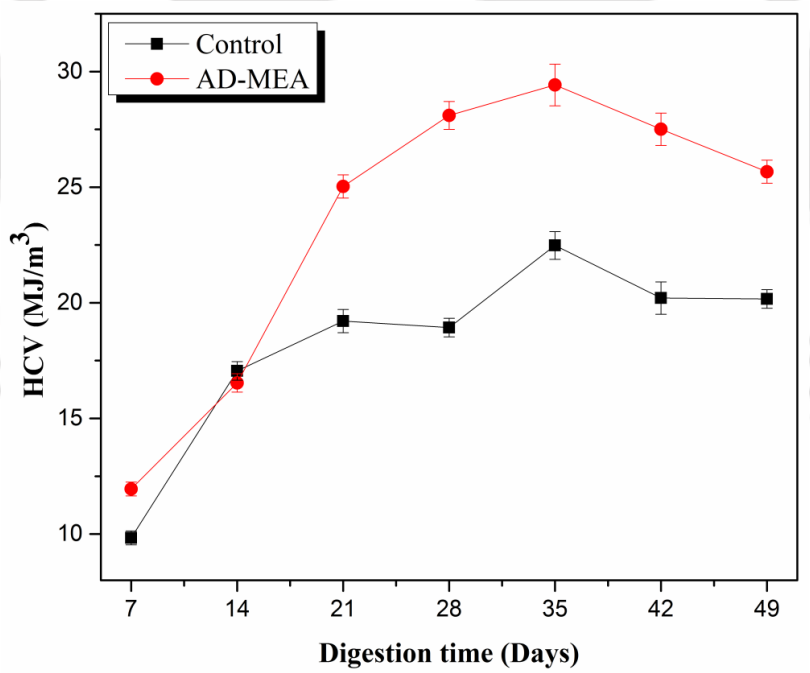


**Fig. 6.5** HCV of control and AD-MEA system

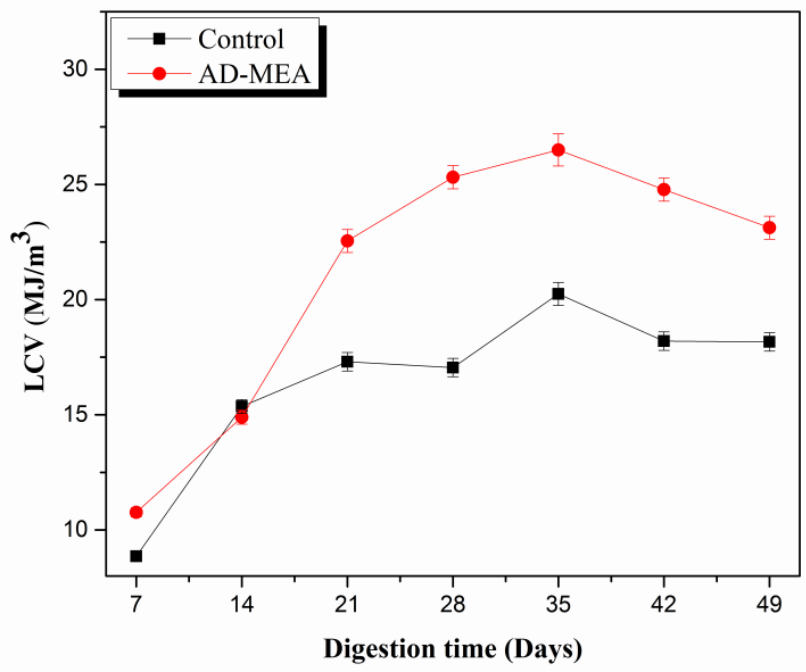


**Fig. 6.6** LCV of control and AD-MEA system

### 6.3.4 VOLTAGE AND POWER GENERATIONS IN AD-MEA

With the construction of the AD-MEA, the open circuit voltage (OCV) was documented on a daily basis with the help of a digital multimeter. Figure 6.7 shows the voltage (OCV) with respect to time of the hybridized AD-MEA. Initially, the OCV of the system increased rapidly till the 8$^{th}$ day of operation, and thereafter the OCV entered into a state of saturation until the 27$^{th}$ day. During this period, the average OCV remained in the range of 445±6.2 mV. After this period, some fluctuations were observed along with an increase in the OCV up to the 30$^{th}$ day. After this period, the OCV again entered into a saturation state up to day 40. The potentials of the two electrodes are dependent on the activity of electrogens, the area of the electrodes, and also temperature. The AD-MEA system was operated at ambient temperature and had equal electrode sizes.

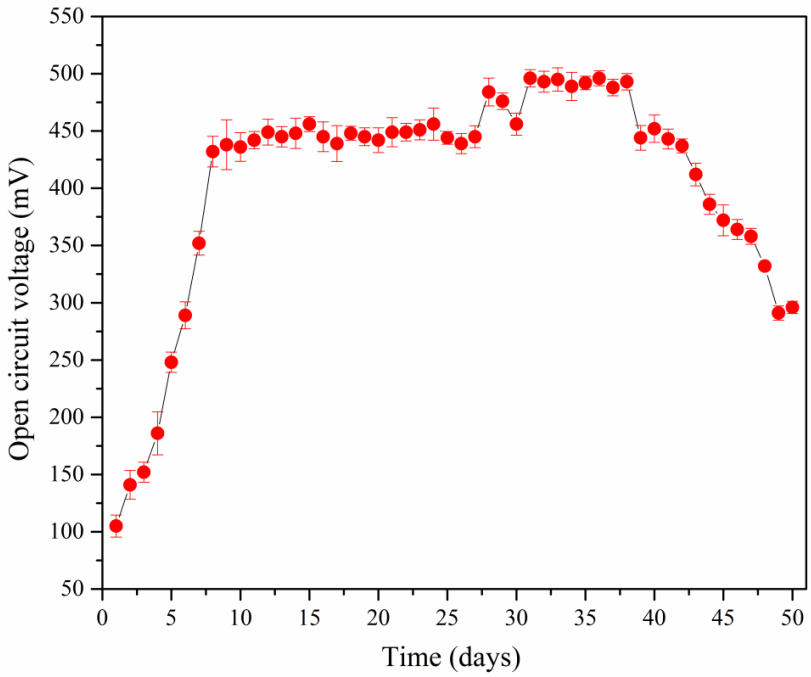


**Fig. 6.7** Open circuit voltage with respect to the time of the AD-MEA system

It is expected that after the period of 30 days, the colonization of microbes on the electrode surface attained saturation level when a maximum OCV of 496±7 mV was observed. Also, the HRT for biogas digesters in the experimental location is 55 days, and hence, beyond day 40, the reduction in the magnitude of OCV was also observed. In this saturation period, the AD-MEA was polarized with different values of resistors in order to obtain the polarization curves. The characteristics of the AD-MEA, such as the current density, the power density, and the I-V characteristics, were studied with the polarization curve. Different resistor values, such as 1MΩ, 560kΩ, 470kΩ, 390kΩ, 220kΩ, 150kΩ, 100kΩ, 56kΩ, 22kΩ, 10kΩ, 1kΩ, 750Ω, 560Ω, 220Ω and 100Ω were connected one at a time, with the terminals of the anode and the cathode for a duration of 10 minutes, and the respective voltages across the resistors were documented. Once the potentials were recorded, the respective current and power through the resistors were calculated using Ohm's law and the power equation.

Figure 6.8 represents the polarization curve obtained from the AD-MEA. From the polarization data, it was observed that the AD-MEA could produce a maximum average power density of 2.87 $mW/m^2$ and about 70 $mA/m^2$ current density, respectively.

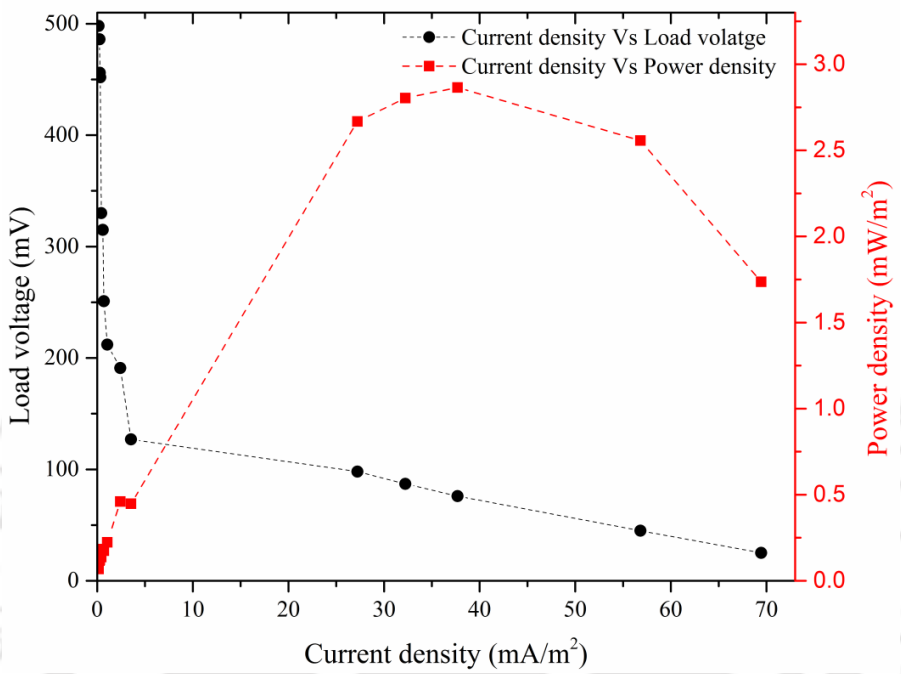


**Fig. 6.8** Polarization curve of the AD-MEA system

Current and power densities are subject to incubation conditions, reactor volume, microbial load, the material of the electrode, and geometric area of the electrode [Choi, 2015; Chung, et al., 2019]. Using the maximum power transfer theorem, which states that maximum power can be dissipated when the load resistance is equal to that of the power source resistance, the internal resistance of the AD-MEA was obtained. In this study, the internal resistance of the system was close to 560Ω, which is a relatively low value for the system. The current density of the AD-MEA followed a rapid drop in the low current range of up to 10 $mA/m^2$. The greater slope of the current density curve in the lower range of current signifies the activation losses. However, beyond 10 $mA/m^2$ and until the higher current range, the slope of the curve is very small. The

lesser slope of the current density in the higher range of current is due to less mass transfer limitation. Based on requirements, these power and current ratings can be increased by increasing the number of AD-MEA setups and connecting them either in series or in parallel or in combinations of both.

### 6.3.5 MORPHOLOGICAL CHARACTERIZATION OF BIOFILM

Figure 6.9 shows the FESEM images of blank carbon cloth and the anaerobic electrode at 10 KX, 50 KX, and 100 KX magnifications, respectively. Woven carbon fibre bundles are distinctly visible in the FESEM image of the blank electrode. It is seen from the micrographs that electrogenic microorganisms form a biofilm on the surface of the electrode in contact with the organic substrate. Moreover, the biofilm formed shows the presence of high-density, cluster-shaped microbial growth, ubiquitously connecting bacteria to bacteria and bacteria to the electrode surface, suggesting the cluster is electrically conductive. From the results, it is anticipated that hybridization of AD with MEA stimulates methanogenic reactions in the AD-MEA system by providing a surface for biofilm formation, thus promoting electron exchange through IHT [Aziz et al., 2011].

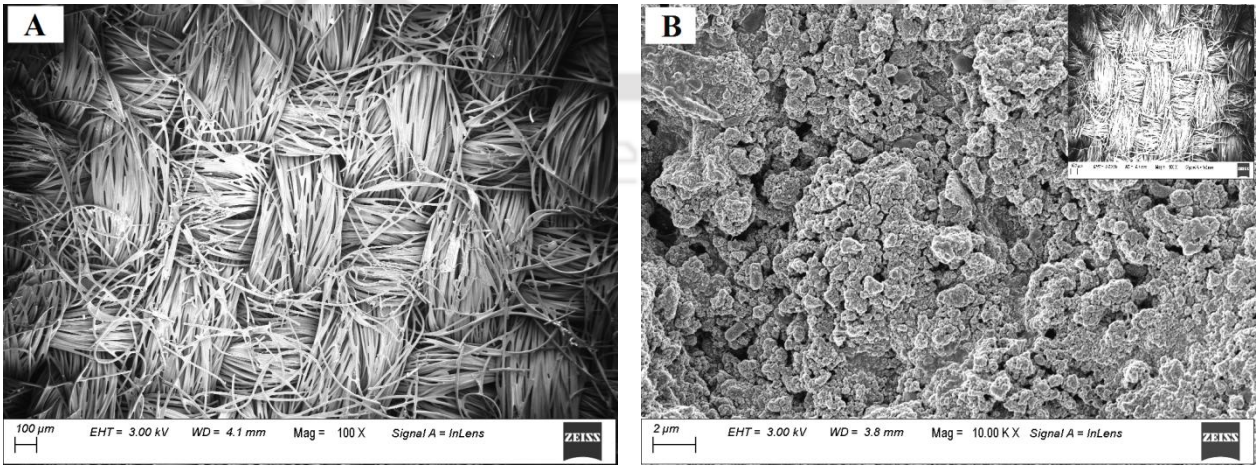

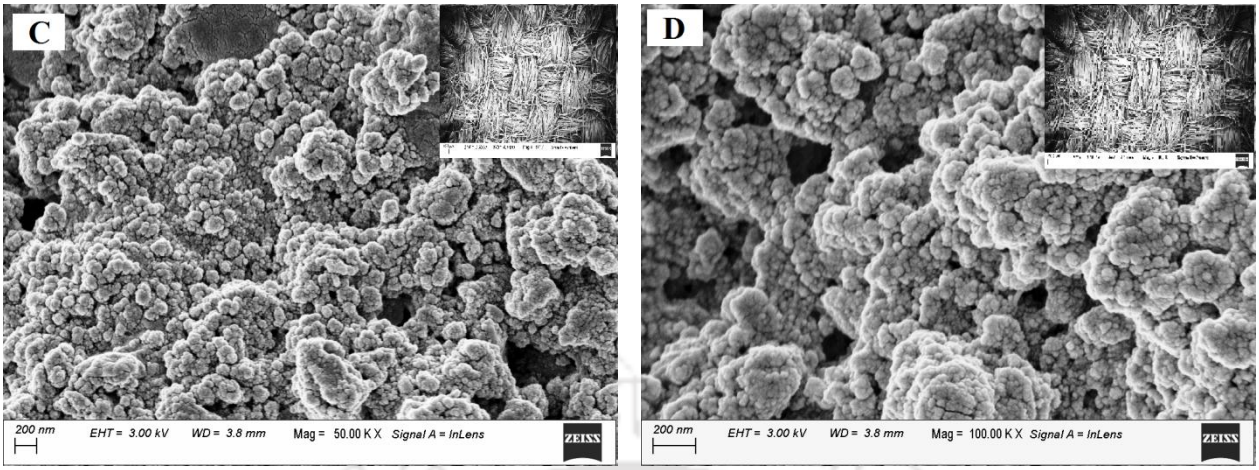


**Fig. 6.9** FESEM images of (A) blank anode (carbon cloth), (B) biofilm formation on anode at 10 KX, (C) biofilm formation on anode at 50 KX, (D) biofilm formation on anode at 100 KX

### 6.3.6 MICROSCOPIC STUDY OF THE BACTERIA ON THE ANODE SURFACE

Figure 6.10 shows the microscopic images of a microbial colony on the anode surface. The microbial culture did not retain the Gram stain and hence is Gram (-ve), which may be considered advantageous for supporting the electrogenic activity of the MEA, as they are anticipated to have higher power generation capacity [Juang et al., 2011]. The microscopic images clearly show the microbial colonies as either clusters or chain-like structures, which is in agreement with the FESEM images. However, further detailed studies of the microbial consortia may be conducted to understand the mechanisms contributing towards $CO_2$ conversion to methane and subsequent power generation.

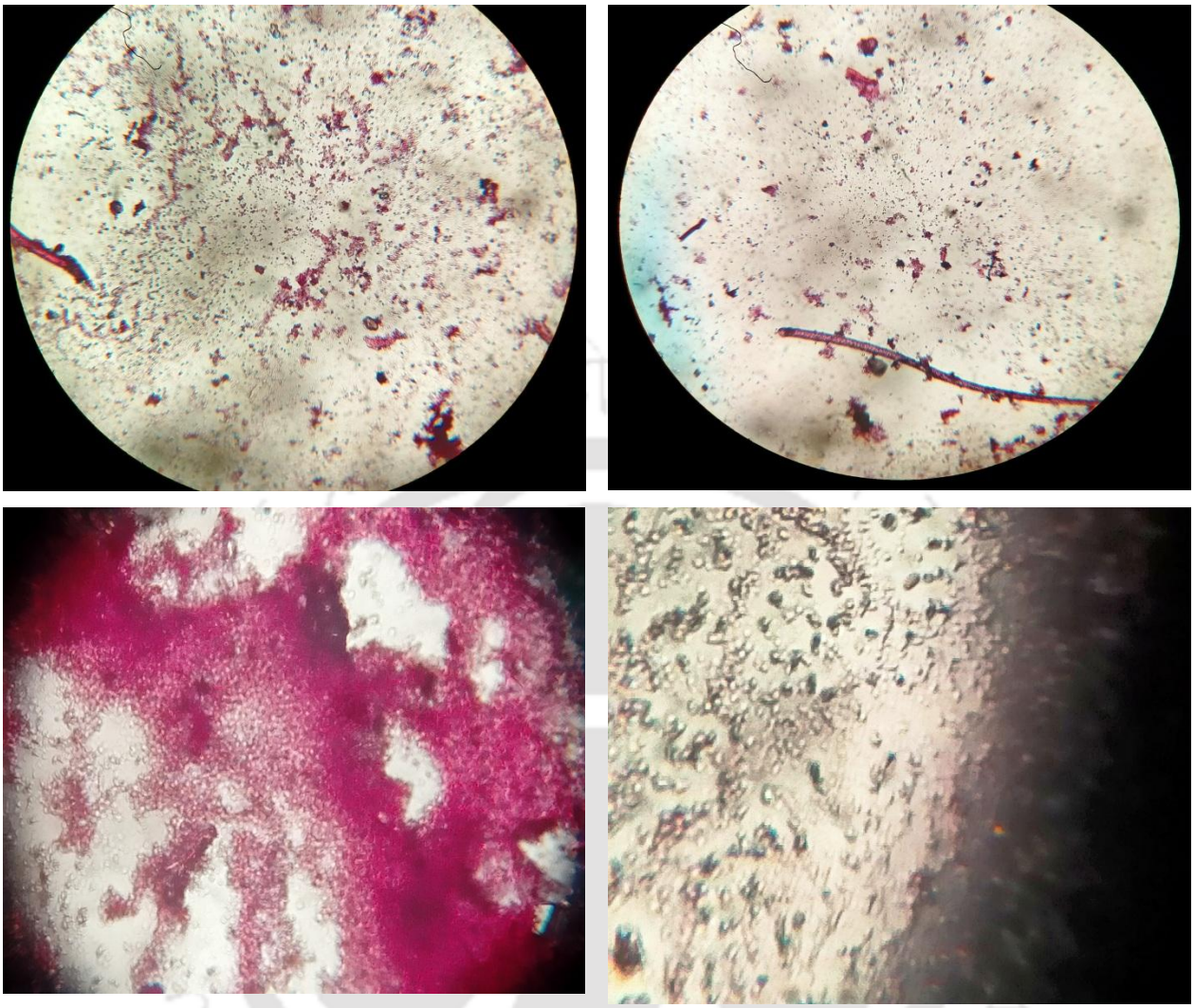

**Fig. 6.10** Microscope images of bacteria on the anode surface

### 6.3.7 ELECTROCHEMICAL STUDIES OF THE ELECTRODE IN AD-MEA SETUP

The cyclic voltammetry (CV) study was performed on the anode electrode under two different conditions. The control CV was performed with a carbon cloth as the working electrode and phosphate buffer as the electrolyte. For the experimental setup, the CV was performed in the MEA portion of the AD-MEA system. Figure 6.11 shows the comparative results of the blank and experimental setups. The anode incubated in cattle dung slurry showed increased voltage as

well as current compared to the blank electrode, thereby affirming the presence of electrogenic bacteria in the cattle dung slurry. Moreover, the cyclic voltammogram of the anode in the experimental setup showed an oxidation peak at -0.545 V (vs. Ag/AgCl), which is absent for the blank condition. The oxidation current indicates the presence of electrogenic bacteria, which is anticipated to facilitate the syntrophic interactions among co-existing microorganisms for enhancing $CH_4$ production [Feng et al., 2018].

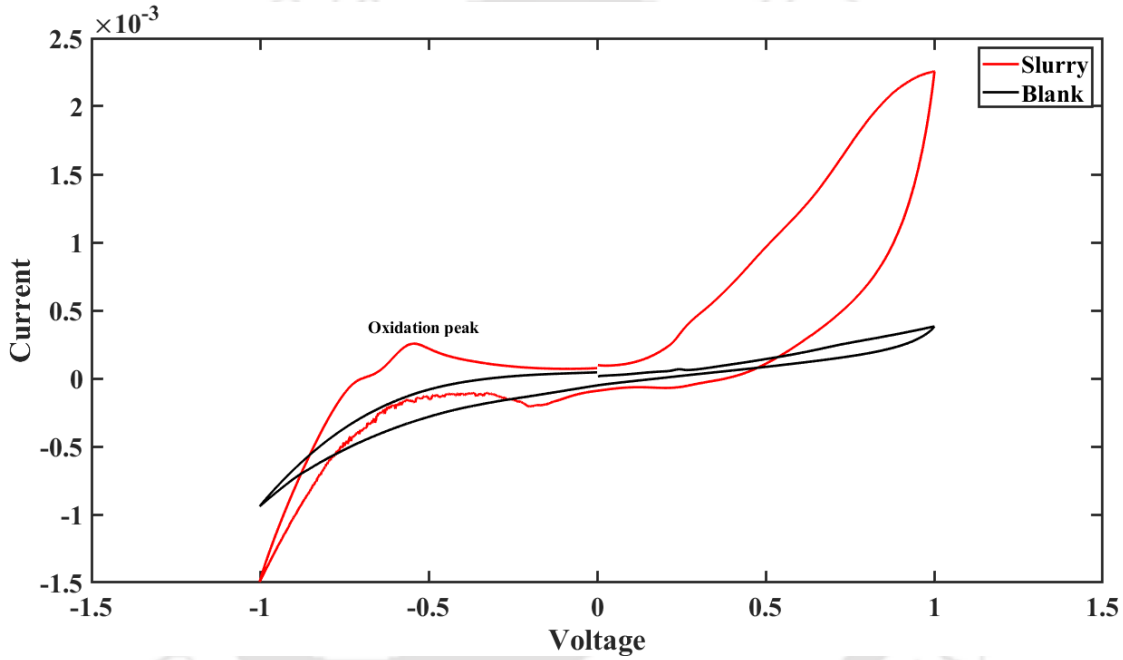


**Fig. 6.11** A comparative study of the CV of blank vs. slurry electrode in AD-MEA

Many authors reported that electrogenic bacteria could directly transfer electrons to the extracellular electron acceptors, which are usually present in anaerobic systems, such as digestion slurry [Rotaru et al., 2014; Yoon et al., 2007]. However, there is a need for an external driving force for the enhancement of the activities of electrogenic bacteria [Feng et al., 2017]. In conventional anaerobic digestion systems, there is very limited syntrophic interaction amongst microorganisms for the reduction of $CO_2$, which in this case could be overcome by hybridization

of the AD with an MEA system. The results obtained from gas chromatography, which features $CH_4$ enrichment in the AD-MEA as compared to the control system, further support this statement.

### 6.3.8 KINETIC MODELS FOR DATA FIT

The experimental data of biogas production obtained from the control and AD-MEA systems were checked for the goodness fit using three non-linear mathematical models, viz., the modified Gompertz function, the Logistic model, and the Transference model. The three kinetic models were used to determine the maximum biogas production rate, biogas production potential, and lag phase for anaerobic digestion by fitting the measured biogas yields [Donoso-Bravo et al., 2010; Luo et al., 2016; Rajput et al., 2018].

As shown in equation 6.9, the Modified Gompertz equation has been widely used in the fields of methane and hydrogen production.

$$B = P\exp(-\exp(\frac{R_m.e}{P}(\lambda - t) + 1)) \qquad (6.9)$$

The Logistic function, as shown in Eq. 6.10, was used to predict the kinetics of biogas production. This model has been used for the process of anaerobic fermentation as well as for the estimation of methane production in landfill leachate [Pommier et al., 2006].

$$B = \frac{P}{1+\exp(\frac{4R_m(\lambda - t)}{P}+2)} \qquad (6.10)$$

The transference function (Eq. 6.11) is mainly used for control purposes and, in some cases; it has been implemented in anaerobic digestion processes [Li et al., 2012].

$$B = P(1 - \exp\left(-\frac{R_m(t-\lambda)}{P}\right)) \qquad (6.11)$$

Where B represents the cumulative biogas production, P is the maximum biogas production potential, $R_m$ is the maximum biogas production rate, λ is the lag phase, t is the retention time, and e is Euler's function equal to 2.7183. The kinetic parameters for the control and AD-MEA systems were calculated by best fitting the experimental data of cumulative biogas production into equations (6.9)–(6.11) using the non-linear regression method (Matlab® 2018b). The statistical indicators such as coefficient of determination ($R^2$) and root mean square error (RMSE) were also calculated from the analysis. Consequently, to evaluate the kinetic parameters and goodness of the model results, the predicted cumulative biogas values from all three models were plotted against the experimental values. Figures 6.12–6.14 show the model fit (solid line) with the experimental data using the Modified Gompertz function, the Logistic, and the Transference model for both control and AD-MEA systems.

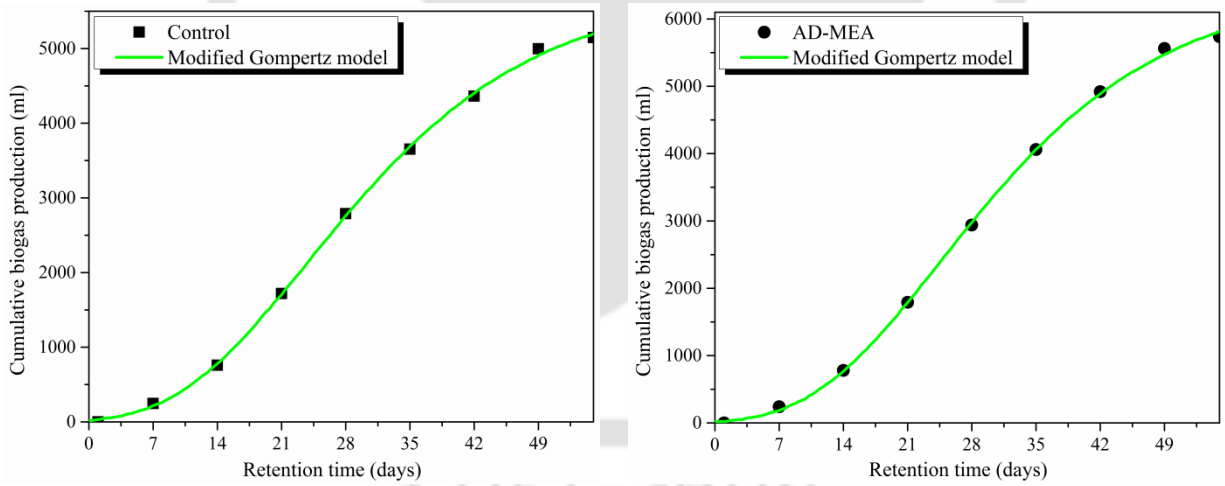


**Fig. 6.12** Experimental and Modified Gompertz model data of cumulative biogas production from cattle dung using control and AD-MEA system

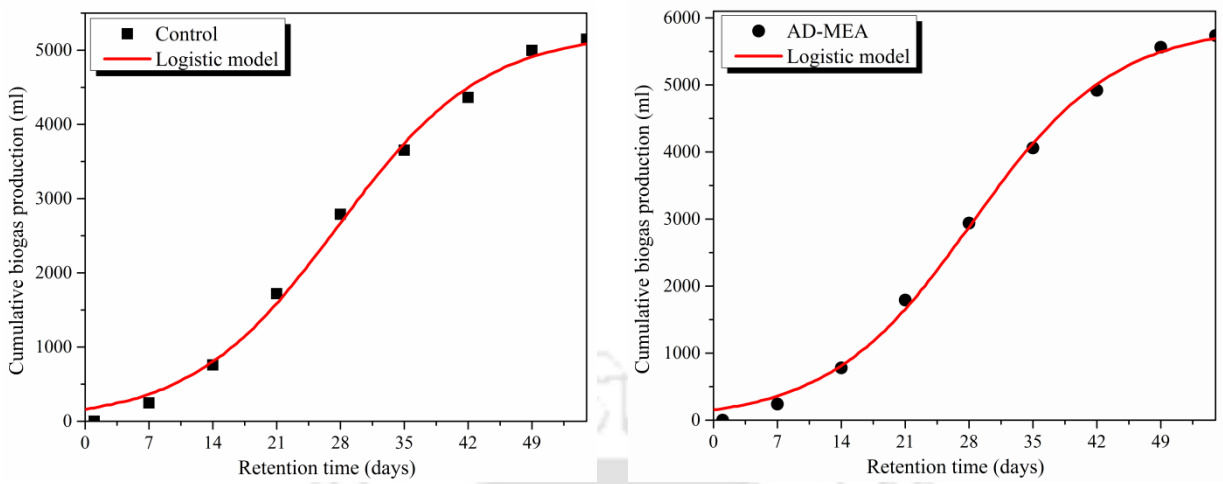


**Fig. 6.13** Experimental and Logistic model data of cumulative biogas production from cattle dung using control and AD-MEA system

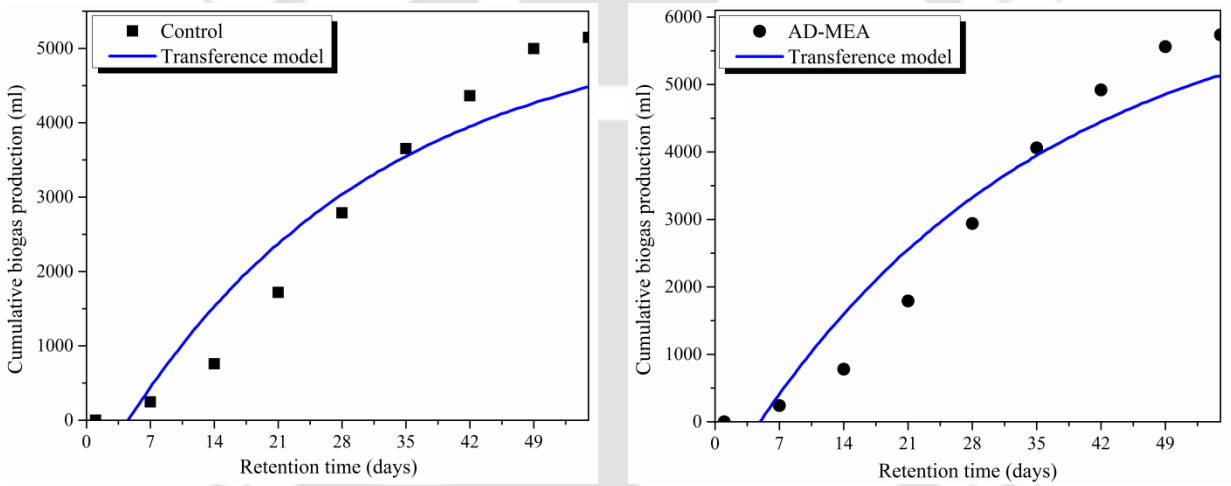


**Fig. 6.14** Experimental and Transference model data of cumulative biogas production from cattle dung using control and AD-MEA system

**Table 6.2** Parameters and goodness fit obtained with the evaluated models

| Parameters | Modified Gompertz equation | | Logistic function | | Transference function | |
|---|---|---|---|---|---|---|
| | **Control** | **AD-MEA** | **Control** | **AD-MEA** | **Control** | **AD-MEA** |
| P (ml) | 5798 | 6507 | 5263 | 5894 | 5385 | 6552 |
| $R_m$ (ml $d^{-1}$) | 151.1 | 172.1 | 164 | 187.9 | 190.9 | 200.6 |
| $\lambda$ (day) | 9.695 | 10.62 | 11.64 | 12.64 | 4.549 | 4.871 |
| $R^2$ | 0.99 | 0.99 | 0.99 | 0.99 | 0.91 | 0.92 |
| RMSE[#] | 54.8 | 57.26 | 140.4 | 120.1 | 683.5 | 729.8 |
| SSE[#] | $1.802 \times 10^4$ | $1.967 \times 10^4$ | $1.183 \times 10^5$ | $8.656 \times 10^4$ | $2.803\times 10^6$ | $3.196 \times 10^6$ |

[#]RMSE = Root mean squared error, SSE = Sum of squares due to error

The estimated kinetic parameters of biogas production, such as maximum biogas production rate, biogas production potential, and lag phase, obtained from all the three models based on cumulative biogas production data are summarized in Table 6.2. When comparing the performances of all the three models, the best fitted curves were obtained using the Modified Gompertz function and the Logistic model for both the control and AD-MEA systems, with the highest coefficient of determination ($R^2$ = 0.99), which shows an overall agreement between the models and the experimental data. All three models, as shown in Table 6.2, predicted an increase in the biogas production rate ($R_m$) and biogas production potential (P) of the AD-MEA system as compared to the control anaerobic system. Thus, for both the systems, the kinetic evaluation was focused mainly on the values of $R_m$ and P, considering that in biogas production, the nominal difference in the lag phase is negligible. The modified Gompertz and the logistic function model under the batch AD condition assume that the specific growth rate of methanogens is proportional to the produced gas with a sigmoidal production trend [Donoso-Bravo et al., 2010]. The Transference function model is usually used in nearly low or zero lag phases and ponders only the stationary and exponential phases in biogas production [Li et al., 2012]. The $R^2$ of the Transference function model for biogas production data of the control and AD-MEA systems was 0.91 and 0.92, respectively. Thus, considering all kinetic parameters, the Modified Gompertz model was best fitted to the experimental biogas production data, followed by Logistic and Transference function models.

## 6.4 SUMMARY OF THE CHAPTER

In the present study, an investigation was performed on a bio-electrochemical system by integration of an anaerobic digester with a membrane electrode assembly to support electrogenic microbial activity for co-generation of enriched biogas and electricity as a byproduct. The

experiment showed enrichment of $CH_4$ in the biogas, while the AD was hybridized with the MEA. The highest concentration of $CH_4$ in control was 56.3±1.5% whereas in AD-MEA, the concentration of $CH_4$ increased to 73.7±3.9%. Thus, the incorporation of conductive surface in the anaerobic chamber of the AD-MEA system could promote the enrichment of methane by stimulating syntrophic interactions among exoelectrogens and hydrogenotrophic methanogens for conversion of $CO_2$ directly to $CH_4$. Also, the hybridized AD-MEA system could produce a maximum of 496±7 mV OCV, with a maximum average power density of 2.87 $mW/m^2$ and 70 $mA/m^2$ current density. Furthermore, three non-linear mathematical model fittings were performed with the average experimental data of biogas production obtained from the control and AD-MEA systems. Considering all kinetic parameters, the modified Gompertz model with an $R^2$ of 0.99 was best fitted to the experimental biogas production data, followed by the Logistic and Transference function models.

The next chapter outline the findings related to the characterization, and selection of scrubbing agents and adsorbents along with the removal of $CO_2$ and $H_2S$ by the processes of absorption and adsorption. Furthermore, it demonstrates the functioning of the hybridized AD-MEA system for cogeneration of enriched biogas and electricity.

# Chapter 7

## Conclusions and Suggestions for Future Work

# CHAPTER 7: CONCLUSIONS AND SUGGESTIONS FOR FUTURE WORK

## 7.1 CONCLUSIONS

The thesis reports the performance efficiency of scrubbing agents prepared from locally available biomass based on their physico-chemical properties for the purification of biogas. Natural base ash solutions prepared from different parts of banana plants, such as banana pseudostem (BPS), *Musa balbisiana* peel (MBP) and *Musa acuminata* peel (MAP), were used for $CO_2$ removal from raw biogas by the process of absorption. Biomass-derived adsorbents *viz.* bamboo biochar (BB), banana peel biochar (BPB) and biochar-clay composite (BCC) were used to remove $H_2S$ from biogas by the process of adsorption. Additionally, it also discussed the hybridized system developed by the application of anaerobic digestion and microbial fuel cell technology for the enrichment of methane in biogas. For the hybridized bio-electrochemical system, an anaerobic digester (AD) was integrated with a membrane electrode assembly (MEA) to support electrogenic microbial activity. The developed system was evaluated for the co-generation of methane-enriched biogas and electricity.

### 7.1.1 BIOMASS SELECTION AS SCRUBBING AGENTS AND ADSORBENTS

Duckweed, *Musa balbisiana* peel, banana pseudostem, pine saw dust, and *Musa acuminata* peel were initially chosen for absorption, while leaf waste, bamboo (Bhaluka), banana peel, clay composite, and areca nut were initially chosen for adsorption. Based on the survey, available literature, and physico-chemical properties like ash content and pH, three types of biomass-based scrubbing agents (BPS, MBP, MAP) and adsorbents (BB, BPB, and BCC) were selected for further characterization using different techniques such as TGA, EDX, FESEM, Flame

photometry, and BET. The highest pH recorded for each biomass ash was 11.48 for BPS, 12.77 for MBP and 11.63 for MAP, and the surface pH recorded for BB, BPB, and BCC were 10.67, 10.95, and 9.96, respectively. Results indicated that the scrubbing agents and adsorbents are naturally alkaline.

### 7.1.2 BIOMASS CHARACTERIZATION AS SCRUBBING AGENTS AND ADSORBENTS

EDX analysis showed that the major elements detected in the ash samples (BPS, MBP, and MAP) were O, K, and C, followed by small amounts of Ca, P, Mg, and Si. MBP ash contained the highest potassium quantity (38.4 wt%), followed by MAP ash (34.2 wt%) and BPS (31.8 wt%). As compared to potassium, the weight percentage of calcium in the biomass ash samples was very low at 4.4%, 1.3%, and 1.7% for BPS, MBP, and MAP, respectively. The potassium content of BPB (31.7 wt%) was found to be higher amongst all adsorbents, followed by BB (8.5 wt%) and BCC (3.8 wt%). The weight percentage of silicon (10.7 wt%) in BCC was found to be higher than in BB and BPB, indicating quartz as the major component of the clay material. Further flame photometry confirmed the presence of potassium as the major cationic constituent in MBP (228.40 mg/g), followed by MAP (209.72 mg/g) and BPS (189.64 mg/g). However, as anticipated, the concentrations of sodium and calcium were relatively low as compared to potassium. The BET surface area for BPB was measured at 9.32 $m^2/g$, followed by BB (7.53 $m^2/g$) and BCC (3.36 $m^2/g$). From BET and FESEM images, it was observed that the porosity and surface area of BPB and BB were comparatively higher than those of BCC, which was expected to facilitate the adsorption of $H_2S$ by physico-chemical reactions within the surface and pores. Thus, the findings indicate that the biomass-derived scrubbing agents and adsorbents can be utilized for the removal of $CO_2$ and $H_2S$ from raw biogas.

### 7.1.3 $H_2S$ REMOVABILITY FROM BIOGAS USING NATURALLY ALKALINE ADSORBENTS DERIVED FROM BIOMASS

Application of BB, BPB, and BCC in a portable biogas purification system to remove $H_2S$ from a decentralized biogas plant by the process of adsorption was reported. The characterization of the adsorbents in fresh and adsorbed states was done by employing analytical techniques such as surface pH, BET, EDX, FESEM, XRD, and FTIR along with onsite experiments at ambient conditions to test the potential of the adsorbents for $H_2S$ removal. Amongst the three types of adsorbents prepared, BPB was found to be the most promising adsorbent, with the highest $H_2S$ removal efficiency of 89.2%, followed by BB (87.7%) and BCC (78.4%), which are also in agreement with the analytical observations. The pH of the saturated adsorbents BB, BPB, and BCC was reduced significantly to 8.41, 8.59, and 8.81, respectively, after passing the raw biogas through them. From the EDX analysis, it was evident that S was absent in the fresh adsorbent samples, but after treatment with the raw biogas, the saturated adsorbents exhibited a presence of S of about 2.2 wt% in BB, 2.6 wt% in BPB, and 0.5 wt% in BCC. This ensures the sorption of $H_2S$ by the respective adsorbents through certain physiochemical reactions. All the biochars had heterogeneous morphology with a rough surface and scattered micropores, which along with the high surface pH, pores, and mineral elements on the surface of biochar could be the reason for $H_2S$ adsorption due to various physiochemical reactions. The noticeable differences observed in the XRD and FTIR spectra of the biochars before and after $H_2S$ sorption further confirmed the above results. The presence of high-intensity peaks of elemental sulphur and sulphurous compounds in $H_2S$ adsorbed samples showed the ability of biochars to adsorb $H_2S$ due to high pH and the presence of supported K, Ca, and other compounds on the surface of biochars. Furthermore, from the study of four kinetic models, viz. pseudo-first-order, pseudo-

second-order, intraparticle diffusion, and Elovich, the calculated equilibrium adsorption value ($q_e$) obtained from the pseudo-second-order model (BB, $q_{e\ cal}$ = 3.53 mg $H_2S$ $g^{-1}$ biochar; BPB, $q_{e\ cal}$ = 3.57 mg $H_2S$ $g^{-1}$ biochar; and BCC, $q_{e\ cal}$ = 1.41 mg $H_2S$ $g^{-1}$ biochar) was best fitted for all the adsorbents with a correlation coefficient of $R^2$ = 0.99. This showed that the pseudo-second-order model can clearly describe the $H_2S$ adsorption process, and it was concluded that the chemical sorption process on the adsorbents was the dominant control step during the whole sorption process. Moreover, the process can be easily implemented in rural areas as an appropriate technique for $H_2S$ removal from decentralized biogas plants as the raw materials for the adsorbents prepared are easily available and cost-effective. Another advantage is that the biochars used are naturally alkaline and no pre-treatment is required to enhance their alkalinity, which makes them more convenient for $H_2S$ removal from raw biogas.

### 7.1.4 $CO_2$ ABSORPTION FROM BIOGAS USING NATURAL BASE ASH SOLUTIONS AND COMPARISON WITH KOH

For the scrubbing of $CO_2$ from biogas, different concentrations of KOH (0.1, 0.3, 0.5, 0.7, and 1.0 M) and natural base ash solutions (BPS, MBP, and MAP) were compared. The methane content of the untreated biogas analyzed in a gas chromatograph was found to be 56.9%. The scrubber with MBP could enrich the methane content in biogas from 56.9% to 86.3%, followed by MAP (78.4%) and BPS (76.8%), which is nearly equivalent to 0.3 M KOH (88.6%). Experimental results revealed that NBAS possess varying pH and have nearly equivalent potential to KOH for $CO_2$ absorption from biogas. The kinetics of $CO_2$ absorption by different solvents was evaluated by plotting the graph of absorption time against dimensionless biogas concentration. It was found that the rate constant *k* for MBP was nearly equivalent to that of 0.5 M and 0.7 M KOH. The $\tau$ value was highest for MBP amongst the three natural base solutions,

which is also in agreement with the experimental values. Moreover, the $R^2$ value of 0.99 for 0.5 M KOH and MBP indicates a higher capacity for $CO_2$ absorption and thereby reflects good linear relationships. The study also indicated that $CO_2$ absorption by various chemicals as well as NBA solutions is transient and has to be replenished after saturation. The process performance is fully reliant on factors such as scrubber dimensions, the concentration of scrubbing agents, raw biogas composition, gas pressure, and flow rates. The findings indicate the potential of NBA solutions to be used as substitutes for chemical solvents for $CO_2$ scrubbing with the added advantage of being environmentally friendly, abundant in resource availability, easy to prepare, and cost-effective.

### 7.1.5 HYBRIDIZED ANAEROBIC DIGESTER-MEMBRANE ELECTRODE ASSEMBLY FOR CO-GENERATION OF METHANE-ENRICHED BIOGAS AND ELECTRICITY

The design arrangement makes the AD-MEA system compact and simultaneously allows the production of enriched biogas along with electricity. GC analysis showed enrichment of $CH_4$ in the biogas while the AD was hybridized with the MEA. The highest concentration of $CH_4$ and $CO_2$ in control was 56.3±1.5% and 43.7±0.9% whereas in AD-MEA the concentration of $CH_4$ increased to 73.7±3.9% and $CO_2$ reduced to 26.3±0.5% respectively, with an increment of 17.4% $CH_4$. Also, in AD-MEA, the volume of biogas production is enhanced as compared to the control system. The presence of a non-biological conductive surface in the anaerobic chamber stimulates syntrophic interactions among electrogens and hydrogenotrophic methanogens for the conversion of $CO_2$ directly to $CH_4$. The methanogenic communities used the conductive surface to facilitate electron transfers between them, improving rates of methane production. Stable voltage generation was observed from the $8^{th}$ day to almost the $43^{rd}$ day with an average OCV of

456±22.6 mV. The hybridized AD-MEA setup could produce as much as 496±7 mV of OCV with a maximum average power density of 2.87 $mW/m^2$ and a 70 $mA/m^2$ current density, respectively. Furthermore, the CV showed an oxidation peak at -0.545 V, which confirms the presence of electrogenic bacteria in the cattle dung slurry. Also, three non-linear mathematical model fittings were performed using the modified Gompertz function, the Logistic model, and the Transference model with the average experimental data of biogas production obtained from the control and AD-MEA systems. Considering all kinetic parameters, the modified Gompertz model ($R^2$ = 0.99) was best fitted to the experimental biogas production data, followed by the Logistic and Transference function models. Thus, the AD-MEA system facilitates the coexistence and functioning of methanogenic and electrogenic microorganisms while simultaneously supporting biogas production, biogas enrichment, and electricity generation. The system can be reused simply by cleaning the chambers and electrode surface and by substitution with fresh organic waste slurry. By increasing the number of AD-MEA setups and connecting them in series, parallel, or a combination of the two, power for real-time applications can be increased.

## 7.2 SIGNIFICANT FINDINGS FROM THIS THESIS

The significant findings from the work reported in this thesis are listed below:

1. Biomass-derived scrubbing agents (BPS, MBP, and MAP) and adsorbents (BB, BPB, and BCC) have great potential for the removal of $CO_2$ and $H_2S$ from raw biogas.
2. All the scrubbing agents and adsorbents are rich in minerals such as potassium, calcium, magnesium, and silicon and are found to be naturally alkaline.
3. BPB had the highest $H_2S$ removal efficiency of 89.2%, followed by BB (87.7%) and

BCC (78.4%), respectively.

4. The pseudo-second-order model could clearly describe the $H_2S$ adsorption process, indicating the chemical sorption process on the adsorbents, which was also confirmed by the XRD analysis.
5. MBP could reduce the amount of $CO_2$ by 68%, which was found to be the best among the selected scrubbing agents (BPS, MBP, and MAP) and is nearly equivalent to 0.3 M KOH.
6. The rate constant *k* for MBP was nearly equivalent to that of 0.5 M and 0.7 M KOH, which is very encouraging.
7. As compared with the control, the AD-MEA system could enrich the concentration of $CH_4$ from 56.3% to 73.7%, with an increment of 17.4%.
8. Along with $CH_4$ enrichment, the hybridized AD-MEA setup could produce as much as 496 mV of OCV, 2.87 $mW/m^2$ of power density, and 70 $mA/m^2$ of current density, respectively.
9. The AD-MEA system facilitates syntrophic interactions among methanogenic and electrogenic microorganisms, simultaneously supporting biogas production, biogas enrichment, and electricity generation.
10. The modified Gompertz model, with an $R^2$ of 0.99, was best fitted to the experimental biogas production data, followed by the Logistic and Transference function models.

## 7.3 SUGGESTIONS FOR FUTURE WORK

Some of the suggestions for future work are bulleted below:

- This work considered only selected biomass for the preparation of scrubbing agents and adsorbents. The same study can be repeated with other locally available biomass like rice husk, rice straw, vegetable and fruit wastes as scrubbing agents or adsorbents for the

removal of $CO_2$ and $H_2S$ from biogas.

- In the present work, a small-scale scrubber was used, and there is scope in the design for modification to medium or large scale for enhancing the removal of $CO_2$ and $H_2S$ for large-scale biogas plants.

- Further research may be carried out on the application of $H_2S$ adsorbed biochar as a nutrient-rich amendment for sulphur-deficient soil.

- The AD-MEA work was conducted in a batch mode in a laboratory-scale digester. So, in the future, the same experiment can be repeated in continuous mode. Further scale-up effects can be achieved at medium and large scales. Moreover, based on the present data, a simulation study can be done on the AD-MEA system for $CH_4$ enrichment and electricity generation by varying the size of electrodes, feedstock compositions, reactor temperature, and pH of the slurry.

# References

# REFERENCES


- Abatzoglou, N., and Boivin, S., 2008, A review of biogas purification processes. Biofuels, Bioproducts & Biorefining. 3(1), 42-71.
- Abdeen, F.R.H., Mel, M., Jami, M.S., Ihsan, S.I., and Ismail, A.F., 2016, A review of chemical absorption of carbon dioxide for biogas upgrading. Chinese Journal of Chemical Engineering. 24, 693–702.
- Aboudheir, A., Tontiwachwuthikul, P., Chakma, A., and Idem, R., 2003, Kinetics of the reactive absorption of carbon dioxide in high $CO_2$-loaded, concentrated aqueous monoethanolamine solutions. Chemical Engineering Science. 58, 5195-5210.
- Abushammala, M.F.M., Qazi, W.A., Azam, M.H., Mehmood, U.A., Al-Mufragi, G.A., and Alrawahi, N.A., 2016, Generation of Electricity from Biogas in Oman. 3rd MEC International Conference on Big Data and Smart City.
- Achak, M., Hafidi, A., Ouazzani, N., Sayadi, S., and Mandi, L., 2009, Low cost biosorbent ―banana peel for the removal of phenolic compounds from olive mill wastewater: Kinetic and equilibrium studies. Journal of Hazardous Materials. 166, 117–125.
- Adib, F., Bagreev, A., and Bandosz, T.J., 2000, Analysis of the relationship between $H_2S$ removal capacity and surface properties of unimpregnated activated carbons. Environmental Science & Technology. 34, 686–692.
- Agneessens, L.M., Ottosen, L.D.M., Voigt, N.V., Nielsen, J.L., de Jonge, N., Fischer, C.H., and Kofoed, M.V.W., 2017, In-situ biogas upgrading with pulse $H_2$ additions: the relevance of methanogen adaption and inorganic carbon level. Bioresource Technology. 233, 256–263.
- Akio, E., Kelly, H., and Thea, W., 2012, Characterization of biochars to evaluate recalcitrance and agronomic performance. Bioresource Technology. 114, 644–653.
- Allegue, L.B., and Hinge, J., 2012, Report: biogas and bio-syngas upgrading. Danish Technological Institute. https://www.teknologisk.dk/ _/media/52679_Report-Biogasandsyngasupgrading.pdf

- Amani, T., Nosrati, M., and Sreekrishnan, T.R., 2010, Anaerobic digestion from the viewpoint of microbiological, chemical, and operational aspects—A review. Environmental Reviews. 18, 255–278.
- An, Z., Feng, Q., Zhao, R., and Wang, X., 2020, Bioelectrochemical Methane Production from Food Waste in Anaerobic Digestion Using a Carbon-Modified Copper Foam Electrode. Processes. 8, 416.
- Andersson, J., and Nordberg, Å., 2017, Biogas upgrading using ash from combustion of wood fuels: Laboratory experiments. Energy and Environment Research. 7, 1–7.
- Andriani, D., Wresta, A., Atmaja, T.D., and Saepudin, A., 2014, A review on optimization production and upgrading biogas through $CO_2$ removal using various techniques. Applied Biochemistry and Biotechnology. 172, 1909-1928.
- Angelidaki, I., Treu, L., Tsapekos, P., Luo, G., Campanaro, S., Wenzel, H., and Kougias, P.G., 2018, Biogas upgrading and utilization: current status and perspectives. Biotechnology Advances. 2, 452–466.
- Appleby, A., 1996, Fuel cell technology: status and future prospects. Energy, 21(7), 521–653.
- Awe, O.W., Zhao, Y., Nzihou, A., Minh, D.P., and Lyczko, N., 2017, A review of biogas utilisation, purification and upgrading technologies. Waste and Biomass Valorization. 8, 267–283.
- Aziz, S.Q., Aziz, H.A., Yuso, M.S., and Bashir, M.J.K., 2011, Landfill leachate treatment using powdered activated carbon augmented sequencing batch reactor (SBR) process: Optimization by response surface methodology. Journal of Hazardous Materials. 189, 404–413.
- Bagreev, A., and Bandosz, T.J., 2001, $H_2S$ adsorption/oxidation on unmodified activated carbons: importance of prehumidification. Carbon. 39, 2303–2311.
- Bandosz, T.J., 2006, Carbonaceous materials as desulfurization media. in: Loureiro, J.M., Kartel, M.T. (Eds.). Combined and Hybrid Adsorbents: Fundamentals and Applications. 145–164.
- Bansal, N., Srivastava, V.K., and Kheraluwala, J., 2019, Renewable Energy in India: Policies to Reduce Greenhouse Gas Emissions. Greenhouse Gas Emissions, Energy, Environment, and Sustainability. 161-178.

- Barua, S., and Dhar, B.R., 2017, Advances towards understanding and engineering direct interspecies electron transfer in anaerobic digestion. Bioresource Technology. 244, 698–707.
- Basu, S., Khan, A., Cano-Odena, A., Liu, C., and Vankelecom, I., 2010, Membrane-based technologies for biogas separations. Chemical Society Reviews. 39, 750–768.
- Batstone, D.J., Keller, J., Angelidaki, I., Kalyuzhnyi, S.V., Pavlostathis, S.G., Rozzi, A., Sanders, W.T., Siegrist, H., and Vavilin, V.A., 2002, The IWA anaerobic digestion model no 1 (ADM1). Water Science and Technology. 45, 65–73.
- Bauer, F., Persson, T., Hulteberg, C., and Tamm, D., 2013, Biogas upgrading – technology overview, comparison and perspectives for the future. Biofuels, Bioproducts and Biorefining. 7, 499–511.
- Belmabkhout, Y., Weireld, G.D., and Sayari, A., 2009, Amine-Bearing Mesoporous Silica for $CO_2$ and $H_2S$ Removal from Natural Gas and Biogas. Langmuir. 25(23), 13275-13278.
- Ben-Mansour, R.M., Habib, A.O., Bamidele, E.M., Basha, N.A., Qasem, A., Peedikakkal, A., and Ali, E., 2016, Carbon capture by physical adsorption: Materials, experimental investigations and numerical modeling and simulations - A review. Applied Energy, 161, 225–255.
- Berk, R.S., and Canfield, J.H., 1964, Bioelectrochemical energy conversion. Journal of Applied Microbiology. 12, 10–12.
- Bhattacharya, S. C., and Khai, P. Q., 1987, Kinetics of anaerobic cow dung digestion. Energy. 12 (6), 497-500.
- Biernat, K., Gis, W., and Samson-brek, I., 2011, Review of technology for cleaning biogas to natural gas quality. Chemik. 65(5), 435–444.
- Biswas, T. D., 1977, Removal of carbon-dioxide from biogas. Proc. Nat. Symp. on Biogas Technology, IARI, New Delhi. Nov. 29-30.
- Borah, A.J., Singh, S., Goyal, A., and Moholkar, V.S., 2016, An assessment of invasive weeds as multiple feedstocks for biofuels production. RSC Advances. 6, 47151-47163.
- Brooks, A. A., 2008, Ethanol production potential of local yeast strains isolated from ripe banana peels. African Journal of Biotechnology. 7 (20), 3749–3752.

- Castrillon, M.C., Moura, K.O., Alves, C.A., Bastos-Neto, M., Azevedo, D.C.S., Hofmann, J., Möllmer, J., Einicke, W.D., and Gläser, R., 2016, $CO_2$ and $H_2S$ removal from $CH_4$-rich streams by adsorption on activated carbons modified with $K_2CO_3$, NaOH, or $Fe_2O_3$. Energy Fuels. 30, 9596–9604.
- Cavenati, S., Grande, C.A., and Rodrigues, A.E., 2005, Upgrade of methane from landfill gas by pressure swing adsorption. Energy Fuels. 19(6), 2545–2555.
- Chandra, R., Vijay, V.K., Subbarao, P.M.V., and Khura, T.K., 2011, Performance evaluation of a constant speed IC engine on CNG methane enriched biogas and biogas. Applied Energy. 88 (11), 3969–3977.
- Chen, B., Chen, Z., and Lv, S., 2011, A novel magnetic biochar efficiently sorbs organic pollutants and phosphate. Bioresource Technology. 102, 716–723.
- Chen, S., Frank Cheng, Y., and Voordouw, G., 2017, A comparative study of corrosion of 316L stainless steel in biotic and abiotic sulfide environments. International Biodeterioration and Biodegradation. 120, 91–96.
- Chen, S., Zhang, X., Singh, D., Yu, H., and Yang, X., 2010, Biological pretreatment of lignocellulosics: potential, progress and challenges. Biofuels. 1(1), 177–199.
- Chen, X.Y., Vinh-Thang, H., Ramirez, A.A., Rodrigue, D., and Kaliaguine, S., 2015, Membrane gas separation technologies for biogas upgrading. RSC Advances. 5, 24399–24448.
- Chen, Y., Cheng, J.J., and Creamer, K.S., 2008, Inhibition of anaerobic digestion process: A review. Bioresource Technology. 99, 4044–4064.
- Choi, S., 2015, Microscale Microbial Fuel Cells: Advances and Challenges. Biosensors Bioelectronics. 69, 8-25.
- Choudhury, A., and Lansing, S., 2021, Adsorption of hydrogen sulfide in biogas using a novel iron-impregnated biochar scrubbing system. Journal of Environmental Chemical Engineering. 9, 104837.
- Chung, R., Kang, E. Y., Shin, Y. J., Park, J. J., Park, P. S., Han, C. H., Kim, B., Moon, S. I., Park, J., and Chung, P. S., 2019, Development of a Consolidated Anaerobic Digester and Microbial Fuel Cell to Produce Biomethane and Electricity from Cellulosic Biomass Using Bovine Rumen Microorganisms. Journal of Sustainable Bioenergy Systems. 9, 17-28.

- Costa, C., Cornacchia, M., Pagliero, M., Fabiano, B., Vocciante, M., and Reverberi, A.P., 2020, Hydrogen Sulfide Adsorption by Iron Oxides and Their Polymer Composites: A Case-Study Application to Biogas Purification. Materials, 13, 4725.
- Creamer, A.E., Gao, B., and Zhang, M., 2014, Carbon dioxide capture using biochar produced from sugarcane bagasse and hickory wood. Chemical Engineering Journal. 249, 174–179.
- Dean, J. A., 1999, Lange's Handbook of Chemistry, 15th ed. McGraw- Hill, New York.
- Deka, D.C., and Talukdar, N.N., 2007, Chemical and spectroscopic investigation of kolakhar and its commercial importance. Indian Journal of Traditional knowledge. 6 (1), 72-78.
- Demirbas, A., 2010, Use of algae as biofuel sources. Energy Conversion and Management. 5(1), 2738-2749.
- Deublein, D., and Steinhauser, A., 2010, Biogas from Waste and Renewable Resources: An Introduction. Second ed. John Wiley & Sons, Weinheim.
- Diaz, I., Perez, S.I., Ferrero, E.M., and Fdz-Polanco, M., 2011, Effect of oxygen dosing point and mixing on the microaerobic removal of hydrogen sulphide in sludge digesters. Bioresource Technology. 102(4), 3768-3775.
- Dolfing, J., Jiang, B., Henstra, A.M., Stams, A.J., and Plugge, C.M., 2008, Syntrophic growth on formate: a new microbial niche in anoxic environments. Applied and Environmental Microbiology. 74, 6126–6131.
- Donoso-Bravo, A., Pérez-Elvira, S.I., and Fdz-Polanco, F., 2010, Application of simplified models for anaerobic biodegradability tests. Evaluation of pre-treatment processes. Chemical Engineering Journal. 160, 607–614.
- Du, Z., Li, H., and Gu, T., 2007, A state of the art review on microbial fuel cells: a promising technology for wastewater treatment and bioenergy. Biotechnology Advances. 25, 464-482.
- Dubey, A. K., 2000, Wet scrubbing of carbon dioxide. Annual report of CIAE, Bhopal, India.
- Farooq, M., Chaudhry, I.A., Hussain, S., Ramzan, N., and Ahmed, M., 2012, Biogas upgradation for power generation applications in Pakistan. Journal of Quality and Technology Management. VIII (II), 107–118.

- Feng, Q., Song, Y.C., Yoo, K., Kuppanan, N., Subudhi, S., and Lal, B., 2017, Bioelectrochemical enhancement of direct interspecies electron transfer in upflow anaerobic digester with effluent recirculation for acidic distillery wastewater. Bioresource Technology. 241, 171–180.
- Feng, Q., Song, Y.C., Yoo, K., Kuppanan, N., Subudhi, S., and Lal, B., 2018, Polarized electrode enhances biological direct interspecies electron transfer for methane production in upflow anaerobic bioelectrochemical digester. Chemosphere. 204, 186–192.
- Fernández-Delgado Juárez, M., Mostbauer, P., Knapp, A., Müller, W., Tertsch, S., Bockreis, A., and Insam, H., 2018, Biogas purification with biomass ash. Waste Management. 71, 224–232.
- Fortuny, M., Gamisans, X., Deshusses, M.A., Lafuente, J., Casas, C., and Gabriel, D., 2011, Operational aspects of the desulfurization process of energy gases mimics in biotrickling filters. Water Research. 45, 5665–5674.
- Fradler, K.R., Kim, J.R., Shipley, G., Massanet-Nicolau, J., Dinsdale, R.M., Guwy, A.J., and Premier, G.C., 2014, Operation of a Bioelectrochemical System as a Polishing Stage for the Effluent from a Two-Stage Biohydrogen and Biomethane Production Process. Biochemical Engineering Journal. 85, 125-131.
- Galante, C.G., Pezzola, L., Priano, N., Scaramellini, S., and Sottocornola, A., 2012, Methane from biogas: the process, cleaning and projects. Norewegian University of Science and Technology, Trondheim.
- Garg, S., Li, M., Weber, A.Z., Ge, L., Li, L., Rudolph, V., Wanga, G., and Rufford, T.E., 2020, Advances and challenges in electrochemical $CO_2$ reduction processes: an engineering and design perspective looking beyond new catalyst materials. Journal of Materials Chemistry. A, Issue 4.
- Gerardi, M., 2003, The Microbiology of Anaerobic Digesters. Waste water Microbiology Series, John Wiley & Sons, Inc. United States of America, 7.
- Goffeng, B., 2013, Crynotechnology for biogas. Dept of Chem Eng, Lund University.
- Gomes, V.G., and Hassan, M.M., 2001, Coal seam methane recovery by vacuum swing adsorption. Separation and Purification Technology. 24, 189–96.

- Gondal, S., Asif, N., Svendsen, H.F., and Knuutila, H., 2015, Kinetics of the absorption of carbon dioxide into aqueous hydroxides of lithium, sodium and potassium and blends of hydroxides and carbonates. Chemical Engineering Science. 123, 487–499.
- Grande, C.A., 2012, Advances in pressure swing adsorption for gas separation. ISRN Chemical Engineering.
- Green, D.W., and Perry, R.H., 2008, Perry's chemical engineers' hand book (8th Ed.). New York: McGraw-Hill Companies Inc.
- Guo, Y., Zhao, C., Chen, X., and Li, C., 2015, $CO_2$ capture and sorbent regeneration performances of some wood ash materials. Applied Energy. 137, 26–36.
- Gupta, V.K., and Suhas., 2009, Application of low-cost adsorbents for dye removal–a review. Journal of Environmental Management. 90(8), 2313–2342.
- Hagelqvist, A., and Granström, K., 2016, Co-digestion of manure with grass silage and pulp and paper mill sludge using nutrient additions. Environmental technology. 37, 2113–2123.
- Hagen, M., and Polman, E., 2001, Adding gas from biomass to the gas grid. Final report submitted to Danish Gas Agency. 26–47.
- Han, X., Chen, H., Liu, Y., and Pan, J., 2020, Study on removal of gaseous hydrogen sulfide based on macroalgae biochars. Journal of Natural Gas Science and Engineering. 73, 103068.
- Hao, X., Hou, G., Zheng, P., Liu, R., and Liu, C., 2016, $H_2S$ in-situ removal from biogas using a tubular zeolite/$TiO_2$ photocatalytic reactor and the improvement on methane production. Chemical Engineering Journal. 294, 105–110.
- Happi, E.T., Ronkart, S.N., Robert, C., Wathelet, B., and Paquot, M., 2008, Characterisation of pectins extracted from banana peels (Musa AAA) under different conditions using an experimental design. Food Chemistry. 108, 463–471.
- Harnisch, F., and Schröder, U., 2009, Selectivity versus Mobility: Separation of Anode and Cathode in Microbial Bioelectrochemical Systems. ChemSusChem. 2 (10), 921-926.
- He, R., Xia, F.F., Wang, J., Pan, C.L., and Fang, C.R., 2011, Characterization of adsorption removal of hydrogen sulfide by waste biocover soil, an alternative landfill cover. Journal of Hazardous Materials. 186, 773–778.

- Hemanta, M.R., Mane, V.K., and Bhagwat, A., 2014, Analysis of traditional food additive kolakhar for its physico-chemical parameters and antimicrobial activity. European Academic Research. II(8), 10531-10536.
- Higgins, S.R., Lopez, R.J., Pagaling, E., Yan, T., Cooney, M.J., 2013, Towards a hybrid anaerobic digester-microbial fuel cell integrated energy recovery system: An overview of the development of an electrogenic biofilm. Enzyme and Microbial Technology. 52, 344–351.
- Horikawa, M.S., Rossi, F., Gimenes, M.L., Costa, C.M.M., and da Silva, M.G.C., 2004, Chemical absorption of $H_2S$ for biogas purification. Brazilian Journal of Chemical Engineering. 21 (03), 415 – 422.
- Hotta, S.K., Sahoo, N., and Mohanty, K., 2019, Comparative assessment of a spark ignition engine fueled with gasoline and raw biogas. Renewable Energy. 134, 1307-1319.
- International Energy Agency, https://www.iea.org/reports/key-world-energy-statistics-2021/supply
- Inyang, M., Gao, B., Yao, Y., Xue, Y.W., and Zimmerman, A., 2012, Removal of heavy metals from aqueous solution by biochars derived from anaerobically digested biomass. Bioresource Technology. 110, 50–56.
- IRENA (International Renewable Energy Agency), 2017, Biogas for Road Vehicles Technology Brief, http://www.irena.org/DocumentDownloads/ Publications/IRENA_ Biogas_for_Road_Vehicles_2017.pdf.
- Jakab, E., Faix, O., and Till, F., 1997, Thermal decomposition of milled wood lignins studied by thermogravimetry/mass spectrometry. Journal of Analytical and Applied Pyrolysis. 40–41, 171–186.
- Janssen, A., Ruitenberg, R., and Buisman, C., 2001, Industrial applications of new sulfur biotechnology. Water Science and Technology. 44, 85–90.
- Jeihanipour, A., Aslanzadeh, S., Rajendran, K., Balasubramanian, G., and Taherzadeh, M.J., 2013, High-rate biogas production from waste textiles using two-stage process. Renewable Energy. 52, 128–135.
- Juang, D.F., Yang, P.C., Lee, C.H. Hsueh, S.C., and Kuo, T.H., 2011, Electrogenic capabilities of gram negative and gram positive bacteria in microbial fuel cell combined

with biological wastewater treatment. International journal of Environmental Science and Technology. 8 (4), 781-792.

- Juárez, M.F.D., Mostbauer, P., Knapp, A., Müller, W., Tertsch, S., Bockreis, A., and Insam, H., 2018, Biogas purification with biomass ash. Waste Management. 71, 224-232.
- K Vasanth, K., 2006, Linear and non-linear regression analysis for the sorption kinetics of methylene blue onto activated carbon. Journal of Hazardous Materials. 137, 1538–1544.
- Kadam, R., and Panwar, N.L., 2017, Recent advancement in biogas enrichment and its applications. Renewable and Sustainable Energy Reviews. 73, 892–903.
- Kanjanarong, J., Giri, B.S., Jaisi, D.P., Oliveira, F.R., Boonsawang, P., Chaiprapat, S., Singh, R.S., Balakrishna, A., and Khanal, S.K., 2016, Removal of hydrogen sulfide generated during anaerobic treatment of sulfate-laden wastewater using biochar: Evaluation of efficiency and mechanisms. Bioresource Technology. 234, 115–121.
- Kapdi, S.S., Vijay, V.K., Rajesh, S.K., and Prasad, R., 2005, Biogas scrubbing, compression and storage: Perspective and prospectus in Indian context. Renewable Energy. 30(8), 1195-1202.
- Kapoor, R., Ghosh, P., Kumar, M., and Vijay, V.K., 2019, Evaluation of biogas upgrading technologies and future perspectives: a review. Environmental Science and Pollution Research. 26, 11631–11661.
- Karim, G.A., Wierzba, I., 1992, Methane-carbon dioxide mixtures as a fuel, SAE technical paper 921557. Warrendale, USA.
- Karki, A.B., Shrestha, J.N., and Bajgain, S., 2005, Biogas: as renewable source of energy in Nepal, theory and development. BSP-Nepal. 1–189.
- Kato, S., Hashimoto, K., and Watanabe, K., 2012, Methanogenesis facilitated by electric syntrophy via (semi) conductive iron- oxide minerals. Environmental Microbiology. 14, 1646–1654.
- Kim I.S., Chae K.J., Choi M.J., and Verstraete, W., 2008, Microbial fuel cells: recent advances, bacterial communities and application beyond electricity generation. Environmental Engineering Research. 13 (2), 51–65.

- Kim, J.R., Cheng, S., Oh, S.E., and Logan, B.E., 2007, Power Generation Using Different Cation, Anion, and Ultrafiltration Membranes in Microbial Fuel Cells. Environmental Science & Technology. 41, 3, 1004–1009.
- Kim, J.R., Min, B., and Logan, B.E., 2006, Evaluation of procedures to acclimate a microbial fuel cell for electricity generation. Applied Microbiology and Biotechnology. 68, 23–30.
- Kim, T., An, J., Jang, J.K., and Chang, I.S., 2015, Coupling of Anaerobic Digester and Microbial Fuel Cell for COD Removal and Ammonia Recovery. Bioresource Technology. 195, 217-222.
- Kondaveeti, S., Lee, J., Kakarla, R., Kim, H.S., and Min, B., 2014, Low-cost separators for enhanced power production and field application of microbial fuel cells (MFCs). Electrochimica Acta. 132, 434-440.
- Kougias, P.G., Treu, L., Benavente, D.P., Boe, K., Campanaro, S., and Angelidaki, I., 2017, Ex-situ biogas upgrading and enhancement in different reactor systems. Bioresource Technology. 225, 429–437.
- Krischan, J., Makaruk, A., and Harasek, M., 2010, Design and scale-up of an oxidative scrubbing process for selective removal of hydrogen sulfide from biogas. Journal of Hazardous Materials. 49, 215–216.
- Krishijagran.com
- Laplanche, A., Bonnin, C., Darmon, D., in: Vignerons, S., Hermia, J., and Chaduki, J., (Eds.), 1994, Characterization and control of odorous and VOC in the process industries. Studies in Environmental Science. 61, 277-291.
- Lecker, B., Illi, L., Lemmer, A., and Oechsner, H., 2017, Biological hydrogen methanation—a review. Bioresource Technology. 245, 1220–1228.
- Lee, E.Y., Lee, N.Y., Cho, K.S., and Ryu, H.W., 2006, Removal of hydrogen sulfide by sulfate-resistant acidithiobacillus thiooxidans AZ11. Journal of Bioscience and Bioengineering. 101(4), 309–314.
- Lee, W.Y., Park, S.Y., Lee, K.B., and Nam, S.C., 2020, Simultaneous Removal of $CO_2$ and $H_2S$ from Biogas by Blending Amine Absorbents: A Performance Comparison Study. Energy Fuels. 34, 1992−2000.

- Leonzio, G., 2016, Upgrading of biogas to bio-methane with chemical absorption process: simulation and environmental impact. Journal of Cleaner Production. 131, 364-75.
- Li, K., Liu, R., and Sun, C., 2015, Comparison of anaerobic digestion characteristics and kinetics of four livestock manures with different substrate concentrations. Bioresource Technology. 198, 133–140.
- Li, L., Kong, X., Yang, F., Li, D., Yuan, Z., and Sun, Y., 2012, Biogas production potential and kinetics of microwave and conventional thermal pretreatment of grass. Applied Biochemistry and Biotechnology. 166 (5), 1183–1191.
- Li, W.W., and Yu, H.Q., 2016, Advances in energy-producing anaerobic biotechnologies for municipal wastewater treatment. Engineering. 2, 438–446.
- Li, Y., Liu, H., Yan, F., Su, D., Wang, Y., and Zhou, H., 2017, High-calorific biogas production from anaerobic digestion of food waste using a two-phase pressurized biofilm (TPPB) system. Bioresource Technology. 224, 56–62.
- Li, Y., Zhang, R., He, Y., Zhang, C., Liu, X., Chen, C., and Liu, G., 2014, Anaerobic co-digestion of chicken manure and corn stover in batch and continuously stirred tank reactor (CSTR). Bioresource Technology. 156, 342–347.
- Lim, S.L., and Wu, T.Y., 2015, Determination of maturity in the vermicompost produced from palm oil mill effluent using spectroscopy, structural characterization and thermogravimetric analysis. Ecological Engineering. 84, 515-519.
- Lin, W.C., Chen, Y.P., and Tseng, C.P., 2013, Pilot-scale chemical–biological system for efficient $H_2S$ removal from biogas. Bioresource Technology. 135, 283–291.
- Liu, Y., and Whitman, W.B., 2008, Metabolic, phylogenetic, and ecological diversity of the methanogenic archaea. Annals of the New York Academy of Sciences. 1125, 171–189.
- Lo, K., Liao, P., and Gao, Y., 1994, Anaerobic Treatment of Swine Wastewater Using Hybrid UASB Reactors. Bioresource Technology. 47, 153-157.
- Logan, B.E., Hamelers, B., Rozendal, R.A., Schroder, U., Keller, J., Freguia, S., Aelterman, P., Verstraete, W., and Rabaey, K., 2006, Microbial fuel cells: methodology and technology. Environmental Science & Technology. 40, 5181–5192.

- Logan, B.E., and Regan, J.M., 2006, Microbial Fuel Cells-Challenges and Applications. Environmental Science & Technology. 40, 5172-5180.
- Luo, G., and Angelidaki, I., 2013, Co-digestion of manure and whey for in situ biogas upgrading by the addition of $H_2$: process performance and microbial insights. Applied Microbiology and Biotechnology. 97, 1373–1381.
- Luo, G., Li, J., Li, Y., Wang, Z., Li, W.T., and Li, A.M., 2016, Performance, kinetics behaviors and microbial community of internal circulation anaerobic reactor treating wastewater with high organic loading rate: Role of external hydraulic circulation. Bioresource Technology. 222, 470–477.
- Mahanta, P., Dewan, A., Saha, U.K., Kalita, P., and Buragohain, B., 2005, Biogas digester: A discussion on factors affecting biogas production and field investigation of a novel duplex digester. Journal of Solar Society of India (SESI) Journal. 15 (2), 1-12.
- Malla, F.A., Khan, S.A., and Gupta, N., 2016, Application of alkaline chemicals for biogas methane enrichment. Ecology, Environment and Conservation. 22 (2), 475-84.
- Mamun, M.R.A., Karim, M.R., Rahman, M.M., Asiri, A.M., and Torii, S., 2016, Methane enrichment of biogas by carbon dioxide fixation with calcium hydroxide and activated carbon. Journal of the Taiwan Institute of Chemical Engineers. 58, 476- 481.
- Mann, G., Schlegel, M., Schumann, R., and Sakalauskas, A., 2009, Biogas-conditioning with microalgae. Agronomy Research. 7(1), 33-38.
- Mel, M., Sharuzaman, M. A. H., and Setyobudi, R. H., 2016, Removal of $CO_2$ from Biogas Plant using Chemical Absorption Column. Advances of Science and Technology for Society. AIP Conference Proceedings. 1755, 050005-1–050005-6.
- Memon, J.R., Memon, S.Q., Bhanger, M.I., Memon, G.Z., El-Turki, A., and Allen, G.C., 2008, Characterization of banana peel by scanning electron microscopy and FT-IR spectroscopy and its use for cadmium removal. Colloids and Surfaces B. 66, 260–265.
- Meszaros, E., Varhegyi, G., Jakab, E., and Marosvolgyi, B., 2004, Thermogravimetric and reaction kinetic analysis of biomass samples from an energy plantation. Energy & Fuels. 18, 497-507.
- Mezenner, N.Y., and Bensmaili, A., 2009, Kinetics and thermodynamic study of phosphate adsorption on iron hydroxide-eggshell waste. Chemical Engineering Journal. 147, 87–96.

- Miltner, M., Makaruk, A., Krischan J., and Harasek, M., 2012, Chemical-oxidative scrubbing for the removal of hydrogen sulphide from raw biogas: potentials and economics. Water Science and Technology. 66, 1354–1360.
- Mittal, S., Ahlgren, E.O., and Shukla, P.R., 2018, Barriers to biogas dissemination in India: A review. Energy Policy. 112, 361–370.
- Monnet, F., 2003, An introduction to anaerobic digestion of organic waste. Final report, Remade Scotland, November.
- Mulu, E., M'Arimi, M.M., Ramkat, R.C., and Mecha, A.C., 2021, Potential of wood ash in purification of biogas. Energy for Sustainable Development. 65, 45–52.
- Muñoz, R., Meier, L., Diaz, I., and Jeison, D., 2015, A review on the state-of-the-art of physical/chemical and biological technologies for biogas upgrading. Reviews in Environmental Science and Bio/Technology. 14, 727–759.
- Muthuraman, G., Chung, S. J., and Moon, I. S., 2012, A review on an electrochemically assisted scrubbing process for environmental harmful pollutant's destruction. Journal of Industrial and Engineering Chemistry. 18, 1540–1550.
- Mwandila, G., Musonda, G., and Mugala, A. N., 2016, A Procedure for the Development of a Low-Cost Treatment Technology of Raw Biogas for Application in a Gas Engine. A Case of Sizing a Carbon Dioxide Removal Unit. Chemical Engineering Communications. 203, 995–1000.
- Nelabhotla, A.B.T., and Dinamarca, C., 2019, Bioelectrochemical $CO_2$ Reduction to Methane: MES Integration in Biogas Production Processes. Applied Sciences. 9, 1056.
- Ni, P., Lyu, T., Sun, H., Dong, R., and Wu, S., 2017, Liquid digestate recycled utilization in anaerobic digestion of pig manure: Effect on methane production, system stability and heavy metal mobilization. Energy. 141, 1695–1704.
- Nie, H., Jiang, H., Chong, D., Wu, Q., Xu, C., and Zhou, H., 2013, Comparison of Water Scrubbing and Propylene Carbonate Absorption for Biogas Upgrading Process. Energy & Fuels. 27, 3239−3245.
- Niesner, J., Jecha, D., and Stehlik, P., 2013, Biogas upgrading techniques: state of art review in European region. Chemical Engineering Transactions. 35, 517–522.

- Nordi, G.H., Palacios-Bereche, R., Gallego, A.G., and Nebra, S.A., 2017, Electricity production from municipal solid waste in Brazil. Waste Management & Research. 35, 709-720.
- Ofori-Boateng, C., and Kwofie, E.M., 2009, Water Scrubbing: A Better Option for Biogas Purification for Effective Storage. World Applied Sciences Journal. 5 (Special Issue for Environment), 122-125.
- Oh, S., Min, B., and Logan, B.E., 2004, Cathode performance as a factor in electricity generation in microbial fuel cells. Environmental Science & Technology. 38, 4900–4904.
- Osorio, F., Sánchez, M., and Torres, J. C., 2014, Preliminary Studies for Obtaining Biofuel by Absorption with Mono-ethanol-amine from Anaerobic Digestion Biogas in a Wastewater Treatment Plant. Energy Sources, Part A. 36, 2043–2051.
- Osorio, F., and Torres, J.C., 2009, Biogas purification from anaerobic digestion in a wastewater treatment plant for biofuel production. Renewable Energy. 34, 2164-71.
- Ostrem, K., 2004, Greening waste: Anaerobic digestion for treating the organic fraction of municipal solid waste. M.S. Thesis, Department of Earth and Environmental Engineering, Columbia University, New York, NY.
- Ou, H.W., Chou, M.S., and Chang, H.Y., 2020, Removal of Hydrogen Sulfide from Biogas Using a Bubbling Tank Fed with Aerated Wastewater. Aerosol and Air Quality Research. 20, 643–653.
- Pagés-Díaz, J., Pereda-Reyes, I., Taherzadeh, M.J., Sárvári-Horváth, I., and Lundin, M., 2014, Anaerobic co-digestion of solid slaughterhouse wastes with agro-residues: Synergistic and antagonistic interactions determined in batch digestion assays. Chemical Engineering Journal. 245, 89-98.
- Pan, M., Lin, X., Xie, J., and Huang, X., 2017, Kinetic, equilibrium and thermodynamic studies for phosphate adsorption on aluminum hydroxide modified palygorskite nano-composites. RSC Advances. 7, 4492–4500.
- Patel, S.K.S., Kumar, P., Singh, M., Lee, J.K., and Kalia, V.C., 2015, Integrative approach to produce hydrogen and polyhydroxybutyrate from biowaste using defined bacterial cultures. Bioresource Technology. 176, 136-341.

- Patterson, T., Esteves, S., Dinsdale, R., and Guwy, A., 2011, An evaluation of the policy and techno-economic factors affecting the potential for biogas upgrading for transport fuel use in the UK. Energy Policy. 39(3), 1806–1816.
- Pelaez-Samaniego, M.R., Smith, M.W., Zhao, Q., Garcia-Perez, T., Frear, C., and Garcia-Perez, M., 2018, Charcoal from anaerobically digested dairy fiber for removal of hydrogen sulfide within biogas. Waste Management. 76, 374–382.
- Persson, M., 2003, Evaluation of upgrading techniques for biogas [Internet] Lund School of Environmental Engineering. Available from, http://www.sgc.se/document/ Evaluation.pdf.
- Persson, T., 2013, Country Report Sweden. Seoul, South Korea: IEA Bioenergy Task 37.
- Pertiwiningrum, A., Harto, A.W., Wuri, M.A., and Budiarto, R., 2018, Assessment of Calorific Value of Biogas after Carbon Dioxide Adsorption Process Using Natural Zeolite and Biochar. International Journal of Environmental Science and Development. 9 (11), 327- 330.
- Petersson, A., and Wellinger, A., 2009, Biogas upgrading technologies–developments and innovations. IEA Bioenergy. 20.
- Pommier, S., Chenu, D., Quintard, M., and Lefebvre, X., 2006, A logistic model for the prediction of the influence of water on the solid waste methanization in landfills. Biotechnology and Bioengineering. 97, 473–482.
- Premier, G.C., Kim, J.R., Massanet-Nicolau, J., Kyazze, G., Esteves, S.R.R., Penumathsa, B.K.V., Rodríguez, J., Maddy, J., Dinsdale, R.M., and Guwy, A.J., 2013, Integration of Biohydrogen, Biomethane and Bioelectrochemical Systems. Renewable Energy. 49, 188-192.
- Qin, F., Wang, S., Hartono, A., Svendsen, H.F., and Chen, C., 2010, Kinetics of $CO_2$ absorption in aqueous ammonia solution. International Journal of Greenhouse Gas Control, 4, 729–738.
- Rabaey, K., Read, S.T., Clauwaert, P., Freguia, S., Bond, P.L., Blackall, L.L., and Keller, J., 2008, Cathodic oxygen reduction catalyzed by bacteria in microbial fuel cells. ISME Journal. 2, 519–527.

- Rachbauer, L., Voitl, G., Bochmann, G., and Fuchs, W., 2016, Biological biogas upgrading capacity of a hydrogenotrophic community in a trickle bed reactor. Applied Energy. 180, 483–490.
- Rahimnejad, M., Ghoreyshi, A., Najafpour, G., Younesi, H., and Shakeri, M., 2012, A novel microbial fuel cell stack for continuous production of clean energy. International Journal of Hydrogen Energy. 37, 5992-6000.
- Rahimnejad, M., Jafary, T., Haghparast, F., Najafpour, G.D., and Ghoreyshi, A.A., 2010, Nafion as a nanoproton conductor in microbial fuel cells. Turkish Journal of Engineering and Environmental Sciences. 34 (4), 289 – 291.
- Rajput, A.A., Zeshan, and Visvanathan, C., 2018, Effect of thermal pretreatment on chemical composition, physical structure and biogas production kinetics of wheat straw. Journal of Environmental Management. 221, 45–52.
- Ramírez-Sáenz, D., Zarate-Segura, P. B., Guerrero-Barajas, C., and Garcia-Peña, E. I., 2009, $H_2S$ and volatile fatty acids elimination by biofiltration: Clean-up process for biogas potential use. Journal of Hazardous Materials. 163, 1272–1281.
- Rasi, S., Läntelä, J., and Rintala, J., 2011, Trace compounds affecting biogas energy utilisation – A review. Energy Conversion and Management. 52, 3369–3375.
- Rasi, S., Veijanen, A., and Rintala, J., 2007, Trace compounds of biogas from different biogas production plants. Energy. 32, 1375–1380.
- Ray, N.H.S., Mohanty, M.K., and Mohanty, R.C., 2016, Biogas Compression and Storage System for Cooking Applications in Rural Households. International Journal of Renewable Energy Research. 6(2), 593-98.
- Rotaru, A.E., Shrestha, P.M., Liu, F., Shrestha, M., Shrestha, D., Embree, M., and Lovley, D.R., 2014, A new model for electron flow during anaerobic digestion: Direct interspecies electron transfer to Methanosaeta for the reduction of carbon dioxide to methane. Energy & Environmental Science. 7, 408–415.
- Rupf, G.V., Bahri, P.A., de Boer, K., and McHenry, M.P., 2015, Barriers and opportunities of biogas dissemination in Sub-Saharan Africa and lessons learned from Rwanda, Tanzania, China, India, and Nepal. Renewable and Sustainable Energy Reviews. 52, 468–476.

- Ryckebosch, E., Drouillon, M., and Vervaeren, H., 2011, Techniques for transformation of biogas to biomethane. Biomass & Bioenergy. 1; 35(5), 1633–1645.
- Sahota, S., Vijay, V. K., Subbarao, P.M.V., Chandra, R., Ghosh, P., Shah, G., Kapoor, R., Vijay, V., Koutu, V., and Thakur, I. S., 2018, Characterization of leaf waste based biochar for cost effective hydrogen sulfide removal from biogas. Bioresource Technology. 250, 635–641.
- Sakar, S., Yetilmezsoy, K., and Kocak, E., 2009, Anaerobic Digestion Technology in Poultry and Livestock Waste Treatment—A Literature Review. Waste Management & Research. 27, 3-18.
- Savery, W.C., and Cruzon, D.C., 1972, Methane recovery from chicken manure. Journal (Water Pollution Control Federation). 44, 2349–54.
- Scholz, M., Melin, T., and Wessling, M., 2013, Transforming biogas into biomethane using membrane technology. Renewable and Sustainable Energy Reviews. 17, 199–212.
- Seppala, M., Pyykkanen, V., Vaisanen, A., Rintala, J., 2013, Biomethane production from maize and liquid cow manure-effect of the share of maize, post methanation potential and digestate characteristics. Fuel. 107, 209-216.
- Seredych, M., Strydom, C., and Bandosz, T.J., 2008, Effect of fly ash addition on the removal of hydrogen sulfide from biogas and air on sewage sludge-based composite adsorbents. Waste Management. 28, 1983–1992.
- Sethupathi, S., Zhang, M., Rajapaksha, A.U., Lee, S.R., Nor, N.M., Mohamed, A.R., Al-Wabel, M., Lee, S.S., and Ok, Y.S., 2017, Biochars as Potential Adsorbers of $CH_4$, $CO_2$ and $H_2S$. Sustainability. 9, 121.
- Shang, G., Shen, G., Liu, L., Chen, Q., and Xu, Z., 2013, Kinetics and mechanisms of hydrogen sulfide adsorption by biochars. Bioresource Technology. 133, 495–499.
- Sharma, R., Wooten, J., Baliga, V., Lin, X., and Chan, W., 2004, Characterization of chars from pyrolysis of lignin. Fuel. 83, 1469–1482.
- Shinogi, Y., and Kanri, Y., 2003, Pyrolysis of plant, animal and human waste: physical and chemical characterization of the pyrolytic products. Bioresource Technology. 90, 241–247.
- Shukla, P.R., 2007, Biomass Energy Strategies for Aligning Development and Climate Goals in India. Netherlands Environmental Assessment Agency.

- Shyam, M., 2002, Promising renewable energy technologies, AICRP technical bulletin number CIAE. 88, 47-48.
- Siddique, R., 2012, Conservation and recycling utilization of wood ash in concrete manufacturing. Resources, Conservation and Recycling. 67, 27–33.
- Singh, D., and Dwivedi, A.K., 2019, Removal of $CO_2$ from Raw Biogas using Water Scrubbing based Up-Gradation Method. International Research Journal of Engineering and Technology. 06 (11), 1565-1568.
- Singh, K.M., Pandya, P.R., Parnerkar, S., Tripathi, A.K., Rank, D.N., Kothari, R.K., and Joshi, C.G., 2011, Molecular identification of methanogenic archaea from surti buffaloes (bubalus bubalis), reveals more hydrogenotrophic methanogens phylotypes. Brazilian Journal of Microbiology. 42, 132-139.
- Singhal, S., Agarwal, S., Arora, S., Sharma, P., and Singhal, N., 2017, Upgrading techniques for transformation of biogas to bio-CNG: a review. International Journal of Energy Research.
- Sitthikhankaew, R., Chadwick, D., Assabumrungrat, S., and Laosiripojana, N., 2014, Effects of humidity, $O_2$, and $CO_2$ on $H_2S$ adsorption onto upgraded and KOH impregnated activated carbons. Fuel Processing Technology. 124, 249–257.
- Skodras, G., Grammelis, O.P., Basinas, P., Kakaras, E., and Sakellaropoulos, G., 2006, Pyrolysis and combustion characteristics of biomass and waste-derived feedstock. Industrial & Engineering Chemistry Research. 45, 3791-3799.
- Srivastava, P., Yadav, A.K., and Mishra, B.K., 2015, The effects of microbial fuel cell integration into constructed wetland on the performance of constructed wetland. Bioresource Technology. 195, 223-30.
- Steinhauser, A., 2008, Biogas from waste and renewable resources, dieter doublein. Wiley-VCH.
- Sun, Q., Li, H., Yan, J., Liu, L., Yu, Z., and Yu, X., 2015, Selection of appropriate biogas upgrading technology-a review of biogas cleaning, upgrading and utilisation. Renewable and Sustainable Energy Reviews. 51, 521–532.
- Surra, E., Nogueira, M.C., Bernardo, M., Lapa, N., Esteves, I., and Fonseca, I., 2019, New adsorbents from maize cob wastes and anaerobic digestate for $H_2S$ removal from biogas. Waste Management. 94, 136–145.

- Tagliabue, M., Farrusseng, D., Valencia, S., Aguado, S., Ravon, U., Rizzo, C., Corma, A., and Mirodatos, C., 2009, Natural gas treating by selective adsorption: material science and chemical engineering interplay. Chemical Engineering Journal. 155(3), 553–566.
- Tahir, M.S., Shahzad, K., Shahid, Z., Sagir, M., Rehan, M., and Nizami, A., 2015, Producing methane enriched biogas using solvent absorption method. Chemical Engineering Transactions. 45, 1309-1314.
- Takuwa, Y., Matsumoto, T., Oshita, K., Takaoka, M., Morisawa S., and Takeda, N., 2009, Characterization of trace constituents in landfill gas and a comparison of sites in Asia. Journal of Material Cycles and Waste Management. 11, 305–311.
- Tamta, P., Rani N., and Yadav, A.K., 2020, Enhanced wastewater treatment and electricity generation using stacked constructed wetland-microbial fuel cells. Environmental Chemistry Letters. 18, 871-879.
- Tan, Z., Lin, C.S.K., Ji, X., and Rainey, T.J., 2017, Returning biochar to fields: a review. Applied Soil Ecology. 116, 1–11.
- Thiruselvi, D., Kumar, P.S., Kumar, M.A., Lay, C.H., Aathika, S., Mani, Y., Jagadiswary, D., Dhanasekaran, A., Shanmugam, P., Sivanesan, S., Show, P.L., 2021, A critical review on global trends in biogas scenario with its up-gradation techniques for fuel cell and future perspectives. International Journal of Hydrogen Energy. 46, 16734-16750.
- Tilahun, E., Sahinkaya, E., and Çalli, B., 2018, A hybrid membrane gas absorption and bio-oxidation process for the removal of hydrogen sulfide from biogas. International Biodeterioration & Biodegradation. 127, 69–76.
- Tippayawong, N., and Thanompongchart, P., 2010, Biogas quality upgrade by simultaneous removal of $CO_2$ and $H_2S$ in a packed column reactor. Energy. 35, 4531-4535.
- Van-Zwieten, L., Kimber, S., Morris, S., Chan, K.Y., and Downie, A., 2010, Effects of biochar from slow pyrolysis of papermill waste on agronomic performance and soil fertility. Plant Soil. 327(1–2), 235–246.
- Viyaj, K.V., Chandra, R., Subbarao, P. M. V., and Kapid, S. S., 2006, Biogas purification and Bottling into CNG Cylinders: Producing Bio-CNG from Biomass for Rural

Automotive Applications. A paper presentation at The 2nd Joint International Conference on Sustainable Energy and Environment (SEE) on 21-23 November, Bangkok, Thailand.

- Wang, H., Qu, Y., Li, D., Zhou, X., and Feng, Y., 2015, Evaluation of an integrated continuous stirred microbial electrochemical reactor: Wastewater treatment, energy recovery and microbial community. Bioresource Technology. 195, 89–95.
- Wang, W., Xie, L., Luo, G., Zhou, Q., and Angelidaki, I., 2013, Performance and microbial community analysis of the anaerobic reactor with coke oven gas biomethanation and in situ biogas upgrading. Bioresource Technology. 146, 234–239.
- Weiland, P., 2010, Biogas production: current state and perspectives. Applied Microbiology and Biotechnology. 85, 849–860.
- Wellinger, A., and Lindberg, A., 1999, Biogas upgrading and utilization. IEA Bioenergy, Task 24: Energy from biological conversion of organic wastes. 1–19.
- Werner, J.J., Knights, D., Garcia, M.L., Scalfone, N.B., Smith, S., Yarasheski, K., Cummings, T.A., Beers, A.R., Knight, R., and Angenent, L.T., 2011, Bacterial community structures are unique and resilient in full-scale bioenergy systems. Proceedings of the National Academy of Sciences of the United States of America. 108, 4158–4163.
- Wise, D.L., 1981, Analysis of systems for purification of fuel gas. Fuel gas production from biomass, vol 2. Boca Raton, FL: CRC Press.
- World Energy Council, 2013, World energy resources: bioenergy. https://www.worldenergy.org/wp-content/uploads/2017/03/WEResources_Bioenergy 2016.pdf.
- www.fao.org/production/faostat
- Xiao, Y., and Li, X., 2014, Removal of Carbon Dioxide from Biogas with Pilot Chemical Absorption System at Different Operating Conditions. Asian Journal of Chemistry. 26, No. 11, 3204-3208.
- Xiao, Y., Yuan, H., Pang, Y., Chen, S., Zhu, B., Zou, D., Ma, J., Yu, L., and Li, X., 2014, $CO_2$ Removal from Biogas by Water Washing System. Chinese Journal of Chemical Engineering. 22, 950–953.
- Xu, X., Cao, X., Zhao, L., and Sun, T., 2014, Comparison of sewage sludge- and pig manure derived biochars for hydrogen sulfide removal. Chemosphere. 111, 296–303.

- Yadav, D., Barbora, L., Bora, D., Mitra, S., Rangan, L., and Mahanta, P., 2017, An assessment of duckweed as a potential lignocellulosic feedstock for biogas production. International Biodeterioration & Biodegradation. 119, 253-259.
- Yadvika, Santosh, Sreekrishnan, T.R., Kohli, S., and Rana, V., 2004, Enhancement of biogas production from solid substrates using different techniques – a review. Bioresource Technology. 95, 1–10.
- Yan, S., He, Q., Zhao, S., Zhai, H., Cao, M., Ai, P., 2015, $CO_2$ removal from biogas by using green amino acid salts: Performance evaluation. Fuel Processing Technology. 129, 203–212.
- Yang, H., Xu, Z., Fan, M., Gupta, R., Slimane, R.B., and Bland, A.E., 2008, Progress in carbon dioxide separation and capture: a review. Journal of Environmental Sciences. 20, 14–27.
- Yeh, J. T., and Pennline, H. W., 2001, Study of $CO_2$ Absorption and Desorption in a Packed Column. Energy & Fuels. 15 (2), 274-278.
- Yin, R., Liu, R., Mei, Y., Fei, W., and Sun, X., 2013, Characterization of bio-oil and bio-char obtained from sweet sorghum bagasse fast pyrolysis with fractional condensers. Fuel. 112, 96-104.
- Yoon, S.M., Choi, C.H., Kim, M., Hyun, M.S., Shin, S.H., Yi, D.H., and Kim, H.J., 2007, Enrichment of electrochemically active bacteria using a three-electrode electrochemical cell. Journal of Microbiology and Biotechnology. 17, 110–115.
- Zanfir, M., and Gavriilidis, A., 2005, Carbon Dioxide Absorption in a Falling Film Microstructured Reactor: Experiments and Modeling. Industrial & Engineering Chemistry Research. 44, 1742-1751.
- Zhang, P., Whistler, R.L., Bemiller, J.N., and Hamaker, B.R., 2005, Banana starch: Production, physicochemical properties, and digestibility-a review. Carbohydrate Polymers. 59, 443–458.
- Zhang, X., Tang, Y., Qu, S., Da, J., and Hao, Z., 2015, $H_2S$-Selective catalytic oxidation: catalysts and processes. ACS Catalysis. 5, 1053–1067.
- Zhang, Y., Sunarso, J., Liu, S., and Wang, R., 2013, Current status and development of membranes for $CO_2/CH_4$ separation: a review. International Journal of Greenhouse Gas Control. 12, 84–107.

- Zhao, G., Ma, F., Wei, L., Chua, H., Chang, C.C., and Zhang, X.J., 2012, Electricity generation from cattle dung using microbial fuel cell technology during anaerobic acidogenesis and the development of microbial populations. Waste Management. 32, 1651–1658.
- Zhao, Q., Leonhardt, E., MacConnell, C., Frear, C., and Chen, S., 2010, Purification technologies for biogas generated by anaerobic digestion. Climate friendly farming, compressed biomethane, 1–24. CSANR research report, [chapter9].
- Zheng, Y., Zhao, J., Xu, F., and Li, Y., 2014, Pretreatment of lignocellulosic biomass for enhanced biogas production. Progress in Energy and Combustion Science. 35–53.
- Zulkefli, N.N., Masdar, M.S., Wan Isahak, W.N.R., Jahim, J.M., Rejab, S.A.M., and Lye, C.C., 2019, Removal of hydrogen sulfide from a biogas mimic by using impregnated activated carbon adsorbent. PLOS ONE. 1-25.

# Annexure

# Annexure

**Annexure A: BJH pore size distribution curves of adsorbents**

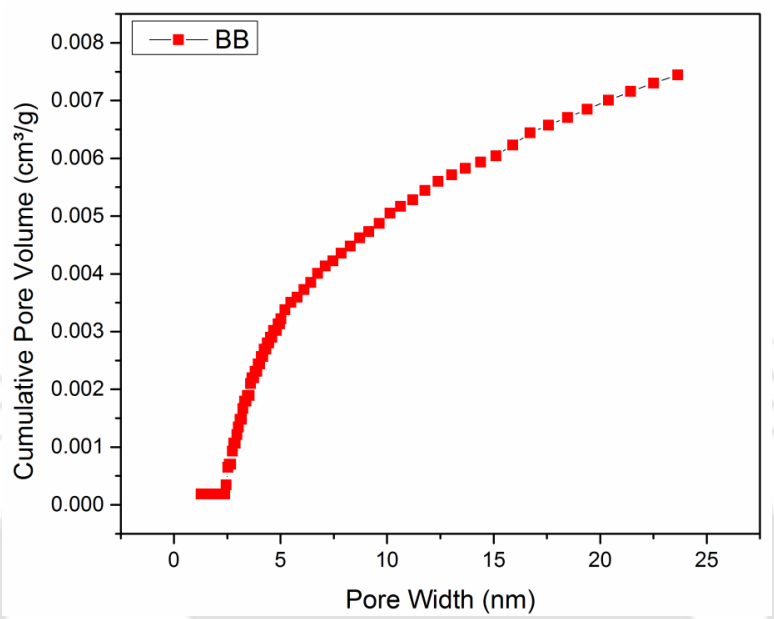


**Figure A1** Cumulative pore volume vs. pore width of BB

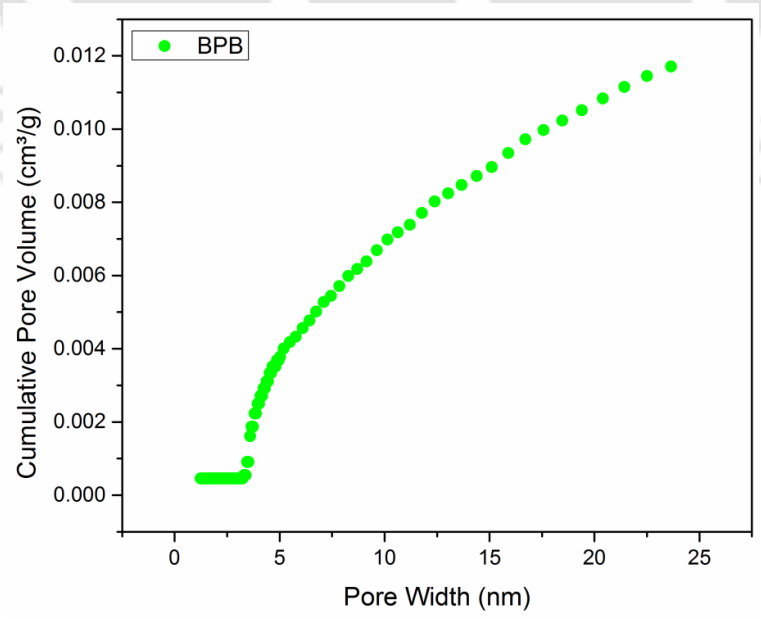


**Figure A2** Cumulative pore volume vs. pore width of BPB

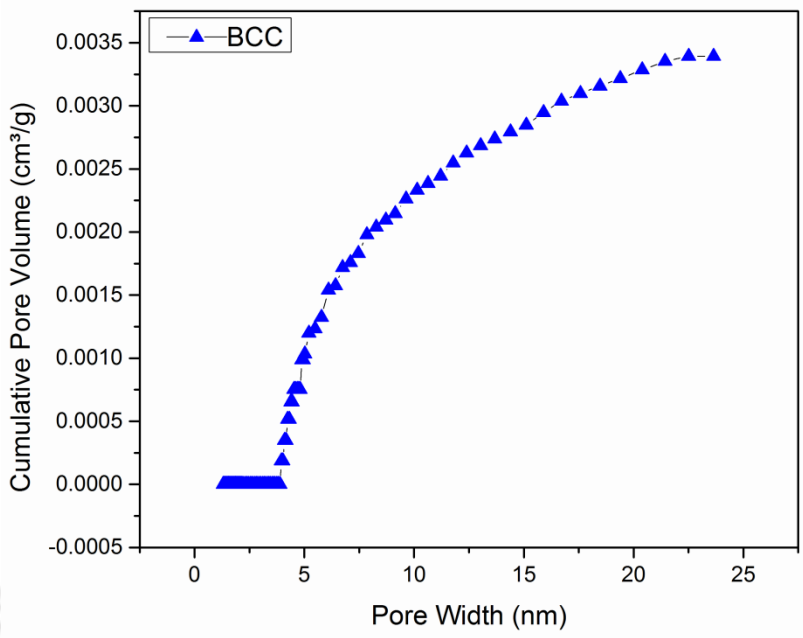


**Figure A3** Cumulative pore volume vs. pore width of BCC

The BJH (Barrett-Joyner-Halenda) pore-size distribution curves of the prepared adsorbents (BB, BPB and BCC) are shown in Fig. A1, A2 and A3. The highest cumulative pore size volume was observed for BPB followed by BB and BCC which satisfied the results obtained from the $N_2$ adsorption-desorption data which was discussed in sub section 3.3.8.

## Annexure B: Survey of biogas plants and locally available biomass

**Figure B1** Survey of biogas plants

A survey was conducted in different districts of Assam to understand the problems faced by the beneficiaries and also in search of locally available biomass to be used as scrubbing agents and adsorbents.

## Annexure C: Experimental setups

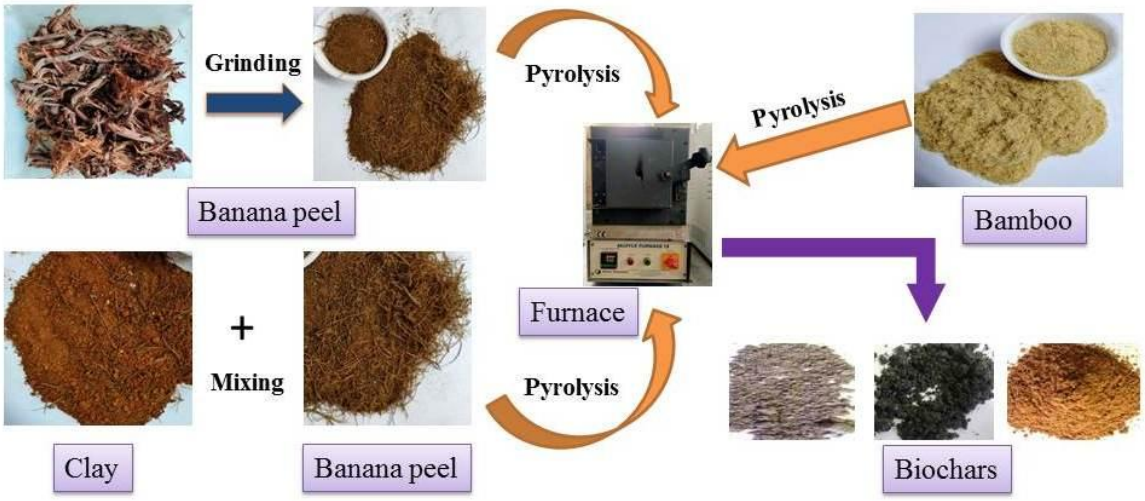


**Figure C1** Preparation process of adsorbents

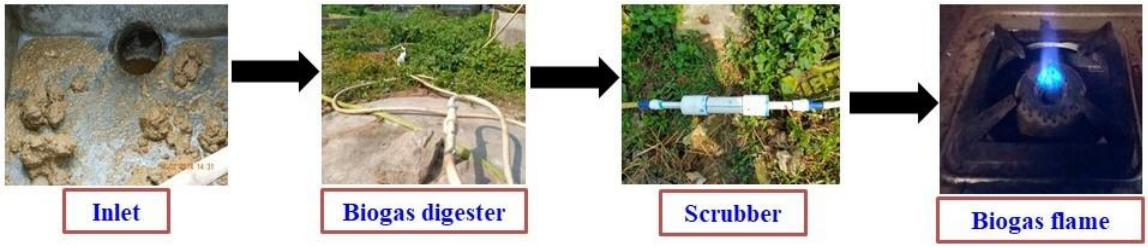


**Figure C2** Route of adsorption


**Figure C3** Route to NBAS

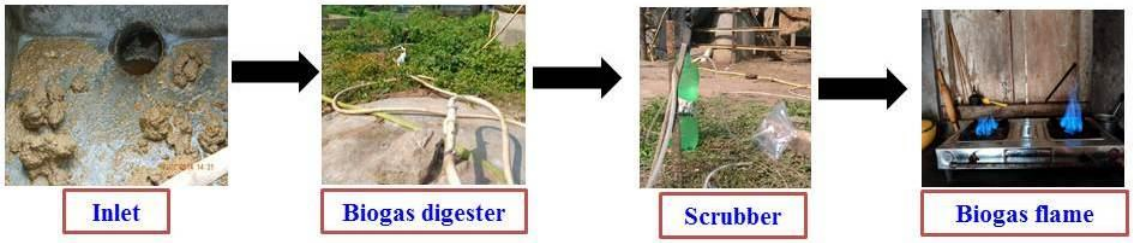


**Figure C4** Route of absorption

**Figure C5** Experimental site of biogas plant at Aaoni ati satra

**Figure C6** Experimental setup of AD-MEA

**Annexure D:** SEM and EDX images of adsorbents

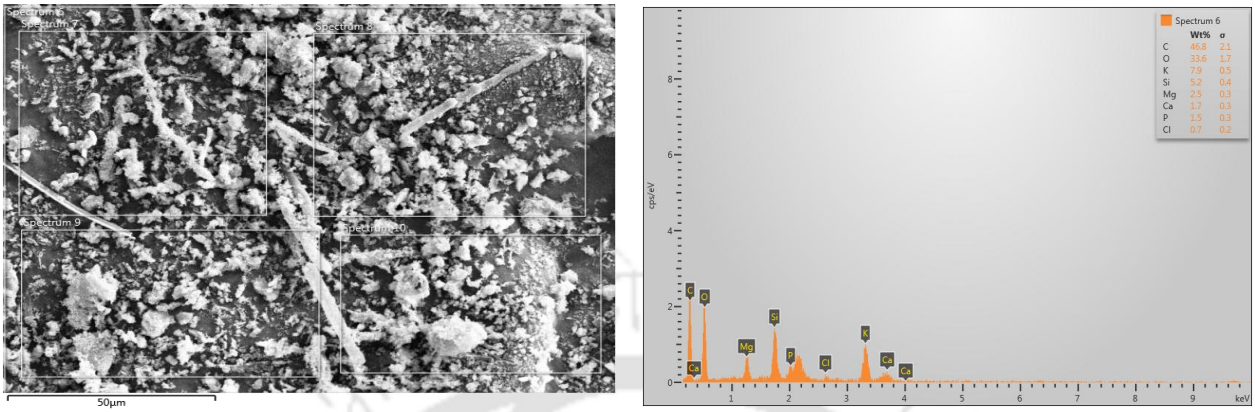


**Figure D1** SEM and EDX images of BB

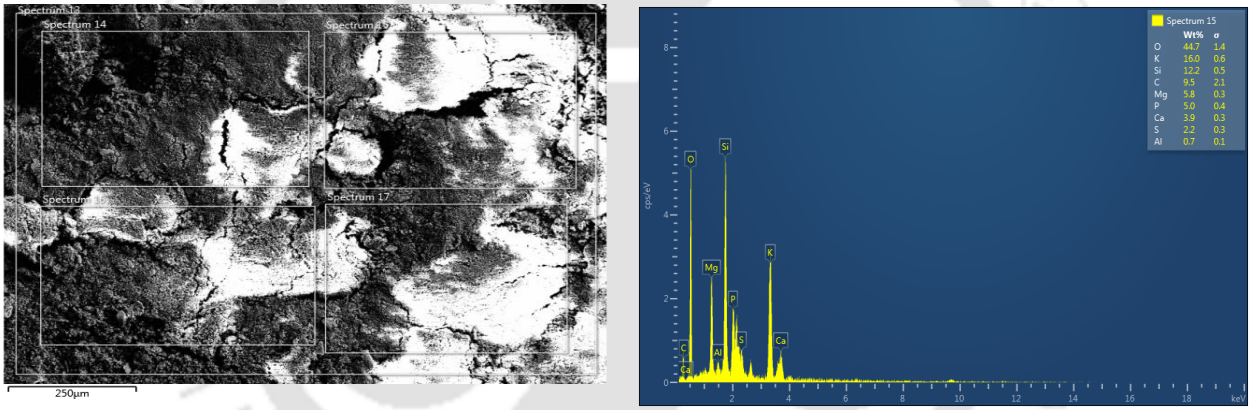


**Figure D2** SEM and EDX images of $BBH_2S$

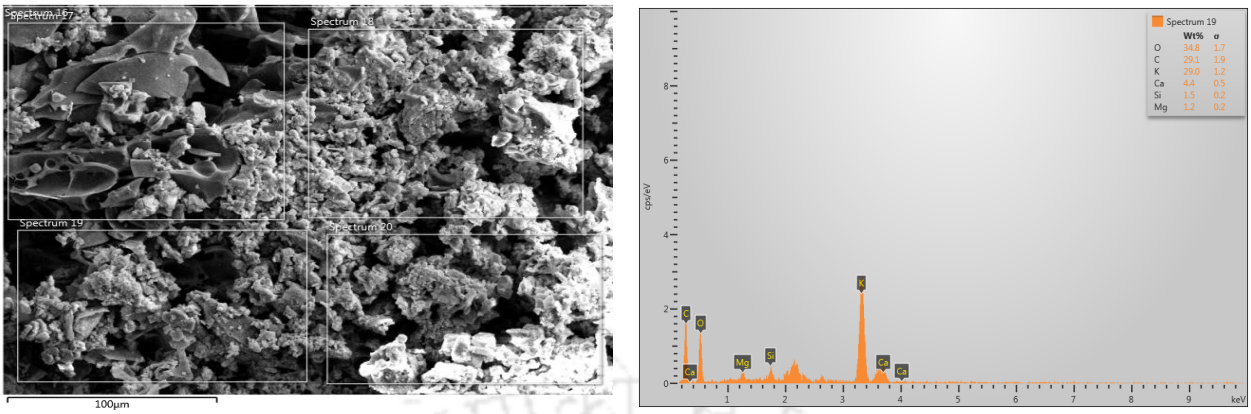


**Figure D3** SEM and EDX images of BPB

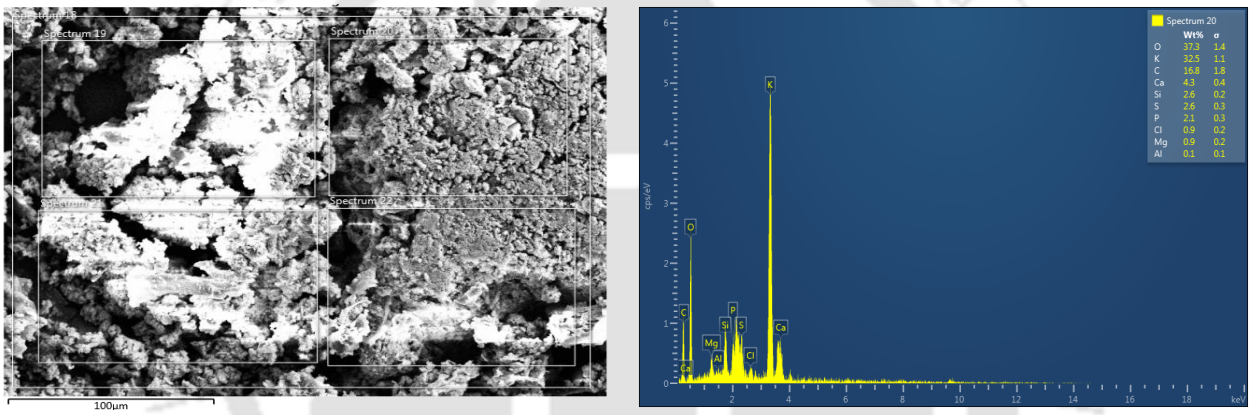


**Figure D4** SEM and EDX images of $BPBH_2S$

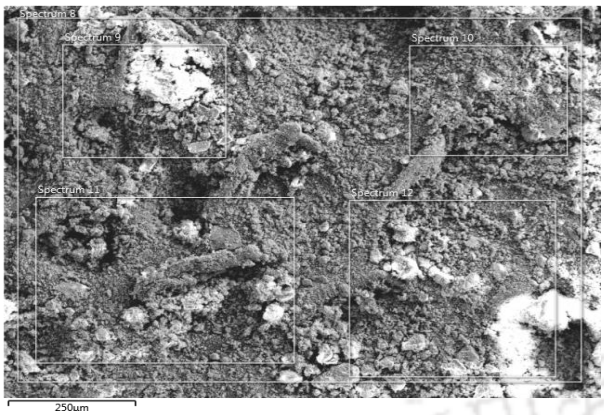


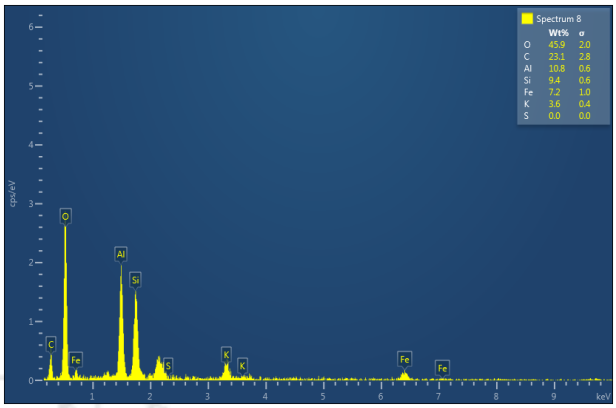


**Figure D5** SEM and EDX images of BCC

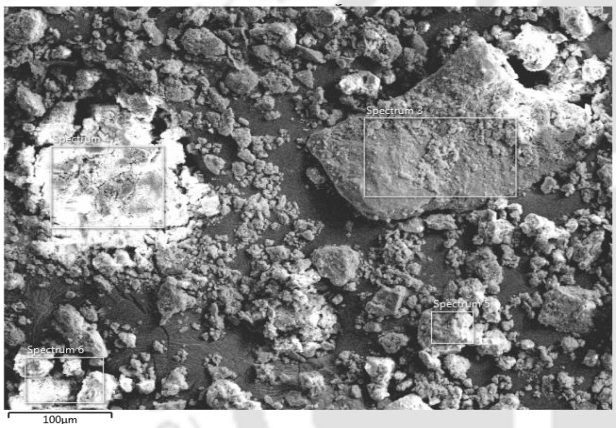


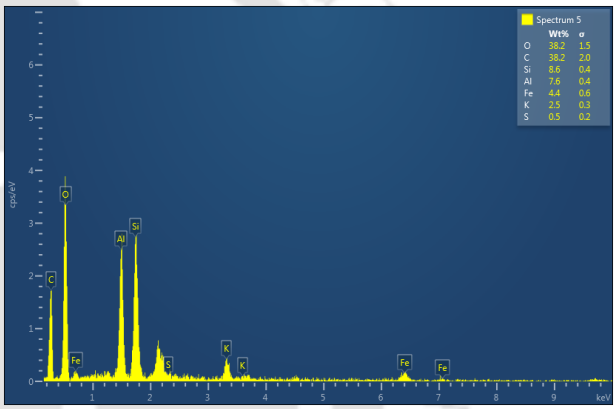


**Figure D6** SEM and EDX images of BCC$H_2S$

Figures D1, D2, D3, D4, D5 and D6 shows the SEM and EDX images of the respective adsorbents in raw and $H_2S$ adsorbed form. As discussed in section 4.3.4, the surface morphology of BB and BPB after $H_2S$ adsorption leads to agglomerate formation whereas in case of BCC no agglomerate is visible which may be due to the disintegration of particles of the biochar clay particles on penetration of $H_2S$. Also, the EDX image shows clear figure on adsorption of $H_2S$, depicting the presence of S in the spectrum.

# PhD RESEARCH OUTPUT

**A. Journals**

- Deep Bora, Arup Dutta, Pinakeswar Mahanta, Pranab Goswami, Devard Stom and Lepakshi Barbora, Membrane Electrode Assembly Hybridized Anaerobic Digester for Co-generation of Methane Enriched Biogas and Electricity, Fuel, 316, 123315, 2022.

- Deep Bora, Lepakshi Barbora and Pinakeswar Mahanta, An Assessment of Natural Base Solution Prepared from different parts of Musa sp. as a Scrubbing Agent of $CO_2$ from Biogas, Journal of Basic and Applied Engineering Research (JBAER), 6 (1), 1-4, 2019.

- Dipti Yadav, Lepakshi Barbora, Deep Bora, Sudip Mitra, Latha Rangan and Pinakeswar Mahanta, An assessment of duckweed as a potential lignocellulosic feedstock for biogas production, International Biodeterioration & Biodegradation, 119, 253-259, 2017.

**B. Book chapters**

- Deep Bora, Lepakshi Barbora and Pinakeswar Mahanta, Synthesis of a Low Cost, Natural Base Solution for $CO_2$ Scrubbing from Biogas and its Comparison with KOH, In: Mahanta P., Kalita P., Paul A., Banerjee A. (eds), Advances in Thermofluids and Renewable Energy, Lecture Notes in Mechanical Engineering, Springer, Singapore, pp. 365-376, 2021.

- Deep Bora, Lepakshi Barbora, Arup Jyoti Borah and Pinakeswar Mahanta, A Comparative Assessment of Biogas Upgradation Techniques and Its Utilization as an Alternative Fuel in Internal Combustion Engines, In: Singh A.P., Kumar D., Agarwal A.K. (eds), Alternative Fuels and Advanced Combustion Techniques as Sustainable Solutions for Internal Combustion Engines. Energy, Environment, and Sustainability. Springer, Singapore, pp. 95-115, 2021.

- Deep Bora, Lepakshi Barbora and Pinakeswar Mahanta, Purification of Biogas for Methane Enrichment Using Biomass Biochar and Biochar–Clay Composite, In: K.M. Pandey, R.D. Misra, P.K. Patowari, and U.S. Dixit (eds), Recent Advances in Mechanical Engineering, Lecture Notes in Mechanical Engineering. Springer, Singapore, pp. 573-581, 2021.

**C. Conferences**

- Deep Bora, Lepakshi Barbora and Pinakeswar Mahanta, Performance Assessment of Natural Base Ash Solutions for Removal of Hydrogen Sulfide from Raw Biogas, *2nd International Conference on Recent Advances in Fluid and Thermal sciences (iCRAFT2020)*, organized by Department of Mechanical Engineering, Birla Institute of Technology and Science Dubai Campus, 19 – 21 March, 2021.

- Deep Bora, Lepakshi Barbora and Pinakeswar Mahanta, Synthesis of a Low Cost, Natural Base Solution for $CO_2$ Scrubbing from Biogas and its Comparison with KOH, *International Conference on Recent Trends in Developments of Thermo-fluids and Renewable Energy (TFRE 2020)*, organized by Department of Electrical Engineering and Department of Mechanical Engineering, NIT Arunachal Pradesh in collaboration with Knowledge Incubation Cell for TEQIP (KIT), IIT Guwahati, NIT Mizoram, NIT Nagaland, NIT Manipur and NIT Meghalaya, November 26 – 28, 2020.

- Deep Bora, Lepakshi Barbora and Pinakeswar Mahanta, Purification of Biogas for Methane Enrichment using Biomass Biochar and Biochar-Clay Composite, *International Conference on Recent Advancements in Mechanical Engineering (ICRAME 2020)*, organized by Department of Mechanical Engineering, NIT Silchar, India, 07-09 February 2020.

- Deep Bora, Lepakshi Barbora and Pinakeswar Mahanta, Utilization of Banana Peel Biochar for Enrichment of Biogas, *National Conference on Issues & Challenges in Water Treatment and Allied Research for Sustainable Environment (WATER 2020)*, organized by Centre for Environment, IIT Guwahati, India, 23-25 January 2020.

- Deep Bora, Lepakshi Barbora and Pinakeswar Mahanta, An Assessment of Natural Base Solution Prepared from different parts of *Musa sp*. as a Scrubbing Agent of $CO_2$ from Biogas, *International Conference on Basic/Applied Sciences, Bioprocess Techniques, Environmental Engineering and Clean Energy Technologies for Sustainable Swachha Bharat (SYNERGY 2019)*, organized by Krishi Sanskriti, Jawaharlal Nehru University, New Delhi, India, 9 February 2019.

- Dipti Yadav, Deep Bora, Munmi Bhattacharya, Lepakshi Barbora, Latha Rangan and Pinakeswar Mahanta, Lignocellulosic Biomass to Bioenergy: A review on sustainable routes for bioenergy conversion, production and processing of biofuels with co-products, *Research Conclave 2016 "An amalgamation of Academia, Industry & Start-up"*, organized by Student Academic Board (SAB), Indian Institute of Technology Guwahati, 17-20 March, 2016.

**D. Patent**

- Lepakshi Barbora, Deep Bora, Arup Dutta, Pinakeswar Mahanta, Jon Mani Kalita and Saurav Khuttiya Deori, "Anaerobic Digester-Membrane Electrode Assembly (AD-MEA) System For Producing Enriched Biogas And Electricity" Patent Application number: 202131014785, Patent no.: 401901. (Granted).

**E. Manuscript under review/ preparation**

- Deep Bora, Kuldeep Roy, Pinakeswar Mahanta, and Lepakshi Barbora, Hydrogen Sulfide Removal from Biogas using Biomass-derived Naturally Alkaline Biochars: Performance analysis and Kinetics.

- Deep Bora, Lepakshi Barbora and Pinakeswar Mahanta, Performance Assessment of Natural Base Ash Solutions for Removal of Hydrogen Sulfide from Raw Biogas.

- Deep Bora, Kuldeep Roy, Pinakeswar Mahanta, and Lepakshi Barbora, Experimental and Kinetic Study on Biogas Production using Membrane Electrode Assembly Hybridized Anaerobic Digester.

- Deep Bora, Lepakshi Barbora and Pinakeswar Mahanta, Biochar-Clay Composite as Adsorbent for $H_2S$ Removal from Raw Biogas: Experimental and Kinetics.